ISSN 1007-9327 (print)
ISSN 2219-2840 (online)

World Journal of *Gastroenterology*

World J Gastroenterol 2024 February 7; 30(5): 424-515

Published by Baishideng Publishing Group Inc

World Journal of Gastroenterology

Contents

Weekly Volume 30 Number 5 February 7, 2024

LETTER TO THE EDITOR

Contents

NAME OF JOURNAL
World Journal of Gastroenterology

ISSN
ISSN 1007-9327 (print) ISSN 2219-2840 (online)

LAUNCH DATE
October 1, 1995

FREQUENCY
Weekly

EDITORS-IN-CHIEF
Andrzej S Tarnawski

EXECUTIVE ASSOCIATE EDITORS-IN-CHIEF
Xian-Jun Yu (Pancreatic Oncology), Jian-Gao Fan (Chronic Liver Disease), Hou-Bao Liu (Biliary Tract Disease)

EDITORIAL BOARD MEMBERS
http://www.wjgnet.com/1007-9327/editorialboard.htm

PUBLICATION DATE
February 7, 2024

PUBLISHING PARTNER
Shanghai Pancreatic Cancer Institute and Pancreatic Cancer Institute, Fudan University
Biliary Tract Disease Institute, Fudan University

INSTRUCTIONS TO AUTHORS
https://www.wjgnet.com/bpg/gerinfo/204

GUIDELINES FOR ETHICS DOCUMENTS
https://www.wjgnet.com/bpg/GerInfo/287

GUIDELINES FOR NON-NATIVE SPEAKERS OF ENGLISH
https://www.wjgnet.com/bpg/gerinfo/240

PUBLICATION ETHICS
https://www.wjgnet.com/bpg/GerInfo/288

PUBLICATION MISCONDUCT
https://www.wjgnet.com/bpg/gerinfo/208

POLICY OF CO-AUTHORS
https://www.wjgnet.com/bpg/GerInfo/310

ARTICLE PROCESSING CHARGE
https://www.wjgnet.com/bpg/gerinfo/242

STEPS FOR SUBMITTING MANUSCRIPTS
https://www.wjgnet.com/bpg/GerInfo/239

ONLINE SUBMISSION
https://www.f6publishing.com

PUBLISHING PARTNER's OFFICIAL WEBSITE
https://www.shca.org.cn
https://www.zs-hospital.sh.cn

World Journal of Gastroenterology

Submit a Manuscript: https://www.f6publishing.com

World J Gastroenterol 2024 February 7; 30(5): 424-428

DOI: 10.3748/wjg.v30.i5.424

ISSN 1007-9327 (print) ISSN 2219-2840 (online)

EDITORIAL

Leveraging machine learning for early recurrence prediction in hepatocellular carcinoma: A step towards precision medicine

Abhimati Ravikulan, Kamran Rostami

Specialty type: Gastroenterology and hepatology

Provenance and peer review: Invited article; Externally peer reviewed.

Peer-review model: Single blind

Peer-review report's scientific quality classification

Grade A (Excellent): 0
Grade B (Very good): B, B
Grade C (Good): 0
Grade D (Fair): 0
Grade E (Poor): 0

P-Reviewer: Lu GR, China; Morya AK, India

Received: November 21, 2023
Peer-review started: November 21, 2023
First decision: December 5, 2023
Revised: December 19, 2023
Accepted: January 12, 2024
Article in press: January 12, 2024
Published online: February 7, 2024

Abhimati Ravikulan, Kamran Rostami, Department of Gastroenterology, Palmerston North Hospital, Palmerston North 4442, New Zealand

Corresponding author: Abhimati Ravikulan, Doctor, Research Fellow, Researcher, Department of Gastroenterology, Palmerston North Hospital, 50 Ruahine Street, Roslyn, Palmerston North 4442, New Zealand. arav175@aucklanduni.ac.nz

Abstract

The high rate of early recurrence in hepatocellular carcinoma (HCC) post curative surgical intervention poses a substantial clinical hurdle, impacting patient outcomes and complicating postoperative management. The advent of machine learning provides a unique opportunity to harness vast datasets, identifying subtle patterns and factors that elude conventional prognostic methods. Machine learning models, equipped with the ability to analyse intricate relationships within datasets, have shown promise in predicting outcomes in various medical disciplines. In the context of HCC, the application of machine learning to predict early recurrence holds potential for personalized postoperative care strategies. This editorial comments on the study carried out exploring the merits and efficacy of random survival forests (RSF) in identifying significant risk factors for recurrence, stratifying patients at low and high risk of HCC recurrence and comparing this to traditional COX proportional hazard models (CPH). In doing so, the study demonstrated that the RSF models are superior to traditional CPH models in predicting recurrence of HCC and represent a giant leap towards precision medicine.

Key Words: Machine learning; Artificial intelligence; Hepatocellular carcinoma; Hepatology; Early recurrence; Liver resection

Core Tip: This study addresses the crucial issue of early recurrence in hepatocellular carcinoma, emphasizing the significance of aggressive tumour characteristics. random survival forests, a machine learning model, surpasses conventional COX proportional hazard models, offering improved prediction, clinical usefulness, and overall performance. The model's ability to stratify risk facilitates targeted postoperative strategies, showcasing its potential as a guide for personalized patient care.

Citation: Ravikulan A, Rostami K. Leveraging machine learning for early recurrence prediction in hepatocellular carcinoma: A step towards precision medicine. *World J Gastroenterol* 2024; 30(5): 424-428
URL: https://www.wjgnet.com/1007-9327/full/v30/i5/424.htm
DOI: https://dx.doi.org/10.3748/wjg.v30.i5.424

INTRODUCTION

Developing a reliable pre-operative prediction model for postoperative recurrence of hepatocellular carcinoma (HCC) is essential in guiding individualized treatment and prognostication process of HCC.

In this issue of *World Journal of Gastroenterology*, Zeng *et al*[1] endeavour to identify key variables in pre-operative clinical and imaging data using machine learning algorithms to construct multiple risk prediction models for early postoperative recurrence of HCC.

HCC remains a significant challenge in the realm of oncology, particularly due to its propensity for early recurrence following curative resection[2,3]. It is the sixth most common cancer worldwide[4]. Though surgical resection remains the mainstay of curative therapy for HCC, early recurrence of HCC (within 1 year) stands as a substantial barrier to positive patient outcomes[3,5]. Survival rates in early recurrence of HCC can be as low as 25% at 3-5 years post resection[5]. There are no current approved therapeutic regimens available for the recurrence of HCC[6].

This raises a significant need to improve models for the early detection of patients at risk of recurrence. Many factors have been identified in predicting risk of recurrence of HCC[2] and this editorial explores the promising avenue in the quest for precision medicine[1] the development of a machine learning model as highlighted by the authors aimed at predicting early recurrence after surgical intervention[7]. The advent of machine learning provides a unique opportunity to harness vast datasets, identifying subtle patterns and factors that elude conventional prognostic methods[8,9].

Machine learning models, equipped with the ability to analyse intricate relationships within datasets, have shown promise in predicting outcomes in various medical disciplines[8]. In the context of HCC, the application of machine learning to predict early recurrence holds potential for personalized postoperative care strategies[10].

Traditionally, predictive models, such as COX proportional hazard (CPH) models, have been employed, but their limitations have spurred the exploration of innovative methodologies[9-11]. This study undertakes a critical examination, comparing the efficacy of random survival forests (RSF) with CPH models in forecasting early recurrence for HCC patients following curative resection.

Drawing from a comprehensive cohort of 4758 patients across two medical centres, this study utilized 15 key features to construct the RSF model. Features encompassed demographic, clinical, and tumour-specific factors. The RSF model was rigorously evaluated for discrimination, calibration, clinical utility, and overall performance, benchmarked against traditional models.

Out of 5686 patients with HCC undergoing definitive surgical therapy at Eastern Hepatobiliary Surgery Hospital (January 2008 to December 2015), 4376 met inclusion criteria. The study included patients with Child-Pugh A cirrhosis or B7 Liver function, without extrahepatic metastases, and complete resection of macroscopic tumour with histological evidence of tumour free margins. Exclusions (n = 1310) were due to preoperative anticancer treatment, history of other malignancies, palliative surgery, loss to follow up within 2 months of surgery, and perioperative death. The training cohort comprised 3370 patients (January 2008 to December 2013), internal validation cohort 1006 patients (January 2014 to December 2015), and external validation cohort 382 patients from Mengchao Hepatobiliary Hospital of Fujian Medical University.

The RSF model was constructed and used as a regression algorithm with faster training and lower estimation bias. This was achieved by using techniques of random forests such as feature and sample bragging. The model was constructed using fifteen factors including age, gender, aetiology, platelet count, albumin, total bilirubin, alpha-fetoprotein (AFP), tumour size, tumour number, microvascular invasion, macrovascular invasion, Edmondson-Steiner grade, tumour capsular, satellite nodules and liver cirrhosis. As 200 survival trees were built, the prediction error was significantly low and at 500 trees constructed, the variable importance for all 15 features was also generated. Utilizing cut-off values (50^{th} and 85^{th} centiles) from the training cohort's risk index, RSF classified patients into low-risk, intermediate-risk, and high-risk groups, providing valuable insights for postoperative follow-up and adjuvant therapy. Kaplan-Meier analysis validated the stratification in all cohorts ($P < 0.0001$) (Figure 1).

Model performance was assessed across several methods including model discrimination, model calibration, clinical usefulness and overall performance. In training, internal, and external validation cohorts, RSF outperformed existing models with C-index values of 0.725, 0.762, and 0.747, respectively. Overall performance time-dependent Brier (2 years) were 0.147, 0.129, and 0.156. RSF excelled against five other models that follow CPH. Decision curve analysis affirmed RSF's superior net benefit over other models (Table 1).

Table 1 Comparison of random survival forests model performance *vs* 5 other models following Cox proportional hazard format to predict early recurrence

Performance	Cohort	RSF	ERASL	Korean	AJCC TNM	BCLC	Chinese
Model Discrimination: (Harrell's C-Index)	Training	0.725	0.706	0.658	0.674	0.635	0.684
	Internal	0.762	0.726	0.672	0.711	0.646	0.709
	External	0.747	0.727	0.722	0.711	0.658	0.696
Overall Performance: Time dependent Brier (2 years)	Training	0.147	0.156	0.174	0.160	0.167	0.161
	Internal	0.129	0.143	0.159	0.144	0.154	0.146
	External	0.156	0.162	0.161	0.169	0.180	0.176
Clinical Usefulness: Net benefit at threshold 50%	Training	0.166	0.154	0.093	0.139	0.137	0.137
	Internal	0.121	0.092	0.041	0.095	0.073	0.073
	External	0.206	0.190	0.222	0.185	0.154	0.154

RSF: Random survival forest; ERASL: Early Recurrence After Surgery for Liver tumours; AJCC TNM: American Joint Committee on Cancer tumour-node-metastasis; BCLC: Barcelona Clinic Liver Cancer stage.

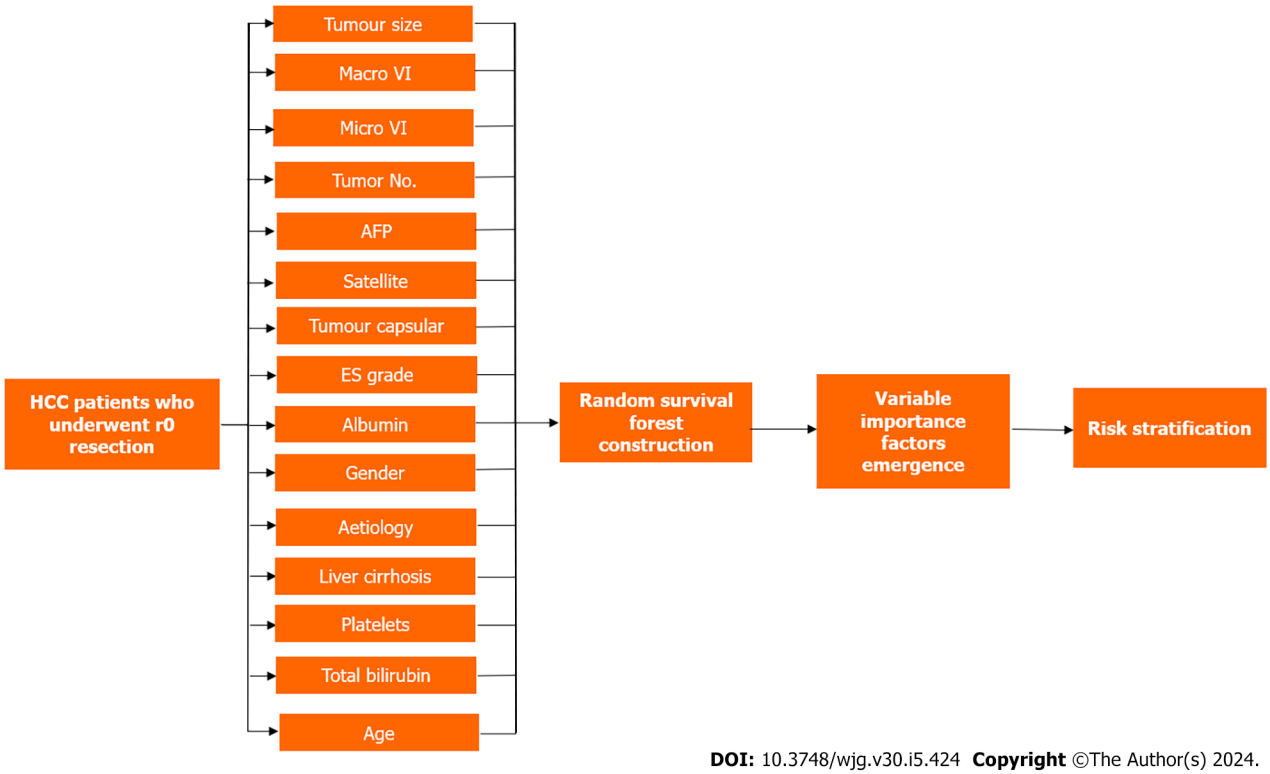

DOI: 10.3748/wjg.v30.i5.424

Figure 1 Construction of random survival forests model. 15 factors used to construct random survival forests model in hepatocellular carcinoma patients who underwent R0 resection with variable importance factors emergence and risk stratification applied. HCC: Hepatocellular carcinoma; AFP: Alpha-fetoprotein.

The RSF model, employing 500 survival trees, showcased superior predictive power. Key factors influencing recurrence were tumour size (which was the most significant risk factor for early recurrence), followed by macrovascular invasion, microvascular invasion, tumour number, and AFP levels.

The limitations to this study include selection bias as the cohort of patients largely had liver disease secondary to hepatitis B, which leaves a large space to question the applicability of these outcomes to other aetiologies of liver disease, and indeed, the RSF model did not consider aetiology and liver cirrhosis as important predictors of recurrence. Further studies will need to be conducted with the RSF model using patients of different aetiologies of liver disease to validate its use across different demographics in predicting HCC recurrence and reduce selection bias.

The user-friendly aspect of the web-tool developed, encompasses multiple complex aspects of the predictive model to increase its application in clinical practice.

In conclusion, the RSF model emerges as a beacon in the quest for precision postoperative care in HCC. Its demonstrated superiority over traditional models, coupled with its ability to stratify risk, ushers in a new era of individualized treatment strategies. The future role of artificial intelligence (AI) in evaluating hepatic diseases holds tremendous promise for revolutionizing diagnostic and treatment approaches. AI technologies, particularly machine learning algorithms, can analyse vast amounts of medical data, including imaging studies, laboratory results, and patient histories, to identify patterns and subtle anomalies that may escape the human eye. In hepatic diseases, AI can play a crucial role in early detection, risk assessment, and personalized treatment planning. Advanced imaging techniques, such as magnetic resonance imaging (MRI) and computed tomography (CT) scans, can be enhanced by AI algorithms to provide more accurate and timely diagnoses of liver conditions. Machine learning models can also predict disease progression, helping healthcare professionals tailor interventions based on individual patient profiles.

As we navigate this machine learning odyssey, the RSF model stands poised to redefine the landscape of HCC prognostication and guide clinicians toward more informed and personalized patient care.

CONCLUSION

In conclusion, the RSF model emerges as a beacon in the quest for precision postoperative care in HCC. Its demonstrated superiority over traditional models, coupled with its ability to stratify risk, ushers in a new era of individualized treatment strategies. The future role of AI in evaluating hepatic diseases holds tremendous promise for revolutionizing diagnostic and treatment approaches. AI technologies, particularly machine learning algorithms, can analyse vast amounts of medical data, including imaging studies, laboratory results, and patient histories, to identify patterns and subtle anomalies that may escape the human eye. In hepatic diseases, AI can play a crucial role in early detection, risk assessment, and personalized treatment planning. Advanced imaging techniques, such as MRI and CT scans, can be enhanced by AI algorithms to provide more accurate and timely diagnoses of liver conditions. Machine learning models can also predict disease progression, helping healthcare professionals tailor interventions based on individual patient profiles.

As we navigate this machine learning odyssey, the RSF model stands poised to redefine the landscape of HCC prognostication and guide clinicians toward more informed and personalized patient care.

FOOTNOTES

Author contributions: Ravikulan A wrote the first draft; Rostami K reviewed the manuscript; and both authors finalized the editorial.

Conflict-of-interest statement: The authors declare no conflict of interest.

Country/Territory of origin: New Zealand

ORCID number: Abhimati Ravikulan 0009-0000-6702-2958; Kamran Rostami 0000-0002-2114-2353.

S-Editor: Qu XL
L-Editor: A
P-Editor: Yu HG

REFERENCES

1 **Zeng J**, Zeng J, Lin K, Lin H, Wu Q, Guo P, Zhou W, Liu J. Development of a machine learning model to predict early recurrence for hepatocellular carcinoma after curative resection. *Hepatobiliary Surg Nutr* 2022; **11**: 176-187 [PMID: 35464276 DOI: 10.21037/hbsn-20-466]

2 **Nevola R**, Ruocco R, Criscuolo L, Villani A, Alfano M, Beccia D, Imbriani S, Claar E, Cozzolino D, Sasso FC, Marrone A, Adinolfi LE, Rinaldi L. Predictors of early and late hepatocellular carcinoma recurrence. *World J Gastroenterol* 2023; **29**: 1243-1260 [PMID: 36925456 DOI: 10.3748/wjg.v29.i8.1243]

3 **Poon RT**, Fan ST, Lo CM, Liu CL, Wong J. Long-term survival and pattern of recurrence after resection of small hepatocellular carcinoma in patients with preserved liver function: implications for a strategy of salvage transplantation. *Ann Surg* 2002; **235**: 373-382 [PMID: 11882759 DOI: 10.1097/00000658-200203000-00009]

4 **Sung H**, Ferlay J, Siegel RL, Laversanne M, Soerjomataram I, Jemal A, Bray F. Global Cancer Statistics 2020: GLOBOCAN Estimates of Incidence and Mortality Worldwide for 36 Cancers in 185 Countries. *CA Cancer J Clin* 2021; **71**: 209-249 [PMID: 33538338 DOI: 10.3322/caac.21660]

5 **Portolani N**, Coniglio A, Ghidoni S, Giovanelli M, Benetti A, Tiberio GA, Giulini SM. Early and late recurrence after liver resection for hepatocellular carcinoma: prognostic and therapeutic implications. *Ann Surg* 2006; **243**: 229-235 [PMID: 16432356 DOI:

10.1097/01.sla.0000197706.21803.a1]

6 **Gao YX**, Ning QQ, Yang PX, Guan YY, Liu PX, Liu ML, Qiao LX, Guo XH, Yang TW, Chen DX. Recent advances in recurrent hepatocellular carcinoma therapy. *World J Hepatol* 2023; **15**: 460-476 [PMID: 37206651 DOI: 10.4254/wjh.v15.i4.460]

7 **Wang D**, Xiao M, Wan ZM, Lin X, Li QY, Zheng SS. Surgical treatment for recurrent hepatocellular carcinoma: Current status and challenges. *World J Gastrointest Surg* 2023; **15**: 544-552 [PMID: 37206072 DOI: 10.4240/wjgs.v15.i4.544]

8 **Ngiam KY**, Khor IW. Big data and machine learning algorithms for health-care delivery. *Lancet Oncol* 2019; **20**: e262-e273 [PMID: 31044724 DOI: 10.1016/S1470-2045(19)30149-4]

9 **Christou CD**, Tsoulfas G. Challenges and opportunities in the application of artificial intelligence in gastroenterology and hepatology. *World J Gastroenterol* 2021; **27**: 6191-6223 [PMID: 34712027 DOI: 10.3748/wjg.v27.i37.6191]

10 **Singal AG**, Mukherjee A, Elmunzer BJ, Higgins PD, Lok AS, Zhu J, Marrero JA, Waljee AK. Machine learning algorithms outperform conventional regression models in predicting development of hepatocellular carcinoma. *Am J Gastroenterol* 2013; **108**: 1723-1730 [PMID: 24169273 DOI: 10.1038/ajg.2013.332]

11 **Pickett KL**, Suresh K, Campbell KR, Davis S, Juarez-Colunga E. Random survival forests for dynamic predictions of a time-to-event outcome using a longitudinal biomarker. *BMC Med Res Methodol* 2021; **21**: 216 [PMID: 34657597 DOI: 10.1186/s12874-021-01375-x]

World Journal of Gastroenterology

Submit a Manuscript: https://www.f6publishing.com

World J Gastroenterol 2024 February 7; 30(5): 429-439

DOI: 10.3748/wjg.v30.i5.429

ISSN 1007-9327 (print) ISSN 2219-2840 (online)

REVIEW

Nicotinamide adenine dinucleotide phosphate oxidase in pancreatic diseases: Mechanisms and future perspectives

Ya-Wei Bi, Long-Song Li, Nan Ru, Bo Zhang, Xiao Lei

Specialty type: Gastroenterology and hepatology

Provenance and peer review: Invited article; Externally peer reviewed.

Peer-review model: Single blind

Peer-review report's scientific quality classification

Grade A (Excellent): 0
Grade B (Very good): 0
Grade C (Good): C, C, C
Grade D (Fair): 0
Grade E (Poor): 0

P-Reviewer: Chen Z, China; Soni S, United States

Received: September 26, 2023
Peer-review started: September 26, 2023
First decision: December 7, 2023
Revised: December 17, 2023
Accepted: January 12, 2024
Article in press: January 12, 2024
Published online: February 7, 2024

Ya-Wei Bi, Long-Song Li, Nan Ru, Bo Zhang, Department of Gastroenterology, The First Medical Center of Chinese PLA General Hospital, Beijing 100853, China

Xiao Lei, Department of Radiation Oncology, Chinese PLA General Hospital, Beijing 100853, China

Corresponding author: Xiao Lei, PhD, Chief Physician, Doctor, Department of Radiation Oncology, Chinese PLA General Hospital, No. 28 Fuxing Road, Haidian District, Beijing 100853, China. 18601758966@163.com

Abstract

Pancreatitis and pancreatic cancer (PC) stand as the most worrisome ailments affecting the pancreas. Researchers have dedicated efforts to unraveling the mechanisms underlying these diseases, yet their true nature continues to elude their grasp. Within this realm, oxidative stress is often believed to play a causal and contributory role in the development of pancreatitis and PC. Excessive accumulation of reactive oxygen species (ROS) can cause oxidative stress, and the key enzyme responsible for inducing ROS production in cells is nicotinamide adenine dinucleotide phosphate hydrogen oxides (NOX). NOX contribute to pancreatic fibrosis and inflammation by generating ROS that injure acinar cells, activate pancreatic stellate cells, and mediate macrophage polarization. Excessive ROS production occurs during malignant transformation and pancreatic carcinogenesis, creating an oxidative microenvironment that can cause abnormal apoptosis, epithelial to mesenchymal transition and genomic instability. Therefore, understanding the role of NOX in pancreatic diseases contributes to a more in-depth exploration of the exact pathogenesis of these diseases. In this review, we aim to summarize the potential roles of NOX and its mechanism in pancreatic disorders, aiming to provide novel insights into understanding the mechanisms underlying these diseases.

Key Words: Nicotinamide adenine dinucleotide phosphate hydrogen oxides; Pancreatitis; Pancreatic cancer; Reactive oxygen species; Mechanism

Core Tip: Nicotinamide adenine dinucleotide phosphate hydrogen oxides (NOX) plays a significant role in the development of pancreatitis and pancreatic cancer (PC) by contributing to pancreatic fibrosis and inflammation. It achieves this by generating reactive oxygen species, which damage acinar cells, activate pancreatic stellate cells, and induce macrophage polarization. Moreover, NOX promotes PC progression by interfering with abnormal cell apoptosis, initiating the epithelial to mesenchymal transition processes, and leading to cell genomic instability. A thorough understanding of NOX's involvement in pancreatic diseases is crucial for comprehending the underlying mechanisms of pancreatitis and PC. This review provides a summary of NOX's potential roles and mechanisms in pancreatic disorders, emphasizing areas that require further investigation.

Citation: Bi YW, Li LS, Ru N, Zhang B, Lei X. Nicotinamide adenine dinucleotide phosphate oxidase in pancreatic diseases: Mechanisms and future perspectives. *World J Gastroenterol* 2024; 30(5): 429-439
URL: https://www.wjgnet.com/1007-9327/full/v30/i5/429.htm
DOI: https://dx.doi.org/10.3748/wjg.v30.i5.429

INTRODUCTION

Incidence of diseases of the pancreas, including acute and chronic pancreatitis (CP) and pancreatic cancer (PC) are rising globally[1-3]. Acute pancreatitis (AP) is the leading cause for gastrointestinal-disease related hospital admissions and is associated with significant morbidity, mortality and socioeconomic burden[4]. CP causes persistent pain, as well as exocrine and endocrine pancreatic insufficiency. It also poses a risk factor for the development of PC[5]. PC is the malignancies with an incidence/mortality ratio of as high as 94% and a 5-year survival rate of about 9%[6]. Although researchers have been dedicated to exploring these diseases, the precise pathogenesis remains unclear. Research indicates that aberrant redox homeostasis occurs in both pancreatitis and PC. Reactive oxygen species (ROS) exert oxidative stress on the pancreatic cells, deregulating the redox homeostasis and promoting inflammation and tumorigenesis by initiating an aberrant induction of signaling networks[7,8].

Nicotinamide adenine dinucleotide phosphate hydrogen oxidases (NOX) is indeed a primary source of cellular ROS. During the development of PC and pancreatitis, the levels of ROS in pancreatic tissue are significantly increased, the source of these ROS is related to dysregulation of NOX in pancreatic cells[9,10]. The dysregulation of NOX plays an important role in pancreatitis and PC. Therefore, to clarify the regulatory mechanism of NOX in pancreatic cells will be more conducive to understanding the pathological process of pancreatitis and PC. In a word, we will present the existing evidence regarding the role and the mechanism of NOX in both pancreatitis and PC.

NOX IN AP

AP occurs as a result of the abnormal activation of pancreatic enzymes, which leads to the digestion of the pancreas itself and surrounding organs[11]. It is primarily characterized by localized inflammation of the pancreas and can even cause systemic organ dysfunction. Acinar cell injury leading to premature activation of pancreatic enzymes is considered the primary factor in the initiation of AP[12]. The subsequent inflammation triggered by the necrosis of acinar cells plays a crucial role in the progression of the disease[13]. Among the immune cells responding to the released chemotactic factors from injured acinar cells during pancreatitis, macrophages are among the earliest[14]. Therefore, both acinar cells and macrophages play significant roles in the development of AP. As the disease worsens, AP can even cause multiple organ dysfunction, known as severe AP, which has a high mortality rate and attracts significant clinical attention[15]. Therefore, this section focuses on exploring the regulatory role of NOX in acinar cells, macrophages, and other organ failures associated with AP.

NOX causes acinar cell damage

Pancreatic acinar cells are secretory cells that primarily synthesize, store and ultimately release digestive enzymes into the duodenum[16]. However, when exposed to harmful stimuli, acinar cells exhibit inflammatory characteristics by activating signaling transduction pathways associated with the expression of inflammatory mediators[17]. The injury or death of acinar cells can initiate inflammatory cascades, which is the main pathogenesis of AP.

Pancreatic acinar cells constitutively express NOX subunits p67phox and p47phox in the cytosol, as well as NOX1 and p22phox in the membrane, which could be activated by cerulein[18]. Upon activation, a complex of the cytosolic subunits translocates to the membrane and facilitates NOX-dependent formation of superoxide and other secondary ROS. In the early stage of AP, the NOX activity of acinar cells is significantly upregulated, leading to the activation of downstream nuclear factor kappa-B (NF-κB) pathway and stimulation of interleukin (IL)-6 expression[18]. In addition to inducing AP, NOX can also participate in a series of inflammatory cascade reactions to promote the progression of AP.

NOX hyperactivity disrupts mitochondrial membrane potential, leading to ATP depletion and subsequent injury in pancreatic acinar cells[19]. The excessive production of ROS by NOX induced zymogen activation, mitochondrial dysfunction and cytokine expression, which further injury to pancreatic acinar cells[20,21]. And the use of the NOX1

inhibitor could suppress these responses and alleviate inflammation in alcoholic AP model. To further investigate the mechanism of NOX action on acinar cells in AP, Ju *et al*[22] discovered that NOX mediated the activation of Janus kinase (JAK)2/signal transducer and activator of transcription and mitogen-activated protein kinases (MAPKs) (ERK, JNK, p38) to induce the expression of transforming growth factor (TGF)-β1 in cerulein-stimulated pancreatic acinar cells, thereby facilitating the progress of AP. Furthermore, NOX is believed to be involved in acinar cell death. NOX upregulates IL-6 and mediates ROS-induced apoptosis in pancreatic acinar cells stimulated with the cholecystokinin analogue cerulein [23]. It is known that cerulein induced the expression of apoptosis-inducing factor (AIF) in pancreatic acinar cell. During the process of cell apoptosis, AIF relocates from the mitochondria to the cytoplasm, and subsequently enters the cell nucleus, resulting in the aggregation and fragmentation of nuclear DNA, ultimately inducing apoptosis in pancreatic acinar cells[24,25]. Previous studies have indicated that NOX activation might be the upstream events of AIF expression, leading to cerulein-induced apoptosis in pancreatic acinar cells[26].

NOX is involved in the M1 polarization of macrophage in AP

Accumulating evidences shows that both the number and activation of macrophages play a crucial role in determining the severity of AP[27-29]. Damaged pancreatic acinar cells release cell contents including trypsin, zymogen granules, cytokines, cell-free DNA and other damage-related molecular patterns, which recruit and activate inflammatory macrophages[30]. Macrophages can be categorized into two main subtypes, M1 and M2, based on their stimuli and function *in vitro*[31]. M1 macrophages are responsible for producing cytokines and inflammatory mediators, which contribute to the amplification of local and systemic inflammation. As a result, they dominate the pro-inflammatory phase of AP. On the other hand, M2-like macrophages are prevalent during the process of pancreas repair/regeneration [32]. Therefore, M1 macrophages are dominated during the development of AP.

NOX-induced ROS production has a role in maintaining the polarization of M1 macrophage[33,34]. The involvement of NOX in mediating macrophage M1 polarization has been studied in various organs. For instance, NOX4 has been shown to induce macrophage M1 polarization following spinal cord injury[35]. In breast cancer, M1 macrophages exhibited significantly increased levels of ROS and mRNA expression of NOX2, NOX5, and CYBA (p22phox) compared to M2 macrophages[36]. Moreover, it is reported that NOX2 could mediate macrophage M1 polarization in traumatic brain injury through NF-κB pathway[37]. Regarding the pancreas, Han *et al*[38] discovered that NOX-mediated oxidative stress the polarization of M1 macrophages in the pancreas, thereby promoting the progression of AP *via* the activation of NF-κB and inflammasome pathways. Accordingly, NOX is capable of mediating the polarization of M1 polarization and contributing to the progression of AP. Further research is warranted to elucidate the underlying mechanisms by which NOX maintains M1 macrophages in the context of AP.

NOX is involved in AP-associated organ dysfunction

Despite the mild nature of AP in most patients, about 20%-30% experience a severe form that frequently results in dysfunction of one or multiple organs, requiring intensive care[39]. Moreover, recent studies have uncovered a link between NOX and organ dysfunction in AP, in addition to its role in inducing local inflammation in the pancreas.

Carrascal *et al*[40] showed that circulating exosomes involved in the progression of inflammation from the pancreas to distant organs leading to organ dysfunction in AP. Interestingly, these exosomes' impact is dependent on NOX. Specifically, NOX is activated by proteins carried by exosomes, resulting in the production of free radicals and the promotion of an inflammatory response. Furthermore, NOX inhibitor pretreatment blocked the expression of IL-1β and tumour necrosis factor alpha mRNAs induced by exosomes obtained from patients with severe AP.

NOX is widely distributed and is participated in various pathological processes of different organs. Yang *et al*[41] showed that NOX regulate the activity of downstream p-AKT and glycogen synthase kinase (GSK)-3β by regulating ROS levels, thereby affecting the release of inflammatory mediators and regulating AP-related kidney injury. Jin *et al*[42] found NOX2 and NOX4 were upregulated in lung tissue of severe AP and NOX-mediated ROS could activate NACHT, LRR, and PYD domains-containing protein 3 inflammasome and NF-κB signaling and facilitate AP-associated lung injury. Wen *et al*[43] showed that hyperactivity of NOX underlies myocardial injury in severe AP by promoting ROS generation with increased oxidative stress and cardiomyocyte apoptosis *via* activating the MAPK pathway. Moreover, NOX is involved in the process of intestinal barrier damage in sever AP, which was associated with an increase in the systemic concentration of cytokines, oxidative stress and activated NF-κB and p38 MAPK expression[44].

In summary, NOX promotes the development of AP by causing acinar cell damage and inducing macrophage polarization into M1 type (Figure 1). Moreover, NOX also be involved in distant organ dysfunction in AP. While the specific mechanism of NOX act on acinar cell and macrophages needs further study, which help us to further elucidate the pathogenesis of AP.

NOX IN CP

CP manifests from a long-term inflammation, which results in a significant replacement of the parenchyma by extracellular matrix (ECM)-rich connective tissue (*i.e.*, fibrosis) and permanent organ damage[45]. Notably, fibrosis is the hallmark histological feature of CP[46]. Fibrosis is a post-injury repair response in which tissue homeostasis is disrupted and fibrotic changes occur under the action of specific cytokines and a pro-oxidative environment, eventually leading to organ dysfunction[47]. The current clinical treatment of CP is limited to symptomatic treatment and management of complications. Thus, a better understanding of the mechanism underlying the pathogenesis of CP is necessary in order to develop more effective therapeutic options to attenuate the progression of the disease. Clarifying the mechanism of

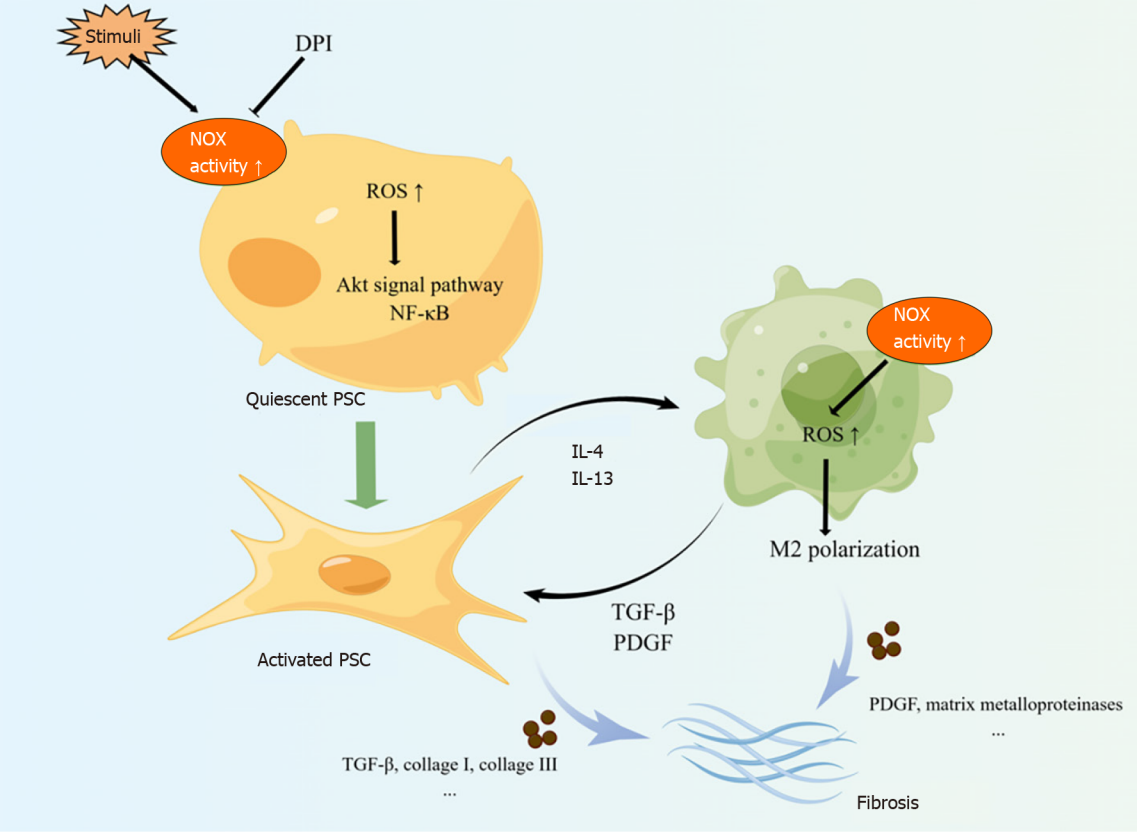

DOI: 10.3748/wjg.v30.i5.429

Figure 1 The scheme of the potential roles of nicotinamide adenine dinucleotide phosphate hydrogen oxides in pancreatic acinar cells and macrophages, which leading the development of acute pancreatitis. NOX: Nicotinamide adenine dinucleotide phosphate hydrogen oxides; AIF: Apoptosis inducing factor; ROS: Reactive oxygen species; NF-κB: Nuclear factor kappa-B; IL: Interleukin; TGF: Transforming growth factor; PDGF: Platelet-derived growth factor; PSC: Pancreatic stellate cell; DPI: Diphenylene iodium.

pancreatic fibrosis in CP and exploring therapeutic methods to delay or reverse pancreatic fibrosis are the basis to finding effective treatment for CP.

NOX induce pancreatic stellate cell activation

The activation of pancreatic stellate cells (PSCs) is the core to CP pathological processes. PSCs exist in two forms, the quiescent state and the activated state. Under physiological conditions, PSCs are in a quiescent state and secrete some growth-promoting cytokines to maintain the basic structure and function of the pancreas. When pancreas tissue damaged or in response to stimulation, PSCs are activated and transformed from their quiescent into myofibroblast-like phenotype, characterized by the disappearance of intracellular lipid droplets and the expression of α-smooth muscle actin (α-SMA) and ECM components such as type I collagen, type III collagen, and fibronectin[48]. PSCs express key components of NOX, p22phox, p47phox, NOX1, gp91phox/NOX2 and NOX4[49]; and NOX is recognized to be involved in PSCs activation.

Masamune *et al*[49] found that upregulating NOX activity in PSCs could induce PSCs activation and proliferation. Furthermore, diphenylene iodium (DPI) abolished ROS production in isolated PSCs and inhibited transformation of freshly isolated PSCs to a myofibroblast-like phenotype. NOX-mediated ROS in PSCs could accelerate fibrosis progression in CP. Xia *et al*[50] found Nox1-derived ROS in PSCs mediate the fibrotic process of CP by activating the downstream redox-sensitive signaling pathways AKT and NF-κB, up-regulating metalloproteases (MMP)-9 and Twist, and producing α-SMA and collagen I and III. However, limited research has been focused on exploring the mechanism of NOX promoting PSCs activation. More studies are needed in this topic.

NOX is involved in the M2 polarization of macrophage in CP

In the pancreatic tissue of CP, M2 macrophages are the dominant type of macrophages[51]. These M2 macrophages secret cytokines including TGF-β, platelet-derived growth factor, IL-10 and various matrix metalloproteinases, which play a role in the progression of fibrosis and chronic inflammation in CP[52]. Furthermore, M2 macrophages can activate PSCs, and the cross-talk between activated PSCs and M2 macrophages initiates and sustains the fibrotic process in CP[53]. NOX-mediated ROS can act as second messengers playing an extremely important role in the regulation of macrophage polarization[54-56]. Previous studies showed NOX was involved in M2 polarization of macrophages. Reduced NOX2 expression improves the wound healing functions of M2 macrophages in degrading disulphide protein[57]. Furthermore, the interaction between M2 macrophages with apoptotic bodies triggers instability of NOX2 mRNAs through binding

blockade of RNA-binding protein SYNCRIP to NOX2 3′ untranslated region. And this further defect the ROS production and leads to M2 macrophage polarization[58]. Mongue *et al*[59] found cardiomyocyte NOX4 modulated macrophage polarization toward M2 phenotype in myocardial injury mice model. Intervention of antioxidant butylated hydroxy anisole by inhibiting NOX-mediated O^{2-} production blocked monocyte differentiation to M2 type[60]. These results suggest that NOX may play a role in regulating M2 polarization of macrophages in the pancreas of CP. Further studies are needed to investigate this relationship.

In summary, NOX is involved in the progression of CP (Figure 2). NOX promotes the activation of PSC in the fibrotic process of CP. Moreover, the application of NOX inhibitors *in vitro* effectively inhibits the activation of PSC. Additionally, several studies have shown that NOX induces M2 polarization of macrophages in other organs. It has been established that M2 macrophages promote the occurrence and development of CP. Therefore, further research is needed to investigate whether NOX also plays a regulatory role in the M2 polarization of macrophages in CP.

NOX IN PC

The global burden of PC has increased dramatically over the past few decades and is expected to continue to represent a leading cause of cancer-related mortality[61]. Although efforts are being made to explore the pathological process of PC, its specific etiology remains unclear. Furthermore, PC shows resistance to chemotherapy, and there is currently no effective clinical treatment available[62]. Therefore, elucidating the underlying mechanisms of PC and identifying potential therapeutic targets have been topics of great interest.

KRAS promotes NOX activity

The oncogenic KRAS mutation is the major event in PC; it confers permanent activation of the KRAS protein, which acts as a molecular drive common phenotypes that expose specific vulnerabilities[63]. KRAS transformed PC cells have increased NOX activity and superoxide levels, as compared to parental cells[64,65]. Moreover, several reports have indicated that in human PC, expression of NOX family members is increased when compared to non-transformed pancreatic tissue[66-68]. KRAS gene mutations can lead cells to depart from common phenotypes and expose specific vulnerabilities. One example of such a phenotype is abnormal redox homeostasis, with excessive accumulation of ROS playing a crucial role in causing this aberrant redox homeostasis[69]. The ROS generated by KRAS, primarily relies on NOX production. ROS exerts oxidative stress on cells, which disrupts redox homeostasis and promotes tumor formation. This occurs due to an abnormal activation of signaling networks that initiate tumorigenesis[70]. NOX is a multi-subunit enzyme which is activated through the small GTPase Rac1[71,72]. Consequently, in PC cell lines, presence of oncogenic KRAS links to increased Rac1 activity and superoxide production; and KRAS-induced ROS production can be inhibited by downregulation of p47phox, the cytosolic regulatory subunit of NOX[73,74]. Therefore, there is a close correlation between NOX and the development of PC caused by the oncogenic KRAS gene mutation.

NOX regulates PC cells from apoptosis

One reason why PC is highly aggressive and unresponsive to treatments is its resistance to apoptosis. ROS induce apoptosis indirectly through damage to DNA, proteins and lipids, or more directly through the activation of pro-apoptotic signaling cascades such as SAPK/JNK, ERK1/2, and p38 upon the induction of the MAPK pathways[75]. However, at high concentrations, ROS, especially as H_2O_2, can inhibit caspases, resulting in irreversible damage to cell components and leading to necrosis[76]. Conversely, in certain cases, NOX-produced ROS can trigger an anti-apoptotic effect by activating NF-κB or Akt/ASK1 transduction pathways[77].

Study have found that growth factors can induce the production of ROS by mediating NOX in PC cells, thus protecting the cells from apoptosis[72]. The oncosuppressor p53 gene plays a crucial role in the process of apoptosis in cancer cells. Research has found that NOX1 inhibits tumor cell apoptosis by regulating p53 deacetylation, suppressing its transcriptional activity, and activating the SIRT1 pathway[78]. Mochizuki *et al*[77] noted that ROS, generated by NOX4, transmits signals for cell survival through the AKT-ASK1 pathway. Furthermore, Lee *et al*[66] demonstrated that NOX4-generated ROS promote PC cell survival by inhibiting JAK2 dephosphorylation. Study has discovered that the application of a NOX inhibitor, Tyrosine, effectively inhibits cell proliferation of human and hamster PC cells by inhibiting the G1 phase of the cell cycle with cyclin D1 downregulation and inactivation of AKT-GSK3β and ERK1/2 signaling pathways[79]. Therefore, NOX could regulate PC cells from death.

NOX facilitates epithelial to mesenchymal transition in PC

The epithelial to mesenchymal transition (EMT) is a crucial mechanism by which tumor cells acquire motility and invasiveness[80]. More and more evidence indicates that EMT plays a vital role in the pathogenesis, invasion, metastasis, and drug resistance of PC[81,82]. It is worth noting that recently, it has been discovered that many important EMT regulators are sensitive to redox reactions, thereby being able to elucidate the molecular basis of EMT from a redox perspective[83].

NOX4, a subunit of NOX, has been implicated in the EMT process in PC[84]. NOX4 mRNA correlation with EMT gene expression such as collagen (COL1A2, COL3A1, COL5A2), MMP2, MMP9 and fibronectin (FN1)[85]. Additionally, studies have discovered that NOX4-derived ROS transmit TGF-β-triggered EMT signals through PTP1B in PC[86]. Furthermore, Witte *et al*[87] proposed that TGF-β1-induced EMT in PC cells is mediated through RAC1/NOX4/ROS/p38 MAPK cascade. More recent research has demonstrated that NOX4 caused inactivation of lysine demethylase 5A, leading to increased methylation modification of histone H3 and regulation of transcription of EMT-associated gene SNAIL1.

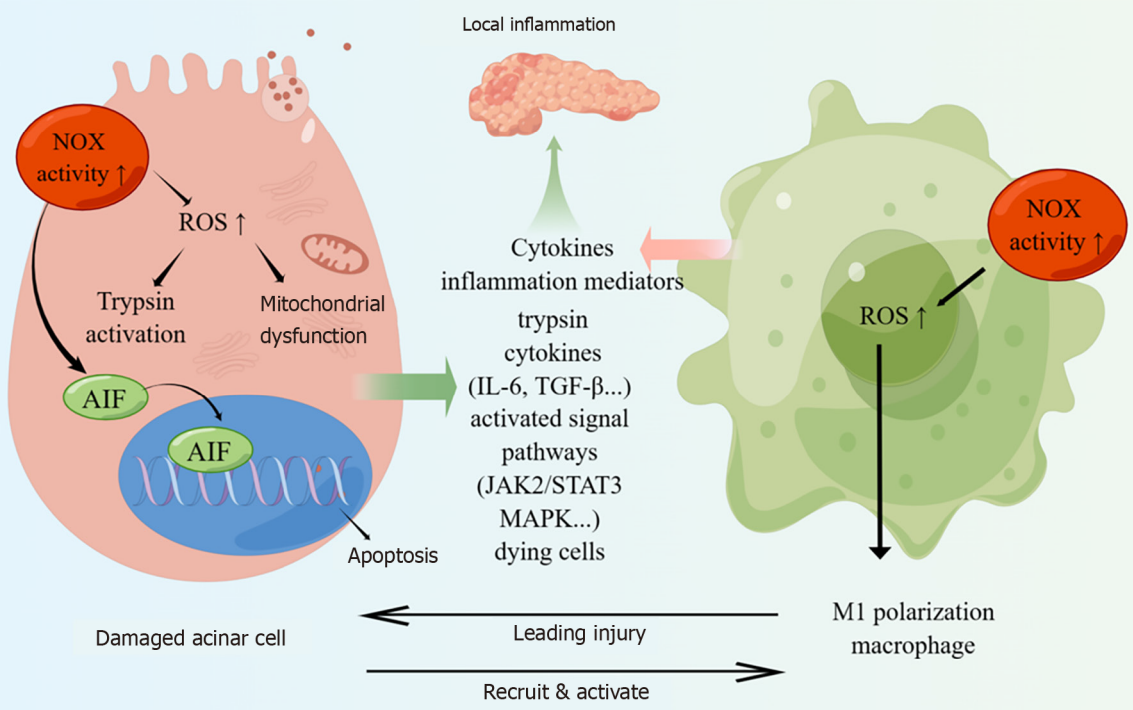

DOI: 10.3748/wjg.v30.i5.429

Figure 2 The scheme of the potential roles of nicotinamide adenine dinucleotide phosphate hydrogen oxides in pancreatic stellate cells and macrophages, which facilitating pancreatic fibrosis of chronic pancreatitis. NOX: Nicotinamide adenine dinucleotide phosphate hydrogen oxides; AIF: Apoptosis inducing factor; ROS: Reactive oxygen species; TGF: Transforming growth; IL: Interleukin; JAK: Janus kinase; STAT: Signal transducer and activator of transcription; MAPK: Mitogen-activated protein kinase.

Moreover, the deficiency of NOX4 has been shown to suppress hypoxia-induced EMT in PC cells[88].

NOX and genomic instability

Extensive reviews have investigated the impact of ROS on DNA damage. Cell exposure to chronic oxidative stress has been reported to elicit genomic instability. Moreover, there is evidence indicating elevated ROS levels in genomically unstable clones[89,90]. Although the precise function of NOX in cellular transformation remains unclear, several studies provide suggestive evidence for its role. NOX4 induces the production of ROS, which damages mitochondrial DNA and leads to mitochondrial dysfunction[91]. In addition to its known involvement in chromosomal instability, NOX1, NOX2, NOX4, and DUOX have been associated with the regulation of p53 transcription factor activity[92-94]. Moreover, p53 mutation can "transform" NOX4 from a protective and good prognostic indicator into a harmful one by promoting programs favorable to cancer progression, including EMT, cell migration, cell adhesion, and angiogenesis[85].

There are studies suggest a relationship between NOX and oncogene in PC. Ogrunc *et al*[95] demonstrated that NOX4 promotes the transformation of PC cells expressing oncogenes by generating mitogenic ROS. This transformation leads to a compromised DNA damage response and oncogene-induced cellular senescence bypass. Ju *et al*[96] identified that NOX4 as a critical factor that facilitates the interaction between KRAS activation and p16 inactivation, promoting the occurrence of PC.

In summary, NOX plays a crucial role in the progression of PC. NOX could regulate PC cells from death, promote the EMT process, and induce genomic instability (Figure 3). Furthermore, NOX is also involved in the key oncogenic process of abnormal redox homeostasis induced by the oncogene KRAS in PC. It is worth noting that that among the subunits of NOX, NOX4 has been extensively studied in relation to PC and has been found to promote PC through various mechanisms. Therefore, NOX4 may represent a potential therapeutic target for PC, but further research is needed to confirm this.

PERSPECTIVE

As we known, NOX is a membrane-bound multi-component enzyme complex. Different isoforms of NOX are distributed in different tissues, cells, and subcellular structures, exerting specific functions under physiological and pathological conditions. Although studies have demonstrated the significant role of NOX in pancreatitis and PC, the exact subunit of NOX responsible for these conditions remains unclear. NOX subunits express differently in acinar cells, PSCs and macrophages. Identifying the specific subunits participate in promoting pancreatic disorders progression help us better understand the pathogenesis of pancreatitis and PC. Further studies are needed to explore this topic.

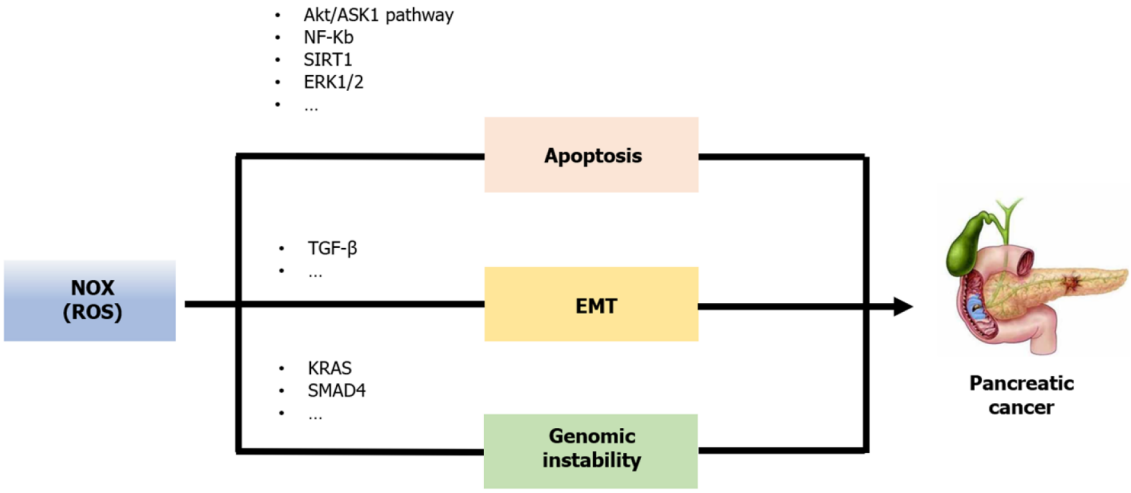

DOI: 10.3748/wjg.v30.i5.429

Figure 3 The scheme of the potential roles of nicotinamide adenine dinucleotide phosphate hydrogen oxides in pancreatic cancer. ASK: Apoptosis signal regulating kinase; TGF: Transforming growth; SIRT: Silent information regulator; NF-κB: Nuclear factor kappa-B; ERK: Extracellular regulated protein kinases; SMAD: Drosophila mothers against decapentaplegic protein; NOX: Nicotinamide adenine dinucleotide phosphate hydrogen oxides; AIF: Apoptosis inducing factor; ROS: Reactive oxygen species; EMT: Epithelial to mesenchymal transition.

Although numerous studies were conducted on the investigation of pancreatitis and PC, no effective methods of prevention and treatment have been developed. Since NOX play an important role in both pancreatitis and PC, it may be considered as a therapeutic target. Study showed inhibition of NOX by DPI suppresses apoptosis of pancreatic acinar cells by reducing the expression of apoptosis-associated genes and caspase-3 activity[97]. NOX2 inhibitor, GSK2795039, caused about 50% reduction in the level of serum amylase activity in AP mice[98]. Apocynin is a specific inhibitor of NOX. Recent studies proved that apocynin could prevent AP and AP-associated organs injury[41-44]. NOX1 knockout alleviate pancreatic fibrosis in CP mice[50]. In terms of PC, drug resistance is the main reason why chemotherapy drugs cannot achieve ideal treatment effects. It is worth noting that NOX is associated with chemotherapy resistance[99-101]. Recent breakthroughs in cancer treatment consisting of new combinations of existing medications. It reminds us that chemotherapy with NOX inhibitor may achieve better therapeutic effects in PC. More studies are needed to verify the therapeutic effect of NOX in pancreatic diseases.

Though they are distinct diseases of pancreas that pancreatitis is benign and PC is malignant, numerous studies indicate that pancreatitis is linked to PC[102,103]. The exact nature of this association is not fully elaborated. Aberrant redox homeostasis is the common features in the pathogenesis of pancreatitis and PC, which could be mediated by NOX. Therefore, further study may focus on the role of NOX in the transformation of pancreatitis and PC which help us clarify the complex relationship between them.

CONCLUSION

In conclusion, NOX plays a role in the occurrence and development of pancreatitis by regulating various types of pancreatic cells, such as acinar cells, PSCs, and macrophages. Additionally, it promotes PC progression by participating in abnormal cell apoptosis, triggering the EMT processes, and causing cell genomic instability. Understanding the role of NOX in pancreatic diseases is crucial for a gaining a deeper understanding of the underlying mechanisms of pancreatitis and PC. Further research is needed to uncover the specific functions of different subtypes within the NOX family in these diseases. Moreover, the development of NOX-specific inhibitors is necessary to validate the feasibility of targeting NOX as a treatment approach for pancreatic diseases.

FOOTNOTES

Co-first authors: Ya-Wei Bi and Long-Song Li.

Author contributions: Bi YW, Li LS, and Ru N retrieved concerned literatures and made the manuscript; Bi YW and Zhang B designed the figures; Lei X participated in the revision of manuscript; and all authors read and approved the final manuscript.

Supported by Youth Independent Innovation Science Fund Project from Chinese PLA General Hospital, No. 22QNFC075.

Conflict-of-interest statement: All the authors report no relevant conflicts of interest for this article.

Country/Territory of origin: China

ORCID number: Ya-Wei Bi 0000-0003-3762-5920; Long-Song Li 0000-0002-4000-7501; Nan Ru 0009-0008-6212-6385; Bo Zhang 0000-0002-4333-0750; Xiao Lei 0000-0002-0428-1749.

S-Editor: Wang JJ
L-Editor: A
P-Editor: Yu HG

REFERENCES

1 **Iannuzzi JP**, King JA, Leong JH, Quan J, Windsor JW, Tanyingoh D, Coward S, Forbes N, Heitman SJ, Shaheen AA, Swain M, Buie M, Underwood FE, Kaplan GG. Global Incidence of Acute Pancreatitis Is Increasing Over Time: A Systematic Review and Meta-Analysis. *Gastroenterology* 2022; **162**: 122-134 [PMID: 34571026 DOI: 10.1053/j.gastro.2021.09.043]

2 **Beyer G**, Habtezion A, Werner J, Lerch MM, Mayerle J. Chronic pancreatitis. *Lancet* 2020; **396**: 499-512 [PMID: 32798493 DOI: 10.1016/S0140-6736(20)31318-0]

3 **Klein AP**. Pancreatic cancer epidemiology: understanding the role of lifestyle and inherited risk factors. *Nat Rev Gastroenterol Hepatol* 2021; **18**: 493-502 [PMID: 34002083 DOI: 10.1038/s41575-021-00457-x]

4 **Peery AF**, Crockett SD, Murphy CC, Jensen ET, Kim HP, Egberg MD, Lund JL, Moon AM, Pate V, Barnes EL, Schlusser CL, Baron TH, Shaheen NJ, Sandler RS. Burden and Cost of Gastrointestinal, Liver, and Pancreatic Diseases in the United States: Update 2021. *Gastroenterology* 2022; **162**: 621-644 [PMID: 34678215 DOI: 10.1053/j.gastro.2021.10.017]

5 **Le Cosquer G**, Maulat C, Bournet B, Cordelier P, Buscail E, Buscail L. Pancreatic Cancer in Chronic Pancreatitis: Pathogenesis and Diagnostic Approach. *Cancers (Basel)* 2023; **15** [PMID: 36765725 DOI: 10.3390/cancers15030761]

6 **Chen X**, Zeh HJ, Kang R, Kroemer G, Tang D. Cell death in pancreatic cancer: from pathogenesis to therapy. *Nat Rev Gastroenterol Hepatol* 2021; **18**: 804-823 [PMID: 34331036 DOI: 10.1038/s41575-021-00486-6]

7 **Badgley MA**, Kremer DM, Maurer HC, DelGiorno KE, Lee HJ, Purohit V, Sagalovskiy IR, Ma A, Kapilian J, Firl CEM, Decker AR, Sastra SA, Palermo CF, Andrade LR, Sajjakulnukit P, Zhang L, Tolstyka ZP, Hirschhorn T, Lamb C, Liu T, Gu W, Seeley ES, Stone E, Georgiou G, Manor U, Iuga A, Wahl GM, Stockwell BR, Lyssiotis CA, Olive KP. Cysteine depletion induces pancreatic tumor ferroptosis in mice. *Science* 2020; **368**: 85-89 [PMID: 32241947 DOI: 10.1126/science.aaw9872]

8 **de Jesus DS**, Bargi-Souza P, Cruzat V, Yechoor V, Carpinelli AR, Peliciari-Garcia RA. BMAL1 modulates ROS generation and insulin secretion in pancreatic β-cells: An effect possibly mediated *via* NOX2. *Mol Cell Endocrinol* 2022; **555**: 111725 [PMID: 35868425 DOI: 10.1016/j.mce.2022.111725]

9 **Morgan MJ**, Liu ZG. Crosstalk of reactive oxygen species and NF-κB signaling. *Cell Res* 2011; **21**: 103-115 [PMID: 21187859 DOI: 10.1038/cr.2010.178]

10 **Cao WL**, Xiang XH, Chen K, Xu W, Xia SH. Potential role of NADPH oxidase in pathogenesis of pancreatitis. *World J Gastrointest Pathophysiol* 2014; **5**: 169-177 [PMID: 25133019 DOI: 10.4291/wjgp.v5.i3.169]

11 **Mederos MA**, Reber HA, Girgis MD. Acute Pancreatitis: A Review. *JAMA* 2021; **325**: 382-390 [PMID: 33496779 DOI: 10.1001/jama.2020.20317]

12 **Boxhoorn L**, Voermans RP, Bouwense SA, Bruno MJ, Verdonk RC, Boermeester MA, van Santvoort HC, Besselink MG. Acute pancreatitis. *Lancet* 2020; **396**: 726-734 [PMID: 32891214 DOI: 10.1016/S0140-6736(20)31310-6]

13 **Liu L**, Zhang Y, Li X, Deng J. Microenvironment of pancreatic inflammation: calling for nanotechnology for diagnosis and treatment. *J Nanobiotechnology* 2023; **21**: 443 [PMID: 37996911 DOI: 10.1186/s12951-023-02200-x]

14 **Stojanovic B**, Jovanovic IP, Stojanovic MD, Jovanovic M, Vekic B, Milosevic B, Cvetkovic A, Spasic M, Stojanovic BS. The Emerging Roles of the Adaptive Immune Response in Acute Pancreatitis. *Cells* 2023; **12** [PMID: 37296616 DOI: 10.3390/cells12111495]

15 **Baron TH**, DiMaio CJ, Wang AY, Morgan KA. American Gastroenterological Association Clinical Practice Update: Management of Pancreatic Necrosis. *Gastroenterology* 2020; **158**: 67-75.e1 [PMID: 31479658 DOI: 10.1053/j.gastro.2019.07.064]

16 **Choi J**, Oh TG, Jung HW, Park KY, Shin H, Jo T, Kang DS, Chanda D, Hong S, Kim J, Hwang H, Ji M, Jung M, Shoji T, Matsushima A, Kim P, Mun JY, Paik MJ, Cho SJ, Lee IK, Whitcomb DC, Greer P, Blobner B, Goodarzi MO, Pandol SJ, Rotter JI; North American Pancreatitis Study 2 (NAPS2) Consortium, Fan W, Bapat SP, Zheng Y, Liddle C, Yu RT, Atkins AR, Downes M, Yoshihara E, Evans RM, Suh JM. Estrogen-Related Receptor γ Maintains Pancreatic Acinar Cell Function and Identity by Regulating Cellular Metabolism. *Gastroenterology* 2022; **163**: 239-256 [PMID: 35461826 DOI: 10.1053/j.gastro.2022.04.013]

17 **Dios ID**. Inflammatory role of the acinar cells during acute pancreatitis. *World J Gastrointest Pharmacol Ther* 2010; **1**: 15-20 [PMID: 21577290 DOI: 10.4292/wjgpt.v1.i1.15]

18 **Yu JH**, Lim JW, Kim H, Kim KH. NADPH oxidase mediates interleukin-6 expression in cerulein-stimulated pancreatic acinar cells. *Int J Biochem Cell Biol* 2005; **37**: 1458-1469 [PMID: 15833277 DOI: 10.1016/j.biocel.2005.02.004]

19 **Gukovsky I**, Pandol SJ, Gukovskaya AS. Organellar dysfunction in the pathogenesis of pancreatitis. *Antioxid Redox Signal* 2011; **15**: 2699-2710 [PMID: 21834686 DOI: 10.1089/ars.2011.4068]

20 **Lee J**, Lim JW, Kim H. Lycopene Inhibits Oxidative Stress-Mediated Inflammatory Responses in Ethanol/Palmitoleic Acid-Stimulated Pancreatic Acinar AR42J Cells. *Int J Mol Sci* 2021; **22** [PMID: 33672594 DOI: 10.3390/ijms22042101]

21 **Ku L**, Lee J, Lim JW, Jin L, Seo JT, Kim H. Docosahexaenoic acid inhibits ethanol/palmitoleic acid-induced necroptosis in AR42J cells. *J Physiol Pharmacol* 2020; **71** [PMID: 33077696 DOI: 10.26402/jpp.2020.3.15]

22 **Ju KD**, Lim JW, Kim KH, Kim H. Potential role of NADPH oxidase-mediated activation of Jak2/Stat3 and mitogen-activated protein kinases

and expression of TGF-β1 in the pathophysiology of acute pancreatitis. *Inflamm Res* 2011; **60**: 791-800 [PMID: 21509626 DOI: 10.1007/s00011-011-0335-4]

23 **Yu JH**, Lim JW, Kim KH, Morio T, Kim H. NADPH oxidase and apoptosis in cerulein-stimulated pancreatic acinar AR42J cells. *Free Radic Biol Med* 2005; **39**: 590-602 [PMID: 16085178 DOI: 10.1016/j.freeradbiomed.2005.04.019]

24 **Wang X**, Yang C, Chai J, Shi Y, Xue D. Mechanisms of AIF-mediated apoptotic DNA degradation in Caenorhabditis elegans. *Science* 2002; **298**: 1587-1592 [PMID: 12446902 DOI: 10.1126/science.1076194]

25 **Cregan SP**, Dawson VL, Slack RS. Role of AIF in caspase-dependent and caspase-independent cell death. *Oncogene* 2004; **23**: 2785-2796 [PMID: 15077142 DOI: 10.1038/sj.onc.1207517]

26 **Yu JH**, Kim KH, Kim H. Role of NADPH oxidase and calcium in cerulein-induced apoptosis: involvement of apoptosis-inducing factor. *Ann N Y Acad Sci* 2006; **1090**: 292-297 [PMID: 17384272 DOI: 10.1196/annals.1378.031]

27 **Wu J**, Zhang R, Hu G, Zhu HH, Gao WQ, Xue J. Carbon Monoxide Impairs CD11b(+)Ly-6C(hi) Monocyte Migration from the Blood to Inflamed Pancreas *via* Inhibition of the CCL2/CCR2 Axis. *J Immunol* 2018; **200**: 2104-2114 [PMID: 29440506 DOI: 10.4049/jimmunol.1701169]

28 **Sendler M**, Weiss FU, Golchert J, Homuth G, van den Brandt C, Mahajan UM, Partecke LI, Döring P, Gukovsky I, Gukovskaya AS, Wagh PR, Lerch MM, Mayerle J. Cathepsin B-Mediated Activation of Trypsinogen in Endocytosing Macrophages Increases Severity of Pancreatitis in Mice. *Gastroenterology* 2018; **154**: 704-718.e10 [PMID: 29079517 DOI: 10.1053/j.gastro.2017.10.018]

29 **Xue J**, Habtezion A. Carbon monoxide-based therapy ameliorates acute pancreatitis *via* TLR4 inhibition. *J Clin Invest* 2014; **124**: 437-447 [PMID: 24334457 DOI: 10.1172/JCI71362]

30 **Hu F**, Lou N, Jiao J, Guo F, Xiang H, Shang D. Macrophages in pancreatitis: Mechanisms and therapeutic potential. *Biomed Pharmacother* 2020; **131**: 110693 [PMID: 32882586 DOI: 10.1016/j.biopha.2020.110693]

31 **Locati M**, Curtale G, Mantovani A. Diversity, Mechanisms, and Significance of Macrophage Plasticity. *Annu Rev Pathol* 2020; **15**: 123-147 [PMID: 31530089 DOI: 10.1146/annurev-pathmechdis-012418-012718]

32 **Wu J**, Zhang L, Shi J, He R, Yang W, Habtezion A, Niu N, Lu P, Xue J. Macrophage phenotypic switch orchestrates the inflammation and repair/regeneration following acute pancreatitis injury. *EBioMedicine* 2020; **58**: 102920 [PMID: 32739869 DOI: 10.1016/j.ebiom.2020.102920]

33 **Tan HY**, Wang N, Li S, Hong M, Wang X, Feng Y. The Reactive Oxygen Species in Macrophage Polarization: Reflecting Its Dual Role in Progression and Treatment of Human Diseases. *Oxid Med Cell Longev* 2016; **2016**: 2795090 [PMID: 27143992 DOI: 10.1155/2016/2795090]

34 **Zheng W**, Umitsu M, Jagan I, Tran CW, Ishiyama N, BeGora M, Araki K, Ohashi PS, Ikura M, Muthuswamy SK. An interaction between Scribble and the NADPH oxidase complex controls M1 macrophage polarization and function. *Nat Cell Biol* 2016; **18**: 1244-1252 [PMID: 27694890 DOI: 10.1038/ncb3413]

35 **Bermudez S**, Khayrullina G, Zhao Y, Byrnes KR. NADPH oxidase isoform expression is temporally regulated and may contribute to microglial/macrophage polarization after spinal cord injury. *Mol Cell Neurosci* 2016; **77**: 53-64 [PMID: 27729244 DOI: 10.1016/j.mcn.2016.10.001]

36 **Griess B**, Mir S, Datta K, Teoh-Fitzgerald M. Scavenging reactive oxygen species selectively inhibits M2 macrophage polarization and their pro-tumorigenic function in part, *via* Stat3 suppression. *Free Radic Biol Med* 2020; **147**: 48-60 [PMID: 31863907 DOI: 10.1016/j.freeradbiomed.2019.12.018]

37 **Wang J**, Ma MW, Dhandapani KM, Brann DW. Regulatory role of NADPH oxidase 2 in the polarization dynamics and neurotoxicity of microglia/macrophages after traumatic brain injury. *Free Radic Biol Med* 2017; **113**: 119-131 [PMID: 28942245 DOI: 10.1016/j.freeradbiomed.2017.09.017]

38 **Han X**, Ni J, Wu Z, Wu J, Li B, Ye X, Dai J, Chen C, Xue J, Wan R, Wen L, Wang X, Hu G. Myeloid-specific dopamine D(2) receptor signalling controls inflammation in acute pancreatitis *via* inhibiting M1 macrophage. *Br J Pharmacol* 2020; **177**: 2991-3008 [PMID: 32060901 DOI: 10.1111/bph.15026]

39 **Dellinger EP**, Forsmark CE, Layer P, Lévy P, Maraví-Poma E, Petrov MS, Shimosegawa T, Siriwardena AK, Uomo G, Whitcomb DC, Windsor JA; Pancreatitis Across Nations Clinical Research and Education Alliance (PANCREA). Determinant-based classification of acute pancreatitis severity: an international multidisciplinary consultation. *Ann Surg* 2012; **256**: 875-880 [PMID: 22735715 DOI: 10.1097/SLA.0b013e318256f778]

40 **Carrascal M**, Areny-Balagueró A, de-Madaria E, Cárdenas-Jaén K, García-Rayado G, Rivera R, Martin Mateos RM, Pascual-Moreno I, Gironella M, Abian J, Closa D. Inflammatory capacity of exosomes released in the early stages of acute pancreatitis predicts the severity of the disease. *J Pathol* 2022; **256**: 83-92 [PMID: 34599510 DOI: 10.1002/path.5811]

41 **Yang X**, Zhao K, Deng W, Zhao L, Jin H, Mei F, Zhou Y, Li M, Wang W. Apocynin Attenuates Acute Kidney Injury and Inflammation in Rats with Acute Hypertriglyceridemic Pancreatitis. *Dig Dis Sci* 2020; **65**: 1735-1747 [PMID: 31617131 DOI: 10.1007/s10620-019-05892-0]

42 **Jin HZ**, Yang XJ, Zhao KL, Mei FC, Zhou Y, You YD, Wang WX. Apocynin alleviates lung injury by suppressing NLRP3 inflammasome activation and NF-κB signaling in acute pancreatitis. *Int Immunopharmacol* 2019; **75**: 105821 [PMID: 31437787 DOI: 10.1016/j.intimp.2019.105821]

43 **Wen Y**, Liu R, Lin N, Luo H, Tang J, Huang Q, Sun H, Tang L. NADPH Oxidase Hyperactivity Contributes to Cardiac Dysfunction and Apoptosis in Rats with Severe Experimental Pancreatitis through ROS-Mediated MAPK Signaling Pathway. *Oxid Med Cell Longev* 2019; **2019**: 4578175 [PMID: 31210840 DOI: 10.1155/2019/4578175]

44 **Deng W**, Abliz A, Xu S, Sun R, Guo W, Shi Q, Yu J, Wang W. Severity of pancreatitisassociated intestinal mucosal barrier injury is reduced following treatment with the NADPH oxidase inhibitor apocynin. *Mol Med Rep* 2016; **14**: 3525-3534 [PMID: 27573037 DOI: 10.3892/mmr.2016.5678]

45 **Peery AF**, Crockett SD, Murphy CC, Lund JL, Dellon ES, Williams JL, Jensen ET, Shaheen NJ, Barritt AS, Lieber SR, Kochar B, Barnes EL, Fan YC, Pate V, Galanko J, Baron TH, Sandler RS. Burden and Cost of Gastrointestinal, Liver, and Pancreatic Diseases in the United States: Update 2018. *Gastroenterology* 2019; **156**: 254-272.e11 [PMID: 30315778 DOI: 10.1053/j.gastro.2018.08.063]

46 **Chang M**, Chen W, Xia R, Peng Y, Niu P, Fan H. Pancreatic Stellate Cells and the Targeted Therapeutic Strategies in Chronic Pancreatitis. *Molecules* 2023; **28** [PMID: 37513458 DOI: 10.3390/molecules28145586]

47 **Kleeff J**, Whitcomb DC, Shimosegawa T, Esposito I, Lerch MM, Gress T, Mayerle J, Drewes AM, Rebours V, Akisik F, Muñoz JED, Neoptolemos JP. Chronic pancreatitis. *Nat Rev Dis Primers* 2017; **3**: 17060 [PMID: 28880010 DOI: 10.1038/nrdp.2017.60]

48 **Bynigeri RR**, Jakkampudi A, Jangala R, Subramanyam C, Sasikala M, Rao GV, Reddy DN, Talukdar R. Pancreatic stellate cell: Pandora's box for pancreatic disease biology. *World J Gastroenterol* 2017; **23**: 382-405 [PMID: 28210075 DOI: 10.3748/wjg.v23.i3.382]

49 **Masamune A**, Watanabe T, Kikuta K, Satoh K, Shimosegawa T. NADPH oxidase plays a crucial role in the activation of pancreatic stellate cells. *Am J Physiol Gastrointest Liver Physiol* 2008; **294**: G99-G108 [PMID: 17962358 DOI: 10.1152/ajpgi.00272.2007]

50 **Xia D**, Halder B, Godoy C, Chakraborty A, Singla B, Thomas E, Shuja JB, Kashif H, Miller L, Csanyi G, Sabbatini ME. NADPH oxidase 1 mediates caerulein-induced pancreatic fibrosis in chronic pancreatitis. *Free Radic Biol Med* 2020; **147**: 139-149 [PMID: 31837426 DOI: 10.1016/j.freeradbiomed.2019.11.034]

51 **Zeng XP**, Wang LJ, Guo HL, He L, Bi YW, Xu ZL, Li ZS, Hu LH. Dasatinib ameliorates chronic pancreatitis induced by caerulein *via* anti-fibrotic and anti-inflammatory mechanism. *Pharmacol Res* 2019; **147**: 104357 [PMID: 31356863 DOI: 10.1016/j.phrs.2019.104357]

52 **Lin Y**, Chen Y, Feng W, Hua R, Zhang J, Huo Y, Jiang H, Yin B, Yang X. Neddylation pathway alleviates chronic pancreatitis by reducing HIF1α-CCL5-dependent macrophage infiltration. *Cell Death Dis* 2021; **12**: 273 [PMID: 33723230 DOI: 10.1038/s41419-021-03549-3]

53 **Xue J**, Sharma V, Hsieh MH, Chawla A, Murali R, Pandol SJ, Habtezion A. Alternatively activated macrophages promote pancreatic fibrosis in chronic pancreatitis. *Nat Commun* 2015; **6**: 7158 [PMID: 25981357 DOI: 10.1038/ncomms8158]

54 **Zhou J**, Liu W, Zhao X, Xian Y, Wu W, Zhang X, Zhao N, Xu FJ, Wang C. Natural Melanin/Alginate Hydrogels Achieve Cardiac Repair through ROS Scavenging and Macrophage Polarization. *Adv Sci (Weinh)* 2021; **8**: e2100505 [PMID: 34414693 DOI: 10.1002/advs.202100505]

55 **Chen Y**, Wu G, Li M, Hesse M, Ma Y, Chen W, Huang H, Liu Y, Xu W, Tang Y, Zheng H, Li C, Lin Z, Chen G, Liao W, Liao Y, Bin J, Chen Y. LDHA-mediated metabolic reprogramming promoted cardiomyocyte proliferation by alleviating ROS and inducing M2 macrophage polarization. *Redox Biol* 2022; **56**: 102446 [PMID: 36057161 DOI: 10.1016/j.redox.2022.102446]

56 **Lu Y**, Rong J, Lai Y, Tao L, Yuan X, Shu X. The Degree of Helicobacter pylori Infection Affects the State of Macrophage Polarization through Crosstalk between ROS and HIF-1α. *Oxid Med Cell Longev* 2020; **2020**: 5281795 [PMID: 33376580 DOI: 10.1155/2020/5281795]

57 **Balce DR**, Li B, Allan ER, Rybicka JM, Krohn RM, Yates RM. Alternative activation of macrophages by IL-4 enhances the proteolytic capacity of their phagosomes through synergistic mechanisms. *Blood* 2011; **118**: 4199-4208 [PMID: 21846901 DOI: 10.1182/blood-2011-01-328906]

58 **Kuchler L**, Giegerich AK, Sha LK, Knape T, Wong MS, Schröder K, Brandes RP, Heide H, Wittig I, Brüne B, von Knethen A. SYNCRIP-dependent Nox2 mRNA destabilization impairs ROS formation in M2-polarized macrophages. *Antioxid Redox Signal* 2014; **21**: 2483-2497 [PMID: 24844655 DOI: 10.1089/ars.2013.5760]

59 **Mongue-Din H**, Patel AS, Looi YH, Grieve DJ, Anilkumar N, Sirker A, Dong X, Brewer AC, Zhang M, Smith A, Shah AM. NADPH Oxidase-4 Driven Cardiac Macrophage Polarization Protects Against Myocardial Infarction-Induced Remodeling. *JACC Basic Transl Sci* 2017; **2**: 688-698 [PMID: 29445778 DOI: 10.1016/j.jacbts.2017.06.006]

60 **Zhang Y**, Choksi S, Chen K, Pobezinskaya Y, Linnoila I, Liu ZG. ROS play a critical role in the differentiation of alternatively activated macrophages and the occurrence of tumor-associated macrophages. *Cell Res* 2013; **23**: 898-914 [PMID: 23752925 DOI: 10.1038/cr.2013.75]

61 **GBD 2017 Pancreatic Cancer Collaborators**. The global, regional, and national burden of pancreatic cancer and its attributable risk factors in 195 countries and territories, 1990-2017: a systematic analysis for the Global Burden of Disease Study 2017. *Lancet Gastroenterol Hepatol* 2019; **4**: 934-947 [PMID: 31648972 DOI: 10.1016/S2468-1253(19)30347-4]

62 **Cao D**, Song Q, Li J, Jiang Y, Wang Z, Lu S. Opportunities and challenges in targeted therapy and immunotherapy for pancreatic cancer. *Expert Rev Mol Med* 2021; **23**: e21 [PMID: 34906271 DOI: 10.1017/erm.2021.26]

63 **Buscail L**, Bournet B, Cordelier P. Role of oncogenic KRAS in the diagnosis, prognosis and treatment of pancreatic cancer. *Nat Rev Gastroenterol Hepatol* 2020; **17**: 153-168 [PMID: 32005945 DOI: 10.1038/s41575-019-0245-4]

64 **Du J**, Nelson ES, Simons AL, Olney KE, Moser JC, Schrock HE, Wagner BA, Buettner GR, Smith BJ, Teoh ML, Tsao MS, Cullen JJ. Regulation of pancreatic cancer growth by superoxide. *Mol Carcinog* 2013; **52**: 555-567 [PMID: 22392697 DOI: 10.1002/mc.21891]

65 **Wang P**, Sun YC, Lu WH, Huang P, Hu Y. Selective killing of K-ras-transformed pancreatic cancer cells by targeting NAD(P)H oxidase. *Chin J Cancer* 2015; **34**: 166-176 [PMID: 25963558 DOI: 10.1186/s40880-015-0012-z]

66 **Lee JK**, Edderkaoui M, Truong P, Ohno I, Jang KT, Berti A, Pandol SJ, Gukovskaya AS. NADPH oxidase promotes pancreatic cancer cell survival *via* inhibiting JAK2 dephosphorylation by tyrosine phosphatases. *Gastroenterology* 2007; **133**: 1637-1648 [PMID: 17983808 DOI: 10.1053/j.gastro.2007.08.022]

67 **Lu W**, Hu Y, Chen G, Chen Z, Zhang H, Wang F, Feng L, Pelicano H, Wang H, Keating MJ, Liu J, McKeehan W, Luo Y, Huang P. Novel role of NOX in supporting aerobic glycolysis in cancer cells with mitochondrial dysfunction and as a potential target for cancer therapy. *PLoS Biol* 2012; **10**: e1001326 [PMID: 22589701 DOI: 10.1371/journal.pbio.1001326]

68 **Wu Y**, Lu J, Antony S, Juhasz A, Liu H, Jiang G, Meitzler JL, Hollingshead M, Haines DC, Butcher D, Roy K, Doroshow JH. Activation of TLR4 is required for the synergistic induction of dual oxidase 2 and dual oxidase A2 by IFN-γ and lipopolysaccharide in human pancreatic cancer cell lines. *J Immunol* 2013; **190**: 1859-1872 [PMID: 23296709 DOI: 10.4049/jimmunol.1201725]

69 **Hayes JD**, Dinkova-Kostova AT, Tew KD. Oxidative Stress in Cancer. *Cancer Cell* 2020; **38**: 167-197 [PMID: 32649885 DOI: 10.1016/j.ccell.2020.06.001]

70 **Moloney JN**, Cotter TG. ROS signalling in the biology of cancer. *Semin Cell Dev Biol* 2018; **80**: 50-64 [PMID: 28587975 DOI: 10.1016/j.semcdb.2017.05.023]

71 **Pick E**. Role of the Rho GTPase Rac in the activation of the phagocyte NADPH oxidase: outsourcing a key task. *Small GTPases* 2014; **5**: e27952 [PMID: 24598074 DOI: 10.4161/sgtp.27952]

72 **Vaquero EC**, Edderkaoui M, Pandol SJ, Gukovsky I, Gukovskaya AS. Reactive oxygen species produced by NAD(P)H oxidase inhibit apoptosis in pancreatic cancer cells. *J Biol Chem* 2004; **279**: 34643-34654 [PMID: 15155719 DOI: 10.1074/jbc.M400078200]

73 **Du J**, Liu J, Smith BJ, Tsao MS, Cullen JJ. Role of Rac1-dependent NADPH oxidase in the growth of pancreatic cancer. *Cancer Gene Ther* 2011; **18**: 135-143 [PMID: 21037555 DOI: 10.1038/cgt.2010.64]

74 **Park MT**, Kim MJ, Suh Y, Kim RK, Kim H, Lim EJ, Yoo KC, Lee GH, Kim YH, Hwang SG, Yi JM, Lee SJ. Novel signaling axis for ROS generation during K-Ras-induced cellular transformation. *Cell Death Differ* 2014; **21**: 1185-1197 [PMID: 24632950 DOI: 10.1038/cdd.2014.34]

75 **Irani K**. Oxidant signaling in vascular cell growth, death, and survival : a review of the roles of reactive oxygen species in smooth muscle and endothelial cell mitogenic and apoptotic signaling. *Circ Res* 2000; **87**: 179-183 [PMID: 10926866 DOI: 10.1161/01.res.87.3.179]

76 **Blaser H**, Dostert C, Mak TW, Brenner D. TNF and ROS Crosstalk in Inflammation. *Trends Cell Biol* 2016; **26**: 249-261 [PMID: 26791157 DOI: 10.1016/j.tcb.2015.12.002]

77 **Mochizuki T**, Furuta S, Mitsushita J, Shang WH, Ito M, Yokoo Y, Yamaura M, Ishizone S, Nakayama J, Konagai A, Hirose K, Kiyosawa K, Kamata T. Inhibition of NADPH oxidase 4 activates apoptosis *via* the AKT/apoptosis signal-regulating kinase 1 pathway in pancreatic cancer PANC-1 cells. *Oncogene* 2006; **25**: 3699-3707 [PMID: 16532036 DOI: 10.1038/sj.onc.1209406]

78 **Puca R**, Nardinocchi L, Starace G, Rechavi G, Sacchi A, Givol D, D'Orazi G. Nox1 is involved in p53 deacetylation and suppression of its transcriptional activity and apoptosis. *Free Radic Biol Med* 2010; **48**: 1338-1346 [PMID: 20171273 DOI: 10.1016/j.freeradbiomed.2010.02.015]

79 **Kato A**, Naiki-Ito A, Nakazawa T, Hayashi K, Naitoh I, Miyabe K, Shimizu S, Kondo H, Nishi Y, Yoshida M, Umemura S, Hori Y, Mori T, Tsutsumi M, Kuno T, Suzuki S, Kato H, Ohara H, Joh T, Takahashi S. Chemopreventive effect of resveratrol and apocynin on pancreatic carcinogenesis *via* modulation of nuclear phosphorylated GSK3β and ERK1/2. *Oncotarget* 2015; **6**: 42963-42975 [PMID: 26556864 DOI: 10.18632/oncotarget.5981]

80 **Dongre A**, Weinberg RA. New insights into the mechanisms of epithelial-mesenchymal transition and implications for cancer. *Nat Rev Mol Cell Biol* 2019; **20**: 69-84 [PMID: 30459476 DOI: 10.1038/s41580-018-0080-4]

81 **Alvarez MA**, Freitas JP, Mazher Hussain S, Glazer ES. TGF-β Inhibitors in Metastatic Pancreatic Ductal Adenocarcinoma. *J Gastrointest Cancer* 2019; **50**: 207-213 [PMID: 30891677 DOI: 10.1007/s12029-018-00195-5]

82 **Rhim AD**, Mirek ET, Aiello NM, Maitra A, Bailey JM, McAllister F, Reichert M, Beatty GL, Rustgi AK, Vonderheide RH, Leach SD, Stanger BZ. EMT and dissemination precede pancreatic tumor formation. *Cell* 2012; **148**: 349-361 [PMID: 22265420 DOI: 10.1016/j.cell.2011.11.025]

83 **Jiang J**, Wang K, Chen Y, Chen H, Nice EC, Huang C. Redox regulation in tumor cell epithelial-mesenchymal transition: molecular basis and therapeutic strategy. *Signal Transduct Target Ther* 2017; **2**: 17036 [PMID: 29263924 DOI: 10.1038/sigtrans.2017.36]

84 **Bi Y**, Lei X, Chai N, Linghu E. NOX4: a potential therapeutic target for pancreatic cancer and its mechanism. *J Transl Med* 2021; **19**: 515 [PMID: 34930338 DOI: 10.1186/s12967-021-03182-w]

85 **Ma WF**, Boudreau HE, Leto TL. Pan-Cancer Analysis Shows TP53 Mutations Modulate the Association of NOX4 with Genetic Programs of Cancer Progression and Clinical Outcome. *Antioxidants (Basel)* 2021; **10** [PMID: 33557266 DOI: 10.3390/antiox10020235]

86 **Hiraga R**, Kato M, Miyagawa S, Kamata T. Nox4-derived ROS signaling contributes to TGF-β-induced epithelial-mesenchymal transition in pancreatic cancer cells. *Anticancer Res* 2013; **33**: 4431-4438 [PMID: 24123012]

87 **Witte D**, Bartscht T, Kaufmann R, Pries R, Settmacher U, Lehnert H, Ungefroren H. TGF-β1-induced cell migration in pancreatic carcinoma cells is RAC1 and NOX4-dependent and requires RAC1 and NOX4-dependent activation of p38 MAPK. *Oncol Rep* 2017; **38**: 3693-3701 [PMID: 29039574 DOI: 10.3892/or.2017.6027]

88 **Li H**, Peng C, Zhu C, Nie S, Qian X, Shi Z, Shi M, Liang Y, Ding X, Zhang S, Zhang B, Li X, Xu G, Lv Y, Wang L, Friess H, Kong B, Zou X, Shen S. Hypoxia promotes the metastasis of pancreatic cancer through regulating NOX4/KDM5A-mediated histone methylation modification changes in a HIF1A-independent manner. *Clin Epigenetics* 2021; **13**: 18 [PMID: 33499904 DOI: 10.1186/s13148-021-01016-6]

89 **Yang Y**, Karakhanova S, Hartwig W, D'Haese JG, Philippov PP, Werner J, Bazhin AV. Mitochondria and Mitochondrial ROS in Cancer: Novel Targets for Anticancer Therapy. *J Cell Physiol* 2016; **231**: 2570-2581 [PMID: 26895995 DOI: 10.1002/jcp.25349]

90 **Bonora M**, Missiroli S, Perrone M, Fiorica F, Pinton P, Giorgi C. Mitochondrial Control of Genomic Instability in Cancer. *Cancers (Basel)* 2021; **13** [PMID: 33921106 DOI: 10.3390/cancers13081914]

91 **Ago T**, Kuroda J, Pain J, Fu C, Li H, Sadoshima J. Upregulation of Nox4 by hypertrophic stimuli promotes apoptosis and mitochondrial dysfunction in cardiac myocytes. *Circ Res* 2010; **106**: 1253-1264 [PMID: 20185797 DOI: 10.1161/CIRCRESAHA.109.213116]

92 **Salmeen A**, Park BO, Meyer T. The NADPH oxidases NOX4 and DUOX2 regulate cell cycle entry *via* a p53-dependent pathway. *Oncogene* 2010; **29**: 4473-4484 [PMID: 20531308 DOI: 10.1038/onc.2010.200]

93 **Eid AA**, Ford BM, Block K, Kasinath BS, Gorin Y, Ghosh-Choudhury G, Barnes JL, Abboud HE. AMP-activated protein kinase (AMPK) negatively regulates Nox4-dependent activation of p53 and epithelial cell apoptosis in diabetes. *J Biol Chem* 2010; **285**: 37503-37512 [PMID: 20861022 DOI: 10.1074/jbc.M110.136796]

94 **Boudreau HE**, Casterline BW, Burke DJ, Leto TL. Wild-type and mutant p53 differentially regulate NADPH oxidase 4 in TGF-β-mediated migration of human lung and breast epithelial cells. *Br J Cancer* 2014; **110**: 2569-2582 [PMID: 24714748 DOI: 10.1038/bjc.2014.165]

95 **Ogrunc M**, Di Micco R, Liontos M, Bombardelli L, Mione M, Fumagalli M, Gorgoulis VG, d'Adda di Fagagna F. Oncogene-induced reactive oxygen species fuel hyperproliferation and DNA damage response activation. *Cell Death Differ* 2014; **21**: 998-1012 [PMID: 24583638 DOI: 10.1038/cdd.2014.16]

96 **Ju HQ**, Ying H, Tian T, Ling J, Fu J, Lu Y, Wu M, Yang L, Achreja A, Chen G, Zhuang Z, Wang H, Nagrath D, Yao J, Hung MC, DePinho RA, Huang P, Xu RH, Chiao PJ. Mutant Kras- and p16-regulated NOX4 activation overcomes metabolic checkpoints in development of pancreatic ductal adenocarcinoma. *Nat Commun* 2017; **8**: 14437 [PMID: 28232723 DOI: 10.1038/ncomms14437]

97 **Yu JH**, Kim KH, Kim DG, Kim H. Diphenyleneiodonium suppresses apoptosis in cerulein-stimulated pancreatic acinar cells. *Int J Biochem Cell Biol* 2007; **39**: 2063-2075 [PMID: 17625947 DOI: 10.1016/j.biocel.2007.05.021]

98 **Hirano K**, Chen WS, Chueng AL, Dunne AA, Seredenina T, Filippova A, Ramachandran S, Bridges A, Chaudry L, Pettman G, Allan C, Duncan S, Lee KC, Lim J, Ma MT, Ong AB, Ye NY, Nasir S, Mulyanidewi S, Aw CC, Oon PP, Liao S, Li D, Johns DG, Miller ND, Davies CH, Browne ER, Matsuoka Y, Chen DW, Jaquet V, Rutter AR. Discovery of GSK2795039, a Novel Small Molecule NADPH Oxidase 2 Inhibitor. *Antioxid Redox Signal* 2015; **23**: 358-374 [PMID: 26135714 DOI: 10.1089/ars.2014.6202]

99 **Chang G**, Chen L, Lin HM, Lin Y, Maranchie JK. Nox4 inhibition enhances the cytotoxicity of cisplatin in human renal cancer cells. *J Exp Ther Oncol* 2012; **10**: 9-18 [PMID: 22946340]

100 **Yang WH**, Huang Z, Wu J, Ding CC, Murphy SK, Chi JT. A TAZ-ANGPTL4-NOX2 Axis Regulates Ferroptotic Cell Death and Chemoresistance in Epithelial Ovarian Cancer. *Mol Cancer Res* 2020; **18**: 79-90 [PMID: 31641008 DOI: 10.1158/1541-7786.MCR-19-0691]

101 **Ju HQ**, Gocho T, Aguilar M, Wu M, Zhuang ZN, Fu J, Yanaga K, Huang P, Chiao PJ. Mechanisms of Overcoming Intrinsic Resistance to Gemcitabine in Pancreatic Ductal Adenocarcinoma through the Redox Modulation. *Mol Cancer Ther* 2015; **14**: 788-798 [PMID: 25527634 DOI: 10.1158/1535-7163.MCT-14-0420]

102 **Sadr-Azodi O**, Oskarsson V, Discacciati A, Videhult P, Askling J, Ekbom A. Pancreatic Cancer Following Acute Pancreatitis: A Population-based Matched Cohort Study. *Am J Gastroenterol* 2018; **113**: 1711-1719 [PMID: 30315287 DOI: 10.1038/s41395-018-0255-9]

103 **Hao L**, Zeng XP, Xin L, Wang D, Pan J, Bi YW, Ji JT, Du TT, Lin JH, Zhang D, Ye B, Zou WB, Chen H, Xie T, Li BR, Zheng ZH, Wang T, Guo HL, Liao Z, Li ZS, Hu LH. Incidence of and risk factors for pancreatic cancer in chronic pancreatitis: A cohort of 1656 patients. *Dig Liver Dis* 2017; **49**: 1249-1256 [PMID: 28756974 DOI: 10.1016/j.dld.2017.07.001]

World Journal of Gastroenterology

Submit a Manuscript: https://www.f6publishing.com

World J Gastroenterol 2024 February 7; 30(5): 440-449

DOI: 10.3748/wjg.v30.i5.440

ISSN 1007-9327 (print) ISSN 2219-2840 (online)

ORIGINAL ARTICLE

Retrospective Study

Evaluation of the efficacy and safety of endoscopic band ligation in the treatment of bleeding from mild to moderate gastric varices type 1

Yue Deng, Ya Jiang, Tong Jiang, Ling Chen, Hai-Jun Mou, Bi-Guang Tuo, Guo-Qing Shi

Specialty type: Gastroenterology and hepatology

Provenance and peer review: Unsolicited article; Externally peer reviewed.

Peer-review model: Single blind

Peer-review report's scientific quality classification

Grade A (Excellent): 0
Grade B (Very good): B, B
Grade C (Good): 0
Grade D (Fair): 0
Grade E (Poor): 0

P-Reviewer: Christodoulidis G, Greece; Popovic DD, Serbia

Received: October 3, 2023
Peer-review started: October 3, 2023
First decision: December 4, 2023
Revised: December 15, 2023
Accepted: January 11, 2024
Article in press: January 11, 2024
Published online: February 7, 2024

Yue Deng, Tong Jiang, Ling Chen, Hai-Jun Mou, Bi-Guang Tuo, Guo-Qing Shi, Department of Gastroenterology, Digestive Disease Hospital, The Affiliated Hospital of Zunyi Medical University, Zunyi 563000, Guizhou Province, China

Yue Deng, Department of Gastroenterology, Guizhou Hospital of the First Affiliated Hospital, Sun Yat-sen University, Guiyang 550000, Guizhou Province, China

Ya Jiang, Department of Gastroenterology, Yinjiang Autonomous County People's Hospital, Tongren 554300, Guizhou Province, China

Corresponding author: Guo-Qing Shi, MM, Chief Doctor, Department of Gastroenterology, Digestive Disease Hospital, The Affiliated Hospital of Zunyi Medical University, No. 149 Dalian Road, Zunyi 563000, Guizhou Province, China. sgqing973@sina.com

Abstract

BACKGROUND

According to practice guidelines, endoscopic band ligation (EBL) and endoscopic tissue adhesive injection (TAI) are recommended for treating bleeding from esophagogastric varices. However, EBL and TAI are known to cause serious complications, such as hemorrhage from dislodged ligature rings caused by EBL and hemorrhage from operation-related ulcers resulting from TAI. However, the optimal therapy for mild to moderate type 1 gastric variceal hemorrhage (GOV1) has not been determined. Therefore, the aim of this study was to discover an individualized treatment for mild to moderate GOV1.

AIM

To compare the efficacy, safety and costs of EBL and TAI for the treatment of mild and moderate GOV1.

METHODS

A clinical analysis of the data retrieved from patients with mild or moderate GOV1 gastric varices who were treated under endoscopy was also conducted. Patients were allocated to an EBL group or an endoscopic TAI group. The differences in the incidence of varicose relief, operative time, operation success rate, mortality rate within 6 wk, rebleeding rate, 6-wk operation-related ulcer healing rate, complication rate and average operation cost were compared

between the two groups of patients.

RESULTS

The total effective rate of the two treatments was similar, but the efficacy of EBL (66.7%) was markedly better than that of TAI (39.2%) ($P < 0.05$). The operation success rate in both groups was 100%, and the 6-wk mortality rate in both groups was 0%. The average operative time (26 min) in the EBL group was significantly shorter than that in the TAI group (46 min) ($P < 0.01$). The rate of delayed postoperative rebleeding in the EBL group was significantly lower than that in the TAI group (11.8% *vs* 45.1%) ($P < 0.01$). At 6 wk after the operation, the healing rate of operation-related ulcers in the EBL group was 80.4%, which was significantly greater than that in the TAI group (35.3%) ($P < 0.01$). The incidence of postoperative complications in the two groups was similar. The average cost and other related economic factors were greater for the EBL than for the TAI ($P < 0.01$).

CONCLUSION

For mild to moderate GOV1, patients with EBL had a greater one-time varix eradication rate, a greater 6-wk operation-related ulcer healing rate, a lower delayed rebleeding rate and a lower cost than patients with TAI.

Key Words: Gastric varices; Type 1 gastric variceal hemorrhage; Endoscopic band ligation; Tissue adhesive injection

Core Tip: Endoscopic band ligation (EBL) and endoscopic tissue adhesive injection for the treatment of type 1 gastric variceal hemorrhage (GOV1) are often associated with various complications, which we believe are due to the lack of individualized treatment. Different treatment methods should be used for different degrees of varicose veins. Therefore, this study was based on mild to moderate GOV1 and explored individualized treatment. Ultimately, the use of EBL for mild to moderate GOV1 can achieve better outcomes and reduce both rebleeding rates and treatment costs.

Citation: Deng Y, Jiang Y, Jiang T, Chen L, Mou HJ, Tuo BG, Shi GQ. Evaluation of the efficacy and safety of endoscopic band ligation in the treatment of bleeding from mild to moderate gastric varices type 1. *World J Gastroenterol* 2024; 30(5): 440-449
URL: https://www.wjgnet.com/1007-9327/full/v30/i5/440.htm
DOI: https://dx.doi.org/10.3748/wjg.v30.i5.440

INTRODUCTION

Esophageal and gastric variceal bleeding (EGVB) is a common cause of death worldwide in patients with cirrhosis, a liver-related disease, with an incidence of approximately 5%-15%. The 6-wk mortality rate can reach 20%, and rebleeding rates can reach 60%, placing an enormous burden on the global economy[1,2]. The main endoscopic treatments for EGVB include endoscopic band ligation (EBL), endoscopic tissue adhesive injection (TAI) and endoscopic injection sclerotherapy (EIS)[3]. However, during the treatment of type 1 gastric variceal hemorrhage (GOV1), EBL, EIS and TAI can cause serious complications, such as hemorrhage from dislodged ligature rings caused by EBL and hemorrhage from operation-related ulcers resulting from TAI, which are major problems for patients and endoscopists. It is important to choose the appropriate treatment modality according to the type, morphology and severity of varicose veins to further improve the treatment efficacy and minimize the incidence of associated complications. However, there are no detailed recommendations in the guidelines or published literature, especially for GOV1. Currently, there is no consensus on the recommended endoscopic treatment for GOV1. Currently, most endoscopists use a "modified sandwich method" (lauromacrogol-tissue adhesive-lauromacrogol)[4], which is highly effective but has a high incidence of rebleeding in patients with mild-to-moderate GOV1[5,6]. Therefore, we stratified the risk factors for mild-to-moderate GOV1 and observed the efficacy, safety, and costs of EBL and TAI to provide more precise and individualized treatment.

MATERIALS AND METHODS

Materials

Patients with mild-to-moderate GOV1 disease who visited Zunyi Medical University and Yinjiang Autonomous County People's Hospital between January 2017 and December 2022 were selected. The inclusion criteria were as follows: (1) Patients diagnosed with cirrhotic decompensation with GOV1 based on their past medical history, clinical presentation and ancillary investigations[7]; (2) Patients who underwent primary or secondary prevention measures; (3) Patients who completed the 6-wk follow-up after endoscopic gastroscopy treatment; (4) Patients with mild-to-moderate GOV1 with gastric varices in the shape of a stripe and a diameter ≤ 10 mm; (5) Patients with no contraindications to endoscopy; (6) Those who had not undergone surgery or transjugular intrahepatic portosystemic shunt for portal hypertension; and (7)

Patients and their families who were willing to cooperate with the treatment and signed a treatment consent form. The exclusion criteria were as follows: (1) Previous endoscopic treatment for gastric varices; (2) Lost to follow-up; (3) Severe comorbidities involving other organ systems; (4) Combined malignant tumors; and (5) Combined hepatic encephalopathies, disorders of consciousness, or other psychiatric-psychological disorders. The study protocol conformed to the ethical guidelines of the 1975 Helsinki Declaration and was approved by the Institutional Review Board.

Data collection

Patient data, including age, sex, and disease etiology (chronic hepatitis B, chronic hepatitis C, alcoholic liver disease, autoimmune hepatitis, hepatitis B combined with alcohol consumption and others), were collected during hospitalization. The results of the radiographic examinations [diameter of gastric varices (mm) and diameter of portal vein (mm)] and Child-Pugh classification were collected at enrollment.

Definitions

The classification of the gastric variceal size was similar to that of esophageal varices. Esophageal varices[8] were classified as mild gastric varices (G1): Rectilinear or slightly tortuous varices < 3 mm in diameter; moderate gastric varices (G2): Serpentine tortuous bulging varices 3-10 mm in diameter; and severe gastric varices (G3): Beaded, nodular or verrucous varices > 10 mm in diameter.

Instruments

The following instruments were used: An electronic gastroscope (Olympus GIF-260), a disposable endoscopic injection needle (Poco, 25G), a multiband variceal ligator (Poco 7-ring ligature), N-butyl-2-cyanoacrylate (0.5 mL/pc; Beijing Fuaile Technology Development Co., Ltd., China), and lauromacrogol (10 mL/pc; Shaanxi Tianyu Pharmaceutical Co., Ltd., China).

Methods of operation

Tests, including routine blood, coagulation, and biochemistry tests, as well as electrocardiogram and portal vein imaging, were completed on admission. The patient's general condition was assessed, drugs were administered to suppress gastric acid and lower the portal pressure, and painless endoscopic treatment was administered once the patient's vital signs had stabilized. All the procedures were performed by our team of doctors experienced in EGVB treatment.

In the EBL group, the lateral vein of the lesser curvature was ligated from the cardia toward the fundus of the stomach *via* a ligature *via* reverse endoscopy. TAI group: TAI treatment was performed using a "modified sandwich method" (lauromacrogol-tissue adhesive-lauromacrogol).

Both groups were treated for esophageal varices after the completion of GV treatment. The patients in both groups received proton pump inhibitors and vasoconstrictors. The TAI group received prophylactic antibiotics. The patients in both groups were followed up for at 6 wk after gastroscopy to judge the effectiveness of the varices eradication and to assess whether continuation of treatment was necessary. Patients in both groups were followed up at 3 months, 6 months and 1 year postoperatively at regular intervals. Depending on the effect of varices, the choice was made whether to repeat endoscopic treatment.

Efficacy evaluation

GOV1 efficacy is divided into three levels[9,10]: (1) Ineffective: No improvement in the varicose veins; (2) Effective: The condition of the varicose veins improved, indicated by less than 50% shrinkage; and (3) Markedly effective: The massed or nodular veins had changed to cords, had shrunk by more than 50% or had disappeared completely. Total effective rate = (number of effective cases + number of effective cases)/total number of cases × 100%.

Safety evaluation

Operation success was defined as the completion of EBL or TAI without uncontrollable bleeding intraoperatively or resulting in patient death. Operative time: The time from the start of the operation to the end of the operation, including the common time for treatment of gastric varices and esophageal varices. Six-week mortality[11]: Death within 6 wk after surgery.

Rebleeding: The reappearance of signs of upper gastrointestinal bleeding, such as vomiting blood, black stools, decreasing hemoglobin levels and shock, that recurs after the first bleeding has been controlled, with early rebleeding characterized as active bleeding within 6 wk after the bleeding had been controlled and late rebleeding characterized as active bleeding 6 wk after the bleeding had been controlled.

Six-week operation-related ulcer healing rate: Follow-up gastroscopy was performed 6 wk after surgery to observe the healing of the ulcer after EBL or TAI. The ulcer was considered healed if a fibrous scar was formed; otherwise, it was not healed. Adverse events included abdominal pain, infection, ectopic embolism, and perforation.

Economic evaluation

The following were summarized: The average number of hospitalizations, average length of hospitalizations, average total cost of hospitalization, average number of operations and average operation cost.

Statistics

Microsoft Excel 2016 and SPSS 26.0 were used for statistical analysis in this study. Normally distributed data are

expressed as the mean ± SD, quantitative data with a skewed distribution are described by the median, and count data are expressed as the rate. A *t*-test was used to compare differences between the groups; nonnormally distributed measures and rank data were compared using the Mann-Whitney *U* test or Wilcoxon rank sum test, and count data were compared using the χ^2 test and Fisher's test. The test level was $P < 0.05$.

RESULTS

Propensity score matching

According to the inclusion and exclusion criteria, a total of 151 patients were included, including 57 patients in the EBL group and 94 patients in the TAI group. The control variables used were sex, age, etiology, Child-Pugh classification, gastric variceal diameter, and portal vein diameter, and propensity score matching was performed using SPSS software. Then, 51 pairs of 102 patients were matched to the EBL group and the TAI group. The sex, age, etiology, Child-Pugh classification, gastric variceal diameter, and portal vein diameter of the two groups of patients were compared after matching. The differences between the two groups were not statistically significant ($P > 0.05$) (Table 1).

Efficacy

Gastroscopy was performed again 6 wk after the operation to observe if there was relief of the gastric varices after endoscopic treatment in the two groups. The difference in the total effective rate between the EBL group (96.1%) and the TAI group (94.1%) was not statistically significant ($P > 0.05$). However, the percentage of patients in the EBL group (66.7%) was significantly greater than that in the TAI group (39.2%) ($\chi^2 = 7.713$, $P < 0.05$) (Table 2).

Safety

Comparison of the operative time, operation success rate and 6-wk mortality: Both groups of patients successfully completed endoscopic treatment, and there was no intraoperative bleeding that was difficult to control or that led to patient death. The operation success rate of the two groups was 100%. Additionally, there were no deaths for any reason in the two groups of patients 6 wk after the operation. The average operative time in the EBL group (26 min) was significantly shorter than that in the TAI group (46 min) ($P < 0.01$) (Table 3).

Comparison of the 6-wk operation-related ulcer healing rate: After surgery, gastroscopy revealed that the healing rate of the ulcers that developed after dislodgement of the ligature ring in the EBL group reached 80.4%, which was significantly greater than the healing rate of the glue-draining ulcers in the TAI group (35.3%). The difference between the two groups was statistically significant ($P < 0.01$) (Table 4). Many TAI patients presented with glue-draining ulcers and bleeding (Figure 1); however, most EBL patients had healed ulcers (Figure 2).

Comparison of the postoperative rebleeding rates: Patients in both groups were followed up for 1 year after successful endoscopic treatment to focus on rebleeding. The rate of early postoperative rebleeding (within 6 wk after surgery) was slightly lower in the EBL group (7.8%) than in the TAI group (13.7%), but the difference was not statistically significant ($P > 0.05$). The rate of late postoperative rebleeding (from 6 wk postoperatively to 1 year) was significantly lower in the EBL group (11.8%) than in the TAI group (45.1%) ($P < 0.01$) (Table 5).

Comparison of adverse events: The rates of postoperative abdominal pain and infection were similar between the two groups, but the difference was not statistically significant ($P > 0.05$). No heterotopic embolism or perforation occurred in either group (Table 6).

Economic analysis

Follow-up economic indices such as the number of hospitalizations, the total number of days of hospitalization, the total cost of hospitalization, the number of surgeries, the cost of surgical materials and other economic indicators were significantly lower in the two groups one year after the operation in the EBL group than in the TAI group ($P < 0.01$) (Table 7).

DISCUSSION

In liver cirrhosis, increased intrahepatic vascular resistance to portal flow increases the portal pressure and leads to portal hypertension. Once portal hypertension develops, it influences extrahepatic vascular beds in the splanchnic and systemic circulations, causing collateral vessel formation and arterial vasodilation. This process helps to increase blood flow into the portal vein, which exacerbates portal hypertension and eventually aids in the development of hyperdynamic circulatory syndrome. As a result, esophageal varices or ascites develop. Gastric varices are present in 5%-33% of patients with portal hypertension. Gastric varices usually bleed more severely than ruptured esophageal varices, and the mortality rate can reach 45%[1].

Based on Sarin's classification, gastric varices can be classified as GOV1, GOV2, isolated gastric varices type 1 (IGV1) or IGV2. GOV1 is the most common type of gastric varices, accounting for 75%[12] of all gastric varices. GOV2 and IGV1 tend to have varices that have thicker diameters and are continuously exposed to gastric acid and pepsin; thus, TAI is recognized as the treatment of choice, as it has high success rates in hemostasis and one-time varicose vein eradication

Table 1 Comparison of the baseline data between the two groups of patients

	EBL group (*n* = 50)	TAI group (*n* = 50)	χ^2/*t*/U	*P* value
Sex, *n* (%)				
Male	45 (88.2)	43 (84.3)	/	0.487[1]
Female	6 (11.8)	8 (15.7)		
Age (yr, mean ± SD)	52.78 ± 8.50	52.92 ± 9.65	0.076	0.939[2]
Causes of disease, *n* (%)			3.744	0.630[1]
Hepatitis B liver cirrhosis	28 (54.9)	26 (51.0)		
alcoholic cirrhosis	11 (21.6)	13 (25.5)		
Hepatitis C cirrhosis	6 (11.7)	2 (3.9)		
Autoimmune liver cirrhosis	1 (2.0)	3 (5.9)		
Hepatitis B liver cirrhosis with alcoholic cirrhosis	4 (7.8)	6 (11.7)		
Other cause	1 (2.0)	1 (2.0)		
Child-Pugh classification, *n* (%)			-0.377	0.706[3]
A	11 (21.6)	10 (19.6)		
B	37 (72.6)	37 (72.6)		
C	3 (5.8)	4 (7.8)		
Diameter of gastric varices (mm)	15.0	14.0	-1.459	0.135[3]
Diameter of the portal vein (mm)	8.0	9.0	-1.280	0.200[3]

[1]Fisher's test.
[2]*t* test.
[3]Mann-Whitney *U* test.
The values are expressed as the mean ± SD or median. EBL: Endoscopic band ligation; TAI: Tissue adhesive injection.

Table 2 Comparison of treatment efficacy between the two groups of patients, *n* (%)

	Markedly effective	Effective	Ineffective	Total effective rate
EBL group	34 (66.7)	15 (29.4)	2 (3.9)	49 (96.1)
TAI group	20 (39.2)	28 (54.9)	3 (5.9)	48 (94.1)
χ^2	-2.669			
P value	0.008[1]			> 0.999[2]

[1]Wilcoxon rank sum test.
[2]Fisher's test.
EBL: Endoscopic band ligation; TAI: Tissue adhesive injection.

[13]. GOV1 is characterized by the presence of gastric varices that appear with esophageal varices and extend 2-5 cm below the gastroesophageal junction. The shape of these lesions is similar to that of esophageal varices, and they may appear tortuous, nodular or tumorous in shape. There is no uniform standard for the endoscopic treatment of GOV1. Currently, most endoscopists choose endoscopic TAI, while a few endoscopists use EBL. Recently, a few studies had analyzed and compared the clinical application of EBL and TAI for removing GOV1, but the conclusions have not been consistent. Several studies have shown that there is no statistically significant difference between EBL and TAI in the treatment of GOV1 in terms of acute hemostasis, variceal elimination or risk of rebleeding, but the complication rate of EBL is lower[14]. Several studies have shown that EBL is superior to TAI in terms of reducing the incidence of late rebleeding in patients with acute GOV1[15]. It has also been suggested that TAI is more favorable than EBL because of its significantly reduced rebleeding rate, significantly increased survival time, high hemostasis and survival rate[16-19]. We believe that the inconsistency of the results of the current study compared to other studies may be related to the fact that none of the other studies stratified the risks of the procedures for the study population, and none of them analyzed indicators such as diameter, morphology, or severity of gastric varices. Moreover, all of their studies involved emergency bleeding rather than primary or secondary bleeding prevention. Therefore, these studies failed to individualize the choice

Table 3 Comparison of operative time, operative success rate and 6-wk mortality

	Operative time (min)	Operative success rate, *n* (%)	Week mortality, *n* (%)
EBL group	26	51 (100)	0 (0)
TAI group	46	51 (100)	0 (0)
Z	-8.721	/	/
P value	< 0.001[1]	/	/

[1]Mann-Whitney *U* test.
The operative times are expressed as medians. EBL: Endoscopic band ligation; TAI: Tissue adhesive injection.

Table 4 Comparison of the 6-wk operation-related ulcer healing rate, *n* (%)

	Healed	Non-healed
EBL group	41 (80.4)	10 (19.6)
TAI group	18 (35.3)	33 (64.7)
χ^2	21.268	
P value	< 0.001	

EBL: Endoscopic band ligation; TAI: Tissue adhesive injection.

Table 5 Comparison of rebleeding rates, *n* (%)

	Early rebleeding rate	Delayed rebleeding rate
EBL group	4 (7.8)	6 (11.8)
TAI group	7 (13.7)	23 (45.1)
χ^2	0.917	13.924
P value	0.338	< 0.001

EBL: Endoscopic band ligation; TAI: Tissue adhesive injection.

Table 6 Comparison of adverse events, *n* (%)

	Abdominal pain	Infection	Ectopic embolism	Perforation
EBL group	11 (21.6)	2 (3.9)	0 (0)	0 (0)
TAI group	10 (19.6)	3 (5.9)	0 (0)	0 (0)
χ^2	0.060	/	/	/
P value	0.807[1]	> 0.999[2]	/	/

[1]χ^2 test.
[2]Fisher's test.
EBL: Endoscopic band ligation; TAI: Tissue adhesive injection.

of regimen, which led to different results.

Therefore, we stratified the risk of GOV1 and developed different treatment programs. For high-tension, nodular or tumorous varicose veins with a diameter greater than 1 cm (severe), precise puncture and precise endoscopic injection are feasible; therefore, TAI can achieve very good outcomes. For this kind of varicose vein, if EBL is chosen, incomplete ligation and insufficient vessel occlusion are likely to occur. In contrast, the risk of rebleeding is high[20]. Therefore, it is appropriate to choose the TAI for GOV1. However, for striated varicose veins (mild to moderate) with a diameter less than 1 cm, precise puncture and precise endoscopic injection are difficult because of the low vascular tone. Therefore, rebleeding is characterized by bleeding from a draining ulcer that can develop as a result of TAI[21,22]. On the basis of

Table 7 Comparison of the economic evaluation (median) results

	Average number of hospitalizations (No.)	Average length of hospitalizations (d)	Average total cost of hospitalization (Yuan)	Average number of operations (No.)	Average operation cost (Yuan)
EBL group	2.00	13.00	32128.60	2.00	1680.00
TAI group	3.00	19.00	69380.75	3.00	6548.80
Z	3.596	3.894	6.134	3.631	8.855
P value	< 0.001	< 0.001	< 0.001	< 0.001	< 0.001

EBL: Endoscopic band ligation; TAI: Tissue adhesive injection.

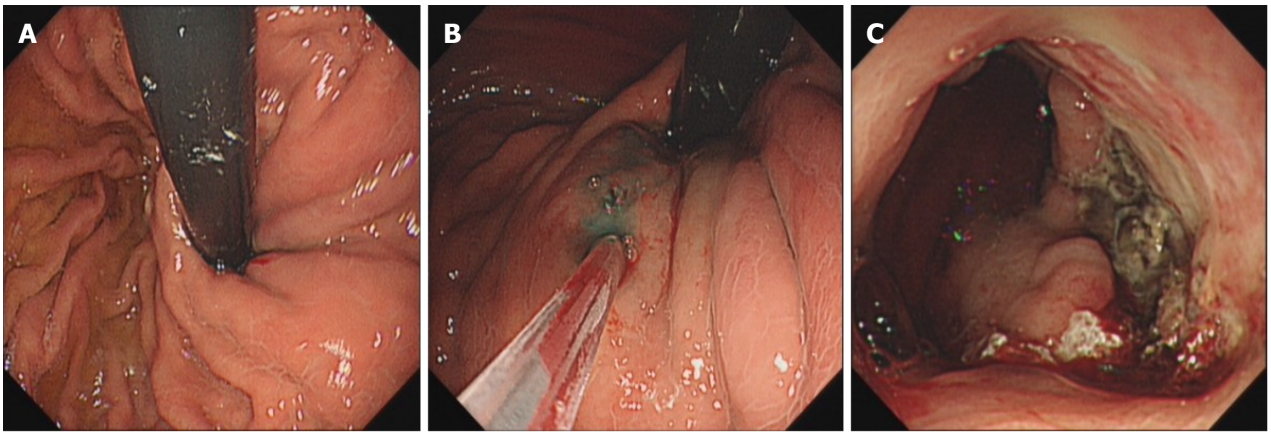

DOI: 10.3748/wjg.v30.i5.440

Figure 1 Endoscopic images of endoscopic tissue adhesive injection for mild to moderate gastric varices type 1. A: Pre-treatment. It showed type 1 gastric variceal hemorrhage; B: In treatment. It was performed using a "modified sandwich method" (lauromacrogol - tissue adhesive - lauromacrogol); C: After 6 wk of treatment. It showed giant glue-draining ulcer after endoscopy.

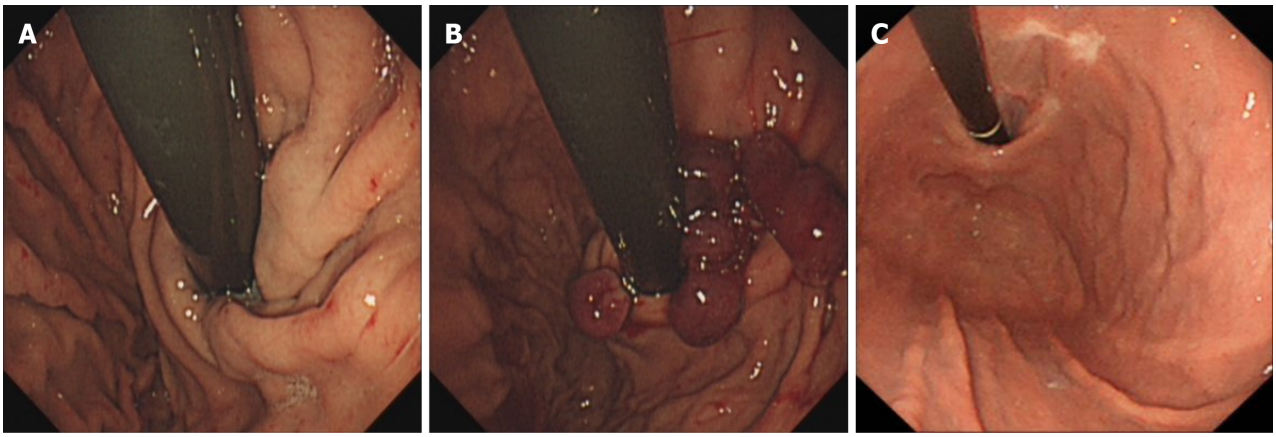

DOI: 10.3748/wjg.v30.i5.440

Figure 2 Endoscopic images of endoscopic band ligation for mild to moderate gastric varices type 1. A: Pre-treatment. It showed type 1 gastric variceal hemorrhage; B: In treatment. The lateral vein of the lesser curvature was ligated from the cardia toward the fundus of the stomach with a ligature through a reverse endoscope; C: After 6 wk of treatment. The ulcer was healed and a fibrous scar was formed.

our clinical findings, EBLs prevent bleeding from glue-draining ulcers. Therefore, our retrospective study compared endoscopic reverse body ligation and TAI for the treatment of mild to moderate GOV1. Our study included patients who were subjected to secondary or primary prophylaxis and did not include only emergency patients.

EBL is a procedure in which the gastroscope enters the fundus of the stomach and then reverses the body to fully expose the fundus, and a ligature ring is used to ligate the varicose vein inside the clear cap at the front of the inhalation

endoscope so that tissue necrosis occurs at the site of the ligature and a thrombus forms to block the varicose vein within 24 to 48 h. The ligature ring eventually detaches and leaves an ulcer, which heals and leaves a fibrous scar, creating a lasting interruption of the blood flow in the vein[23].

Therefore, this study compared the efficacy, safety and cost of endoscopic reverse body ligation and TAI for the treatment of mild and moderate GOV1 gastric varices: (1) Efficacy: The total effective rates of EBL and TAI were similar, but the effective rate of EBL was better than that of TAI. These findings suggest that both EBL and TAI have similar overall efficacy rates, but EBL has a greater rate of effective one-time varicose vein eradication than does TAI. Because of the small diameter of the gastric varices selected for this study and the choice of intensive multiple ring ligation during treatment, the varices could be fully occluded at one time, and the risk of recurrence of residual varices could be reduced; (2) Safety: The data of this study showed that the patients in both the EBL group and the TAI group successfully completed the endoscopic surgery, and none of them had uncontrollable intraoperative bleeding or died. Both EBL and TAI are feasible, safe and effective for the treatment of mild to moderate GOV1. However, the average operative time of EBL was significantly shorter than that of TAI. This finding indicates that performing EBL is easier for endoscopists. EBL can fully expose the gastric fundus to expand the surgical window more openly and clearly locate the varicose vein, which is favorable for surgical operation. Complete ligation under direct vision can be achieved due to the clear visibility of the surgical field, ensuring a safe operation. The early postoperative rebleeding rate in the EBL group was slightly lower than that in the TAI group. The rate of late rebleeding in the postoperative period after surgery for EBL was significantly lower than that in the postoperative period after TAI. A 6-wk postoperative review of patients treated with gastroscopy showed that the healing rate of ulcers after dislodged ligature rings in the EBL group was significantly greater than the glue-draining ulcers in the TAI group. This is because shallow ulcers tend to form after detachment of the ligature ring, and most of the ulcers heal into a fibrous scar within 6 wk. However, after injection of the tissue adhesive, due to poor precision, the tissue glue tends to leak into the submucosa, which results in the formation of a long-lasting and deep glue-discharging ulcer that tends to remain unhealed and bleeds repeatedly even after 6 wk. This is the reason why the rate of delayed rebleeding after surgery was significantly lower in the EBL group than in the TAI group. The rate of postoperative complications was similar between the two groups, which shows that there is no increased risk of treatment with EBL; and (3) Cost: The number of hospitalizations, total number of days of hospitalization, total cost of hospitalization, number of surgeries, and cost of surgical materials in the EBL group were lower than those in the TAI group. The cost of consumables used in the EBL group was lower than that used in the TAI group because the EBL group had higher rates of effective one-time varicose vein eradication and procedure-related ulcer healing at 6 wk postoperatively but a lower rebleeding rate. Therefore, this approach has a significantly lower health care cost and a considerably lighter financial burden on the patient's family and the country.

CONCLUSION

In conclusion, for mild to moderate GOV1, endoscopic reverse body ligation is safer, more effective, more economical and easier to perform than TAI, thus confirming that this approach is beneficial for patients and is worthy of clinical application. EBL is a better treatment for gastric varices in patients with mild or moderate GOV1.

ARTICLE HIGHLIGHTS

Research background

During the treatment of type 1 gastric variceal hemorrhage (GOV1), endoscopic band ligation (EBL), endoscopic tissue adhesive injection (TAI) and endoscopic injection sclerotherapy can cause serious complications. Therefore, individualized treatment is urgently needed.

Research motivation

The optimal individualized therapy for patients with mild or moderate GOV1 has yet to be identified. It is important to choose the appropriate treatment modality according to the type, morphology and severity of varicose veins to further improve the treatment efficacy and minimize the incidence of associated complications. Thus, this new treatment will greatly reduce patient suffering.

Research objectives

We focused on comparing the differences between the EBL and TAI treatments. This study provides new ideas for the treatment of mild and moderate GOV1.

Research methods

This retrospective study compared the efficacy, safety and costs of EBL and TAI. A detailed comparison of the varicose-relief rate, operative time, operation success rate, mortality rate within 6 wk, rebleeding rate, 6-wk operation-related ulcer healing rate, complication rate and average operation cost was performed.

Research results

EBL has a higher one-time varix eradication rate, a higher 6-wk operation-related ulcer healing rate, a lower delayed rebleeding rate and a lower cost than TAI for mild to moderate GOV1.

Research conclusions

This study provides a new method for the treatment of mild to moderate GOV1:EBL.

Research perspectives

EBL has a higher one-time varix eradication rate, higher 6-wk operation-related ulcer healing rate, lower delayed rebleeding rate and lower cost than TAI for mild to moderate GOV1.

ACKNOWLEDGEMENTS

Our research team will expand the sample size and study the treatment of different levels of gastric varices in the future.

FOOTNOTES

Co-first authors: Yue Deng and Ya Jiang.

Author contributions: Deng Y and Jiang Y designed the research study and wrote the paper; Jiang Y, Mou HJ, and Shi GQ contributed to the surgical operations and provided clinical advice; Tuo BG supervised the study; Jiang T and Chen L contributed to the analysis and interpretation of the data; Shi GQ approved the final version of the article to be published.

Supported by the Guizhou Provincial Science and Technology Program, No. [2020]4Y004.

Institutional review board statement: This study was reviewed and approved by the Ethics Committee of the Affiliated Hospital of Zunyi Medical University.

Informed consent statement: Patients were not required to give informed consent to participate in the study because the analysis used anonymous clinical data that were obtained after each patient agreed to the treatment by written consent.

Conflict-of-interest statement: All the authors report no relevant conflicts of interest for this article.

Data sharing statement: No additional data are available.

Country/Territory of origin: China

ORCID number: Yue Deng 0000-0003-3896-1491; Bi-Guang Tuo 0000-0003-3147-3487; Guo-Qing Shi 0000-0003-3597-8255.

S-Editor: Wang JJ
L-Editor: A
P-Editor: Zhao S

REFERENCES

1 **Kim DH**, Cho E, Jun CH, Son DJ, Lee MJ, Park CH, Cho SB, Park SY, Kim HS, Choi SK, Rew JS. Risk Factors and On-site Rescue Treatments for Endoscopic Variceal Ligation Failure. *Korean J Gastroenterol* 2018; **72**: 188-196 [PMID: 30419643 DOI: 10.4166/kjg.2018.72.4.188]

2 **Ginès P**, Krag A, Abraldes JG, Solà E, Fabrellas N, Kamath PS. Liver cirrhosis. *Lancet* 2021; **398**: 1359-1376 [PMID: 34543610 DOI: 10.1016/S0140-6736(21)01374-X]

3 **Gralnek IM**, Camus Duboc M, Garcia-Pagan JC, Fuccio L, Karstensen JG, Hucl T, Jovanovic I, Awadie H, Hernandez-Gea V, Tantau M, Ebigbo A, Ibrahim M, Vlachogiannakos J, Burgmans MC, Rosasco R, Triantafyllou K. Endoscopic diagnosis and management of esophagogastric variceal hemorrhage: European Society of Gastrointestinal Endoscopy (ESGE) Guideline. *Endoscopy* 2022; **54**: 1094-1120 [PMID: 36174643 DOI: 10.1055/a-1939-4887]

4 **Zeng XQ**, Ma LL, Tseng YJ, Chen J, Cui CX, Luo TC, Wang J, Chen SY. Endoscopic cyanoacrylate injection with or without lauromacrogol for gastric varices: A randomized pilot study. *J Gastroenterol Hepatol* 2017; **32**: 631-638 [PMID: 27439114 DOI: 10.1111/jgh.13496]

5 **Nakayama S**, Murashima N. Extrusion of Glue Cast after Sclerotherapy. *Intern Med* 2015; **54**: 2781 [PMID: 26521912 DOI: 10.2169/internalmedicine.54.5599]

6 **Cheng LF**, Wang ZQ, Li CZ, Lin W, Yeo AE, Jin B. Low incidence of complications from endoscopic gastric variceal obturation with butyl cyanoacrylate. *Clin Gastroenterol Hepatol* 2010; **8**: 760-766 [PMID: 20621678 DOI: 10.1016/j.cgh.2010.05.019]

7 **Smith A**, Baumgartner K, Bositis C. Cirrhosis: Diagnosis and Management. *Am Fam Physician* 2019; **100**: 759-770 [PMID: 31845776]

8 **Beppu K**, Inokuchi K, Koyanagi N, Nakayama S, Sakata H, Kitano S, Kobayashi M. Prediction of variceal hemorrhage by esophageal endoscopy. *Gastrointest Endosc* 1981; **27**: 213-218 [PMID: 6975734 DOI: 10.1016/s0016-5107(81)73224-3]

9 **Tripathi D**, Stanley AJ, Hayes PC, Patch D, Millson C, Mehrzad H, Austin A, Ferguson JW, Olliff SP, Hudson M, Christie JM; Clinical Services and Standards Committee of the British Society of Gastroenterology. U.K. guidelines on the management of variceal haemorrhage in cirrhotic patients. *Gut* 2015; **64**: 1680-1704 [PMID: 25887380 DOI: 10.1136/gutjnl-2015-309262]

10 **Wani ZA**, Bhat RA, Bhadoria AS, Maiwall R, Choudhury A. Gastric varices: Classification, endoscopic and ultrasonographic management. *J Res Med Sci* 2015; **20**: 1200-1207 [PMID: 26958057 DOI: 10.4103/1735-1995.172990]

11 **Garcia-Tsao G**, Abraldes JG, Berzigotti A, Bosch J. Portal hypertensive bleeding in cirrhosis: Risk stratification, diagnosis, and management: 2016 practice guidance by the American Association for the study of liver diseases. *Hepatology* 2017; **65**: 310-335 [PMID: 27786365 DOI: 10.1002/hep.28906]

12 **Sarin SK**, Kumar A. Gastric varices: profile, classification, and management. *Am J Gastroenterol* 1989; **84**: 1244-1249 [PMID: 2679046]

13 **Jakab SS**, Garcia-Tsao G. Screening and Surveillance of Varices in Patients With Cirrhosis. *Clin Gastroenterol Hepatol* 2019; **17**: 26-29 [PMID: 29551741 DOI: 10.1016/j.cgh.2018.03.012]

14 **Chang DF**, Mei ZC, He S, Guo JJ, Deng L. [Clinical efficacy of endoscopic gastric variceal ligation vs. gastric variceal obliteration in treating type 1 gastroesophageal varices bleeding]. *J Chongqing Medical University* 2021; **46**: 252-256 [DOI: 10.13406/j.cnki.cyxb.002716]

15 **Hong HJ**, Jun CH, Lee du H, Cho EA, Park SY, Cho SB, Park CH, Joo YE, Kim H, Choi SK, Rew JS. Comparison of Endoscopic Variceal Ligation and Endoscopic Variceal Obliteration in Patients with GOV1 Bleeding. *Chonnam Med J* 2013; **49**: 14-19 [PMID: 23678472 DOI: 10.4068/cmj.2013.49.1.14]

16 **Park SJ**, Kim YK, Seo YS, Park SW, Lee HA, Kim TH, Suh SJ, Jung YK, Kim JH, An H, Yim HJ, Jang JY, Yeon JE, Byun KS. Cyanoacrylate injection versus band ligation for bleeding from cardiac varices along the lesser curvature of the stomach. *Clin Mol Hepatol* 2016; **22**: 487-494 [PMID: 28081588 DOI: 10.3350/cmh.2016.0050]

17 **Tan PC**, Hou MC, Lin HC, Liu TT, Lee FY, Chang FY, Lee SD. A randomized trial of endoscopic treatment of acute gastric variceal hemorrhage: N-butyl-2-cyanoacrylate injection versus band ligation. *Hepatology* 2006; **43**: 690-697 [PMID: 16557539 DOI: 10.1002/hep.21145]

18 **Lo GH**, Lin CW, Perng DS, Chang CY, Lee CT, Hsu CY, Wang HM, Lin HC. A retrospective comparative study of histoacryl injection and banding ligation in the treatment of acute type 1 gastric variceal hemorrhage. *Scand J Gastroenterol* 2013; **48**: 1198-1204 [PMID: 24047398 DOI: 10.3109/00365521.2013.832792]

19 **Qiao W**, Ren Y, Bai Y, Liu S, Zhang Q, Zhi F. Cyanoacrylate Injection Versus Band Ligation in the Endoscopic Management of Acute Gastric Variceal Bleeding: Meta-Analysis of Randomized, Controlled Studies Based on the PRISMA Statement. *Medicine (Baltimore)* 2015; **94**: e1725 [PMID: 26469912 DOI: 10.1097/MD.0000000000001725]

20 **Garcia-Pagán JC**, Barrufet M, Cardenas A, Escorsell A. Management of gastric varices. *Clin Gastroenterol Hepatol* 2014; **12**: 919-28.e1; quiz e51 [PMID: 23899955 DOI: 10.1016/j.cgh.2013.07.015]

21 **Hu Z**, Zhang D, Swai J, Liu T, Liu S. Risk of rebleeding from gastroesophageal varices after initial treatment with cyanoacrylate; a systematic review and pooled analysis. *BMC Gastroenterol* 2020; **20**: 181 [PMID: 32517718 DOI: 10.1186/s12876-020-01333-9]

22 **Nakazawa M**, Imai Y, Sugawara K, Uchida Y, Saitoh Y, Fujii Y, Uchiya H, Ando S, Nakayama N, Tomiya T, Mochida S. Long-term outcomes of patients with cirrhosis presenting with bleeding gastric varices. *PLoS One* 2022; **17**: e0264359 [PMID: 35290384 DOI: 10.1371/journal.pone.0264359]

23 **Nelms DW**, Pelaez CA. The Acute Upper Gastrointestinal Bleed. *Surg Clin North Am* 2018; **98**: 1047-1057 [PMID: 30243446 DOI: 10.1016/j.suc.2018.05.004]

World Journal of Gastroenterology

Submit a Manuscript: https://www.f6publishing.com

World J Gastroenterol 2024 February 7; 30(5): 450-461

DOI: 10.3748/wjg.v30.i5.450

ISSN 1007-9327 (print) ISSN 2219-2840 (online)

ORIGINAL ARTICLE

Retrospective Study

Development and validation of a prediction model for early screening of people at high risk for colorectal cancer

Ling-Li Xu, Yi Lin, Li-Yuan Han, Yue Wang, Jian-Jiong Li, Xiao-Yu Dai

Specialty type: Gastroenterology and hepatology

Provenance and peer review: Unsolicited article; Externally peer reviewed.

Peer-review model: Single blind

Peer-review report's scientific quality classification

Grade A (Excellent): 0
Grade B (Very good): B
Grade C (Good): C
Grade D (Fair): 0
Grade E (Poor): 0

P-Reviewer: Alvarez-Bañuelos MT, Mexico; Bordonaro M, United States

Received: October 16, 2023
Peer-review started: October 16, 2023
First decision: December 6, 2023
Revised: December 19, 2023
Accepted: January 12, 2024
Article in press: January 12, 2024
Published online: February 7, 2024

Ling-Li Xu, Jian-Jiong Li, Xiao-Yu Dai, Department of General Surgery, Ningbo No. 2 Hospital, Ningbo 315000, Zhejiang Province, China

Yi Lin, Center for Health Economics, Faculty of Humanities and Social Sciences, University of Nottingham, Ningbo 315100, Zhejiang Province, China

Li-Yuan Han, Department of Global Health, Ningbo Institute of Life and Health Industry, University of Chinese Academy of Sciences, Ningbo 315000, Zhejiang Province, China

Yue Wang, School of Public Health, Medical College of Soochow University, Suzhou 215123, Jiangsu Province, China

Corresponding author: Xiao-Yu Dai, MD, Chief Physician, Department of General Surgery, Ningbo No. 2 Hospital, No. 41 Northwest Street, Haishu Zone, Ningbo 315000, Zhejiang Province, China. daixiaoyu1968@163.com

Abstract

BACKGROUND

Colorectal cancer (CRC) is a serious threat worldwide. Although early screening is suggested to be the most effective method to prevent and control CRC, the current situation of early screening for CRC is still not optimistic. In China, the incidence of CRC in the Yangtze River Delta region is increasing dramatically, but few studies have been conducted. Therefore, it is necessary to develop a simple and efficient early screening model for CRC.

AIM

To develop and validate an early-screening nomogram model to identify individuals at high risk of CRC.

METHODS

Data of 64448 participants obtained from Ningbo Hospital, China between 2014 and 2017 were retrospectively analyzed. The cohort comprised 64448 individuals, of which, 530 were excluded due to missing or incorrect data. Of 63918, 7607 (11.9%) individuals were considered to be high risk for CRC, and 56311 (88.1%) were not. The participants were randomly allocated to a training set (44743) or validation set (19175). The discriminatory ability, predictive accuracy, and clinical utility of the model were evaluated by constructing and analyzing receiver operating characteristic (ROC) curves and calibration curves and by decision

curve analysis. Finally, the model was validated internally using a bootstrap resampling technique.

RESULTS

Seven variables, including demographic, lifestyle, and family history information, were examined. Multifactorial logistic regression analysis revealed that age [odds ratio (OR): 1.03, 95% confidence interval (CI): 1.02-1.03, $P < 0.001$], body mass index (BMI) (OR: 1.07, 95%CI: 1.06-1.08, $P < 0.001$), waist circumference (WC) (OR: 1.03, 95%CI: 1.02-1.03 $P < 0.001$), lifestyle (OR: 0.45, 95%CI: 0.42-0.48, $P < 0.001$), and family history (OR: 4.28, 95%CI: 4.04-4.54, $P < 0.001$) were the most significant predictors of high-risk CRC. Healthy lifestyle was a protective factor, whereas family history was the most significant risk factor. The area under the curve was 0.734 (95%CI: 0.723-0.745) for the final validation set ROC curve and 0.735 (95%CI: 0.728-0.742) for the training set ROC curve. The calibration curve demonstrated a high correlation between the CRC high-risk population predicted by the nomogram model and the actual CRC high-risk population.

CONCLUSION

The early-screening nomogram model for CRC prediction in high-risk populations developed in this study based on age, BMI, WC, lifestyle, and family history exhibited high accuracy.

Key Words: Colorectal cancer; Early screening model; High-risk population; Nomogram model; Questionnaire survey; Dietary habit; Living habit

Core Tip: This was the first large-scale study to investigate early screening for detection of colorectal cancer (CRC) in Ningbo, China, which was part of the national early screening CRC program. The study focused on collecting information on the general population who attended annual health checks. Our findings showed that the area under the curve was 0.734 for the final validation set receiver operating characteristic (ROC) curve and 0.735 for the training set ROC curve. Therefore, we developed an early screening model with high accuracy for CRC.

Citation: Xu LL, Lin Y, Han LY, Wang Y, Li JJ, Dai XY. Development and validation of a prediction model for early screening of people at high risk for colorectal cancer. *World J Gastroenterol* 2024; 30(5): 450-461
URL: https://www.wjgnet.com/1007-9327/full/v30/i5/450.htm
DOI: https://dx.doi.org/10.3748/wjg.v30.i5.450

INTRODUCTION

Colorectal cancer (CRC) has become the third most common cancer worldwide[1]. The incidence of CRC in China increased from 42.74/100000 in 1990 to 8.95/100000 in 2019 and has been increasing annually in the Yangtze River Delta region[2]. A cross-sectional study on CRC knowledge and awareness in the Caribbean in 2020 revealed that only 54.7% of people were aware of the risk factors for CRC[3]. In addition, a questionnaire survey of diagnostic delays and their predictive factors in 303 CRC patients in southern China in 2020 found that the incidence of prolonged diagnostic delays was 57.8%[4]. The study found that the diagnostic delays were attributed to a variety of factors, such as a lack of knowledge of the risk factors for CRC and a reluctance to undergo CRC screening. This suggests that awareness of high-risk factors for CRC in China is insufficient, and colonoscopic screening has yet to become popular. Therefore, it is critical to identify individuals with high-risk CRC at an early stage.

In 2022, a study conducted at Memorial Sloan-Kettering Cancer Center found that altered bowel habits accounted for 24.7% of the common symptoms of CRC[5]. Some people recognize such symptoms and visit a hospital for treatment; however, a unified approach has yet to be developed in China for early screening of people at high risk of CRC. Previously, CRC screening was based on colonoscopy, fecal occult blood test, and abdominal computed tomography[6], which have some limitations, such as high cost and poor compliance. Therefore, it is important to utilize risk factors that are easily obtained in screening settings to develop simple and convenient early screening models capable of identifying those at high risk of CRC.

Some CRC risk-prediction models have been constructed. For instance, a risk-prediction model for advanced CRC in asymptomatic adults in the United States established by Imperiale *et al*[7], a risk-prediction model for CRC in Caucasian patients in Poland established by Kaminski *et al*[8], and a risk-prediction model for advanced CRC in Germany established by Tao *et al*[9]. Most of these models based their predictions on demographic information. In contrast, most of the CRC risk-prediction models developed in China were based on genomics, lifestyle habits, and dietary habits, such as those developed by Wong *et al*[10] and Sung *et al*[11]. Cai *et al*[12] constructed a CRC risk-prediction model in a retrospective cohort study of a population with poor dietary habits. This model was based on logistic regression and afforded an area under the curve (AUC) of 0.74 [95% confidence interval (CI): 0.70-078], indicating that it has moderate predictive ability. In summary, most of the CRC risk-prediction models are beneficial for screening high-risk CRC individuals in the

general population but are of little use for early screening of populations with high-risk CRC. Moreover, while some models are based on a single method or not well validated, others are complex and thus not feasible or practical for clinical application. Most importantly, compared with the factors affecting CRC incidence in western countries, those affecting CRC incidence in China are more complex. Thus, there is a need for CRC risk-prediction models based on data from the Chinese population, as these will allow the risk of CRC development to be effectively assessed in Chinese people and improve the accuracy of early-screening programs.

CRC has many causes; therefore, assessing and screening high-risk groups for CRC can be complicated. It requires examination of dietary habits[13], lifestyle habits[14], genetic factors[15], environmental factors[16], and emotional and psychological factors[17]. High-calorie, high-fat, and high-protein diets; consumption of pickled foods; and unhealthy lifestyle habits, such as staying up late, smoking, and drinking alcohol, can cause CRC[18]. China is a huge country with 56 ethnic groups, and the large variations in lifestyles, dietary habits, and environmental factors in the country mean that constructing a prediction model for early screening of CRC in high-risk groups may be complex.

Here, we collected the demographic information, living habits, dietary habits, and family history of a large CRC early screening cohort in the China Urban Cancer Early Diagnosis and Treatment Program, Ningbo, from 2014 to 2017. These data were examined *via* a backward Wald logistic regression analysis to identify the risk factors for CRC. These risk factors were used to establish a prediction model for screening groups at high risk for CRC at an early stage. We believe that this model will provide a basis for the accurate identification of high-risk groups in future CRC screening efforts.

MATERIALS AND METHODS

Study design and participants

This retrospective study was conducted in Ningbo Hospital, China, from 2014 to 2017. Of the 64448 participants, 530 were excluded due to missing or incorrect data. Of the remaining participants, 7607 (11.9%) were considered high risk for CRC, and 56311 (88.1%) were not. The inclusion criteria were as follows: (1) Permanent household registration in the city (living in the local area for > 3 years); (2) age 40-74 years; and (3) ability to sign the informed consent form unaided. The exclusion criteria were as follows: (1) An abnormal identifier number; and (2) a previous CRC diagnosis. All the participants provided written informed consent. The study protocol complied with the Declaration of Helsinki and was approved by the Ethical Review Board of Ningbo No. 2 Hospital (approval number: YJ-NBEY-KY-2023-060-01).

Selection of variables

Demographic information, dietary habits, living habits, and family history of the participants in the validation and training sets were obtained *via* questionnaires. The questionnaires collected details of dietary habits, including usual food intake, food preference, and dietary behavior, using the food frequency questionnaire. The questionnaires were administered by uniformly trained and qualified investigators through face-to-face questioning. We selected variables based on prior knowledge of the underlying biology and epidemiology of CRC and relevant predictors. This yielded seven variables that covered basic information, lifestyle, and family history.

Basic information comprised age, sex, ethnicity, body mass index (BMI), and waist circumference (WC). Age was categorized according to the United Nations New Standard for the Classification of Human Ages: young adults ≤ 65 years and middle-aged and older adults > 65 years[19]. Minors < 18 years of age were not included in the study. Sex was categorized as male or female. Ethnicity was divided into Han nationality and other ethnic groups, according to the results of the questionnaire. BMI was based on the BMI classification standard for Chinese adults[20]: Underweight < 18.50 kg/m^2, normal weight 18.50-23.99 kg/m^2, overweight 24.0-27.99 kg/m^2, and obese ≥ 28.0 kg/m^2. The median WC was 80 cm (SD: 50-184 cm).

Lifestyle included dietary habits and living habits. With reference to the standards of Dietary Guidelines for Chinese Residents (2007 edition) and the Dietary Reference Intake of Nutrients for Chinese Residents (2013 edition) and based on the discussion involving a group of relevant experts and scholars, we used the following definitions to determine the intake of substances and their frequencies (dietary habits) and the specific behaviors (living habits) in the questionnaire survey.

Dietary habits included taste, oil consumption, frequency of pickled and sun-cured food intake, and weekly consumption of fresh vegetables, fresh fruits, meat, and coarse grains. Taste was classified into three levels based on salt consumption: double-salt taste (> 5 g/d), moderate-salt taste (5 g/d), and low-salt taste (< 5 g/d). Oil consumption was classified into three levels based on the amount of cooking oil ingested per day: High oil consumption (> 30 g/d), moderate oil consumption (25-30 g/d), and low oil consumption (< 25 g/d). The frequency of pickled and sun-cured food intake was classified into the following three levels: never, < 3 times/wk (*i.e.*, sometimes), and ≥ 3 times/wk (*i.e.*, often). Weekly consumption of fresh vegetables, fresh fruits, meat, and coarse grains was classified as follows: fresh vegetables (0 kg/wk, < 2.5 kg/wk, or ≥ 2.5 kg/wk); fresh fruits (0 kg/wk, < 1.25 kg/wk, or ≥ 1.25 kg/wk); meat (0 kg/wk, < 0.35 kg/wk, or ≥ 0.35 kg/wk), and coarse grains (0 kg/wk, < 0.5 kg/wk, or ≥ 0.5 kg/wk).

Living habits included smoking, alcohol consumption, and physical activity. Smoking was defined as having smoked > 1 cigarette/d for > 6 consecutive or cumulative months, and smoking cessation was defined as not having smoked for ≥ 2 years. Thus, smoking was classified into three levels: never smoker (no), current smoker (yes), and ever smoker but currently not a smoker (quit smoking). Drinking alcohol was defined as having consumed an average of at least 1 drink/wk for > 6 mo, and abstinence was defined as not having had a drink for ≥ 1 year. Thus, alcohol consumption was classified into three levels: never drinker (no), current drinker (yes), and ever drinker but currently abstaining (quit drinking). Physical activity was defined as effective physical activity of > 30 min/session, with an average of ≥ 3

sessions/wk, and was categorized into two levels: ≤ 3 times/wk (no) and > 3 times/wk (yes). Family history was categorized as no family history of CRC (no) and a family history of CRC (yes).

Diagnosis of participants with a high risk of CRC

The diagnosis of participants with a high risk of CRC was made by at least two experienced anorectal surgeons who were experts in the field, based on the following conditions: (1) A positive test for fecal occult blood[21]; (2) a first-degree relative with a history of CRC[22]; (3) a history of intestinal polyps or adenomas[23]; (4) a history of cancer or other malignancies[24]; (5) a change in bowel habits[25]; and (6) any two of the following conditions: chronic diarrhea, chronic constipation, mucus bloody stools, a history of chronic appendicitis or appendectomy, a history of chronic cholecystitis or cholecystectomy, and chronic mental depression[24]. Participants were diagnosed as having a high risk of CRC if they had any one of the conditions from 1 to 5 and any two of the conditions listed in 6. After a series of evaluations, those without any of the above conditions were not considered high risk for CRC.

Statistical analysis

We used χ^2 tests to assess the characteristic differences in baseline data, 2014-2017 separately, between the high-risk and non-high-risk groups. Cluster analysis was used to categorize the participants based on their dietary and living habits as either having a healthy or an unhealthy lifestyle. A healthy lifestyle was considered an intake of fresh vegetables, fresh fruits, and coarse grains and participation in physical activity. An unhealthy lifestyle was considered an intake of meat, pickled and sun-cured food, oily food, and double-salted food; smoking; and alcohol consumption. A random sampling method was used to allocate the participants to a training set or a validation set in the ratio of 7:3. Each participant was considered as a randomized unit with the same probability of being selected. We performed a multifactorial logistic regression analysis by introducing variables with $P < 0.05$ as independent predictor variables into the training set. The strength of the association between predictors and participants with a high risk of CRC was assessed by calculating the ORs and 95%CIs. Meaningful variables were selected based on a backward Wald logistic regression analysis and were used to construct a nomogram model. The discriminative ability, predictive accuracy, and clinical value of the model were evaluated by constructing and analyzing the ROC and calibration curves and by performing decision curve analysis (DCA). Five hundred bootstrap resamples were used to reduce overfitting bias. All of the statistical analyses were conducted using R (version 4.3.0) and SPSS (version 25.0), and $P < 0.05$ was considered to indicate statistical significance.

RESULTS

Basic characteristics and risk factors of participants at high risk for CRC

Table 1 shows the basic information, dietary habits, living habits, and family histories of both groups in 2014-2017. Compared with the CRC non-high-risk group, the basic information revealed that the CRC high-risk group had more men and the participants were older, and had higher BMI and WC. The dietary habits data revealed that the CRC high-risk group had a lower weekly intake of fresh vegetables, fresh fruits, and coarse grains; had a higher weekly intake of meat; had more participants with double-salt taste and high oil consumption; and consumed pickled and sun-cured foods more frequently. Furthermore, participants in the CRC high-risk group were more likely to smoke, drink alcohol, and not perform physical activity. The family history data showed that the CRC high-risk group typically had a family history of the disease.

A cluster analysis of the dietary and living habits of all the participants was performed to categorize them as having a healthy or unhealthy lifestyle. A healthy lifestyle was considered an intake of fresh vegetables, fresh fruits, and coarse grains and participation in physical activities. An unhealthy lifestyle was considered an intake of meat and pickled and sun-cured foods, high oil consumption, a double-salt taste, smoking, and alcohol consumption. The analysis revealed that 39134 (61.2%) participants had a healthy lifestyle and 24783 (38.8%) had an unhealthy lifestyle. All of the participants were then randomly divided into a training set (n = 44743) and a validation set (n = 19175) in a 7:3 ratio.

Table 2 shows the results of univariate and multivariate analyses of the training set. The univariate analysis indicated that BMI and WC were significantly associated with a high risk of CRC, as was lifestyle and family history. The backward Wald logistic regression model, after excluding variables with $P > 0.05$, demonstrated that there were five predictors associated with a high risk of CRC: age, BMI, WC, lifestyle, and family history (Figure 1).

Development and validation of a nomogram model for early screening of individuals with a high risk of CRC

A nomogram for the early screening of individuals at high risk of CRC was constructed based on a logistic regression model (Figure 1). To estimate the probability of high-risk CRC individuals being detected during early screening, each predictor observation was assigned a certain number of points by drawing a vertical line toward the vertex table. The sum of the points for each variable corresponded to the probability of an individual being identified during early screening as having a high risk of CRC. Finally, we analyzed the 500 resamples using the bootstrap method and determined the AUC of the nomogram model as 0.734 for the validation set (Figure 2A) and 0.735 for the training set (Figure 2B). The calibration curves demonstrated good agreement between the actual observations in the model validation set (Figure 3A) and training set (Figure 3B). The DCA of the validation set (Figure 4A) and training set (Figure 4B) indicated that the model has potential clinical value.

Table 1 Basic information, dietary habits, living habits, and family history of colorectal cancer high-risk and non-high-risk groups in 2014-2017

Variable		2014		*P* value	2015		*P* value	2016		*P* value	2017		*P* value
Basic information		Non-high risk group, *n* (%)	High risk group, *n* (%)		Non-high risk group, *n* (%)	High risk group, *n* (%)		Non-high risk group, *n* (%)	High risk group, *n* (%)		Non-high risk group, *n* (%)	High risk group, *n* (%)	
Sex	Male	8514 (43.24)	888 (43.94)	0.545	14277 (53.80)	1486 (57.46)	0.0002	2359 (54.82)	711 (54.61)	0.892	3276 (56.68)	899 (50.70)	0.004
	Female	11177 (56.76)	1133 (56.06)		12260 (46.20)	1092 (42.36)		1944 (45.18)	591 (45.39)		2504 (43.32)	807 (47.30)	
Age (yr)	≤ 65	16311 (82.83)	1573 (77.83)	< 0.001	22960 (86.52)	2139 (82.97)	< 0.001	3186 (74.04)	979 (75.19)	0.405	4499 (77.84)	1287 (75.44)	0.038
	> 65	3380 (17.17)	448 (22.17)		3577 (13.48)	439 (17.03)		1117 (25.96)	323 (24.81)		1281 (22.16)	419 (24.56)	
Ethnicity	The Han nationality	19641 (99.75)	2015 (99.70)	0.717	26474 (99.76)	2572 (99.77)	0.963	4298 (99.88)	1302 (100)	0.219	5766 (99.76)	1701 (99.71)	0.714
	Other	50 (0.25)	6 (0.30)		63 (0.24)	6 (0.23)		5 (0.12)	0 (0.00)		14 (0.24)	5 (0.29)	
BMI (kg/m^2)	< 18.50	541 (2.75)	46 (2.28)	< 0.001	644 (2.43)	59 (2.29)	< 0.001	104 (2.42)	26 (2.00)	< 0.001	132 (2.28)	33 (1.93)	< 0.001
	18.50-23.99	10988 (55.80)	869 (43.00)		16050 (60.48)	1211 (46.97)		2497 (28.03)	694 (53.30)		3376 (58.41)	852 (49.94)	
	24-27.99	6899 (35.04)	773 (38.25)		8586 (32.35)	1011 (39.22)		1502 (34.91)	444 (34.10)		1971 (34.10)	650 (38.10)	
	≥ 28.00	1263 (6.41)	333 (16.48)		1257 (4.74)	297 (11.52)		200 (4.65)	138 (10.60)		301 (5.21)	171 (10.02)	
WC (cm)	≤ 80	10038 (50.98)	762 (37.70)	< 0.001	14239 (53.66)	1139 (44.18)	< 0.001	2225 (51.71)	650 (49.92)	0.259	2951 (51.06)	830 (48.65)	0.081
	> 80	9653 (49.02)	1259 (62.30)		12298 (46.34)	1439 (55.82)		2078 (48.29)	652 (50.08)		2829 (48.94)	876 (51.35)	
Dietary habit													
Fresh vegetables (kg/wk)	0	79 (0.40)	20 (0.99)	< 0.001	151 (0.57)	18 (0.70)	< 0.001	22 (0.51)	10 (0.77)	< 0.001	16 (0.28)	14 (0.82)	< 0.001
	< 2.5	8839 (44.89)	1265 (62.59)		14860 (56.00)	1727 (66.99)		2386 (55.45)	952 (73.12)		3329 (57.60)	1188 (69.64)	
	≥ 2.5	10773 (54.71)	736 (36.42)		11526 (43.43)	833 (32.31)		1895 (44.04)	340 (26.11)		2435 (42.13)	504 (29.54)	
Fresh fruits (kg/wk)	0	472 (2.40)	71 (3.51)	< 0.001	457 (1.72)	228 (8.84)	< 0.001	61 (1.42)	39 (3.00)	< 0.001	62 (1.07)	51 (2.99)	< 0.001
	< 1.25	12209 (62.00)	1496 (74.02)		17073 (64.34)	1793 (69.55)		2722 (63.26)	998 (76.65)		4080 (70.59)	1312 (76.91)	
	≥ 1.25	7010 (35.60)	454 (22.46)		9007 (33.94)	557 (21.61)		1520 (35.32)	265 (20.35)		1638 (28.34)	343 (20.11)	
Meat (kg/wk)	0	641 (3.26)	103 (5.10)	< 0.001	427 (1.61)	49 (1.90)	< 0.001	54 (1.25)	17 (1.31)	0.843	64 (1.11)	22 (1.29)	< 0.001
	< 0.35	12542 (63.69)	1047 (51.81)		17393 (65.54)	1179 (45.73)		2781 (64.63)	830 (63.75)		4123 (71.33)	1075 (63.01)	
	≥ 0.35	6508 (33.05)	871 (43.10)		8717 (32.85)	1350 (52.37)		1468 (34.12)	455 (34.95)		1593 (27.56)	609 (35.70)	

Coarse grains (kg/wk)	0	1090 (5.54)	203 (10.04)	< 0.001	1309 (4.93)	437 (16.95)	< 0.001	296 (6.88)	227 (17.43)	< 0.001	164 (2.84)	133 (7.80)	< 0.001
	< 0.5	13140 (66.73)	1535 (75.95)		18394 (69.31)	1714 (66.49)		2937 (68.25)	947 (72.73)		4277 (74.00)	1314 (77.02)	
	≥ 0.5	5461 (27.73)	283 (14.00)		6834 (25.75)	427 (16.56)		1070 (24.87)	128 (9.83)		1339 (23.17)	259 (15.18)	
Taste	Double salt	2492 (12.66)	522 (25.83)	< 0.001	3073 (11.58)	985 (38.21)	< 0.001	965 (22.43)	754 (57.91)	< 0.001	803 (13.89)	620 (36.34)	< 0.001
	Moderate	13520 (68.66)	1183 (58.54)		19823 (74.70)	1239 (48.06)		2905 (67.51)	482 (37.02)		4351 (75.28)	882 (51.70)	
	Light	3679 (18.68)	316 (15.64)		3641 (13.72)	354 (13.73)		433 (10.06)	66 (5.07)		626 (10.83)	204 (11.96)	
Oil consumption	High oil consumption	1597 (8.11)	536 (26.52)	< 0.001	2311 (8.71)	981 (38.05)	< 0.001	604 (14.04)	585 (44.93)	< 0.001	620 (10.73)	639 (37.46)	< 0.001
	Moderate oil consumption	15323 (77.82)	1271 (62.89)		21196 (79.87)	1364 (52.91)		3318 (77.11)	657 (50.46)		4699(81.30)	921 (53.99)	
	Low oil consumption	2771 (14.07)	214 (10.59)		3030 (11.42)	233 (9.04)		381 (8.85)	60 (4.61)		461 (7.98)	146 (8.56)	
Pickled and sun-cured food	Never	1805 (9.17)	161 (7.97)	< 0.001	1964 (7.40)	138 (5.35)	< 0.001	290 (6.74)	48 (3.69)	< 0.001	550 (9.52)	63 (3.69)	< 0.001
	Sometimes	15686 (79.66)	1385 (68.53)		20894 (78.74)	1430 (55.47)		3114 (72.37)	561 (43.09)		4480 (77.51)	1098 (64.36)	
	Often	2200 (11.17)	475 (23.50)		3679 (13.86)	1010 (39.18)		899 (20.89)	693 (53.23)		750 (12.98)	545 (31.95)	
Living habit													
Smoking	No	14265 (72.44)	1358 (67.19)	< 0.001	21116 (79.57)	1682 (65.24)	< 0.001	3180 (73.90)	810 (62.21)	< 0.001	4338 (75.05)	1047 (61.37)	<0.001
	Yes	4401 (22.35)	521 (25.78)		4445 (16.75)	724 (28.08)		839 (19.50)	364 (27.96)		1127 (19.50)	482 (28.25)	
	Quit smoking	1025 (5.21)	142 (7.03)		976 (3.68)	172 (6.67)		284 (6.60)	128 (9.83)		315 (5.45)	177 (10.38)	
Alcohol drinking	No	14190 (72.06)	1287 (63.68)	< 0.001	20691 (77.97)	1523 (59.08)	< 0.001	3148 (73.16)	789 (60.60)	< 0.001	4352 (75.29)	986 (57.80)	< 0.001
	Yes	4885 (24.81)	647 (32.01)		5177 (19.51)	903 (35.03)		997 (23.17)	445 (34.18)		1247 (21.57)	619 (36.28)	
	Quit drinking	616 (3.13)	87 (4.30)		668 (2.52)	152 (5.90)		158 (3.67)	68 (5.22)		181 (3.13)	101 (5.92)	
Physical activities	No	9188 (46.66)	1094 (54.13)	< 0.001	11132 (41.95)	1477 (57.29)	< 0.001	1917 (44.55)	845 (64.90)	< 0.001	2865 (49.57)	917 (53.75)	0.002
	Yes	10503 (53.34)	927 (45.87)		15405 (58.05)	1101 (42.71)		2386 (55.45)	457 (35.10)		2915 (50.43)	789 (46.25)	
Family history	No	14438 (73.32)	1032 (51.06)	< 0.001	21524 (81.11)	1174 (45.54)	< 0.001	2960 (68.79)	527 (40.48)	< 0.001	3660 (63.32)	486 (28.49)	< 0.001
	Yes	5253 (26.68)	9989 (48.94)		5013 (18.89)	1404 (54.46)		1343 (31.21)	775 (59.52)		2120 (36.68)	1220 (71.51)	

BMI: Body mass index; WC: Waist circumference.

Table 2 Univariate and multivariate analyses of the training set

Variables	Univariate analysis			Multivariate analysis		
	OR	95%CI	*P* value	OR	95%CI	*P* value
Age (≤ 65 yr *vs* >65 yr)	1.03	1.02-1.03	< 0.001	1.03	1.02-1.03	< 0.001
Sex (male *vs* female)	0.98	0.93-1.04	0.540			
Ethnicity (Han nationality *vs* other)	0.90	0.48-1.67	0.731			
BMI (< 18.50 kg/m^2, 18.50-23.99 kg/m^2, 24-27.99 kg/m^2 *vs* ≥ 28.00 kg/m^2)	1.07	1.06-1.08	< 0.001	1.05	1.04-1.06	< 0.001
WC (≤ 80 cm *vs* > 80 cm)	1.03	1.02-1.03	< 0.001	1.02	1.01-1.02	< 0.001
Family history (no *vs* yes)	4.28	4.04-4.54	< 0.001	4.30	4.04-4.56	< 0.001
Lifestyle (unhealthy lifestyle *vs* healthy lifestyle)	0.45	0.42-0.48	< 0.001	0.44	0.41-0.47	< 0.001

BMI: Body mass index; WC: Waist circumference.

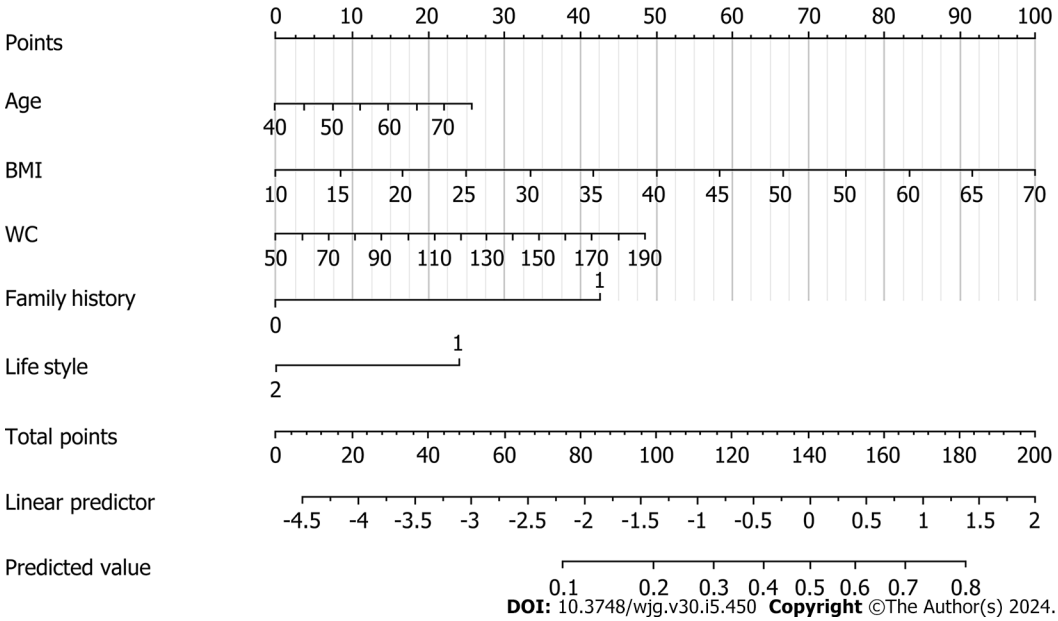

DOI: 10.3748/wjg.v30.i5.450

Figure 1 Nomogram for predicting early screening of individuals at high risk of colorectal cancer. The value of each variable was scored on a point scale from 0 to 100, after which the scores for each variable were added together. The total sum was located on the total points axis, which enabled us to predict the probability of early screening of individuals at high risk of colorectal cancer. Age, body mass index, and waist circumference were used as continuous variables. The family history group 0 = no and 1 = yes, and lifestyle group 1 = unhealthy lifestyle and 2 = healthy lifestyle. BMI: Body mass index; WC: Waist circumference.

DISCUSSION

Our findings indicated that age, BMI, WC, family history, and lifestyle significantly contributed to the prediction of individuals at high risk for CRC. Therefore, these variables were used to validate an early screening model for individuals at high risk for CRC, and the model demonstrated potential clinical utility.

Compared with the current study, a multicenter study combining genetic and environmental risk scores for risk stratification of early-onset CRC[16] placed more emphasis on scores for polygene variants, environmental factors, and lifestyle. The results showed that an increase in the lifestyle score was associated with an increase in the relative risk of early-onset CRC, in line with our findings, which demonstrated a significant association between lifestyle and high risk for CRC. However, unlike this multicenter study, our study incorporated dietary habits in addition to living habits and family history to assess lifestyle. We found five factors to be significantly associated with high risk for CRC, two of which were non-modifiable variables (age and family history), in line with previous findings[22,26]. A healthy lifestyle had an OR of 0.44 (95%CI: 0.41-0.47) in individuals at high risk of CRC, indicating that a healthy lifestyle is a protective factor.

A similar study found that in addition to a high intake of red and processed meat, sex, ethnicity, sedentary lifestyle, and inflammatory bowel disease were associated with a low, intermediate, and high risk of early-onset CRC[27]. The study was a meta-analysis of the literature retrieved from PubMed and Web of Science. Eighteen articles were screened for inclusion, and 10 were ultimately reviewed to afford baseline data on the case group (n = 32843) and control group (n

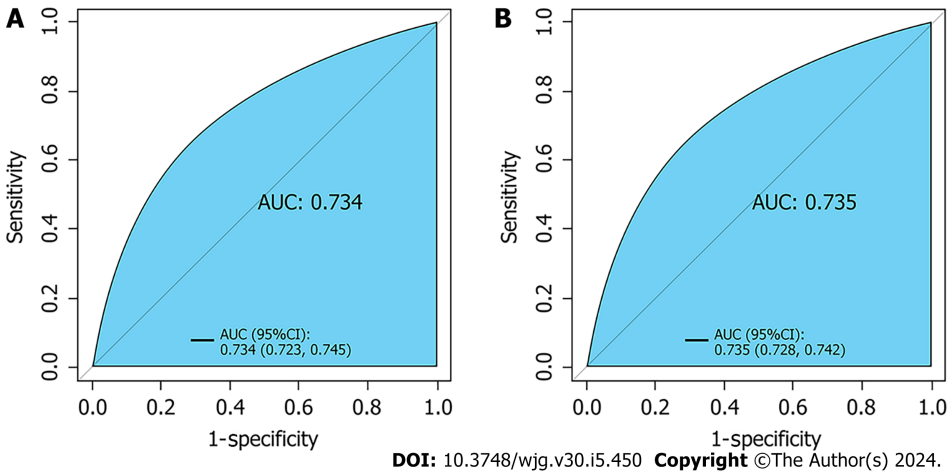

Figure 2 Receiver operating characteristic curves curve for predicting early screening of individuals at high risk of colorectal cancer. A: Validation set: Receiver operating characteristic curves (ROC) curve for the nomogram generated using bootstrap resampling (500 times); B: Training set: ROC curve for the nomogram generated using bootstrap resampling (500 times). AUC: Area under the curve.

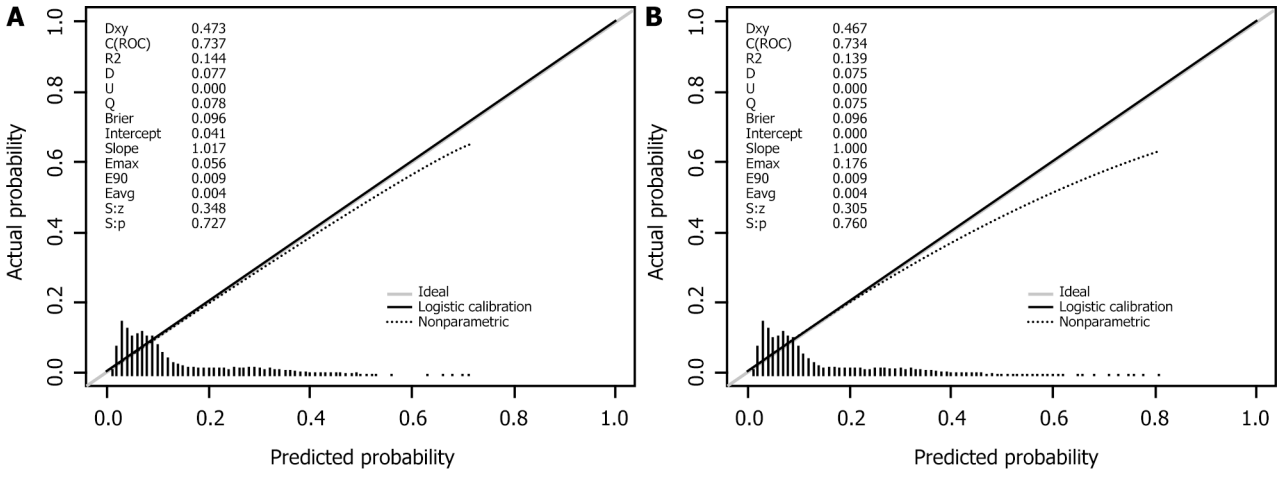

Figure 3 Calibration pot for predicting early screening of individuals at high risk of colorectal cancer. A: Validation set nomogram calibration plot; B: Training set nomogram calibration plot. When the solid line (performance nomogram) is closer to the dotted line (ideal model), the prediction accuracy of the nomogram is better.

= 25806408), which were used to construct a risk assessment model. Risk factors associated with early-onset CRC in the baseline data were screened by meta-analysis, and those with $P < 0.05$ were included in the final model. The model differed from ours in that it categorized the population into low-, intermediate-, and high-risk groups based on risk trend scores. Moreover, their participants were < 50 years of age, thus predominantly comprising young adults. In contrast, the current study consisted of a wider range of age groups, although primarily focusing on those aged 40-74 years. It aimed to develop a prediction model that would enable accurate primary screening of groups at high risk for CRC.

One of the major strengths of our study was that it integrated multiple factors including age, sex, ethnicity, BMI, WC, healthy and unhealthy lifestyle, and family history. Second, our sample size, which was obtained from the population in Ningbo, Zhejiang, China, was large. Third, compared with other models, our model enabled better and earlier screening of CRC in high-risk populations in Ningbo. In addition, previous studies have demonstrated that CRC development can be prevented by altering the modifiable risk factors[28]. In our model, all of the risk factors, except age and family history, could be modified by improving lifestyle habits, changing dietary habits, and increasing physical activities. Age and family history are non-modifiable variables and must be carefully examined in early screening of CRC, especially because they are inextricably linked to CRC development[22,26]. Therefore, the combination of modifiable and non-modifiable risk factors in our model can help facilitate early screening of individuals at high risk for CRC. Furthermore, our model makes it easier to screen patients for CRC risk than colonoscopy, which can be painful and complex. The Colorectal Cancer Early Screening Model can also be convenient for clinicians and may help them improve the rate of clinical diagnosis and reduce the rate of underdiagnosis of CRC in high-risk populations.

However, this study had some limitations. First, given that the study population was from a single region in China (Ningbo, Zhejiang), the model lacked generalizability. China is a large country with differences in living environments, lifestyles and habits, diets, and cultures. Second, although we examined four risk factors, there are many other factors

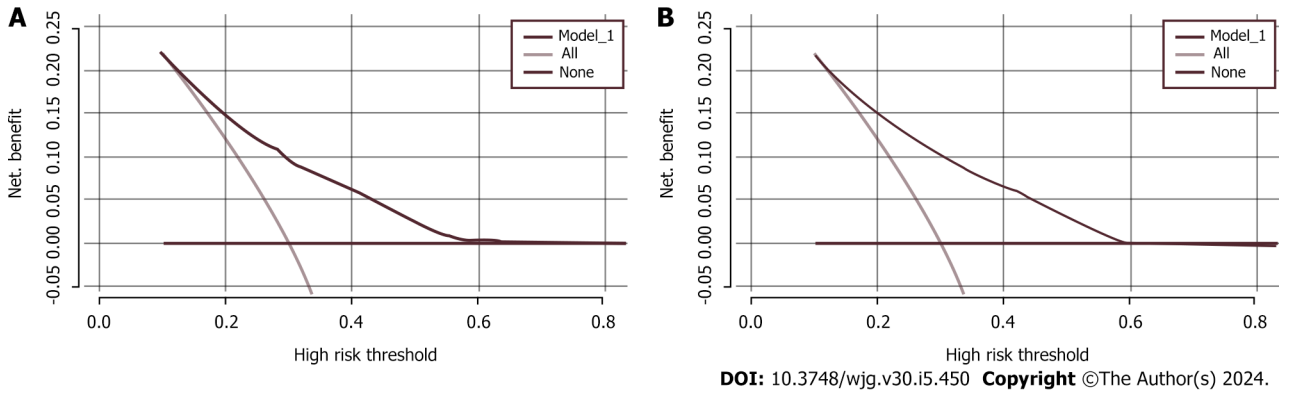

DOI: 10.3748/wjg.v30.i5.450

Figure 4 Decision curve analysis for predicting early screening of individuals at high risk of colorectal cancer. A: Decision curve analysis (DCA) of the validation set prediction model; B: DCA of the training set prediction model. Red solid lines indicate the prediction models, gray solid lines indicate all populations at high risk for colorectal cancer (CRC), and solid horizontal lines indicate non-high-risk populations for CRC. The graph depicts the expected net gain for each individual relative to the high-risk CRC Nuo plot forecast. Net gain increases with the model curve.

associated with dietary habits, living habits, and family history, and our study design could not incorporate them all. Therefore, future studies should include more variables to further validate our model. Third, our model did not include emotional and psychological factors. It is worth noting that a relationship between mental trauma and CRC has been reported in previous studies[29]. Although the exact mechanism underlying this relationship remains unclear, it may be because great mental trauma leads to neurological dysfunction, resulting in bowel disorders and stress ulcers, ultimately leading to the development of malignant intestinal lesions. Alternatively, excessive mental stress weakens the immune system, thereby increasing the susceptibility to disorders of the intestinal flora and the risk of developing CRC[30]. Therefore, future studies must examine the effect of emotional and psychological factors on CRC risk.

CONCLUSION

This study showed that older age, a high BMI, a large WC, an unhealthy lifestyle, and a family history of CRC are significantly associated with a high risk of CRC. A CRC risk-prediction model was also developed for accurate primary screening of groups with a high risk of CRC. This model could enable clinicians to develop early CRC screening strategies and may support public health campaigns for reducing CRC deaths and disease burden.

ARTICLE HIGHLIGHTS

Research background

The establishment of early screening model for high risk of colorectal cancer (CRC) may become a potential new method for early screening. It is different from traditional invasive screening and is a noninvasive, simple and rapid screening methods. Although there are many studies on early screening model for high risk of CRC, there is still a lack of large sample size studies and clinical validation. Our study focused on collecting information in the general population who attended annual health checks. At the same time, this is also the first study with a large sample size for early screening for CRC in Ningbo, China, which was part of national early screening for CRC.

Research motivation

Constructing an early screening model for CRC high-risk groups by means of basic information such as lifestyle has gradually become a major topic in CRC early screening research, which is mainly aimed at solving the problem of the more complicated means of early screening for colorectal cancer high-risk groups.

Research objectives

This study aimed to establish an efficient early screening model to identify individuals at high risk of CRC, and reduce CRC prevalence and mortality.

Research methods

This retrospective study included data from the health screening population in Ningbo Hospital, China from 2014 to 2017 to analyze the basic information, living habits and dietary habits, so that the early screening model of CRC was constructed and conducted for internal verification.

Research results

Retrospective analysis of 63918 individuals eligible for health screening, comprising studies with seven variables. The area under the curve was 0.734 [95% confidence interval (CI): 0.723-0.745] for the final validation set receiver operating characteristic curve (ROC) and 0.735 (95%CI: 0.728-0.742) for the training set ROC curve. The calibration curve demonstrated a high correlation between the CRC high-risk population predicted by the nomogram model and the actual CRC high-risk population.

Research conclusions

This study has an early screening model for high risk of CRC based on basic population information, lifestyle and family history.

Research perspectives

This study has the potential to revolutionize primary detection by accurately identifying groups at high risk of developing CRC.

ACKNOWLEDGEMENTS

The authors would like to thank the participants and participating doctors at Ningbo No. 2 Hospital; Ningbo Institute of Life and Health Science, University of Chinese Academy of Sciences; and students of Medical College of Soochow University, all of whom were staff members of this study.

FOOTNOTES

Co-first authors: Ling-Li Xu and Yi Lin.

Co-corresponding authors: Jian-Jiong Li and Xiao-Yu Dai.

Author contributions: Xu LL, Lin Y, Li JJ and Dai XY participated in the study design; Xu LL and Lin Y statistically analyzed, interpreted, and drafted the manuscript; Xu LL and Lin Y revised the manuscript; Han LY and Wang Y contributed to data collection and organization; all authors contributed to the revision of the final manuscript and approved the final version of the manuscript; Li JJ and Dai XY provided financial support and study supervision.

Supported by the Project of NINGBO Leading Medical Health Discipline, No. 2022-B11; Ningbo Natural Science Foundation, No. 202003N4206; and Public Welfare Foundation of Ningbo, No. 2021S108.

Institutional review board statement: This study was reviewed and approved by the Ethics Committee of the Ningbo No. 2 Hospital.

Informed consent statement: All involved persons gave their informed written consent prior to study inclusion and any and all details that might disclose the identity of the subjects under study were omitted.

Conflict-of-interest statement: The authors declare no potential conflicts of interest.

Data sharing statement: No additional data are available.

Country/Territory of origin: China

ORCID number: Ling-Li Xu 0009-0000-1178-8102; Yi Lin 0000-0003-4417-9455; Li-Yuan Han 0000-0001-9532-5622; Yue Wang 0009-0002-1146-0072; Jian-Jiong Li 0000-0001-6054-4745; Xiao-Yu Dai 0000-0003-3630-6039.

S-Editor: Gong ZM
L-Editor: A
P-Editor: Cai YX

REFERENCES

1 **Baidoun F**, Elshiwy K, Elkeraie Y, Merjaneh Z, Khoudari G, Sarmini MT, Gad M, Al-Husseini M, Saad A. Colorectal Cancer Epidemiology: Recent Trends and Impact on Outcomes. *Curr Drug Targets* 2021; **22**: 998-1009 [PMID: 33208072 DOI: 10.2174/1389450121999201117115717]

2 **GBD 2019 Colorectal Cancer Collaborators**. Global, regional, and national burden of colorectal cancer and its risk factors, 1990-2019: a systematic analysis for the Global Burden of Disease Study 2019. *Lancet Gastroenterol Hepatol* 2022; **7**: 627-647 [PMID: 35397795 DOI: 10.1016/S2468-1253(22)00044-9]

3 **Rocke KD**. Colorectal Cancer Knowledge and Awareness Among University Students in a Caribbean Territory: a Cross-sectional Study. *J Cancer Educ* 2020; **35**: 571-578 [PMID: 30798462 DOI: 10.1007/s13187-019-01499-1]

4 **Jin Y**, Zheng MC, Yang X, Chen TL, Zhang JE. Patient delay to diagnosis and its predictors among colorectal cancer patients: A cross-sectional study based on the Theory of Planned Behavior. *Eur J Oncol Nurs* 2022; **60**: 102174 [PMID: 35952459 DOI: 10.1016/j.ejon.2022.102174]

5 **Park L**, O'Connell K, Herzog K, Chatila W, Walch H, Palmaira RLD, Cercek A, Shia J, Shike M, Markowitz AJ, Garcia-Aguilar J, Schattner MA, Kantor ED, Du M, Mendelsohn RB. Clinical features of young onset colorectal cancer patients from a large cohort at a single cancer center. *Int J Colorectal Dis* 2022; **37**: 2511-2516 [PMID: 36441197 DOI: 10.1007/s00384-022-04286-5]

6 **Wu W**, Huang J, Tan S, Wong MCS, Xu W. Screening methods for colorectal cancer in Chinese populations. *Hong Kong Med J* 2022; **28**: 183-185 [PMID: 35470808 DOI: 10.12809/hkmj219917]

7 **Imperiale TF**, Monahan PO, Stump TE, Glowinski EA, Ransohoff DF. Derivation and Validation of a Scoring System to Stratify Risk for Advanced Colorectal Neoplasia in Asymptomatic Adults: A Cross-sectional Study. *Ann Intern Med* 2015; **163**: 339-346 [PMID: 26259154 DOI: 10.7326/M14-1720]

8 **Kaminski MF**, Polkowski M, Kraszewska E, Rupinski M, Butruk E, Regula J. A score to estimate the likelihood of detecting advanced colorectal neoplasia at colonoscopy. *Gut* 2014; **63**: 1112-1119 [PMID: 24385598 DOI: 10.1136/gutjnl-2013-304965]

9 **Tao S**, Hoffmeister M, Brenner H. Development and validation of a scoring system to identify individuals at high risk for advanced colorectal neoplasms who should undergo colonoscopy screening. *Clin Gastroenterol Hepatol* 2014; **12**: 478-485 [PMID: 24022090 DOI: 10.1016/j.cgh.2013.08.042]

10 **Wong MC**, Lam TY, Tsoi KK, Hirai HW, Chan VC, Ching JY, Chan FK, Sung JJ. A validated tool to predict colorectal neoplasia and inform screening choice for asymptomatic subjects. *Gut* 2014; **63**: 1130-1136 [PMID: 24045331 DOI: 10.1136/gutjnl-2013-305639]

11 **Sung JJY**, Wong MCS, Lam TYT, Tsoi KKF, Chan VCW, Cheung W, Ching JYL. A modified colorectal screening score for prediction of advanced neoplasia: A prospective study of 5744 subjects. *J Gastroenterol Hepatol* 2018; **33**: 187-194 [PMID: 28561279 DOI: 10.1111/jgh.13835]

12 **Cai QC**, Yu ED, Xiao Y, Bai WY, Chen X, He LP, Yang YX, Zhou PH, Jiang XL, Xu HM, Fan H, Ge ZZ, Lv NH, Huang ZG, Li YM, Ma SR, Chen J, Li YQ, Xu JM, Xiang P, Yang L, Lin FL, Li ZS. Derivation and validation of a prediction rule for estimating advanced colorectal neoplasm risk in average-risk Chinese. *Am J Epidemiol* 2012; **175**: 584-593 [PMID: 22328705 DOI: 10.1093/aje/kwr337]

13 **Song M**, Garrett WS, Chan AT. Nutrients, foods, and colorectal cancer prevention. *Gastroenterology* 2015; **148**: 1244-60.e16 [PMID: 25575572 DOI: 10.1053/j.gastro.2014.12.035]

14 **Wang C**, Miller SM, Egleston BL, Hay JL, Weinberg DS. Beliefs about the causes of breast and colorectal cancer among women in the general population. *Cancer Causes Control* 2010; **21**: 99-107 [PMID: 19787437 DOI: 10.1007/s10552-009-9439-3]

15 **Ahmad R**, Singh JK, Wunnava A, Al-Obeed O, Abdulla M, Srivastava SK. Emerging trends in colorectal cancer: Dysregulated signaling pathways (Review). *Int J Mol Med* 2021; **47** [PMID: 33655327 DOI: 10.3892/ijmm.2021.4847]

16 **Archambault AN**, Jeon J, Lin Y, Thomas M, Harrison TA, Bishop DT, Brenner H, Casey G, Chan AT, Chang-Claude J, Figueiredo JC, Gallinger S, Gruber SB, Gunter MJ, Guo F, Hoffmeister M, Jenkins MA, Keku TO, Le Marchand L, Li L, Moreno V, Newcomb PA, Pai R, Parfrey PS, Rennert G, Sakoda LC, Lee JK, Slattery ML, Song M, Win AK, Woods MO, Murphy N, Campbell PT, Su YR, Lansdorp-Vogelaar I, Peterse EFP, Cao Y, Zeleniuch-Jacquotte A, Liang PS, Du M, Corley DA, Hsu L, Peters U, Hayes RB. Risk Stratification for Early-Onset Colorectal Cancer Using a Combination of Genetic and Environmental Risk Scores: An International Multi-Center Study. *J Natl Cancer Inst* 2022; **114**: 528-539 [PMID: 35026030 DOI: 10.1093/jnci/djac003]

17 **Peng YN**, Huang ML, Kao CH. Prevalence of Depression and Anxiety in Colorectal Cancer Patients: A Literature Review. *Int J Environ Res Public Health* 2019; **16** [PMID: 30709020 DOI: 10.3390/ijerph16030411]

18 **Boi-Dsane NAA**, Amarh V, Tsatsu SE, Bachelle SV, Bediako-Bowan AAA, Koney NK, Dzudzor B. Cross-Sectional Study for Investigation of the Association Between Modifiable Risk Factors and Gastrointestinal Cancers at a Tertiary Hospital in Ghana. *Cancer Control* 2023; **30**: 10732748231155702 [PMID: 37129188 DOI: 10.1177/10732748231155702]

19 **Yao A**, Liang L, Rao H, Shen Y, Wang C, Xie S. The Clinical Characteristics and Treatments for Large Cell Carcinoma Patients Older than 65 Years Old: A Population-Based Study. *Cancers (Basel)* 2022; **14** [PMID: 36358648 DOI: 10.3390/cancers14215231]

20 **Kokkinos P**, Faselis C, Myers J, Pittaras A, Sui X, Zhang J, McAuley P, Kokkinos JP. Cardiorespiratory fitness and the paradoxical BMI-mortality risk association in male veterans. *Mayo Clin Proc* 2014; **89**: 754-762 [PMID: 24943694 DOI: 10.1016/j.mayocp.2014.01.029]

21 **Jayasinghe M**, Prathiraja O, Caldera D, Jena R, Coffie-Pierre JA, Silva MS, Siddiqui OS. Colon Cancer Screening Methods: 2023 Update. *Cureus* 2023; **15**: e37509 [PMID: 37193451 DOI: 10.7759/cureus.37509]

22 **Kastrinos F**, Samadder NJ, Burt RW. Use of Family History and Genetic Testing to Determine Risk of Colorectal Cancer. *Gastroenterology* 2020; **158**: 389-403 [PMID: 31759928 DOI: 10.1053/j.gastro.2019.11.029]

23 **Sano W**, Hirata D, Teramoto A, Iwatate M, Hattori S, Fujita M, Sano Y. Serrated polyps of the colon and rectum: Remove or not? *World J Gastroenterol* 2020; **26**: 2276-2285 [PMID: 32476792 DOI: 10.3748/wjg.v26.i19.2276]

24 **Zhu N**, Huang YQ, Song YM, Zhang SZ, Zheng S, Yuan Y. [Efficacy comparison among high risk factors questionnaire and Asia-Pacific colorectal screening score and their combinations with fecal immunochemical test in screening advanced colorectal tumor]. *Zhonghua Wei Chang Wai Ke Za Zhi* 2022; **25**: 612-620 [PMID: 35844124 DOI: 10.3760/cma.j.cn441530-20211127-00478]

25 **Siegel RL**, Jakubowski CD, Fedewa SA, Davis A, Azad NS. Colorectal Cancer in the Young: Epidemiology, Prevention, Management. *Am Soc Clin Oncol Educ Book* 2020; **40**: 1-14 [PMID: 32315236 DOI: 10.1200/EDBK_279901]

26 **Sninsky JA**, Shore BM, Lupu GV, Crockett SD. Risk Factors for Colorectal Polyps and Cancer. *Gastrointest Endosc Clin N Am* 2022; **32**: 195-213 [PMID: 35361331 DOI: 10.1016/j.giec.2021.12.008]

27 **Gu J**, Li Y, Yu J, Hu M, Ji Y, Li L, Hu C, Wei G, Huo J. A risk scoring system to predict the individual incidence of early-onset colorectal cancer. *BMC Cancer* 2022; **22**: 122 [PMID: 35093005 DOI: 10.1186/s12885-022-09238-4]

28 **Keum N**, Giovannucci E. Global burden of colorectal cancer: emerging trends, risk factors and prevention strategies. *Nat Rev Gastroenterol Hepatol* 2019; **16**: 713-732 [PMID: 31455888 DOI: 10.1038/s41575-019-0189-8]

29 **Simonton OC**, Matthews-Simonton S. Cancer and stress: counselling the cancer patient. *Med J Aust* 1981; **1**: 679, 682-683 [PMID: 7278751

DOI: 10.5694/j.1326-5377.1981.tb135959.x]
30 **Geremia A**, Arancibia-Cárcamo CV. Innate Lymphoid Cells in Intestinal Inflammation. *Front Immunol* 2017; **8**: 1296 [PMID: 29081776 DOI: 10.3389/fimmu.2017.01296]

World Journal of Gastroenterology

Submit a Manuscript: https://www.f6publishing.com

World J Gastroenterol 2024 February 7; 30(5): 462-470

DOI: 10.3748/wjg.v30.i5.462

ISSN 1007-9327 (print) ISSN 2219-2840 (online)

ORIGINAL ARTICLE

Retrospective Study

Diagnosis and treatment experience of atypical hepatic cystic echinococcosis type 1 at a tertiary center in China

Yu-Peng Li, Jie Zhang, Zhi-De Li, Chao Ma, Guang-Lei Tian, Yuan Meng, Xiong Chen, Zhi-Gang Ma

Specialty type: Gastroenterology and hepatology

Provenance and peer review: Unsolicited article; Externally peer reviewed.

Peer-review model: Single blind

Peer-review report's scientific quality classification

Grade A (Excellent): 0
Grade B (Very good): B, B
Grade C (Good): 0
Grade D (Fair): 0
Grade E (Poor): 0

P-Reviewer: Eyraud D, France; Goja S, India

Received: November 1, 2023
Peer-review started: November 1, 2023
First decision: December 6, 2023
Revised: December 19, 2023
Accepted: January 11, 2024
Article in press: January 11, 2024
Published online: February 7, 2024

Yu-Peng Li, Jie Zhang, Zhi-De Li, Chao Ma, Guang-Lei Tian, Yuan Meng, Xiong Chen, Zhi-Gang Ma, Department of Hepatobiliary Surgery, People's Hospital of Xinjiang Uygur Autonomous Region, Urumqi 830000, Xinjiang Uygur Autonomous Region, China

Corresponding author: Zhi-Gang Ma, MD, Doctor, Professor, Department of Hepatobiliary Surgery, People's Hospital of Xinjiang Uygur Autonomous Region, No. 91 Tianchi Road, Tianshan District, Urumqi 830000, Xinjiang Uygur Autonomous Region, China.
ma.zhigang@aliyun.com

Abstract

BACKGROUND

Some hydatid cysts of cystic echinococcosis type 1 (CE1) lack well-defined cyst walls or distinctive endocysts, making them difficult to differentiate from simple hepatic cysts.

AIM

To investigate the diagnostic methods for atypical hepatic CE1 and the clinical efficacy of laparoscopic surgeries.

METHODS

The clinical data of 93 patients who had a history of visiting endemic areas of CE and were diagnosed with cystic liver lesions for the first time at the People's Hospital of Xinjiang Uygur Autonomous Region (China) from January 2018 to September 2023 were retrospectively analyzed. Clinical diagnoses were made based on findings from serum immunoglobulin tests for echinococcosis, routine abdominal ultrasound, high-frequency ultrasound, abdominal computed tomography (CT) scan, and laparoscopy. Subsequent to the treatments, these patients underwent reexaminations at the outpatient clinic until October 2023. The evaluations included the diagnostic precision of diverse examinations, the efficacy of surgical approaches, and the incidence of CE recurrence.

RESULTS

All 93 patients were diagnosed with simple hepatic cysts by conventional abdominal ultrasound and abdominal CT scan. Among them, 16 patients were preoperatively diagnosed with atypical CE1, and 77 were diagnosed with simple hepatic cysts by high-frequency ultrasound. All the 16 patients preoperatively diagnosed with atypical CE1 underwent laparoscopy, of whom 14 patients were intraoperatively confirmed to have CE1, which was consistent with the postope-

rative pathological diagnosis, one patient was diagnosed with a mesothelial cyst of the liver, and the other was diagnosed with a hepatic cyst combined with local infection. Among the 77 patients who were preoperatively diagnosed with simple hepatic cysts, 4 received aspiration sclerotherapy of hepatic cysts, and 19 received laparoscopic fenestration. These patients were intraoperatively diagnosed with simple hepatic cysts. During the follow-up period, none of the 14 patients with CE1 experienced recurrence or implantation of hydatid scolices. One of the 77 patients was finally confirmed to have CE complicated with implantation to the right intercostal space.

CONCLUSION

Abdominal high-frequency ultrasound can detect CE1 hydatid cysts. The laparoscopic technique serves as a more effective diagnostic and therapeutic tool for CE.

Key Words: Hepatic echinococcosis; Hepatic cystic echinococcosis type 1; Hepatic cyst; Color Doppler ultrasound; Laparoscopy

Core Tip: This retrospective study investigated the diagnostic methods for atypical hepatic cystic echinococcosis type 1 (CE1) and evaluated the clinical efficacy of laparoscopic surgeries. In total, 93 patients were diagnosed with simple hepatic cysts by conventional abdominal ultrasound and abdominal computed tomography scan. Among them, 16 patients were preoperatively diagnosed with atypical CE1, of whom 14 were diagnosed with CE1 intraoperatively after laparoscopy. The remaining 77 patients were diagnosed with simple hepatic cysts by high-frequency ultrasound, of whom 4 patients received aspiration sclerotherapy of hepatic cysts, and 19 patients were intraoperatively diagnosed with simple hepatic cysts. Abdominal high-frequency ultrasound can detect CE1 hydatid cysts.

Citation: Li YP, Zhang J, Li ZD, Ma C, Tian GL, Meng Y, Chen X, Ma ZG. Diagnosis and treatment experience of atypical hepatic cystic echinococcosis type 1 at a tertiary center in China. *World J Gastroenterol* 2024; 30(5): 462-470
URL: https://www.wjgnet.com/1007-9327/full/v30/i5/462.htm
DOI: https://dx.doi.org/10.3748/wjg.v30.i5.462

INTRODUCTION

Humans can be affected by hepatic hydatid disease, also known as hepatic echinococcosis, by ingesting eggs from *Echinococcus granulosus* through eating contaminated food products[1]. Along with developments in animal husbandry and tourism, hepatic echinococcosis has become a worldwide epidemic disease that threatens public health and hinders social progress. Surveys organized by the World Health Organization (WHO) and Food and Agriculture Organization of the United Nations indicated that alveolar echinococcosis and cystic echinococcosis are the second and third most common foodborne parasitic diseases, respectively[2,3]. The average prevalence of echinococcosis is 1.08% among the population in western China. Globally, the disease affects approximately 66 million people, resulting in an annual economic loss of around 400 million US dollars[4]. Echinococcosis may further aggravate the economic burden in low-income regions. Early-stage hepatic echinococcosis lacks specific clinical symptoms. Some patients may have already missed the opportunity of treatment at the time of diagnosis, leading to a marked deterioration in their quality of life and premature death[5-7]. In endemic areas of hepatic echinococcosis, surgery is the most effective treatment[8]. Given the distinct biological features of this disease, only a few patients with hepatic echinococcosis can receive standardized diagnosis and treatment. This explains the high incidence of complications and high recurrence rate of hepatic echinococcosis, further increasing the likelihood of repeated surgeries. The WHO-Informal Working Group on Echinococcosis (WHO/IWGE) divided cystic echinococcosis (CE) into six types (WHO classification)[9]. CE type 1 (CE1) is defined as a unilocular anechoic cystic lesion, presenting with a hydatid cyst wall and an endocyst that are distinctly demarcated from the surrounding liver tissues. However, some patients with CE1 exhibit atypical clinical manifestations, and findings from laboratory tests and radiographic examinations may not align with typical patterns. In specific cases of CE1, hydatid cysts may lack clearly defined cyst walls or characteristic endocysts. It is challenging to differentiate these lesions from simple hepatic cysts. Erroneous diagnosis and treatment of atypical CE1 may lead to grim consequences[10]. For instance, some atypical CE1 lesions are misdiagnosed and surgically treated as simple hepatic cysts, resulting in the spillage of hydatid fluid, or even anaphylactic shock and death. Developing appropriate diagnostic and therapeutic approaches for atypical CE1 hydatid cysts is of great importance.

In the present study, a high-frequency linear array transducer (5.0-12 MHz) was utilized to scan patients with a history of visiting CE endemic areas. The patients were diagnosed with hepatic cysts by conventional abdominal ultrasound (convex array probe, 3.5-5.0 MHz) and abdominal computed tomography (CT). The purpose was to improve the diagnostic rate of atypical CE1. Laparoscopic procedures were performed to verify the diagnosis of atypical CE1 and to deliver a less invasive treatment, in order to reduce the misdiagnosis rate and the risks associated with potential delays in treatment.

MATERIALS AND METHODS

Subjects

From January 2018 to September 2023, 93 patients received treatments for simple hepatic cysts at the People's Hospital of Xinjiang Uygur Autonomous Region (Urumqi, China). All patients had a history of visiting CE endemic areas. Furthermore, they were diagnosed with simple hepatic cysts for the first time and had no prior history of treatment for these lesions or a record of undergoing abdominal surgery.

Examination methods

Medical history inquiry, physical examinations, and laboratory tests: The main complaints and findings from physical and abdominal examinations were collected. The results of routine blood tests, liver function tests, tumor marker tests, and serum immunoglobulin tests for echinococcosis (colloidal gold-based immunochromatographic strip assay, Colloidal Gold Diagnostic Kit for Echinococcosis by Xinjiang Hydatid Clinical Research Institute, China) were obtained.

Radiographic examinations: Ultrasound scan was performed using the GE LOGIQ E9 ultrasound scanner (GE HealthCare Technologies, Inc., Chicago, IL, United States) and the Philips iu22 ultrasound machine (Philips Healthcare, Best, Netherlands), with a convex array probe for conventional abdominal ultrasound (3.5-5.0 MHz). Upon discovery of hepatic cystic lesions, we changed the convex array probe to the high-frequency linear array transducer (5.0-12 MHz), which allowed for a multi-directional observation of whether the cystic lesion had localized cyst wall thickening or a bilayered wall. If the high-frequency linear array transducer only delivered a limited penetrating power, there would be a change back to the convex array transducer for local magnification to observe whether there was a bilayered wall or local cyst wall thickening.

Abdominal CT scanning was carried out using the Philips 128-slice spiral CT scanner, with a slice thickness of 3 mm and a spacing of 5 mm. Before CT scanning, the patient drank 1000-1500 mL clear water and lay on their back. The CT was performed in the supine position to observe whether the upper and lower layers of the cyst fluid in the simple hepatic lesions had uneven density.

Treatment methods

Patients identified with distinctive signs of hepatic cystic lesions using color Doppler ultrasound, and subsequently diagnosed with atypical CE1, underwent laparoscopic exploration to determine the optimal surgical approach.

Patients received laparotomic/laparoscopic endocystectomy plus partial ectocystectomy or laparotomic/laparoscopic cystectomy if they met the following conditions: (1) The average hydatid cyst diameter was > 5 cm; (2) The average hydatid cyst diameter was ≤ 5 cm , and the lesion was located in the first and second hepatic hila; and (3) The average hydatid cyst diameter was ≤ 5 cm , and patients could not tolerate medication or had poor medication compliance or were unable to tolerate percutaneous-aspiration-injection-reaspiration (PAIR).

Laparoscopic endocystectomy plus partial or intact ectocystectomy was performed as follows: After general anesthesia, a prophylactic intravenous injection of 100 mg of hydrocortisone was given to prevent allergy. The pneumoperitoneum pressure was 10-12 mmHg. Five trocars were placed in the abdominal wall, with the observing trocar situated above the umbilicus and the operating trocars arranged in a fan-shaped pattern, concentrating on the lesion at the center. Gauze soaked with hypertonic saline (20%) was placed around the hydatid cysts to isolate them from abdominal organs. For lesions with thin-walled ectocysts and high tension, aspiration was carried out at the highest point in the cyst wall relative to the body position to aspirate the cyst fluid and to decompress the lesions (the diameter of the aspiration device was small, and the device was connected to a strong negative pressure). An echinococcosis rotary cutter was placed through the aspiration orifice to fully aspirate the cyst content. The cyst was flushed with 20% hypertonic saline, and caution was taken to prevent spillage of cyst content. The ectocyst wall was excised with an ultrasound knife, with preservation of the segment near vital blood vessels that proved challenging for removal. During laparoscopic examination, any identified points of bile leakage in the hydatid cyst wall were closed with 4-0 vascular sutures, if necessary. If leakage still existed after suturing, choledochotomy was performed for T-tube drainage. The gauze saturated with hypertonic saline was carefully placed inside a specimen pouch alongside the ectocyst wall, ensuring no contamination of the pouch exterior. A drainage tube was indwelled in the residual cavity. None of the patients required oral albendazole after intact ectocystectomy. For those receiving laparoscopic endocystectomy plus partial ectocystectomy, these patients received oral albendazole tablets at the daily dose of 10-15 mg/kg (in two equally divided doses) after normal liver function was restored. Each cycle of albendazole treatment lasted 1 month, and 3-6 cycles of treatment were delivered. Two cycles were administered, 7-10 d apart.

Patients diagnosed with asymptomatic simple hepatic cysts received no specific treatments except for follow-up observation.

Patients diagnosed with symptomatic simple hepatic cysts exceeding 5 cm and located in the liver parenchyma underwent aspiration sclerotherapy. Percutaneous liver aspiration was conducted to aspirate the fluid from the cyst, followed by injection of sclerosing agent (absolute alcohol, lauromacrogol). Laparoscopic fenestration of the hepatic cysts was performed for shallow-lying cysts with a larger volume and located no more than 1 cm from the liver capsule. The cyst fluid was aspirated using an aspiration needle under the laparoscope. After checking for the bile leakage point, sclerotherapy was administered by injecting absolute alcohol or lauromacrogol. The lesion was soaked in the sclerosing agent for several minutes before the sclerosing agent was aspirated. The cyst wall protruding outside the liver parenchyma was resected using an ultrasound knife.

Follow-up

Patients with CE received outpatient follow-up once every 3-6 months, and those with simple hepatic cysts received follow-up once every 6-12 months. Patients underwent abdominal ultrasound and liver function tests during the follow-up period until October 2023.

Statistical analysis

Statistical analysis was conducted using SPSS 25.0 software (IBM, Armonk, NY, United States). Quantitative data obeying a normal distribution were expressed as mean ± SD; otherwise, they were presented as median with interquartile range (IQR) (25^{th} and 75^{th}). Pairwise comparisons were conducted using analysis of variance or the Chi-square test. A *P* value less than 0.05 was considered statistically significant.

RESULTS

Patients' general data

A total of 93 patients were recruited, including 30 men and 63 women aged 56.6 ± 12.3 years. All of these patients had a history of visiting CE endemic areas. In addition, 30 patients presented with distension and discomfort in the upper abdomen; 63 patients were found to have nonspecific signs and symptoms, including hepatic cysts during physical check-up.

Serum immunology test for echinococcosis

Among the 93 patients, 21 and 72 patients were CE-positive and CE-negative, respectively.

Radiographic examination

All 93 patients were diagnosed with simple hepatic cysts by abdominal CT scanning (Figure 1A), with a CT value of 6.1 ± 3.4 Hounsfield Units. Notably, 79 patients had single lesions and 14 patients had multiple lesions, and the largest lesion had a diameter of 8.3 ± 3.4 cm. All 93 patients were diagnosed with simple hepatic cysts by color Doppler ultrasound (convex array transducer, 3.5-5.0 MHz) (Figure 1B). Color Doppler ultrasound using a linear array transducer (5.0-12 MHz) identified the double-line sign in the top of the cystic lesion or locally thickened cyst wall in 16 patients (Figure 2). For these patients, the final diagnosis was atypical CE1. Among them, 12 patients had single lesions, and 4 patients had multiple lesions. In addition, 77 patients were diagnosed with simple hepatic cysts.

Treatments and surgical situation

In this study, 16 patients, who were diagnosed with atypical CE1 by color Doppler ultrasound (linear array transducer, 5.0-12 MHz), underwent laparoscopy. Furthermore, 14 patients were intraoperatively diagnosed with CE1, which was consistent with the postoperative pathological diagnosis. One patient was diagnosed with a mesothelial cyst of the liver, and another patient was diagnosed with a hepatic cyst combined with local infection. Among the 14 patients who were intraoperatively diagnosed with CE1, 8 patients underwent laparoscopic endocystectomy plus partial ectocystectomy, 4 patients underwent intact laparoscopic ectocystectomy, and 2 patients underwent open endocystectomy plus intact ectocystectomy. In these 14 patients, the operation time was 3.8 ± 1.0 h, the intraoperative blood loss was 200 (IQR: 125, 350) mL, and the intraoperative blood transfusion volume was 200 (IQR: 125, 350) mL. Furthermore, 2 patients received intraoperative blood transfusion. Of these 14 patients who were intraoperatively diagnosed with CE, 3 were found to have a bile leakage point in the residual cyst wall near the first hepatic hilum after the cyst fluid was completely aspirated intraoperatively. The closure of leaks in these patients involved suturing, followed by the placement of a T-tube for drainage of the common bile duct. In the 14 patients with CE, duration of the abdominal drainage tube was 5.5 (IQR: 4.75, 8.25) d, and the hospital stay was 7.0 (IQR: 5.5, 12.0) d. Additionally, 2 patients experienced post-surgical peritoneal effusion, which was successfully treated by aspiration and drainage.

Among the 77 patients who were diagnosed with simple hepatic cysts, 23 patients had abdominal distension and discomfort, as well as a hepatic cyst greater than 5 cm. Notably, 4 of these 77 patients received aspiration sclerotherapy of hepatic cysts, and 19 patients underwent laparoscopic fenestration. These patients were operatively diagnosed with simple hepatic cysts.

Follow-up

Notably, 14 patients with atypical CE1 received postoperative follow-up for 36.5 (IQR: 15, 50.5) months. No patients were lost to follow-up, and there were no instances of hydatid cyst recurrence or abdominal implantation.

The cohort of 77 patients, initially diagnosed with simple hepatic cysts preoperatively, included one case initially classified as atypical CE1. However, intraoperative confirmation revealed it to be a simple hepatic cyst accompanied by a local infection. The entire cohort underwent a comprehensive follow-up for 26 (IQR: 6, 44.5) months. Among the 77 patients who were preoperatively diagnosed with simple hepatic cysts, one patient later received aspiration sclerotherapy of an intrahepatic lesion (Figure 3). However, this case was diagnosed with CE2 one year after surgery during the follow-up period. There was one lesion implanted in the right intercostal space (Figure 3) and treated by open endocystectomy (Figure 4) plus partial ectocystectomy and removal of the hydatid cyst in the right intercostal space (hydatid cyst combined with bile leakage). No recurrence was found during the 55 months of postoperative follow-up. No misdiagnoses occurred in the remaining 76 patients with simple hepatic cysts during follow-up.

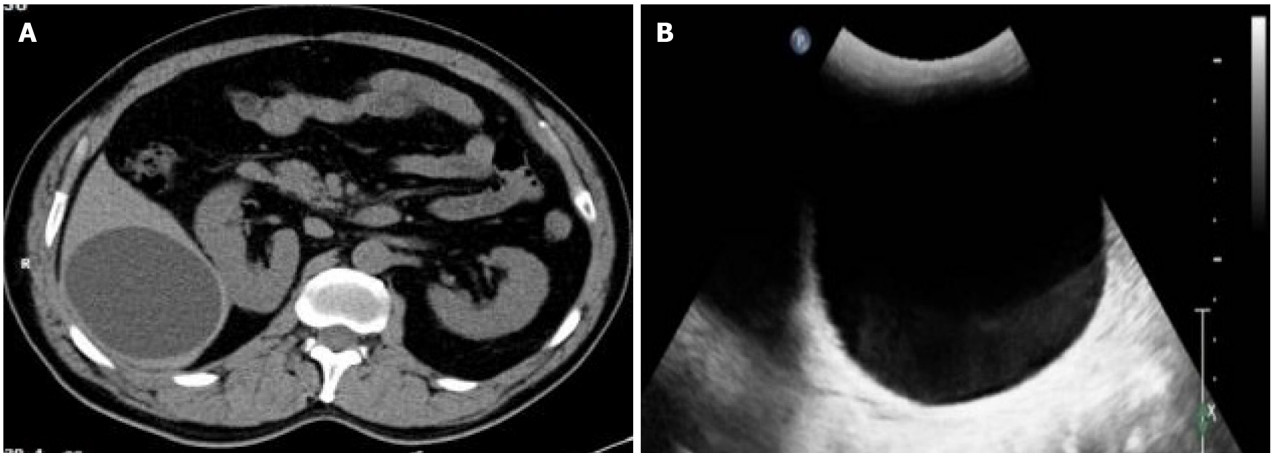

DOI: 10.3748/wjg.v30.i5.462

Figure 1 Hepatic cyst diagnosis. A: Cystic echinococcosis type 1 (CE1) lesion, which was diagnosed as hepatic cyst by computed tomography; B: CE1 lesion, which was diagnosed as hepatic cyst by ultrasound.

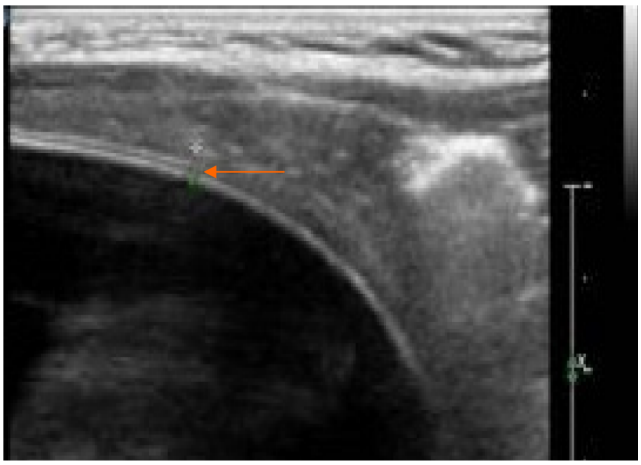

DOI: 10.3748/wjg.v30.i5.462

Figure 2 Hydatid cyst with a localized bilayered wall (arrowhead) detected by a linear array transducer.

One patient, who was preoperatively diagnosed with atypical CE1, was subsequently found to have a mesothelial cyst of the liver by surgery and pathological diagnosis. No recurrence was identified during the 56 months of follow-up.

DISCUSSION

In CE endemic areas, correct diagnostic and therapeutic measures are closely associated with CE-affected patients' health and economic benefits. Color Doppler ultrasound is the preferred option for diagnosing CE[11], and it outperforms CT and magnetic resonance imaging for CE1[12]. However, according to our clinical experience, endocysts may be invisible on abdominal color Doppler ultrasound (convex array transducer, 3.5-5.0 MHz) and abdominal spiral CT scan in some CE1 lesions. CE1 is likely to be misdiagnosed as a simple hepatic cyst, and it is therefore called "atypical CE1". Atypical lesions may be explained by the unique pathological mechanisms involved in the occurrence and development of CE. A fibrous capsule around the hydatid cyst is formed by fibroblasts, and persistent fibrous hyperplasia progresses to create a fibrous wall, identified as the ectocyst. During the early stages of ectocyst formation, fibrous hyperplasia may not be prominently expressed and may manifest as a quasi-circular hypodense lesion on multi-row spiral CT scanning. These lesions typically exhibit smooth edges and it is challenging to differentiate them from the surrounding liver parenchyma. The characteristics observed on the CT scan align with those commonly associated with simple hepatic cysts. There is mainly a lack of a well-defined cyst wall or a bilayered wall that indicates the presence of an endocyst and an ectocyst.

The present study enrolled 93 patients diagnosed with CE for the first time, each with a history of visiting endemic CE areas. All were diagnosed with simple hepatic cysts by spiral CT scanning and abdominal color Doppler ultrasound. Using a linear array transducer, CE1 was diagnosed in 16 cases, and 14 of them were confirmed either by surgery or follow-up observation. The diagnostic accuracy was 87.5%. One patient with a mesothelial cyst of the liver and one case of simple hepatic cyst with local infection were found to have the specific sign of the "bilayered wall" using the linear

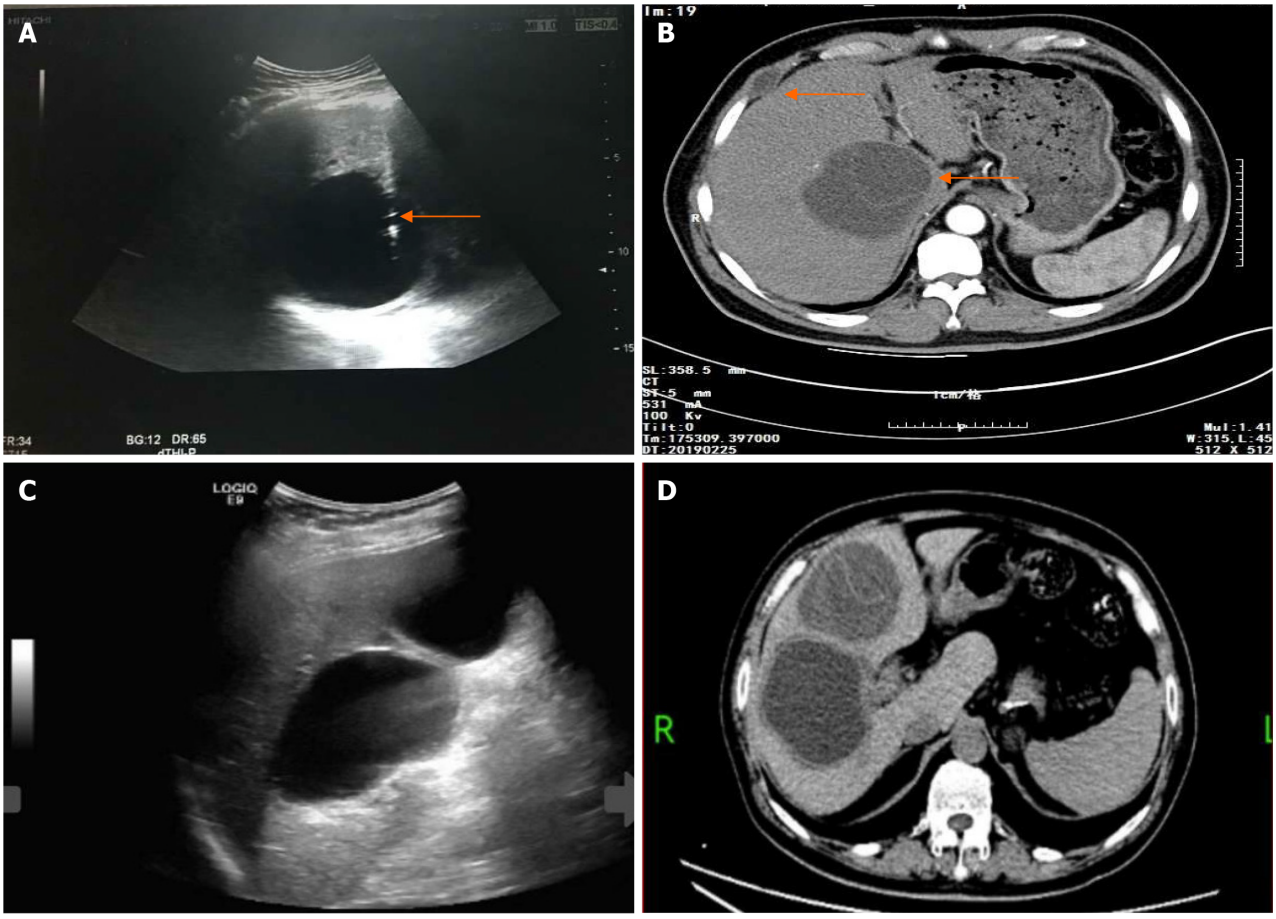

DOI: 10.3748/wjg.v30.i5.462

Figure 3 Hepatic cyst diagnosis and treatment. A: Cystic echinococcosis type 1 (CE1) misdiagnosed as a hepatic cyst and treated by percutaneous aspiration, the arrowhead indicating the aspiration needle; B: Post-treatment follow-up revealing recurrence of a hepatic hydatid cyst (arrowhead) with hydatid implanted in the intercostal space (arrowhead); C: Conventional ultrasound diagnosing two simple hepatic cysts; D: Follow-up examination confirming the diagnosis of CE compressing the right hepatic pedicle.

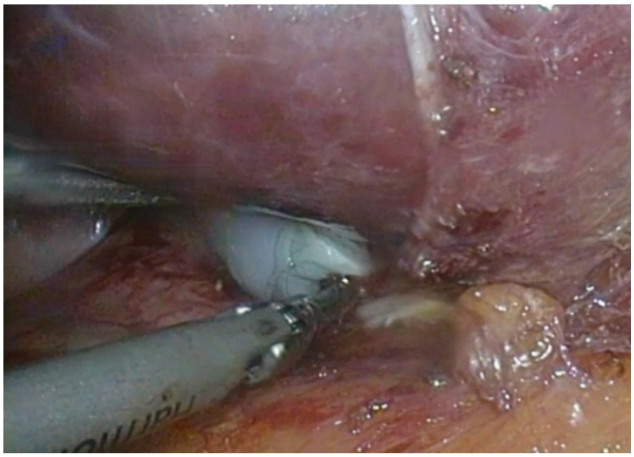

DOI: 10.3748/wjg.v30.i5.462

Figure 4 Endocyst of cystic echinococcosis type 1 under the laparoscope.

array transducer. Fortunately, the misdiagnosis in this case did not lead to adverse outcomes. Among the 77 patients who were diagnosed with simple hepatic cysts using the linear array transducer, one patient receiving aspiration and drainage of the hepatic cyst was found to have CE during the follow-up period. The above results may be explained by limitations of the linear array transducer itself, although the possibility of cystic lesion (CL) could not be completely ruled out at the first diagnosis. The CL-type hydatid cyst is rare and the diagnosis is generally difficult[13]. During sonography, the diagnosis of a simple hepatic cyst is often made if there are multiple lesions (two or more). However, in the present study,

among 15 patients with CE, 11 patients had single lesions and 4 had multiple lesions. Among the 77 patients diagnosed with simple hepatic cysts, 67 patients had single lesions and 10 had multiple lesions (two or more). The distribution of multiple lesions did not significantly differ between the two diseases (P = 0.177, F = 1.821). In addition, one patient was found to have two hepatic cystic lesions at first diagnosis, and both abdominal CT scanning and routine abdominal ultrasound (convex array transducer) diagnosed the lesions as simple hepatic cysts. This patient was not further examined using a linear array transducer. Two years later, the patient was admitted to hospital due to abdominal distension and pain. The diagnosis of CE Type 2 (CE2) was made, and the lesion size was enlarged, which was closely related to the right hepatic pedicle in the first hepatic hilum. This patient subsequently underwent open endocystectomy plus partial ectocystectomy, and suffered from residual cavity of hydatid cyst with bile leakage. A drainage tube was placed in the residual cavity for 40 d and a T-tube in the common bile duct for 2 months. The likelihood of misdiagnosis of CE can be reduced by the supplementary utilization of a linear array transducer during the ultrasound examination of hepatic cystic lesions, and by rectifying the empirical idea that multiple cystic lesions are generally simple hepatic cysts.

Colloidal gold-based immunochromatographic strip assay is an important method for the differential diagnosis of CE, with a sensitivity above 85% and a specificity above 85%[4]. In the present study, among 15 patients with CE, 10 (66.7%) were positive for antibodies against *Echinococcus* and 5 (33.3%) were negative. Among the 77 patients with simple hepatic cysts, 11 (14.3%) were positive for antibodies against *Echinococcus* and 66 (85.7%) were negative. The sensitivity of the colloidal gold-based immunochromatographic strip assay for detecting antibodies against *Echinococcus* was lower than that reported previously, while the specificity was comparable. For simple hepatic cysts causing compression, they can be treated by fenestration. Specifically, aspiration and drainage are performed at the superficial site of the liver and in the thin wall of the cyst and lower pole of the lesion, with resection of parts of the cyst wall. However, the aforementioned procedure contradicts surgical principles for CE. If a patient is misdiagnosed and receives surgery for simple hepatic cysts rather than surgery for atypical CE1, this may lead to extensive implantation of hydatid scolices in the abdomen, or even anaphylactic shock and death. In the present study, one patient was diagnosed with simple hepatic cyst upon admission and received aspiration and drainage. However, during the follow-up period, CE was confirmed in this patient and complicated with implantation of hydatid scolices in the intercostal space. It is noteworthy that this patient was negative for antibodies against *Echinococcus* at first diagnosis. For patients with hepatic cysts and a history of visiting endemic CE areas, CE may still be suspected even if patients are negative for antibodies against *Echinococcus*.

With development in laparoscopy in the field of liver surgery, this technology has demonstrated notable success in treating CE. Cugat *et al*[14] reviewed the data of hepatic echinococcosis treatment in 74 patients. Yagci G *et al*[15] retrospectively analyzed the data of 355 patients undergoing surgery for hepatic echinococcosis over a 10-year period, and they confirmed the safety and effectiveness of laparoscopy. Casulli *et al*[16] presented a case of cerebral CE in a child, along with a comparative molecular analysis of the isolated cyst specimens from the patient and sheep from local farms. Bakinowska *et al*[17] reported the surgical treatment of three different cases of pulmonary echinococcosis. They demonstrated that simple small pulmonary echinococcal lesions could be excised using endostaplers. Mfingwana *et al*[18] described a pediatric cohort diagnosed with pulmonary CE and treated with a combination of medical and surgical therapy. In endemic areas of hepatic echinococcosis, laparoscopy should be performed for hepatic cysts that are highly suspected to be CE, as a diagnostic and therapeutic tool. In the present study, of 2 patients who were preoperatively diagnosed with CE1, laparoscopy confirmed the diagnosis of hepatic cyst in one patient and the diagnosis of a mesothelial cyst of the liver in the other. Thus, the risk of long-term utilization of oral albendazole was avoided, and these patients markedly benefited from laparoscopy. According to the Synopsis of Echinococcosis Diagnosis and Treatment developed by the WHO-IWGE, PAIR is a less invasive and easy-to-use method to diagnose and treat CE. This treatment is recommended for countries and regions that are not fully equipped for surgery, especially for the treatment of CE1[9]. According to our clinical experience, PAIR is recommended for small, deep-lying CE lesions. However, for superficial lesions, PAIR is likely to cause implantation of hydatid scolices in the abdomen or along the puncture path. Besides, PAIR cannot eliminate endocysts, and residual endocysts may lead to infections, typically requiring further aspiration or surgery. In the present study, 4 of 15 patients with CE were found to have bile leakage points in the hydatid cyst wall, which could not be closed by PAIR. These patients may require further surgery due to bile leakage from the cyst cavity.

The mortality of untreated CE is 2%-4%[11]. Early diagnosis and appropriate treatment of CE are highly important for patients' prognosis. Differential diagnosis of atypical CE1 and simple hepatic cysts is necessary for patients with hepatic cysts who have a history of visiting endemic CE areas. A linear array transducer can facilitate the early detection of a bilayered wall or local wall thickening in cysts during color Doppler ultrasound, even before the differential sign becomes fully visible. The combined utilization of a linear array transducer, a convex array transducer, and serum immunoglobulin test for CE can enhance the diagnostic accuracy and reduce the likelihood of missed diagnoses. In cases where differentiation remains challenging using the aforementioned methods, it is recommended that patients undergo laparoscopic procedures to mitigate the potential risk of severe adverse outcomes.

CONCLUSION

Abdominal high-frequency ultrasound can detect CE1 hydatid cysts. Laparoscopy serves as an effective diagnostic and therapeutic tool for CE.

ARTICLE HIGHLIGHTS

Research background

Given the distinct biological features of this disease, only a few patients with hepatic echinococcosis can receive standardized diagnosis and treatment. Some patients with cystic echinococcosis type 1 (CE1) exhibit atypical clinical manifestations, and findings from laboratory tests and radiographic examinations may not align with typical patterns. In specific cases of CE1, hydatid cysts may lack clearly defined cyst walls or characteristic endocysts. It is challenging to differentiate these lesions from simple hepatic cysts. Erroneous diagnosis and treatment of atypical CE1 may lead to grim consequences.

Research motivation

Developing appropriate diagnostic and therapeutic approaches for atypical CE1 hydatid cysts is of great importance.

Research objectives

The purpose of this study was to improve the diagnostic rate of atypical CE1. Laparoscopic procedures were performed to verify the diagnosis of atypical CE1 and to deliver a less invasive treatment, in order to reduce the misdiagnosis rate and the risks associated with potential delays in treatment.

Research methods

Ninety-three patients who received treatments for simple hepatic cysts at the People's Hospital of Xinjiang Uygur Autonomous Region (Urumqi, China) from January 2018 to September 2023 were enrolled in the study. The clinical diagnoses were made based on findings from serum immunoglobulin tests for echinococcosis, routine abdominal ultrasound, high-frequency ultrasound, abdominal computed tomography (CT) scanning, and laparoscopy. Subsequent to treatments, patients with CE were followed up once every 3-6 months, and those with simple hepatic cysts once every 6-12 months. Patients underwent abdominal ultrasound and liver function tests during the follow-up period until October 2023.

Research results

Among the 93 patients, 21 and 72 patients were CE-positive and CE-negative, respectively. All 93 patients were diagnosed with simple hepatic cysts by conventional abdominal ultrasound and abdominal CT scanning. Among them, 16 patients were preoperatively diagnosed with atypical CE1, and 77 were diagnosed with simple hepatic cysts by high-frequency ultrasound. All the 16 patients preoperatively diagnosed with atypical CE1 underwent laparoscopy, of whom 14 patients were intraoperatively confirmed to have CE1, which was consistent with the postoperative pathological diagnosis, one patient was diagnosed with a mesothelial cyst of the liver, and the other was diagnosed with a hepatic cyst combined with local infection. Among the 77 patients who were preoperatively diagnosed with simple hepatic cysts, 4 received aspiration sclerotherapy of hepatic cysts, and 19 received laparoscopic fenestration. These patients were intraoperatively diagnosed with simple hepatic cysts. During the follow-up period, none of the 14 patients with CE1 experienced recurrence or implantation of hydatid scolices. One of the 77 patients was finally confirmed to have CE complicated with implantation to the right intercostal space.

Research conclusions

Abdominal high-frequency ultrasound can detect CE1 hydatid cysts. Laparoscopy serves as an effective diagnostic and therapeutic tool for CE.

Research perspectives

Our findings remain to be further verified by randomized clinical trials.

FOOTNOTES

Author contributions: Li Y designed and performed the research and wrote the manuscript; Ma Z designed the research and supervised the manuscript preparation; Zhang J, Li Z, and Ma C designed the research and contributed to the data analysis; Tian G, Meng Y, and Chen X provided clinical advice; all authors have read and approved the final manuscript to be published.

Institutional review board statement: The protocol was approved by the Ethics Committee of People's Hospital of Xinjiang Uygur Autonomous Region, China.

Informed consent statement: The informed consent was obtained from the subject(s) and/or guardian(s).

Conflict-of-interest statement: The authors declare that there is no conflict of interest.

Data sharing statement: Technical appendix, statistical code, and dataset are accessible through the corresponding author. Participants provided informed consent for sharing their data.

Country/Territory of origin: China

ORCID number: Yu-Peng Li 0009-0000-8930-5457; Zhi-De Li 0000-0002-7780-8337; Guang-Lei Tian 0000-0003-3166-7245; Yuan Meng 0000-0002-2188-527X; Xiong Chen 0000-0003-4209-3797; Zhi-Gang Ma 0000-0003-4412-7487.

S-Editor: Gong ZM
L-Editor: A
P-Editor: Zhao S

REFERENCES

1 **Zhou S**, Wan L, Shao Y, Ying C, Wang Y, Zou D, Xia W, Chen Y. Detection of aortic rupture using post-mortem computed tomography and post-mortem computed tomography angiography by cardiac puncture. *Int J Legal Med* 2016; **130**: 469-474 [PMID: 25773916 DOI: 10.1007/s00414-015-1171-9]
2 **Casulli A**. Recognising the substantial burden of neglected pandemics cystic and alveolar echinococcosis. *Lancet Glob Health* 2020; **8**: e470-e471 [PMID: 32199112 DOI: 10.1016/S2214-109X(20)30066-8]
3 **WHO**. Integrating neglected tropical diseases into global health and development: fourth WHO report on neglected tropical diseases. 2017. Available from: http://apps.who.int/iris/bitstream/handle/10665/255013/WHOHTM-NTD-20170·2-eng.pdf?sequence=1&isAllowed=y
4 **Chinese Doctor Association**, Chinese College of Surgeons (CCS); Chinese Committee for Hadytidology (CCH). Expert consensus on diagnosis and treatment of hepatic cystic and alveolar echinococcosis (2019 edition). *Zhonghua Xiaohua Waike Zazhi* 2019; 18: 71121 [DOI: 10.3760/cma.j.issn.1673-9752.2019.08.002]
5 **McManus DP**, Gray DJ, Zhang W, Yang Y. Diagnosis, treatment, and management of echinococcosis. *BMJ* 2012; **344**: e3866 [PMID: 22689886 DOI: 10.1136/bmj.e3866]
6 **Paternoster G**, Boo G, Wang C, Minbaeva G, Usubalieva J, Raimkulov KM, Zhoroev A, Abdykerimov KK, Kronenberg PA, Müllhaupt B, Furrer R, Deplazes P, Torgerson PR. Epidemic cystic and alveolar echinococcosis in Kyrgyzstan: an analysis of national surveillance data. *Lancet Glob Health* 2020; **8**: e603-e611 [PMID: 32199126 DOI: 10.1016/S2214-109X(20)30038-3]
7 **Tamarozzi F**, Akhan O, Cretu CM, Vutova K, Akinci D, Chipeva R, Ciftci T, Constantin CM, Fabiani M, Golemanov B, Janta D, Mihailescu P, Muhtarov M, Orsten S, Petrutescu M, Pezzotti P, Popa AC, Popa LG, Popa MI, Velev V, Siles-Lucas M, Brunetti E, Casulli A. Prevalence of abdominal cystic echinococcosis in rural Bulgaria, Romania, and Turkey: a cross-sectional, ultrasound-based, population study from the HERACLES project. *Lancet Infect Dis* 2018; **18**: 769-778 [PMID: 29793823 DOI: 10.1016/S1473-3099(18)30221-4]
8 **Dziri C**, Haouet K, Fingerhut A, Zaouche A. Management of cystic echinococcosis complications and dissemination: where is the evidence? *World J Surg* 2009; **33**: 1266-1273 [PMID: 19350321 DOI: 10.1007/s00268-009-9982-9]
9 **WHO Informal Working Group**. International classification of ultrasound images in cystic echinococcosis for application in clinical and field epidemiological settings. *Acta Trop* 2003; **85**: 253-261 [PMID: 12606104 DOI: 10.1016/s0001-706x(02)00223-1]
10 **Mihmanli M**, Idiz UO, Kaya C, Demir U, Bostanci O, Omeroglu S, Bozkurt E. Current status of diagnosis and treatment of hepatic echinococcosis. *World J Hepatol* 2016; **8**: 1169-1181 [PMID: 27729953 DOI: 10.4254/wjh.v8.i28.1169]
11 **Wen H**, Vuitton L, Tuxun T, Li J, Vuitton DA, Zhang W, McManus DP. Echinococcosis: Advances in the 21st Century. *Clin Microbiol Rev* 2019; **32** [PMID: 30760475 DOI: 10.1128/CMR.00075-18]
12 **Brunetti E**, Kern P, Vuitton DA; Writing Panel for the WHO-IWGE. Expert consensus for the diagnosis and treatment of cystic and alveolar echinococcosis in humans. *Acta Trop* 2010; **114**: 1-16 [PMID: 19931502 DOI: 10.1016/j.actatropica.2009.11.001]
13 **Brunetti E**, Tamarozzi F, Macpherson C, Filice C, Piontek MS, Kabaalioglu A, Dong Y, Atkinson N, Richter J, Schreiber-Dietrich D, Dietrich CF. Ultrasound and Cystic Echinococcosis. *Ultrasound Int Open* 2018; **4**: E70-E78 [PMID: 30364890 DOI: 10.1055/a-0650-3807]
14 **Cugat E**, Olsina JJ, Rotellar F, Artigas V, Suárez MA, Moreno-Sanz C, Herrera J, Noguera J, Figueras J, Díaz-Luis H, Güell M, Balsells J. [Initial results of the National Registry of Laparoscopic Liver Surgery]. *Cir Esp* 2005; **78**: 152-160 [PMID: 16420816 DOI: 10.1016/s0009-739x(05)70909-x]
15 **Yagci G**, Ustunsoz B, Kaymakcioglu N, Bozlar U, Gorgulu S, Simsek A, Akdeniz A, Cetiner S, Tufan T. Results of surgical, laparoscopic, and percutaneous treatment for hydatid disease of the liver: 10 years experience with 355 patients. *World J Surg* 2005; **29**: 1670-1679 [PMID: 16311852 DOI: 10.1007/s00268-005-0058-1]
16 **Casulli A**, Pane S, Randi F, Scaramozzino P, Carvelli A, Marras CE, Carai A, Santoro A, Santolamazza F, Tamarozzi F, Putignani L. Primary cerebral cystic echinococcosis in a child from Roman countryside: Source attribution and scoping review of cases from the literature. *PLoS Negl Trop Dis* 2023; **17**: e0011612 [PMID: 37669300 DOI: 10.1371/journal.pntd.0011612]
17 **Bakinowska E**, Kostopanagiotou K, Wojtyś ME, Kiełbowski K, Ptaszyński K, Gajić D, Ruszel N, Wójcik J, Grodzki T, Tomos P. Basic Operative Tactics for Pulmonary Echinococcosis in the Era of Endostaplers and Energy Devices. *Medicina (Kaunas)* 2023; **59** [PMID: 36984545 DOI: 10.3390/medicina59030543]
18 **Mfingwana L**, Goussard P, van Wyk L, Morrison J, Gie AG, Mohammed RAA, Janson JT, Wagenaar R, Ismail Z, Schubert P. Pulmonary Echinococcus in children: A descriptive study in a LMIC. *Pediatr Pulmonol* 2022; **57**: 1173-1179 [PMID: 35122423 DOI: 10.1002/ppul.25854]

World Journal of Gastroenterology

Submit a Manuscript: https://www.f6publishing.com

World J Gastroenterol 2024 February 7; 30(5): 471-484

DOI: 10.3748/wjg.v30.i5.471

ISSN 1007-9327 (print) ISSN 2219-2840 (online)

ORIGINAL ARTICLE

Basic Study

Recombinant adeno-associated virus 8-mediated inhibition of microRNA let-7a ameliorates sclerosing cholangitis in a clinically relevant mouse model

Hui Hua, Qian-Qian Zhao, Miriam Nkesichi Kalagbor, Guo-Zhi Yu, Man Liu, Zheng-Rui Bian, Bei-Bei Zhang, Qian Yu, Yin-Hai Xu, Ren-Xian Tang, Kui-Yang Zheng, Chao Yan

Specialty type: Gastroenterology and hepatology

Provenance and peer review: Invited article; Externally peer reviewed.

Peer-review model: Single blind

Peer-review report's scientific quality classification

Grade A (Excellent): 0
Grade B (Very good): B
Grade C (Good): 0
Grade D (Fair): 0
Grade E (Poor): 0

P-Reviewer: Kotlyarov S, Russia

Received: October 7, 2023
Peer-review started: October 7, 2023
First decision: December 8, 2023
Revised: December 17, 2023
Accepted: January 12, 2024
Article in press: January 12, 2024
Published online: February 7, 2024

Hui Hua, Qian-Qian Zhao, Miriam Nkesichi Kalagbor, Guo-Zhi Yu, Man Liu, Zheng-Rui Bian, Bei-Bei Zhang, Qian Yu, Ren-Xian Tang, Kui-Yang Zheng, Chao Yan, Jiangsu Key Laboratory of Immunity and Metabolism, Department of Pathogenic Biology and Immunology, National Demonstration Center for Experimental Basic Medical Science Education, Laboratory of Infection and Immunity, Xuzhou Medical University, Xuzhou 221004, Jiangsu Province, China

Yin-Hai Xu, Department of Laboratory Medicine, The Affiliated Hospital of Xuzhou Medical University, Xuzhou 221002, Jiangsu Province, China

Corresponding author: Chao Yan, MD, PhD, Academic Research, Professor, Jiangsu Key Laboratory of Immunity and Metabolism, Department of Pathogenic Biology and Immunology, National Demonstration Center for Experimental Basic Medical Science Education, Department of Pathogenic Biology and Immunology, Xuzhou Medical University, No. 209 Tongshan Road, Xuzhou 221004, Jiangsu Province, China. yanchao6957@xzhmu.edu.cn

Abstract

BACKGROUND

Primary sclerosing cholangitis (PSC) is characterized by chronic inflammation and it predisposes to cholangiocarcinoma due to lack of effective treatment options. Recombinant adeno-associated virus (rAAV) provides a promising platform for gene therapy on such kinds of diseases. A microRNA (miRNA) let-7a has been reported to be associated with the progress of PSC but the potential therapeutic implication of inhibition of let-7a on PSC has not been evaluated.

AIM

To investigate the therapeutic effects of inhibition of a miRNA let-7a transferred by recombinant adeno-associated virus 8 (rAAV8) on a xenobiotic-induced mouse model of sclerosing cholangitis.

METHODS

A xenobiotic-induced mouse model of sclerosing cholangitis was induced by 0.1% 3,5-Diethoxycarbonyl-1,4-Dihydrocollidine (DDC) feeding for 2 wk or 6 wk. A single dose of rAAV8-mediated anti-let-7a-5p sponges or scramble control was injected *in vivo* into mice onset of DDC feeding. Upon sacrifice, the liver and the

serum were collected from each mouse. The hepatobiliary injuries, hepatic inflammation and fibrosis were evaluated. The targets of let-7a-5p and downstream molecule NF-κB were detected using Western blot.

RESULTS

rAAV8-mediated anti-let-7a-5p sponges can depress the expression of let-7a-5p in mice after DDC feeding for 2 wk or 6 wk. The reduced expression of let-7a-5p can alleviate hepato-biliary injuries indicated by serum markers, and prevent the proliferation of cholangiocytes and biliary fibrosis. Furthermore, inhibition of let-7a mediated by rAAV8 can increase the expression of potential target molecules such as suppressor of cytokine signaling 1 and Dectin1, which consequently inhibit of NF-κB-mediated hepatic inflammation.

CONCLUSION

Our study demonstrates that a rAAV8 vector designed for liver-specific inhibition of let-7a-5p can potently ameliorate symptoms in a xenobiotic-induced mouse model of sclerosing cholangitis, which provides a possible clinical translation of PSC of human.

Key Words: Primary sclerosing cholangitis; Recombinant adeno-associated virus 8; Let-7a-5p; Therapeutic effects; Inflammation

Core Tip: Primary sclerosing cholangitis (PSC) have a high risk of cholangiocarcinoma with a lack of effective treatment options. Then the present study aimed to investigate the therapeutic effects of inhibition of a microRNA let-7a transferred by recombinant adeno-associated virus 8 (rAAV8) on a 3,5-Diethoxycarbonyl-1,4-Dihydrocollidine-induced mouse model of sclerosing cholangitis. And the results of our study demonstrates that a rAAV8 vector designed for liver-specific inhibition of let-7a-5p can potently ameliorate symptoms in a xenobiotic-induced mouse model of sclerosing cholangitis, which provides a possible clinical human clinical translation of PSC.

Citation: Hua H, Zhao QQ, Kalagbor MN, Yu GZ, Liu M, Bian ZR, Zhang BB, Yu Q, Xu YH, Tang RX, Zheng KY, Yan C. Recombinant adeno-associated virus 8-mediated inhibition of microRNA let-7a ameliorates sclerosing cholangitis in a clinically relevant mouse model. *World J Gastroenterol* 2024; 30(5): 471-484
URL: https://www.wjgnet.com/1007-9327/full/v30/i5/471.htm
DOI: https://dx.doi.org/10.3748/wjg.v30.i5.471

INTRODUCTION

Primary sclerosing cholangitis (PSC) is an idiopathic cholestatic disease and it affects intrahepatic and/or extrahepatic bile ducts characterized by chronic inflammation, ductal stricture, cholestasis, and fibrosis[1,2]. PSC patients can progress to liver cirrhosis and have a great risk of cholangiocarcinoma with liver failure at the end stage. PSC has been considered an orphan disease since the prevalence of PSC is up to 16.2 per 100000 population with variable distribution due to different regions[3-5]. Although the occurrence of PSC is rare, it showed significant morbidity and mortality in PSC patients as there is a very limited medical option to interfere with the course of PSC, and liver transplant is the exclusively therapeutic option at the end-stage of the disease[1,6]. MicroRNA (miRNA) represents a kind of small non-coding RNA with 18-23 nucleotide length. The miRNAs widely participate in various processes in physiological and disease conditions by regulating of expression mRNAs at the post-transcriptional level. Although the etiology and pathogenesis of PSC are complex and largely unknown, increasing data demonstrate that the dysregulation of miRNA can also contribute to the pathogenesis of PSC[7-9]. These aberrant miRNAs have been reported to be involved in almost all aspects of diseases including inflammation, hyperplasia, fibrosis, and malignancy of cholangiocytes in patients or mouse models of PSC[10,11]. Of these miRNAs, the let-7a family is one of the latest identified miRNAs that are dysregulated in cholestasis[12-16], suggesting possible medical targets of let-7a on cholestatic diseases. However, the therapeutic effect of targeting let-7a in cholestasis is yet to be determined.

Recombinant adeno-associated virus (rAAVs) provide a promising vehicle for gene therapy as they can efficiently transfer genes to the target tissue with low immunogenicity, low toxicity, and long persistence[17-23]. rAAV8 is one serotype that can transduce hepatocytes and cholangiocytes with high efficiency and specificity due to its liver tropism and has been implicated in many liver diseases including cholangiopathies[19,24-28]. Increasing data showed that rAAVs also can deliver miRNAs (mimics, precursor, or its antisense) to play the significant therapeutic effects of miRNAs on many other liver diseases[29-32], but there are rare therapeutic data about miRNAs delivered by rAAVs on cholangiopathies. Given the aberrance and importance of let-7a in cholangiopathies especially in PSC, we hypothesize that inhibition of let-7a delivered by rAAV8 has potential therapeutic effects on PSC. To support our hypothesis, we used a well-established mouse model of PSC- a mouse model of sclerosing cholangitis *via* 0.1% 3,5-Diethoxycarbonyl-1,4-Dihydrocollidine (DDC) feeding, following treatment with a single dose injection of rAAV8-delivered inhibitors (anti-

Table 1 The primers used in the present study

Target	Oligonucleotide sequence (5'-3')	
	Forward primer	Reverse primer
let-7a-5p	GGAGGTAGTTCGTTGTGTGGT	
U6	ATGGGTCGAAGTCGTAGCC	TTCTCGGCGTCTTCTTTCTCG
Gfp	TGCTTCAGCCGCTACCC	AGTTCACCTTGATGCCGTTC
β-actin	AACTCCATCATGAAGTGTGA	CTGCGGCTTCTATTGGGGAC
Tnfa	CTTGTTGCCTCCTCTTTTGCTTA	GACTTCAGCACTCAAGACATCC
Il6	TCACAGAAGGAGTGGCTAAGGACC	ACGCACTAGGTTTGCCGAGTAGAT
Acta2	TTCATCGGGATGGAGTCTGCTGG	TCGGTCGGCAATGCCAGGGT
Tgfb	CCACCTGCAAGACCATCGAC	CTGGCGAGCCTTAGTTTGGAC
Ccl2	TTAAAAACCTGGATCGGAACCAA	GCATTAGCTTCAGATTTACGGGT

senses of let-7a sponges) of let-7a for 2 wk or 6 wk. Our data showed that we have successfully developed a possible therapeutic strategy for PSC based on the administration of an AAV8 vector designed for liver-specific inhibition of let-7a. This strategy could markedly ameliorate biliary injuries by the decreased proliferation of cholangiocytes, biliary inflammation, and fibrosis in the mice induced by 0.1% DDC feeding for 2 wk or 6 wk. Furthermore, the therapeutic effects may be associated with the inhibition of NF-κB-mediated hepatic inflammation. The present study demonstrates that the rAAV-mediated miRNAs strategy provides a promising therapeutic opportunity for this debilitating and life-threatening disease.

MATERIALS AND METHODS

Experimental animals and ethics

Female C57BL/6J mice without specific pathogen, 6-wk old, 18-25 g in weight, were raised in a clean-grade animal house, free to eat and drink, and the animal lab environment as the following specifications: temperature range from 20 °C to 26 °C, humidity range from 40% to 70%, and 12 h/12 h light/dark. Tail vein injection and other operations were conducted in the animal barrier experimental operation room of the Experimental Animal Center of Xuzhou Medical University [SYXK (Su) 2016-0028]. Animal care and all experiments in this study were carried out following the guidelines of the National Laboratory Animal Center and were given humanitarian care according to the 3R principle of laboratory animals. The main procedures and protocols were approved by the Animal Care and Use Committee of Xuzhou Medical University (license IACUC: 201801w003).

Mouse model of DDC-feeding induced sclerosing cholangitis and the adeno- associated virus infection

A sclerosing cholangitis mouse model was induced by 0.1% DDC feeding for 2 wk or 6 wk. Specifically, 24 mice were fed DDC food while the other 12 mice were fed chow food as a control. The adeno-associated virus (AAV) labeled with EGFP for targeting knocking down the expression of let-7a-5p in the liver was purchased from Genechem (Shanghai, China). The mice in the two DDC-feeding groups were intravenously injected with 100 μL 4×10^{12} vector genomes (VG)/mL AAV that overexpressed mmu-let-7a-5P-sponges or empty vehicles (4×10^{11} vg per mice). And the 12 normal control mice were injected with the same volume of PBS (LPS-free) in which the AAV original liquid was diluted. Following, half of the mice from each group were sacrificed by euthanasia in 2 wk, while the half of rest were sacrificed in 6 wk. The livers and sera from each mouse were harvested for further experiments. The inhibitor sponges of mmu-let-7a-5P are ACCACACAAgacCTACCTCCcttcACCACACAAgacCTACCTCCcttcACCACACAAgacCTACCTCCatccgtaACCACACAAgacCTACCTCCcttcACCACACAAgacCTACCTCC, and the specific molding method is shown as Figure 1.

RNA extraction and qPCR analysis

Total RNAs from liver tissues were extracted using the TRIZOL reagent (Invitrogen, Carlsbad, CA, United States), following the manufacturer's instructions, and then reverse transcribed into cDNA using the miRcute Plus miRNA First-Strand cDNA Kit (TIANGEN Biotech, Beijing, China) or FastKing RT Kit (With gDNase) (TIANGEN Biotech, Beijing, China). Then, qPCR was performed using the SYBR Green Master Mix (TransGen Biotech, Beijing, China) and run on a StepOne Plus Real-Time PCR System (Roche Applied Science, Mannheim, Germany). The relative expression levels of miRNAs or mRNAs were normalized to *U6* small nuclear RNA (snRNA) or β-actin following the $2^{-\Delta\Delta Ct}$ comparative method. The sequences of the primers used in this study were optimized as Table 1.

Activities of serum enzyme detection

The mouse serum was collected and transported to the Laboratory Department of the Affiliated Hospital of Xuzhou

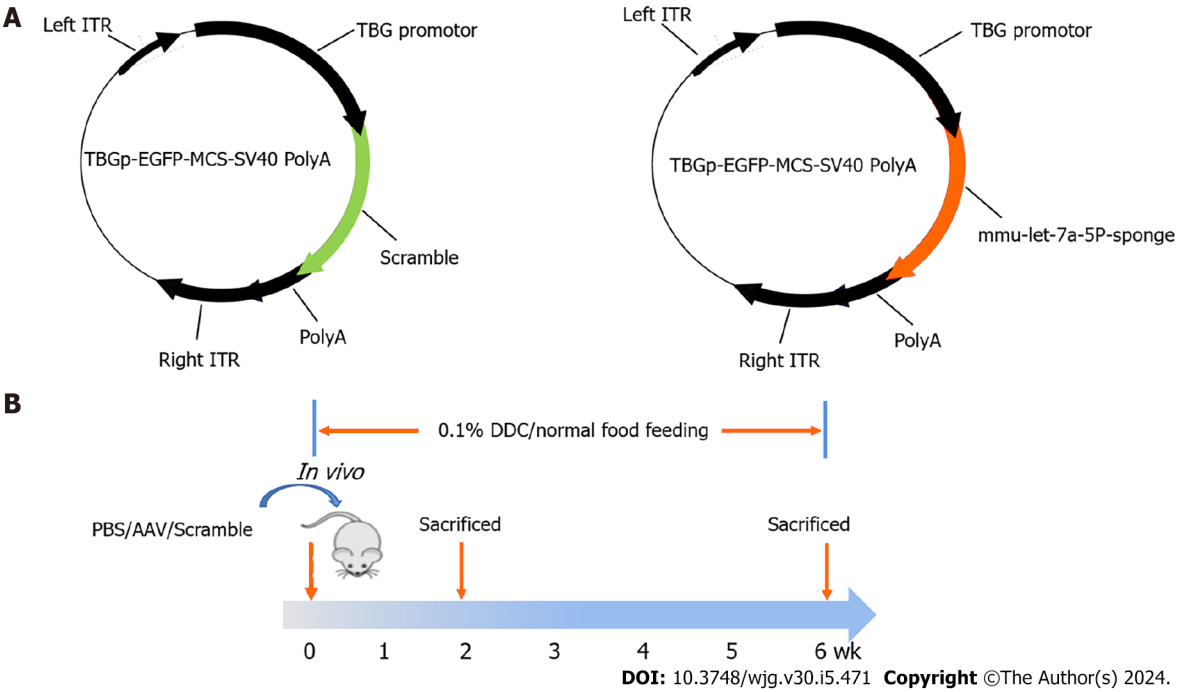

DOI: 10.3748/wjg.v30.i5.471

Figure 1 Schematic representation of recombinant adeno-associated virus 8 delivered let-7a-5p inhibitor and the design of experiment. A: Diagrams of anti-let-7a-5p sponges' vector and anti-scramble control (SCR) control vector; B: The design of the experiment. The mice were divided 3 groups (n = 6 for each group): (1) Normal control mice with feeding chow; (2) 3,5-Diethoxycarbonyl-1,4-Dihydrocollidine (DDC) feeding mice who were iv injected with adeno-associated virus 8-anti-SCR at the dose of 4 × 10^{11} vg per mouse; and (3) DDC feeding mice were iv injected with anti-let-7a-5p sponges (anti-let-7a-5p) at the dose of 4 × 10^{11} vg per mice. The mice in each group were sacrificed at 2 wk and 6 wk after DDC feeding to evaluate the expression of let-7a-5p and the therapeutic effects of let-7a-5p inhibitor. ITR: Invert terminal repeat; TBG: Thyroxine-binding globulin; DDC: 3,5-Diethoxycarbonyl-1,4-Dihydrocollidine; AAV: Adeno-associated virus.

Medical University at low temperature to detect the activities of bile duct injury-related enzymes [alanine aminotransferase (ALT), total bilirubin (BILT), and total bile acid (TBA)].

Hematoxylin and eosin and Sirius red staining

For histological analysis, liver tissues were excised and fixed with 4% paraformaldehyde for 24 h at least. Thereafter, the fixed tissues were embedded in paraffin, sliced to a thickness of 4 μm, and routinely stained with hematoxylin and eosin (H&E) and Sirius red staining according to the recommendation of the manufacturer (Shanghai Xinfan Biotechnology, Shanghai, China), after sealing the slides with neutral adhesive, the pathological changes of stained histological sections were observed by a microscope (Olympus, Japan). The staining pictures were quantitatively analyzed with Image J, 6 pictures zoomed in 100 × were selected for each mouse for quantitative analysis, and the average value was taken as the quantitative value of that mouse, n = 6.

Immunohistochemistry staining

The liver tissue was deparaffinized, hydrated, and heated in citric acid buffer at 95 °C for 15 min and blocked with 5% BSA for 30 min, and then incubated overnight with primary anti-CK19 (1:500, ab52625, Abcam, Cambridge, United States) and then incubated with secondary antibodies for 30 min at room temperature. After washing with PBS, DAB (1:20, ZSGB-BIO, Beijing, China) as an enzyme substrate was added. Six high-power fields (× 100 magnifications, Olympus, Japan) were randomly selected from each mouse staining section and the percentage of CK19 positive area was calculated by ImageJ software (NIH, United States).

Immunofluorescence staining

The slides with liver tissues were fixed in 4% paraformaldehyde, permeabilized with 0.1% Triton X-100, and then blocked with 5% BSA. Slides were incubated with the indicated primary antibodies anti-GFP (1:100; Abcam, Cambridge, MA, United Kingdom) overnight at 4 °C and then incubated with fluorescence-labeled secondary antibodies for 1 h at room temperature. Nuclei were stained using DAPI for 10 min. Six images zoomed in 100 × per mouse were captured under a fluorescence microscope (AX70, Olympus, Japan), and the average signal value from the 6 images was used to represent the value from one mouse liver. Ten fields from each slide were randomly selected, and the positive color area was measured quantitatively using Image-Pro Plus 6.0 software.

Detection of hepatic hydroxyproline contents

Hepatic hydroxyproline (Hyp) content was determined using a commercially available kit according to the manufacturer's recommendations (Jiancheng Institute of Biotechnology, Nanjing, Jiangsu Province, China).

Western blot analysis

Liver homogenates were harvested and washed in cold PBS twice and then were treated with the lysis buffer (Beyotime, Shanghai, China) on ice for 30 min. The lysate was collected into microtubes and centrifuged for 15 min at 12000 rpm at 4 °C. Protein samples (20 mg) were denatured with the 5 × SDS loading buffer at 100 °C for 5 min then were segregated on a 10% SDS polyacrylamide gel electrophoresis and transferred onto 0.2 um nitrocellulose membranes. After 60 min of blocking with 5% fat-free milk, membranes were incubated with suppressor of cytokine signaling 1 (SOCS1) (1:1000; Cell Signaling Technology, United States), Dectin-1 (1:1000; Abclonal, Wuhan, Hubei Province, China), P-p65 (1:1000; Cell Signaling Technology, United States) and GAPDH antibody (1:2000; Abmart, Shanghai, China) overnight at 4 °C. After washing with TBST 3 times, blots were incubated with the anti-rabbit secondary antibody (1:5000; Abclonal, Wuhan, China) for 1 h. After washing, immunoreactive protein bands were detected by using enhanced chemiluminescence reagents (Bio-Rad, California, United States). Band intensities were normalized to GAPDH and analyzed using ImageLab software.

Statistical analysis

All data are presented as means ± SEM. The statistical analysis was performed with the use of the software package SPSS version 19.0 (SPSS Inc, Chicago, United States). One-way ANOVA analysis was used for the comparison of differences among more than two groups, which was followed by the Least Significant Difference test unless otherwise stated. In the case of the comparison of two groups, the differences were evaluated using a two-tailed Student's *t*-test, a value of $P < 0.05$ was considered significant.

RESULTS

Anti-let-7a-5p sponges delivered by rAAV8 depressed the expression of let-7a-5p in the liver of mice with DDC feeding

Since the expression of let-7a-5p is increased in both experimental obstructive cholestasis and patients[12], we investigated the potential therapeutic effects of an inhibitor of let-7a-5p delivered by highly hepatotropic rAAV8 on a mouse model of PSC at 2 wk and 6 wk. To address this, we generated rAAV8 expression plasmids containing either the scramble control (anti-SCR) or anti-let-7a-5p sponges under the control of a liver-specific thyroxine-binding globulin (TBG) promoter (Figure 1A) and injected rAAV8-anti-let-7a-5p (anti-let-7a-5p, 4×10^{11} vg/mouse) or rAAV8-scramble (anti-SCR, 4×10^{11} vg/mouse) with a single dose at the beginning of DDC feeding for 2 wk and 6 wk, respectively ($n = 6$ per group, Figure 1B).

After 2 or 6 wk for DDC feeding, we found that the GFP-flagged rAAVs were extensively observed in the livers of mice injected with rAAVs anti-SCR control or anti-let-7a-5p sponges (Figure 2A-C), and the relative expression of GFP indicating the amounts of virus in the liver were significantly increased both in anti-SCR and inhibitor mice at 2 wk or 6 wk, although it seems that the titer of recombinant adenovirus has dropped from 2 wk to 6 wk. We further evaluated the inhibition efficiency of let-7a-5p using anti-let-7a-5p sponges, it was found that anti-let-7a-5p sponges can significantly depress approximately 50% (at 2 wk) and approximately 60% (at 6 wk) of let-7a-5p in the liver of rAAV8-anti-let-7a-5p-injected mice, compared with anti-SCR mice (Figure 2D and E).

Inhibition of let-7a-5p delivered by rAAV8 alleviates hepato-biliary injuries caused by DDC

Next, we evaluated the amelioratory effects of let-7a-5p on hepato-biliary injuries caused by DDC (Figure 3). We found that DDC feeding for 2 wk or 6 wk both can significantly increase the ratio of liver weight to body weight which may indicate hepatomegaly, but let-7a-5p inhibitor depressed the ratio, compared with anti-SCR control at 2 wk or 6 wk ($P < 0.05$; Figure 3A). In addition, let-7a-5p inhibitor delivered by rAAVs can also reduce the levels of aspartate aminotransferase and BILT that were increased due to hepatic-biliary damages induced by DDC feeding both at 2 wk and 6 wk ($P < 0.05$, Figure 3B and C). At 2 wk, although there was no statistical significance of ALT and alkaline phosphatase (ALP) between anti-let-7a-5p mice and anti-SCR control mice, there are decreasing trends of ALT and ALP activities in anti-let-7a-5p mice than those anti-SCR control mice [$P > 0.05$, Figure 3D and E (upper panel)]. However, after 6 wk, there are significant decreases of ALT and ALP in the sera of anti-let-7a-5p mice, compared with anti-SCR control [$P < 0.05$, Figure 3D and E (nether panner)]. Taken together, let-7a-5p inhibitor delivered by rAAV8 ameliorates the hepato-biliary injuries caused by DDC feeding.

To assess the potential side effects of rAAV delivering anti-let-7a-5p sponges or anti-SCR on kidney function, we also detected serum urea, creatinine, and uric acid in those administrated mice both at 2 wk and 6 wk. Compared with normal control mice, we didn't find any increases in these indexes after injection of rAAV8, suggesting that rAAV8 injection can't induce kidney injuries (Supplementary Figure 1).

let-7a-5p inhibition mediated by rAAV8 ameliorates histologic changes and proliferation of cholangiocytes

H&E staining showed DDC feeding causes a moderated ductular reaction at 2 wk, and DRs became severe with the extended time of DDC feeding at 6 wk (Figure 4A), but rAAV8-let-7a-5p inhibitor injected mice showed a significant amelioration of the ductular reaction both at 2 wk and 6 wk, compared with anti-SCR control mice (Figure 4A). We also stained the CK19-specific marker for cholangiocytes in the liver, we found that the percentage of positive CK19 cells was dramatically increased after DDC feeding, compared with normal control mice, but anti-let-7a-5p mediated by rAAV8 significantly decreased the percent of positive CK19 cholangiocytes both at 2 wk and 6 wk, compared with anti-SCR control mice ($P < 0.05$, Figure 4B and C).

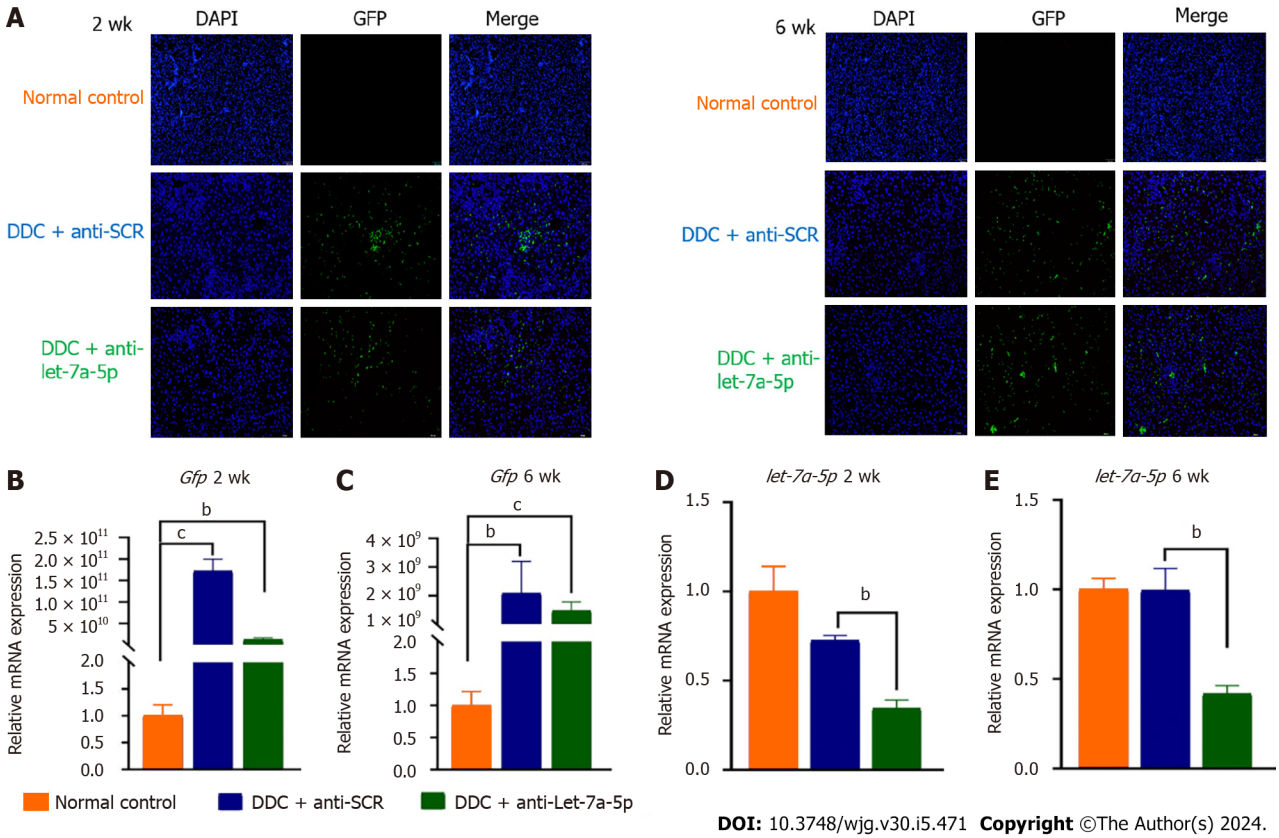

DOI: 10.3748/wjg.v30.i5.471

Figure 2 The expression of let-7a-5p is depressed using anti-let-7a-5p sponges delivered by recombinant adeno-associated virus 8. A: The recombinant adeno-associated virus 8 was extensively distributed in the liver of mice after 2 or 6 wk of 3,5-Diethoxycarbonyl-1,4-Dihydrocollidine (DDC) feeding; B and C: The relative expression of GFP indicates the relative amounts of virus; D and E: The relative expression of let-7a-5p in the liver of mice injected by adeno-associated virus 8-mediated scramble control or anti-let-7a-5p sponges after 2 wk or 6 wk of DDC feeding. DDC: 3,5-Diethoxycarbonyl-1,4-Dihydrocollidine; SCR: Scramble control. $^{b}P < 0.01$, $^{c}P < 0.001$.

rAAV8-delivered let-7a-5p inhibition attenuates liver fibrosis

Sirus-red staining showed there are massive "strip shape" collagen fibers deposition around bile ducts after DDC feeding for 2 wk and 6 wk, however, after treatment with rAAV8 mediated anti-let-7a-5p for 2 or 6 wk, the deposition of these collagen fibers was significantly decreased (Figure 5A). Furthermore, we detected other fibrotic biomarkers such as *Acta2* (encoding α-SMA) and *Tgfb* using qPCR, after 2 or 6 wk of the feeding of DDC, we found that the relative expression of *Acta2* and *Tgfb* was significantly higher in the DDC feeding mice than those in normal control mice without DDC feeding, but the mice injected with let-7a-5p inhibitor delivered by rAAV8 showed a noteworthy drop (almost five times drop) in *Acta2* and *Tgfb* expression, compared with anti-SCR control mice when they were fed with DDC for 2 or 6 wk ($P < 0.001$, Figure 5B and C). We also detected Hyp-another liver fibrosis marker, it was shown that there was no significant difference in anti-SCR control mice and anti-let-7a-5p mice at 2 wk for DDC feeding, but after 6 wk of treatment, the content of Hyp was significantly decreased in anti-let-7a-5p mice, compared with anti-SCR control mice ($P < 0.05$, Figure 5D). Taken together, rAAV8 delivered let-7a-5p inhibition abates liver fibrosis in experimental sclerosing cholangitis.

Let-7a-5p inhibition mediated by rAAV8 increased the expression of SOCS1 and Dectin-1, thus depression of NF-κB-mediated proinflammatory cytokines

Our previous and other studies demonstrated that let-7a-5p can potently regulate immune responses to depression NF-κB-mediated pro-inflammation by targeting several molecules such as SOCS1 and Dectin-1[33]. Therefore, we detected hepatic expression of SOCS1, Dectin-1, and P-p65 in the DDC feeding mice that were injected with rAAV8 mediated anti-SCR control or anti-let-7a-5p. Regarding to 2 wk' DDC feeding, there was no significant differences in the expression of SOCS1 between anti-SCR and anti-let-7a-5p group ($P > 0.05$, Figure 6A and B), but compared with rAAV8 mediated anti-SCR control group, the expression of Dectin-1 in rAAV8 mediated anti-let-7a-5p mice were significantly increased ($P < 0.05$, Figure 6A and C), and the level of downstream inflammatory transfactor P-p65 of NF-κB were remarkably decreased ($P < 0.05$, Figure 6A and D); For 6 wk DDC feeding, anti-let-7a-5p can both depressed the expression of SOCS1 ($P < 0.05$, Figure 6E and F) and Dectin-1 ($P < 0.05$, Figure 6E and G), which induced the lower level of P-p65 of NF-κB ($P < 0.05$, Figure 6E and H).

Sequentially, we further detected the pro-inflammatory cytokines such as IL-6, TNF-α, and CCl2. At 2 wk, DDC feeding induced high levels of *Il6*, *Tnfa*, and *Ccl*$_2$ mRNA production, but rAAV8-mediated let-7a-5p inhibitor depressed the production of these cytokines, compared with an anti-SCR group ($P < 0.01$, Figure 7A-C, upper panel). The

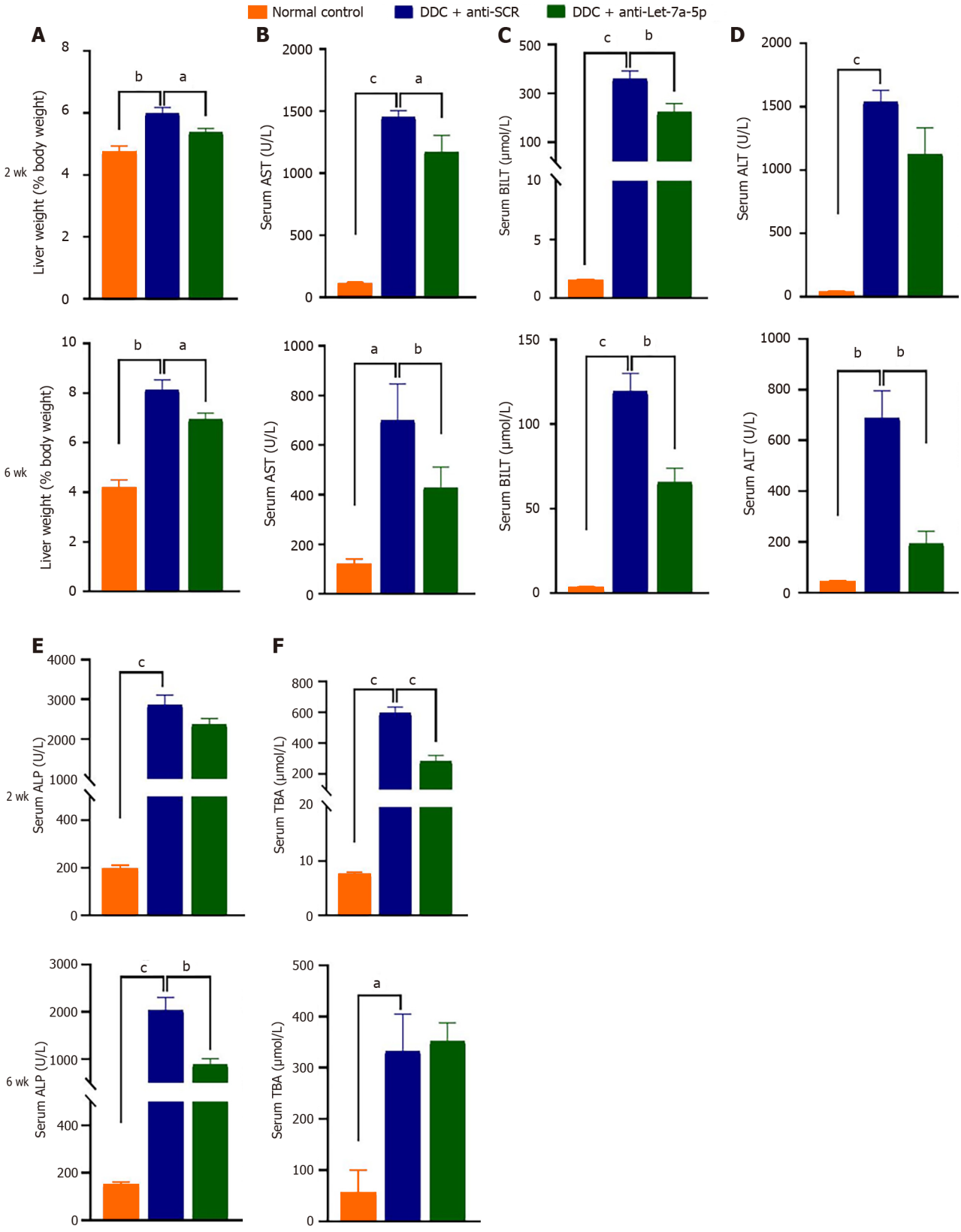

DOI: 10.3748/wjg.v30.i5.471

Figure 3 Recombinant adeno-associated virus 8 mediated anti-let-7a-5p protects from 3,5-Diethoxycarbonyl-1,4-Dihydrocollidine-induced hepato-biliary damages. A: The ratio of Liver weight to body weight; B-E: Serum levels of aspartate aminotransferase, total bilirubin, alanine aminotransferase, and alkaline phosphatase in the normal control, scramble control, and anti-let-7a sponge (anti-let-7a-5p) mice for 3,5-Diethoxycarbonyl-1,4-Dihydrocollidine feeding at the indicated time (2 wk and 6 wk). DDC: 3,5-Diethoxycarbonyl-1,4-Dihydrocollidine; SCR: Scramble control; AST: Aspartate aminotransferase; BILT: Total bilirubin; ALT: Alanine aminotransferase; ALP: Alkaline phosphatase; TBA: Total bile acid. $^{a}P < 0.05$, $^{b}P < 0.01$, $^{c}P < 0.001$.

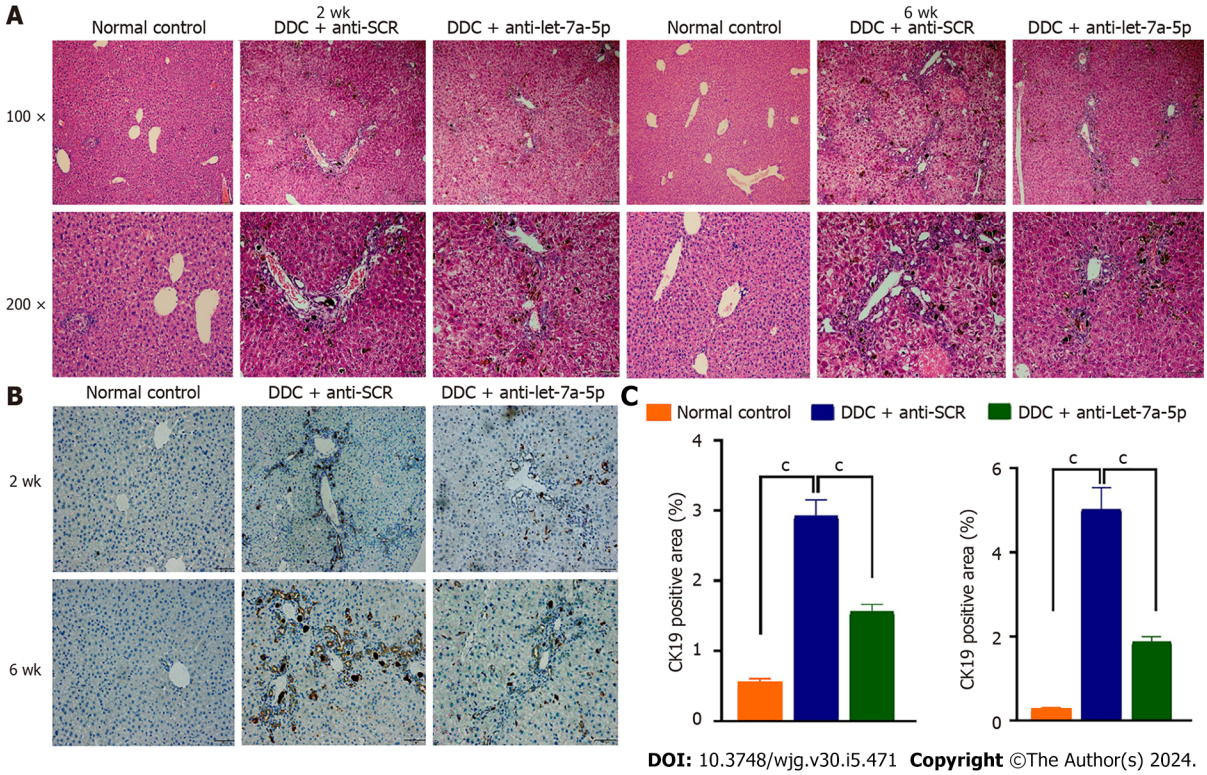

Figure 4 Let-7a-5p inhibition delivered by recombinant adeno-associated virus 8 prevents liver pathology and the proliferation of cholangiocytes. A: Histological changes at 2 and 6 wk was evaluated using hematoxylin and eosin staining. The upper panel was shown in 100 times amplification; the nether panel was shown in 200 times amplification; B: CK19 was stained for indicating the proliferation of cholangiocytes using Immunohistochemistry staining; C: and the percent of CK19 positive cells in the liver was calculated at 2 and 6 wk. DDC: 3,5-Diethoxycarbonyl-1,4-Dihydrocollidine; SCR: Scramble control. $^{c}P < 0.001$.

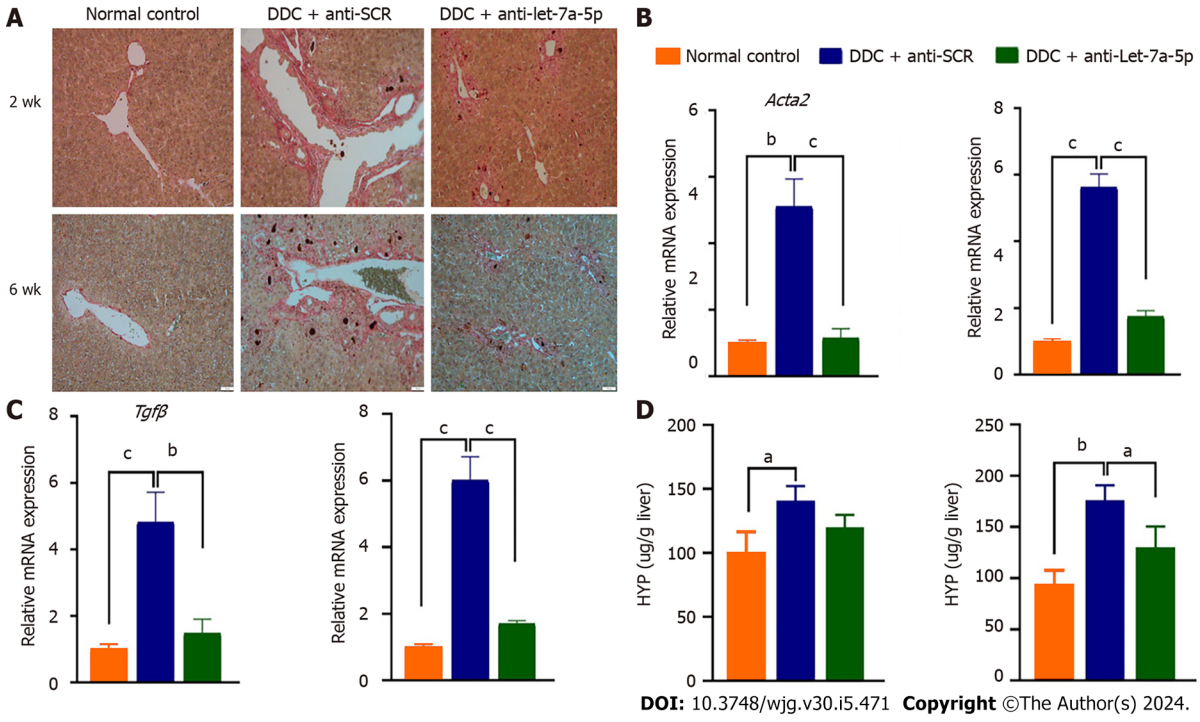

Figure 5 Let-7a-5p inhibition mediated by recombinant adeno-associated virus 8 ameliorates biliary fibrosis in the 3,5-Diethoxycarbonyl-1,4-Dihydrocollidine-induced cholestasis model. A: Sirius Red staining in the liver of mice at 2 wk and 6 wk after 3,5-Diethoxycarbonyl-1,4-Dihydrocollidine feeding; B and C: The fibrosis markers such as *Acta 2* and *Tgfb* were evaluated using qRT-PCR; D: The contents of Hyp in the liver of mice in each group were determined. DDC: 3,5-Diethoxycarbonyl-1,4-Dihydrocollidine; SCR: Scramble control; Hyp: Hydroxyproline. $^{a}P < 0.05$, $^{b}P < 0.01$, $^{c}P < 0.001$.

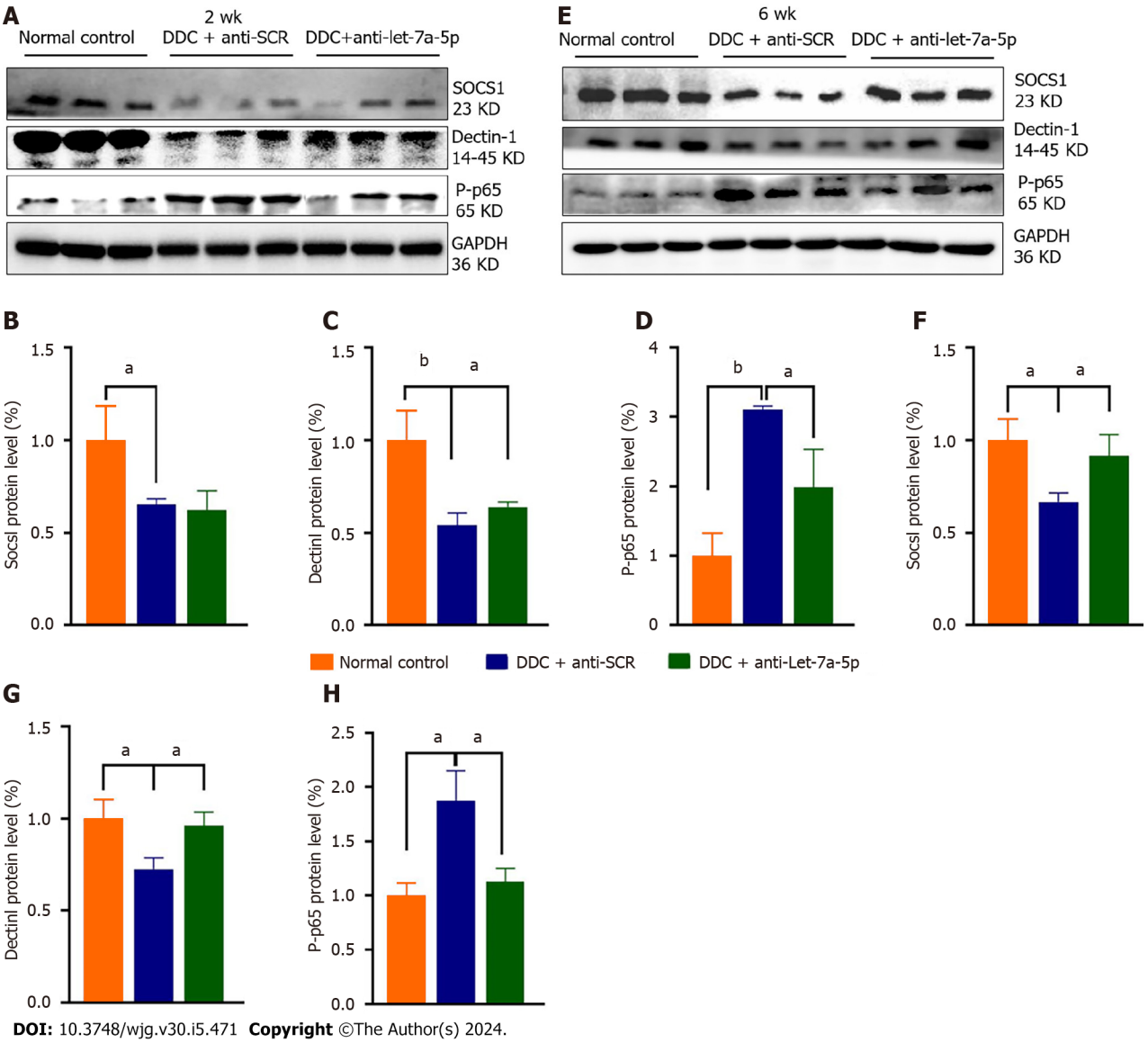

DOI: 10.3748/wjg.v30.i5.471

Figure 6 Recombinant adeno-associated virus 8 mediated let-7a-5p inhibitor interfers suppressor of cytokine signaling 1/Dectin1 mediated NF-κB signaling pathway. The expression of suppressor of cytokine signaling 1 (SOCS1)/Dectin1/P-p65 in each mouse of normal control group, anti-scramble control and anti-let-7a-5p group were assayed by western-blot. A: The blot of SOCS1/Dectin1/ P-p65 in each group after 2 wk 3,5-Diethoxycarbonyl-1,4-Dihydrocollidine (DDC) feeding; B-D: the relative levels of SOCS1, Dectin1, and P-p65 in each group after 2 wk DDC feeding; E: The blot of SOCS1/Dectin1/P-p65 in each group after 6 wk DDC feeding; F-H: relative levels of SOCS1, Dectin1, and P-p65 in each group after 6 wk DDC feeding. DDC: 3,5-Diethoxycarbonyl-1,4-Dihydrocollidine; SCR: Scramble control. $^{a}P < 0.05$, $^{b}P < 0.01$.

production of these cytokines in the mice at 6 wk after DDC feeding seems to be declined compared with those in the mice with DDC feeding for 2 wk, but they were still higher than those in the normal control mice (at least more than 3 times; $P < 0.001$, Figure 7A-C, nether panel); furthermore, the production of these cytokines were also significantly decreased in rAAV8 mediated anti-let-7a-5p mice, compared with anti-SCR group mice when they were feeding DDC for 6 wk ($P < 0.01$, Figure 7D-F, D for *Il6*, E for *Tnfa*, and F for *Ccl*$_2$ nether panel). Taken together, our data demonstrated that anti-let-7a-5p delivered by rAAV8 ameliorate experimental sclerosing cholangitis by targeting at Dectin-1 or SOCS1 - negatively regulated NF-κB.

DISCUSSION

PSC is a rare but life-threatening chronic disease and there is no effective medical option to cure it except liver transplantation. DDC-fed (0.1%) mice are a xenobiotic- induced mouse model of cholangiopathy. It can induce reactive cholangiocytes, biliary inflammation, pericholangitis, periductal fibrosis, and ultimately portal-portal bridging affecting large bile ducts, which more closely resembles human sclerosing cholangitis and biliary fibrosis[34,35]. In the present study, using this experimental model of mice, we found that we demonstrate that a single dose of rAAV8-mediated inhibition of let-7a can protect mice from hepatic (biliary) injuries, biliary inflammation, proliferation, and fibrosis in

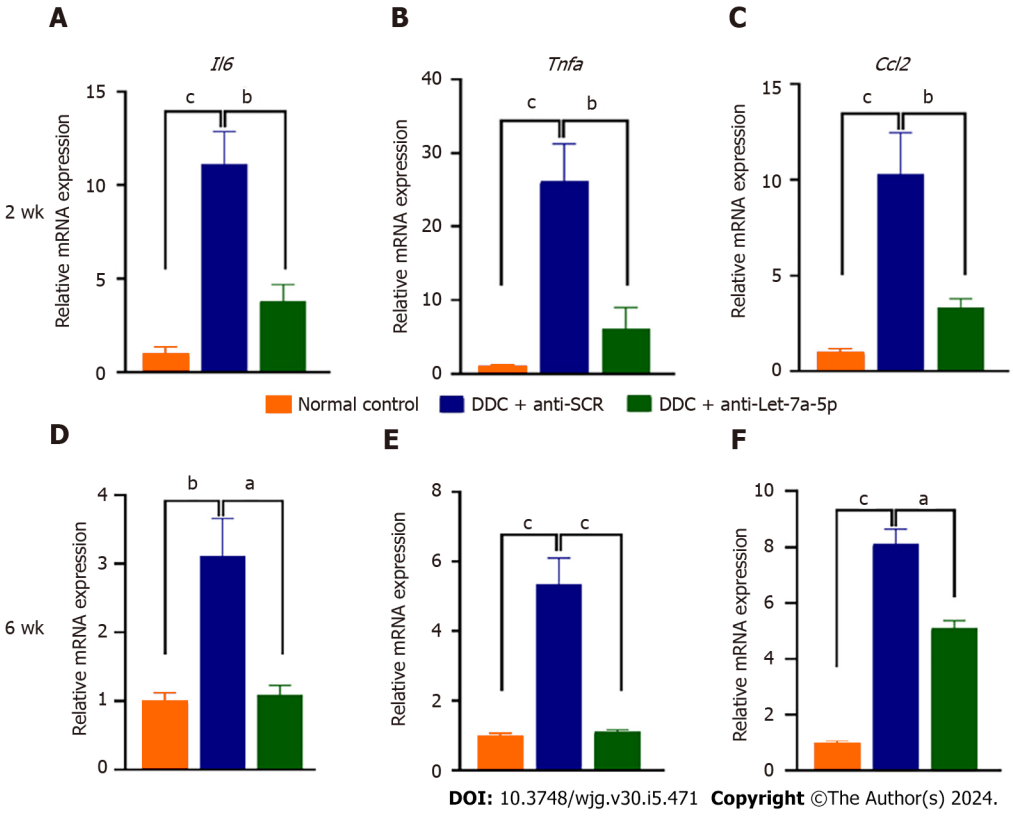

DOI: 10.3748/wjg.v30.i5.471

Figure 7 Let-7a-5p inhibition mediated by adeno-associated virus 8 ameliorates local pro-inflammatary cytokines produced. The levels of *Il6* , *Tnfa*, and *Ccl2* in the liver of mice from each group after 3,5-Diethoxycarbonyl-1,4-Dihydrocollidine (DDC) feeding for 2 or 6 wk were evaluted by qPCR. A-C: The relative levels of *Il6*, *Tnfa*, and *Ccl2* after 2 wk DDC feeding; D-F: The relative levels of *Il6*, *Tnfa*, and *Ccl2* after 6 wk DDC feeding. DDC: 3,5-Diethoxycarbonyl-1,4-Dihydrocollidine; SCR: Scramble control. $^{a}P < 0.05$, $^{b}P < 0.01$, $^{c}P < 0.001$.

experimental sclerosing cholangitis for 2 wk and 6 wk, suggesting that inhibition let-7a delivered by rAAV8 provides a potential therapeutic strategy for sclerosing cholangitis (Figure 8).

rAAV-based therapeutic has proved as the most effective strategy for gene therapy because rAAV8 can provide an effective, safe, and long-lasting vehicle to deliver genes (including miRNAs) to the targeted organs[36,37]. Currently, rAAV has been implicated in clinical trials in some human diseases such as cystic fibrosis, and Parkinson's disease, and Glybera-the commercial drug based on rAAV has been applied in the treatment of lipoprotein lipase deficiency[38-43]. rAAV8 with TBG promoters is a liver-tropism serotype that has been widely used to deliver genes targeting hepatocytes with high transduction efficiency, low immunogenicity, and toxicity to the cell. In our present study, we also found that systematic injection of rAAV8 has no side effects on other organs such as the kidney (Supplementary Figure 1), suggesting that rAAV8 is relatively low side effects on other organs[44,45]. In our present study, we attempted to use rAAV8 as a tool to deliver inhibitors of let-7a (anti-sense of let-7a-5p sponge). After injection, rAAV8 can not only invades hepatocytes but also can transfect cholangiocytes, a study showed that 6.8% and 30.9% of cholangiocytes were rAAV8 positive at 10 d and 56 d of transfection, respectively[24]. These data demonstrated that rAAV8 may act as a useful tool for the intervention of cholangiopathies.

Increasing evidence demonstrates that miRNAs play critical roles in cholangiopathies[6]. Let-7 family is the first identified miRNA and increasing data suggested that let-7a plays pro-inflammatory or anti-inflammatory roles by inhibition of several targets[46-50]. Of these signaling pathways that let-7 is involved in, the TLR/NF-κB signaling pathway that is critical to the induction of pro-inflammatory cytokines can be also well-regulated by let-7. For example, let-7a targeted the SOCS1-the feedback inhibitor of NF-κB to facilitate the transcriptional activity of NF-κB and subsequent production of pro-inflammatory cytokines[51]. Similarly, let-7a has been reported to target A20-another inhibitor of the NF-κB pathway, leading to the increased TNF, IL-1β, and nitrite during Mycobacterium tuberculosis infection[52]. In agreement with these observations, we found that the pro-inflammatory cytokines such as TNF, IL-6, and CCl_2 were decreased after the treatment with anti-let-7a delivered by rAAV8, which may be associated with the increased SOCS1 expression and the increased activities of NF-κB due to the loss of inhibitor effects of let-7a.

Many miRNAs have been demonstrated to participate in cholestasis[53-55]. Of these miRNAs, let-7a-5p is a recently identified miRNA that is dysregulated in animal models of cholangiopathies (such as BDL and *Mdr2* KO mice) and patients with BA or PSC. Intriguing, it seems that let-7a-5p showed multiple contradictory functions in the different contexts of cholangiopathies due to targeting different genes. For example, let-7a decreased cholangiocytes in BDL mice and inhibits the secretin produced by cholangiocytes and S cells by targeting *NGF*, leading to a repression of the proliferation of cholangiocytes[13]. Similarly, in another study, the expression of let-7a was decreased in the liver of *Mdr2* KO mice or human PSC, which probably increase downstream targets of let-7a (such as the NF-κB, IL-13, and NR1H4) and

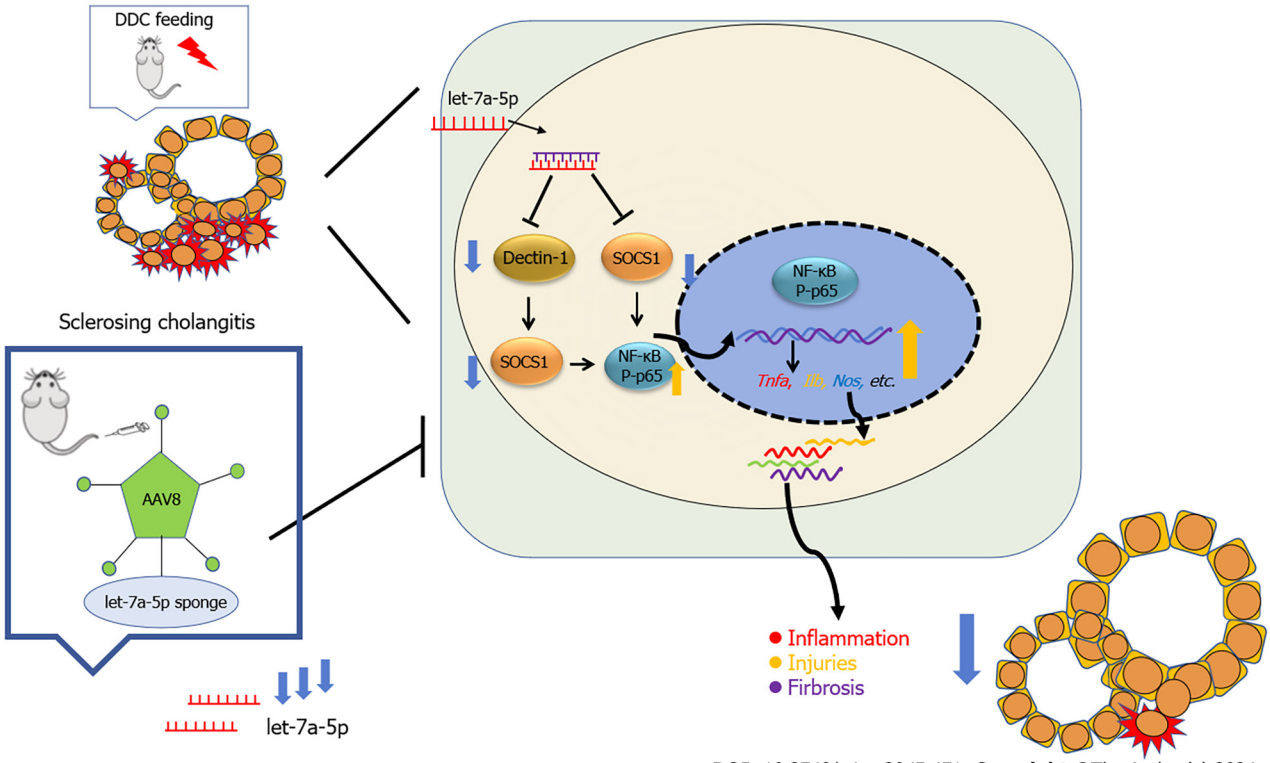

DOI: 10.3748/wjg.v30.i5.471

Figure 8 Schematic summary of an amelioration of sclerosing cholangitis in a clinically relevant mouse model by recombinant adeno-associated virus 8-mediated microRNA let-7a inhibition. DDC: 3,5-Diethoxycarbonyl-1,4-Dihydrocollidine; SOCS: Suppressor of cytokine signaling.

accelerate the severity of disease[14]. However, in another study, an increased let-7a-5p inhibited BCC2/Abcc2 (also known as MRP2) expression in obstructive cholestasis; the latter is critical for biliary excretion of conjugated bilirubin and the deficiency of BCC2 lead to obstructive cholestasis[12]. In our present study, we found that the inhibition of let-7a delivered by rAAV8 showed therapeutic effects on sclerosing cholangitis induced by DDC feeding at early (2 wk) or chronic stage (6 wk). The expression pattern of let-7a is discrepant in different cell types and the role of let-7a seems cell type-dependent in the different contexts of cholangiopathies. Glaser *et al*[13] found that the more than 15-fold increased expression of let-7a in hepatocytes, but deceased in cholangiocytes in the context of BDL mice. This may partly account for the diverse roles of let-7a in different cholangiopathies.

CONCLUSION

In summary, rAAV8 mediated let-7a-5p inhibitor provides powerful therapeutical effects on the DDC-induced sclerosing cholangitis, which can prevent hepato-biliary injuries, ductal reaction, and fibrosis by interfering with pro-inflammatory cytokines production. Our present study provides a possible clinical human clinical translation of PSC using rAAV8 systems to manipulate the expression of let-7a-5p. Other mechanisms by which therapeutic implication of inhibition of let-7a in DDC-induced sclerosing cholangitis are not excluded and further investigations are warranted.

ARTICLE HIGHLIGHTS

Research background

Primary sclerosing cholangitis (PSC) which may progress to cholangiocarcinoma is an idiopathic cholestatic disease and there is a very limited medical option to interfere with the course of PSC. Recombinant adeno-associated virus (rAAV) provides a prospective platform for gene therapy on such kinds of diseases. A microRNA (miRNA) let-7a has been reported to be associated with the progress of PSC but the potential therapeutic implication of inhibition of let-7a on PSC has not been evaluated.

Research motivation

To investigate the potential function and mechanisms of miRNA let-7a-5p transferred by rAAV8 in animal model of PSC.

Research objectives

To study the therapeutic effects of inhibition of let-7a-5p transferred by rAAV8 on a 3,5-Diethoxycarbonyl-1,4-Dihydrocollidine (DDC)-induced mouse model of sclerosing cholangitis.

Research methods

A mouse model of sclerosing cholangitis was induced by 0.1% DDC feeding for 2 wk or 6 wk, and rAAV8-mediated anti-let-7a-5p sponges or scramble control was injected *in vivo* onset of DDC feeding. After sacrifice of the mice, the liver and the serum were collected from each mouse. The hepatobiliary injuries, hepatic inflammation was evaluated. The targets of let-7a-5p and downstream molecule NF-κB were detected using Western blot.

Research results

The reduced expression of let-7a-5p can alleviate hepato-biliary injuries indicated by serum markers, and prevent the proliferation of cholangiocytes and biliary fibrosis. Furthermore, inhibition of let-7a mediated by rAAV8 can increase the expression of potential target molecules such as SOCS1 and Dectin1, which consequently inhibition of NF-κB-mediated hepatic inflammation.

Research conclusions

Our findings suggested that a rAAV8 vector designed for liver-specific inhibition of let-7a-5p can potently ameliorate symptoms in a xenobiotic-induced mouse model of sclerosing cholangitis, which provides a possible therapeutic strategy for PSC.

Research perspectives

The present study demonstrates that the rAAV-mediated miRNAs strategy may provide a promising therapeutic opportunity for this debilitating and life-threatening disease.

FOOTNOTES

Co-corresponding authors: Kui-Yang Zheng and Chao Yan.

Author contributions: Hua H and Zhao QQ performed the majority of experiments; Kalagbor MN, Yu GZ, Liu M, Bian ZR, Zhang BB, Yu Q, Xu YH, and Tang RX contributed to the acquisition of data and improving the manuscript. Zheng KY and Yan C contributed equally to this work as co-corresponding authors; Zheng KY supervised the experiments, corrected the data, and revised the manuscript; Yan C conceived and designed the main content of this study and was responsible for analyzing the research results.

Supported by the National Natural Science Foundation of China, No. 82172297; Natural Science Foundation of Jiangsu Province of China, No. BK20211346 and No. BK20201011; Natural Science Foundation of Jiangsu Higher Education Institutions of China, No. 22KJA310007; and Xuzhou Science and Technology Project, No. KC22055.

Institutional animal care and use committee statement: All procedures involving animals were reviewed and approved by the Animal Care and Use Committee of Xuzhou Medical University License (Approval No. 201801w003).

Conflict-of-interest statement: All authors declare no competing interests.

Data sharing statement: No additional data are available.

ARRIVE guidelines statement: The authors have read the ARRIVE Guidelines, and the manuscript was prepared and revised according to the ARRIVE Guidelines.

Country/Territory of origin: China

ORCID number: Hui Hua 0009-0004-7279-074X; Qian-Qian Zhao 0009-0009-4428-5056; Miriam Nkesichi Kalagbor 0009-0004-7041-0301; Guo-Zhi Yu 0009-0004-3760-7938; Man Liu 0009-0003-2288-7001; Zheng-Rui Bian 0009-0007-4023-6228; Bei-Bei Zhang 0000-0002-3627-2687; Qian Yu 0009-0000-6820-5393; Yin-Hai Xu 0009-0006-9738-884X; Ren-Xian Tang 0009-0001-4451-9168; Kui-Yang Zheng 0000-0002-1896-7485; Chao Yan 0000-0002-7482-9116.

S-Editor: Chen YL
L-Editor: A
P-Editor: Yu HG

REFERENCES

1 **Dyson JK**, Beuers U, Jones DEJ, Lohse AW, Hudson M. Primary sclerosing cholangitis. *Lancet* 2018; **391**: 2547-2559 [PMID: 29452711 DOI: 10.1016/S0140-6736(18)30300-3]

2 **Li ZJ**, Gou HZ, Zhang YL, Song XJ, Zhang L. Role of intestinal flora in primary sclerosing cholangitis and its potential therapeutic value. *World J Gastroenterol* 2022; **28**: 6213-6229 [PMID: 36504550 DOI: 10.3748/wjg.v28.i44.6213]

3 **Villard C**, Friis-Liby I, Rorsman F, Said K, Warnqvist A, Cornillet M, Kechagias S, Nyhlin N, Werner M, Janczewska I, Hagström T, Nilsson E, Bergquist A. Prospective surveillance for cholangiocarcinoma in unselected individuals with primary sclerosing cholangitis. *J Hepatol* 2023; **78**: 604-613 [PMID: 36410555 DOI: 10.1016/j.jhep.2022.11.011]

4 **Hu C**, Iyer RK, Juran BD, McCauley BM, Atkinson EJ, Eaton JE, Ali AH, Lazaridis KN. Predicting cholangiocarcinoma in primary sclerosing cholangitis: using artificial intelligence, clinical and laboratory data. *BMC Gastroenterol* 2023; **23**: 129 [PMID: 37076803 DOI: 10.1186/s12876-023-02759-7]

5 **Tan N**, Lubel J, Kemp W, Roberts S, Majeed A. Current Therapeutics in Primary Sclerosing Cholangitis. *J Clin Transl Hepatol* 2023; **11**: 1267-1281 [PMID: 37577219 DOI: 10.14218/JCTH.2022.00068S]

6 **Tanaka A**. IgG4-Related Sclerosing Cholangitis and Primary Sclerosing Cholangitis. *Gut Liver* 2019; **13**: 300-307 [PMID: 30205418 DOI: 10.5009/gnl18085]

7 **Olaizola P**, Lee-Law PY, Arbelaiz A, Lapitz A, Perugorria MJ, Bujanda L, Banales JM. MicroRNAs and extracellular vesicles in cholangiopathies. *Biochim Biophys Acta Mol Basis Dis* 2018; **1864**: 1293-1307 [PMID: 28711597 DOI: 10.1016/j.bbadis.2017.06.026]

8 **Povero D**, Tameda M, Eguchi A, Ren W, Kim J, Myers R, Goodman ZD, Harrison SA, Sanyal AJ, Bosch J, Ohno-Machado L, Feldstein AE. Protein and miRNA profile of circulating extracellular vesicles in patients with primary sclerosing cholangitis. *Sci Rep* 2022; **12**: 3027 [PMID: 35194091 DOI: 10.1038/s41598-022-06809-0]

9 **Huang C**, Xing X, Xiang X, Fan X, Men R, Ye T, Yang L. MicroRNAs in autoimmune liver diseases: from diagnosis to potential therapeutic targets. *Biomed Pharmacother* 2020; **130**: 110558 [PMID: 32781357 DOI: 10.1016/j.biopha.2020.110558]

10 **Kennedy LL**, Meng F, Venter JK, Zhou T, Karstens WA, Hargrove LA, Wu N, Kyritsi K, Greene J, Invernizzi P, Bernuzzi F, Glaser SS, Francis HL, Alpini G. Knockout of microRNA-21 reduces biliary hyperplasia and liver fibrosis in cholestatic bile duct ligated mice. *Lab Invest* 2016; **96**: 1256-1267 [PMID: 27775690 DOI: 10.1038/labinvest.2016.112]

11 **Song CW**, Qiu W, Zhou XQ, Feng XC, Chen WS. Elevated hepatic MDR3/ABCB4 is directly mediated by MiR-378a-5p in human obstructive cholestasis. *Eur Rev Med Pharmacol Sci* 2019; **23**: 2539-2547 [PMID: 30964181 DOI: 10.26355/eurrev_201903_17402]

12 **Balasubramaniyan N**, Devereaux MW, Orlicky DJ, Sokol RJ, Suchy FJ. Up-regulation of miR-let7a-5p Leads to Decreased Expression of ABCC2 in Obstructive Cholestasis. *Hepatol Commun* 2019; **3**: 1674-1686 [PMID: 31832574 DOI: 10.1002/hep4.1433]

13 **Glaser S**, Meng F, Han Y, Onori P, Chow BK, Francis H, Venter J, McDaniel K, Marzioni M, Invernizzi P, Ueno Y, Lai JM, Huang L, Standeford H, Alvaro D, Gaudio E, Franchitto A, Alpini G. Secretin stimulates biliary cell proliferation by regulating expression of microRNA 125b and microRNA let7a in mice. *Gastroenterology* 2014; **146**: 1795-808. e12 [PMID: 24583060 DOI: 10.1053/j.gastro.2014.02.030]

14 **McDaniel K**, Wu N, Zhou T, Huang L, Sato K, Venter J, Ceci L, Chen D, Ramos-Lorenzo S, Invernizzi P, Bernuzzi F, Wu C, Francis H, Glaser S, Alpini G, Meng F. Amelioration of Ductular Reaction by Stem Cell Derived Extracellular Vesicles in MDR2 Knockout Mice *via* Lethal-7 microRNA. *Hepatology* 2019; **69**: 2562-2578 [PMID: 30723922 DOI: 10.1002/hep.30542]

15 **Xiao Y**, Liu R, Li X, Gurley EC, Hylemon PB, Lu Y, Zhou H, Cai W. Long Noncoding RNA H19 Contributes to Cholangiocyte Proliferation and Cholestatic Liver Fibrosis in Biliary Atresia. *Hepatology* 2019; **70**: 1658-1673 [PMID: 31063660 DOI: 10.1002/hep.30698]

16 **Zhang L**, Yang Z, Huang W, Wu J. H19 potentiates let-7 family expression through reducing PTBP1 binding to their precursors in cholestasis. *Cell Death Dis* 2019; **10**: 168 [PMID: 30778047 DOI: 10.1038/s41419-019-1423-6]

17 **Ronzitti G**, Gross DA, Mingozzi F. Human Immune Responses to Adeno-Associated Virus (AAV) Vectors. *Front Immunol* 2020; **11**: 670 [PMID: 32362898 DOI: 10.3389/fimmu.2020.00670]

18 **Arjomandnejad M**, Dasgupta I, Flotte TR, Keeler AM. Immunogenicity of Recombinant Adeno-Associated Virus (AAV) Vectors for Gene Transfer. *BioDrugs* 2023; **37**: 311-329 [PMID: 36862289 DOI: 10.1007/s40259-023-00585-7]

19 **Pupo A**, Fernández A, Low SH, François A, Suárez-Amarán L, Samulski RJ. AAV vectors: The Rubik's cube of human gene therapy. *Mol Ther* 2022; **30**: 3515-3541 [PMID: 36203359 DOI: 10.1016/j.ymthe.2022.09.015]

20 **Pan XY**, You HM, Wang L, Bi YH, Yang Y, Meng HW, Meng XM, Ma TT, Huang C, Li J. Methylation of RCAN1.4 mediated by DNMT1 and DNMT3b enhances hepatic stellate cell activation and liver fibrogenesis through Calcineurin/NFAT3 signaling. *Theranostics* 2019; **9**: 4308-4323 [PMID: 31285763 DOI: 10.7150/thno.32710]

21 **Chai S**, Wakefield L, Norgard M, Li B, Enicks D, Marks DL, Grompe M. Strong ubiquitous micro-promoters for recombinant adeno-associated viral vectors. *Mol Ther Methods Clin Dev* 2023; **29**: 504-512 [PMID: 37287749 DOI: 10.1016/j.omtm.2023.05.013]

22 **Mücke MM**, Fong S, Foster GR, Lillicrap D, Miesbach W, Zeuzem S. Adeno-associated viruses for gene therapy - clinical implications and liver-related complications, a guide for hepatologists. *J Hepatol* 2023 [PMID: 37890721 DOI: 10.1016/j.jhep.2023.10.029]

23 **Meumann N**, Cabanes-Creus M, Ertelt M, Navarro RG, Lucifora J, Yuan Q, Nien-Huber K, Abdelrahman A, Vu XK, Zhang L, Franke AC, Schmithals C, Piiper A, Vogt A, Gonzalez-Carmona M, Frueh JT, Ullrich E, Meuleman P, Talbot SR, Odenthal M, Ott M, Seifried E, Schoeder CT, Schwäble J, Lisowski L, Büning H. Adeno-associated virus serotype 2 capsid variants for improved liver-directed gene therapy. *Hepatology* 2023; **77**: 802-815 [PMID: 35976053 DOI: 10.1002/hep.32733]

24 **Lee S**, Zhou P, Whyte S, Shin S. Adeno-Associated Virus Serotype 8-Mediated Genetic Labeling of Cholangiocytes in the Neonatal Murine Liver. *Pharmaceutics* 2020; **12** [PMID: 32295003 DOI: 10.3390/pharmaceutics12040351]

25 **Siew SM**, Cunningham SC, Zhu E, Tay SS, Venuti E, Bolitho C, Alexander IE. Prevention of Cholestatic Liver Disease and Reduced Tumorigenicity in a Murine Model of PFIC Type 3 Using Hybrid AAV-piggyBac Gene Therapy. *Hepatology* 2019; **70**: 2047-2061 [PMID: 31099022 DOI: 10.1002/hep.30773]

26 **Weber ND**, Odriozola L, Martínez-García J, Ferrer V, Douar A, Bénichou B, González-Aseguinolaza G, Smerdou C. Gene therapy for progressive familial intrahepatic cholestasis type 3 in a clinically relevant mouse model. *Nat Commun* 2019; **10**: 5694 [PMID: 31836711 DOI: 10.1038/s41467-019-13614-3]

27 **Zhao L**, Yang Z, Zheng M, Shi L, Gu M, Liu G, Miao F, Chang Y, Huang F, Tang N. Recombinant adeno-associated virus 8 vector in gene therapy: Opportunities and challenges. *Genes Dis* 2024; **11**: 283-293 [PMID: 37588223 DOI: 10.1016/j.gendis.2023.02.010]

28 **Yu H**, Zhou L, Loong JHC, Lam KH, Wong TL, Ng KY, Tong M, Ma VWS, Wang Y, Zhang X, Lee TK, Yun JP, Yu J, Ma S. SERPINA12

promotes the tumorigenic capacity of HCC stem cells through hyperactivation of AKT/β-catenin signaling. *Hepatology* 2023; **78**: 1711-1726 [PMID: 36630996 DOI: 10.1097/HEP.0000000000000269]

29 **Kang J**, Huang L, Zheng W, Luo J, Zhang X, Song Y, Liu A. Promoter CAG is more efficient than hepatocytetargeting TBG for transgene expression *via* rAAV8 in liver tissues. *Mol Med Rep* 2022; **25** [PMID: 34779500 DOI: 10.3892/mmr.2021.12532]

30 **He X**, Wang Y, Fan X, Lei N, Tian Y, Zhang D, Pan W. A schistosome miRNA promotes host hepatic fibrosis by targeting transforming growth factor beta receptor III. *J Hepatol* 2020; **72**: 519-527 [PMID: 31738999 DOI: 10.1016/j.jhep.2019.10.029]

31 **Bala S**, Zhuang Y, Nagesh PT, Catalano D, Zivny A, Wang Y, Xie J, Gao G, Szabo G. Therapeutic inhibition of miR-155 attenuates liver fibrosis *via* STAT3 signaling. *Mol Ther Nucleic Acids* 2023; **33**: 413-427 [PMID: 37547286 DOI: 10.1016/j.omtn.2023.07.012]

32 **Jiang LF**, Yang M, Meng HW, Jia PC, Du CL, Liu JY, Lv XW, Cheng-Huang, Li J. The effect of hepatic stellate cell derived-IL-11 on hepatocyte injury in hepatic fibrosis. *Life Sci* 2023; **330**: 121974 [PMID: 37495078 DOI: 10.1016/j.lfs.2023.121974]

33 **Yan C**, Zhou QY, Wu J, Xu N, Du Y, Li J, Liu JX, Koda S, Zhang BB, Yu Q, Yang HM, Li XY, Zhang B, Xu YH, Chen JX, Wu Z, Zhu XQ, Tang RX, Zheng KY. Csi-let-7a-5p delivered by extracellular vesicles from a liver fluke activates M1-like macrophages and exacerbates biliary injuries. *Proc Natl Acad Sci U S A* 2021; **118** [PMID: 34772807 DOI: 10.1073/pnas.2102206118]

34 **Zhang J**, Lyu Z, Li B, You Z, Cui N, Li Y, Huang B, Chen R, Chen Y, Peng Y, Fang J, Wang Q, Miao Q, Tang R, Gershwin ME, Lian M, Xiao X, Ma X. P4HA2 induces hepatic ductular reaction and biliary fibrosis in chronic cholestatic liver diseases. *Hepatology* 2023; **78**: 10-25 [PMID: 36799463 DOI: 10.1097/HEP.0000000000000317]

35 **Shen Y**, Jiang B, Zhang C, Wu Q, Li L, Jiang P. Combined Inhibition of the TGF-β1/Smad Pathway by Prevotella copri and Lactobacillus murinus to Reduce Inflammation and Fibrosis in Primary Sclerosing Cholangitis. *Int J Mol Sci* 2023; **24** [PMID: 37446187 DOI: 10.3390/ijms241311010]

36 **Kleven MD**, Gomes MM, Wortham AM, Enns CA, Kahl CA. Ultrafiltered recombinant AAV8 vector can be safely administered in vivo and efficiently transduces liver. *PLoS One* 2018; **13**: e0194728 [PMID: 29621273 DOI: 10.1371/journal.pone.0194728]

37 **Sen D**, Gadkari RA, Sudha G, Gabriel N, Kumar YS, Selot R, Samuel R, Rajalingam S, Ramya V, Nair SC, Srinivasan N, Srivastava A, Jayandharan GR. Targeted modifications in adeno-associated virus serotype 8 capsid improves its hepatic gene transfer efficiency in vivo. *Hum Gene Ther Methods* 2013; **24**: 104-116 [PMID: 23442071 DOI: 10.1089/hgtb.2012.195]

38 **Lopes-Pacheco M**, Kitoko JZ, Morales MM, Petrs-Silva H, Rocco PRM. Self-complementary and tyrosine-mutant rAAV vectors enhance transduction in cystic fibrosis bronchial epithelial cells. *Exp Cell Res* 2018; **372**: 99-107 [PMID: 30244179 DOI: 10.1016/j.yexcr.2018.09.015]

39 **Yan Z**, Vorhies K, Feng Z, Park SY, Choi SH, Zhang Y, Winter M, Sun X, Engelhardt JF. Recombinant Adeno-Associated Virus-Mediated Editing of the G551D Cystic Fibrosis Transmembrane Conductance Regulator Mutation in Ferret Airway Basal Cells. *Hum Gene Ther* 2022; **33**: 1023-1036 [PMID: 35686451 DOI: 10.1089/hum.2022.036]

40 **Tang Y**, Yan Z, Engelhardt JF. Viral Vectors, Animal Models, and Cellular Targets for Gene Therapy of Cystic Fibrosis Lung Disease. *Hum Gene Ther* 2020; **31**: 524-537 [PMID: 32138545 DOI: 10.1089/hum.2020.013]

41 **Nakamura Y**, Arawaka S, Sato H, Sasaki A, Shigekiyo T, Takahata K, Tsunekawa H, Kato T. Monoamine Oxidase-B Inhibition Facilitates α-Synuclein Secretion In Vitro and Delays Its Aggregation in rAAV-Based Rat Models of Parkinson's Disease. *J Neurosci* 2021; **41**: 7479-7491 [PMID: 34290084 DOI: 10.1523/JNEUROSCI.0476-21.2021]

42 **Croft CL**, Cruz PE, Ryu DH, Ceballos-Diaz C, Strang KH, Woody BM, Lin WL, Deture M, Rodríguez-Lebrón E, Dickson DW, Chakrabarty P, Levites Y, Giasson BI, Golde TE. rAAV-based brain slice culture models of Alzheimer's and Parkinson's disease inclusion pathologies. *J Exp Med* 2019; **216**: 539-555 [PMID: 30770411 DOI: 10.1084/jem.20182184]

43 **Kok CY**, MacLean LM, Ho JC, Lisowski L, Kizana E. Potential Applications for Targeted Gene Therapy to Protect Against Anthracycline Cardiotoxicity: JACC: CardioOncology Primer. *JACC CardioOncol* 2021; **3**: 650-662 [PMID: 34988473 DOI: 10.1016/j.jaccao.2021.09.008]

44 **Greig JA**, Limberis MP, Bell P, Chen SJ, Calcedo R, Rader DJ, Wilson JM. Non-Clinical Study Examining AAV8.TBG.hLDLR Vector-Associated Toxicity in Chow-Fed Wild-Type and LDLR(+/-) Rhesus Macaques. *Hum Gene Ther Clin Dev* 2017; **28**: 39-50 [PMID: 28319449 DOI: 10.1089/humc.2017.014]

45 **Mak KY**, Chin R, Cunningham SC, Habib MR, Torresi J, Sharland AF, Alexander IE, Angus PW, Herath CB. ACE2 Therapy Using Adeno-associated Viral Vector Inhibits Liver Fibrosis in Mice. *Mol Ther* 2015; **23**: 1434-1443 [PMID: 25997428 DOI: 10.1038/mt.2015.92]

46 **Jiang S**. Recent findings regarding let-7 in immunity. *Cancer Lett* 2018; **434**: 130-131 [PMID: 30053607 DOI: 10.1016/j.canlet.2018.07.027]

47 **Gilles ME**, Slack FJ. Let-7 microRNA as a potential therapeutic target with implications for immunotherapy. *Expert Opin Ther Targets* 2018; **22**: 929-939 [PMID: 30328720 DOI: 10.1080/14728222.2018.1535594]

48 **Jin S**, Zeng X, Fang J, Lin J, Chan SY, Erzurum SC, Cheng F. A network-based approach to uncover microRNA-mediated disease comorbidities and potential pathobiological implications. *NPJ Syst Biol Appl* 2019; **5**: 41 [PMID: 31754458 DOI: 10.1038/s41540-019-0115-2]

49 **Li K**, Yan G, Huang H, Zheng M, Ma K, Cui X, Lu D, Zheng L, Zhu B, Cheng J, Zhao J. Anti-inflammatory and immunomodulatory effects of the extracellular vesicles derived from human umbilical cord mesenchymal stem cells on osteoarthritis *via* M2 macrophages. *J Nanobiotechnology* 2022; **20**: 38 [PMID: 35057811 DOI: 10.1186/s12951-021-01236-1]

50 **Lin D**, Chen H, Xiong J, Zhang J, Hu Z, Gao J, Gao B, Zhang S, Chen J, Cao H, Li Z, Lin B, Gao Z. Mesenchymal stem cells exosomal let-7a-5p improve autophagic flux and alleviate liver injury in acute-on-chronic liver failure by promoting nuclear expression of TFEB. *Cell Death Dis* 2022; **13**: 865 [PMID: 36224178 DOI: 10.1038/s41419-022-05303-9]

51 **Meng F**, Glaser SS, Francis H, DeMorrow S, Han Y, Passarini JD, Stokes A, Cleary JP, Liu X, Venter J, Kumar P, Priester S, Hubble L, Staloch D, Sharma J, Liu CG, Alpini G. Functional analysis of microRNAs in human hepatocellular cancer stem cells. *J Cell Mol Med* 2012; **16**: 160-173 [PMID: 21352471 DOI: 10.1111/j.1582-4934.2011.01282.x]

52 **Kumar M**, Sahu SK, Kumar R, Subuddhi A, Maji RK, Jana K, Gupta P, Raffetseder J, Lerm M, Ghosh Z, van Loo G, Beyaert R, Gupta UD, Kundu M, Basu J. MicroRNA let-7 modulates the immune response to Mycobacterium tuberculosis infection *via* control of A20, an inhibitor of the NF-κB pathway. *Cell Host Microbe* 2015; **17**: 345-356 [PMID: 25683052 DOI: 10.1016/j.chom.2015.01.007]

53 **Kumstel S**, Janssen-Peters H, Abdelrahman A, Tang G, Xiao K, Ernst N, Wendt EHU, Palme R, Seume N, Vollmar B, Thum T, Zechner D. MicroRNAs as systemic biomarkers to assess distress in animal models for gastrointestinal diseases. *Sci Rep* 2020; **10**: 16931 [PMID: 33037288 DOI: 10.1038/s41598-020-73972-7]

54 **Rodrigues PM**, Perugorria MJ, Santos-Laso A, Bujanda L, Beuers U, Banales JM. Primary biliary cholangitis: A tale of epigenetically-induced secretory failure? *J Hepatol* 2018; **69**: 1371-1383 [PMID: 30193962 DOI: 10.1016/j.jhep.2018.08.020]

55 **Tadokoro T**, Morishita A, Masaki T. Diagnosis and Therapeutic Management of Liver Fibrosis by MicroRNA. *Int J Mol Sci* 2021; **22** [PMID: 34360904 DOI: 10.3390/ijms22158139]

World Journal of Gastroenterology

Submit a Manuscript: https://www.f6publishing.com

World J Gastroenterol 2024 February 7; 30(5): 485-498

DOI: 10.3748/wjg.v30.i5.485

ISSN 1007-9327 (print) ISSN 2219-2840 (online)

ORIGINAL ARTICLE

Basic Study

Bile acids inhibit ferroptosis sensitivity through activating farnesoid X receptor in gastric cancer cells

Chu-Xuan Liu, Ying Gao, Xiu-Fang Xu, Xin Jin, Yun Zhang, Qian Xu, Huan-Xin Ding, Bing-Jun Li, Fang-Ke Du, Lin-Chuan Li, Ming-Wei Zhong, Jian-Kang Zhu, Guang-Yong Zhang

Specialty type: Gastroenterology and hepatology

Provenance and peer review: Unsolicited article; Externally peer reviewed.

Peer-review model: Single blind

Peer-review report's scientific quality classification

Grade A (Excellent): 0
Grade B (Very good): B
Grade C (Good): 0
Grade D (Fair): 0
Grade E (Poor): 0

P-Reviewer: Kalkum E, Germany

Received: November 21, 2023
Peer-review started: November 21, 2023
First decision: December 8, 2023
Revised: December 12, 2023
Accepted: January 11, 2024
Article in press: January 11, 2024
Published online: February 7, 2024

Chu-Xuan Liu, Xin Jin, Guang-Yong Zhang, Department of General Surgery, Shandong Provincial Qianfoshan Hospital, Shandong University, Jinan 250014, Shandong Province, China

Ying Gao, Department of General Surgery, Linyi People's Hospital, Linyi 276034, Shandong Province, China

Xiu-Fang Xu, Department of Nursing, Huantai TCM Hospital, Zibo 256400, Shandong Province, China

Yun Zhang, Center for Translational medical Research, The First Affiliated Hospital of Shandong First Medical University, Jinan 250014, Shandong Province, China

Qian Xu, Huan-Xin Ding, Bing-Jun Li, Fang-Ke Du, Lin-Chuan Li, Ming-Wei Zhong, Jian-Kang Zhu, Guang-Yong Zhang, Department of General Surgery, The First Affiliated Hospital of Shandong First Medical University, Jinan 250014, Shandong Province, China

Corresponding author: Guang-Yong Zhang, MD, Chief Doctor, Professor, Department of General Surgery, The First Affiliated Hospital of Shandong First Medical University, No. 16766 Jingshi Road, Jinan 250014, Shandong Province, China. guangyongzhang@hotmail.com

Abstract

BACKGROUND

Gastric cancer (GC) is associated with high mortality rates. Bile acids (BAs) reflux is a well-known risk factor for GC, but the specific mechanism remains unclear. During GC development in both humans and animals, BAs serve as signaling molecules that induce metabolic reprogramming. This confers additional cancer phenotypes, including ferroptosis sensitivity. Ferroptosis is a novel mode of cell death characterized by lipid peroxidation that contributes universally to malignant progression. However, it is not fully defined if BAs can influence GC progression by modulating ferroptosis.

AIM

To reveal the mechanism of BAs regulation in ferroptosis of GC cells.

METHODS

In this study, we treated GC cells with various stimuli and evaluated the effect of

BAs on the sensitivity to ferroptosis. We used gain and loss of function assays to examine the impacts of farnesoid X receptor (FXR) and BTB and CNC homology 1 (BACH1) overexpression and knockdown to obtain further insights into the molecular mechanism involved.

RESULTS

Our data suggested that BAs could reverse erastin-induced ferroptosis in GC cells. This effect correlated with increased glutathione (GSH) concentrations, a reduced GSH to oxidized GSH ratio, and higher GSH peroxidase 4 (GPX4) expression levels. Subsequently, we confirmed that BAs exerted these effects by activating FXR, which markedly increased the expression of GSH synthetase and GPX4. Notably, BACH1 was detected as an essential intermediate molecule in the promotion of GSH synthesis by BAs and FXR. Finally, our results suggested that FXR could significantly promote GC cell proliferation, which may be closely related to its anti-ferroptosis effect.

CONCLUSION

This study revealed for the first time that BAs could inhibit ferroptosis sensitivity through the FXR-BACH1-GSH-GPX4 axis in GC cells. This work provided new insights into the mechanism associated with BA-mediated promotion of GC and may help identify potential therapeutic targets for GC patients with BAs reflux.

Key Words: Gastric cancer; Ferroptosis; Bile acids; Chenodeoxycholic acid; Farnesoid X receptor; Glutathione

Core Tip: Gastric cancer (GC) is the fifth most common cancer worldwide and the third leading cause of cancer-related deaths. Bile acids (BAs) reflux is an essential carcinogenic factor in GC, but its role has not been absolutely elaborated. BAs could serve as signaling molecules to regulate the metabolic state in cells, which is closely related to ferroptosis. In the present experiment, we explored the role of BAs in the regulation of ferroptosis in GC cells. Our data suggested that BAs could significantly inhibit the ferroptosis sensitivity of GC cells and that this effect was exerted through the activation of the farnesoid X receptor-BTB and CNC homology 1-glutathione (GSH)-GSH peroxidase 4 axis.

Citation: Liu CX, Gao Y, Xu XF, Jin X, Zhang Y, Xu Q, Ding HX, Li BJ, Du FK, Li LC, Zhong MW, Zhu JK, Zhang GY. Bile acids inhibit ferroptosis sensitivity through activating farnesoid X receptor in gastric cancer cells. *World J Gastroenterol* 2024; 30(5): 485-498

URL: https://www.wjgnet.com/1007-9327/full/v30/i5/485.htm

DOI: https://dx.doi.org/10.3748/wjg.v30.i5.485

INTRODUCTION

Gastric cancer (GC) is the fifth most common cancer worldwide and the third leading cause of cancer-related deaths because of the difficulties associated with early diagnosis [1]. Along with the improvement of life conditions, there is a noticeable decrease in the prevalence of *Helicobacter pylori* infection, which is the major causative factor of GC[2]. Bile acids (BAs) reflux, another etiologic factor for developing GC, is receiving more attentions[3]. BAs are cholesterol-derived sterols. These small-molecule metabolites play essential roles in the human body. They are amphiphilic and can thus participate in cholesterol absorption and secretion in the intestines[4]. Previous work has shown that BAs reflux is an independent risk factor for precancerous gastric lesions and gastric carcinogenesis[5,6]. For example, gastric mucosal damage can be induced by BAs through activation of the IL-6/JAK1/STAT3 pathway[5]. However, the mechanism by which BAs can promote GC progression remains unknown.

By activating BAs receptors, BAs can modulate immune responses, gastrointestinal mucosal barrier function, gestation, metabolic diseases, and carcinogenesis[7-10]. The farnesoid X receptor (FXR, NR1H4) is a typical BA receptor that has been well investigated. Cholic acid (CA) and chenodeoxycholic acid (CDCA) are the two predominant BAs in the human body[11], the latter of which is the most potent physiologic agonist of FXR[12]. FXR activation can remodel the metabolic state of cells, including glucose metabolism and lipid metabolism, which in turn is involved in the development of a variety of metabolic diseases and cancers, such as hepatocellular carcinoma[13]. However, further research on the role of FXR in GC patients with BAs reflux is required.

An altered metabolic state, also known as metabolic reprogramming, is a vital factor in cancer progression[14]. Ferroptosis, which is closely related to metabolism, may be involved in the effects of BAs and FXR in GC[15]. Ferroptosis is a novel type of cell death characterized by intracellular phospholipid peroxidation, distinct from apoptosis, pyroptosis, necroptosis, and autophagy[16,17]. This unique mode of cell death is regulated by a variety of factors, particularly oxidative stress. Glutathione (GSH) peroxidase 4 (GPX4) specifically recognizes peroxidized lipids and scavenges them by converting reduced GSH to oxidized GSH (GSSG) for anti-ferroptosis[18,19]. Therefore, GSH, as the substrate of GPX4, also has a key role in the resistance to ferroptosis. Changes in GSH metabolism will eventually lead to alterations in cellular sensitivity to ferroptosis[20]. Although ferroptosis has been reported in GC development and treatment[21,22],

few studies have described ferroptosis in GC with BAs reflux.

In the present study, we investigated the role of BAs, especially CDCA, in the regulation of ferroptosis sensitivity in GC. We subsequently identified the specific receptors for these BAs and further investigated the molecular mechanism.

MATERIALS AND METHODS

Reagents and antibodies

CA (S3742), dehydrocholic acid (DCA, S4562), CDCA (S1843), erastin (S7242), Ferrostatin-1 (Fer-1, S7243), and GW4064 (S2782) were purchased from Selleck Chemicals (Houston, TX, United States). RSL3 (HY-100218A) was purchased from MedChemExpress (Monmouth Junction, NJ, United States). Anti-GPX4 (67763-1-Ig, 1:2500), anti-β-actin (HRP-66009, 1:5000), anti-FXR (25055-1-Ig, 1:1000), anti-GCLC (12601-1-AP, 1:4000), anti-GCLM (14241-1-AP, 1:4000), anti-GSS (67598-1-Ig, 1:4000), and anti-BTB and CNC homology 1 (BACH1, 14018-1-AP, 1:5000) antibodies were purchased from Proteintech (Wuhan, China).

Cell culture

HGC-27 and MKN-45 cells were purchased from Procell (Wuhan, China) and cultured in MEM (for HGC-27) and RPMI-1640 (for MKN-45) medium (Gibco, Carlsbad, CA, United States) containing 10% fetal bovine serum (FBS; Gibco) and 1% Penicillin/Streptomycin (Gibco) at 37°C and 5% CO_2. The cell lines were correctly identified by short tandem repeat (STR) analysis and periodically tested for mycoplasma.

Cell transfection

Cells were seeded in 6-well plates (5×10^5 cells/well) and incubated for 18 h. Then, overexpression or short hairpin RNA plasmids for the indicated genes were transfected using Lipofectamine 2000 (Invitrogen, Carlsbad, CA, United States) for 48 h according to the manufacturer's instructions.

Cell viability assay

Cells were seeded in 96-well plates (5000 cells/well) in complete medium. After incubation for 18 h, the indicated treatments were added to the cells and incubated for certain times. Then, 100 mL complete medium containing 10 mL cell count kit-8 reagent (CK04, Dojindo Laboratories, Kumamoto, Japan) was added to each well. After incubating the cells for 2 h, the absorbance value for each well was colorimetrically measured at a wavelength of 450 nm.

GSH and Malondialdehyde assay quantification

The cells were collected after indicated stimuli. The GSH concentrations and GSH/GSSG ratio were quantified using the GSSG/GSH Quantification Kit (G263, Dojindo Laboratories, Kumamoto, Japan) according to the manufacturer's instructions. The results were quantified colorimetrically at a wavelength of 405 nm.

After the indicated treatments, the cells were collected and assayed using the Malondialdehyde (MDA) Assay Kit (S0131S, Beyotime, Shanghai, China) following the manufacturer's instructions to measure the levels of MDA. The results were quantified colorimetrically at a wavelength of 532 nm.

Lipid reactive oxygen species assay

After the indicated treatments, BODIPY-589/591 C11 (D3861, Thermo Fisher Scientific, Waltham, MA, USA) was added to each well (10 mM). After incubated at 37°C for 30 min, the cells were washed with PBS for three times. Subsequently, the nuclei were stained with DAPI (C1002, Beyotime) for 30 min at room temperature. Finally, the lipid reactive oxygen species was observed under a fluorescence microscope with 488 nm excitation.

5-ethynyl-2'-deoxyuridin staining

Cell proliferation rates under different treatment conditions were assessed using 5-ethynyl-2'-deoxyuridine (EdU) assays (Beyotime) according to the manufacturer's instructions.

Colony formation assay

Cells were seeded in 6-well plates (500 cells/well), treated with various stimuli, and incubated for 10 to 14 d. The cells were then rinsed three times with PBS and fixed with 4% paraformaldehyde at room temperature for 30 min. Subsequently, the fixed cells were treated with crystal violet at 4°C overnight.

Western blot

Cells were lysed using RIPA buffer containing 1% Phenylmethanesulfonyl fluoride (PMSF, ST505, Beyotime, Shanghai, China) and 2% phosphatase inhibitor. The total protein concentration was quantified using the Bicinchoninic Acid Protein Assay Kit (ST505, Thermo Fisher Scientific, Waltham, MA, United States). Next, protein samples (30 mg) were separated using 10% SDS-PAGE (PG212, EpiZyme, Shanghai, China). Then, the proteins were transferred to PVDF membranes, followed by blocking with 5% BSA (A8020, Solarbio, Beijing, China) at room temperature for 1 h. Afterwards, the membranes were incubated with primary antibodies at 4°C overnight. Subsequently, the membranes were washed with PBST and incubated with a goat anti-mouse or goat anti-rabbit secondary antibody for 1 h at room temperature. Finally,

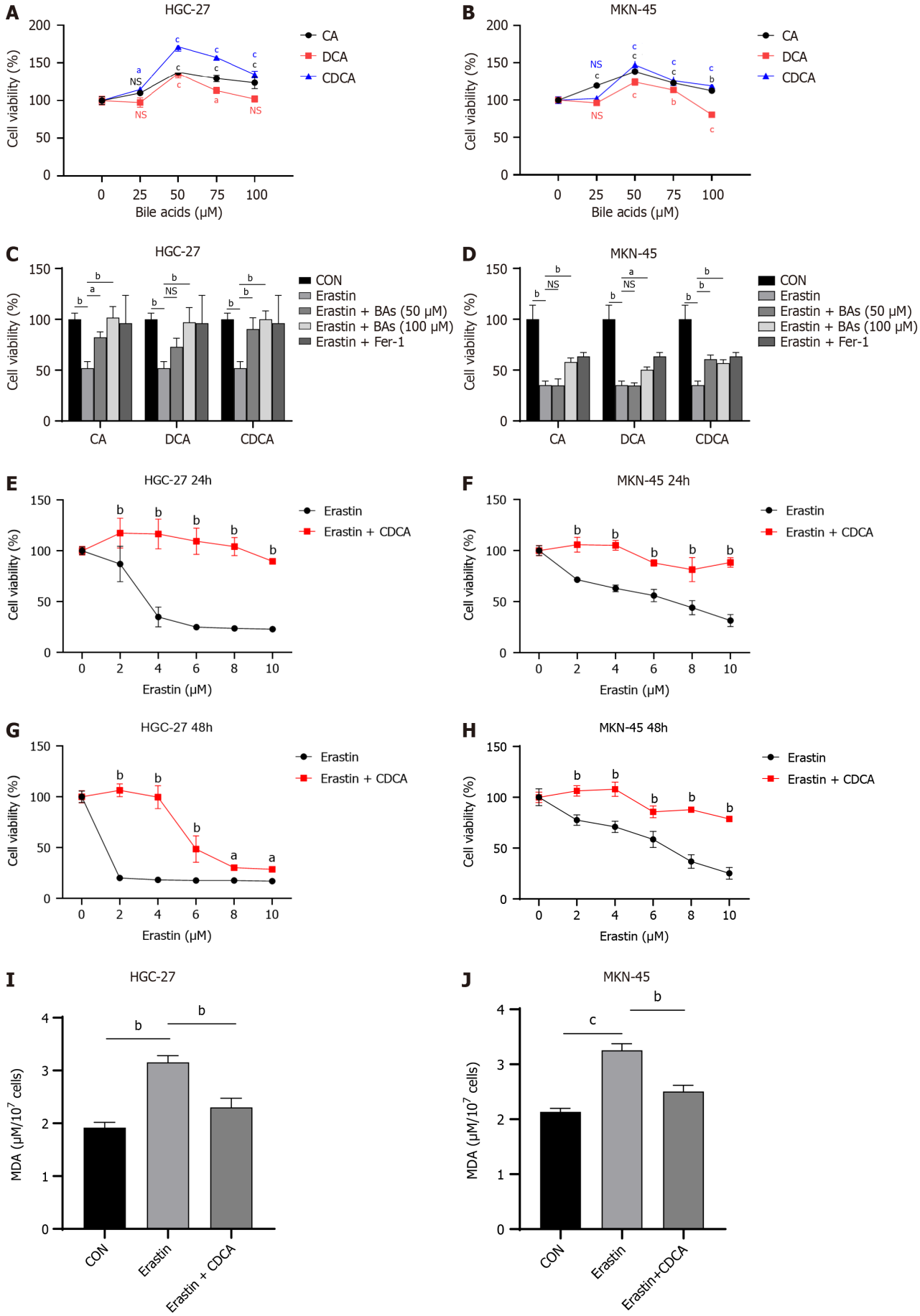
A
HGC-27
Cell viability (%)
Bile acids (μM)
CA
DCA
CDCA
B
MKN-45
C
HGC-27
CON
Erastin
Erastin + BAs (50 μM)
Erastin + BAs (100 μM)
Erastin + Fer-1
D
MKN-45
E
HGC-27 24h
Erastin
Erastin + CDCA
Erastin (μM)
F
MKN-45 24h
G
HGC-27 48h
H
MKN-45 48h
I
HGC-27
MDA (μM/10^7 cells)
Erastin + CDCA
J
MKN-45
Erastin+CDCA

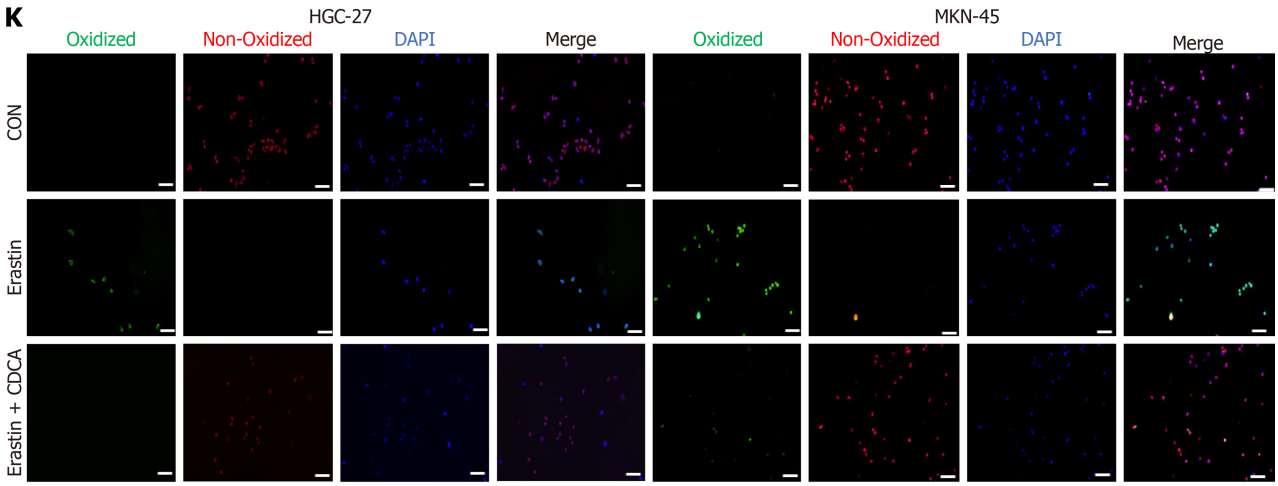

DOI: 10.3748/wjg.v30.i5.485

Figure 1 Bile acids enhanced proliferation and inhibited erastin-induced ferroptosis sensitivity in gastric cancer cells. A and B: Cell viability assay for HGC-27 and MKN-45 cells treated with three Bas; C and D: Cell viability assay for HGC-27 and MKN-45 cells treated with different concentration of BAs together with erastin (5 μM); E-H: Cell viability assay for two gastric cancer cell lines stimulated with erastin followed by chenodeoxycholic acid (50 μM) or control for 24 and 48 h; I and J: Malondialdehyde production in HGC-27 and MKN-45 cells; K: BODIPY-589/591 C11 staining to identify lipid reactive oxygen species in the cell lines under different treatments. Scale bar: 100 μm. $^{a}P < 0.05$, $^{b}P < 0.01$, $^{c}P < 0.001$. These experiments were repeated three times. BAs: Bile acids; CA: Cholic acid; DCA: Dehydrocholic acid; CDCA: Chenodeoxycholic acid; MDA: Malondialdehyde; NS: Not significant.

the protein bands were visualized with ECL (Millipore) and quantified with ImageJ software (National Institutes of Health) the manufacturer's instructions.

Statistical analyses

SPSS 22.0 software (Chicago, IL, United States) was used for data analysis. GraphPad Prism 8.0 (San Diego, CA, United States) software was used to create the images. Data are presented as mean ± SD. One-way ANOVA was used to compare the differences between groups. A *P* value of less than 0.05 indicated statistical significance.

RESULTS

BAs can promote GC cell proliferation and inhibit erastin-induced ferroptosis sensitivity in GC cells

It has been shown that BAs tend to induce gastric intestinal metaplasia prior to causing GC[23]. Thus, two GC cell lines, HGC-27 and MKN-45, were chosen because they were both classified as intestinal type GC cells[24]. Three common BAs including CA, DCA, and CDCA, were chosen to stimulate GC cells *in vitro*. The cell viability assay results suggested that these BAs could significantly promote GC cell proliferation rates, especilly CDCA (Figure 1A and B). Subsequently, to investigate if they could modulate ferroptosis in GC cells, we examined the effects of the three BAs on HGC-27 and MKN-45 cell sensitivity to erastin, a classical inducer of ferroptosis. Interestingly, the GC cells treated with BAs exhibited higher viabilities compared with the controls, suggesting that the BAs possibly could support resistance to the ferroptosis induced by erastin (Figure 1C and D). Because it was the most effective BAs proved by above results and in previous study[23], CDCA was chosen in subsequent experiments. We then examined the effect of CDCA on the sensitivity to erastin-induced ferroptosis in GC cells at 24 and 48 h, respectively. The anti-ferroptosis effect was confirmed (Figure 1E-H). To exclude interference from other types of cell death, we performed the MDA assays (Figure 1I and J) and BODIPY-589/591 C11 staining (Figure 1K), which directly reflected ferroptosis and reconfirmed the anti-ferroptosis function of the BAs.

BAs significantly upregulated GSH and GPX4 Levels in GC cells

The cystine-glumate antiporter (xCT) is an essential anti-ferroptosis protein located on the cytomembrane that exchanges intracellular glutamate for extracellular cystine in a 1:1 ratio[25,26]. Mechanistically, erastin induces ferroptosis by acting on xCT and inhibiting its function. This thereby downregulates the levels of downstream GSH and GPX4, which inhibit the onset of ferroptosis[27]. Additionally, another classical ferroptosis inducer is RSL3, which targets and inactivates GPX4[28]. Therefore, to explore the anti-ferroptosis mechanism of CDCA, we examined its effect on RSL3-induced cell death using cell viability assays. Interestingly, CDCA did not ameliorate RSL3-induced GC cell death (Figure 2A and B), nor could it ameliorate the ferroptosis caused by RSL3 (Figure 2C-E). We therefore speculated that CDCA possibly exerted its anti-ferroptosis effect by upregulating GSH and GPX4 levels. To verify this hypothesis, we examined the GSH concentrations and GSH/GSSG ratio in CDCA-treated cells, finding that CDCA treatment significantly increased them compared with the control group (Figure 2F-I). Besides, CDCA also significantly attenuated the GPX4 protein expression downregulation induced by erastin, as seen with Western blot (WB) analysis (Figure 2J and K).

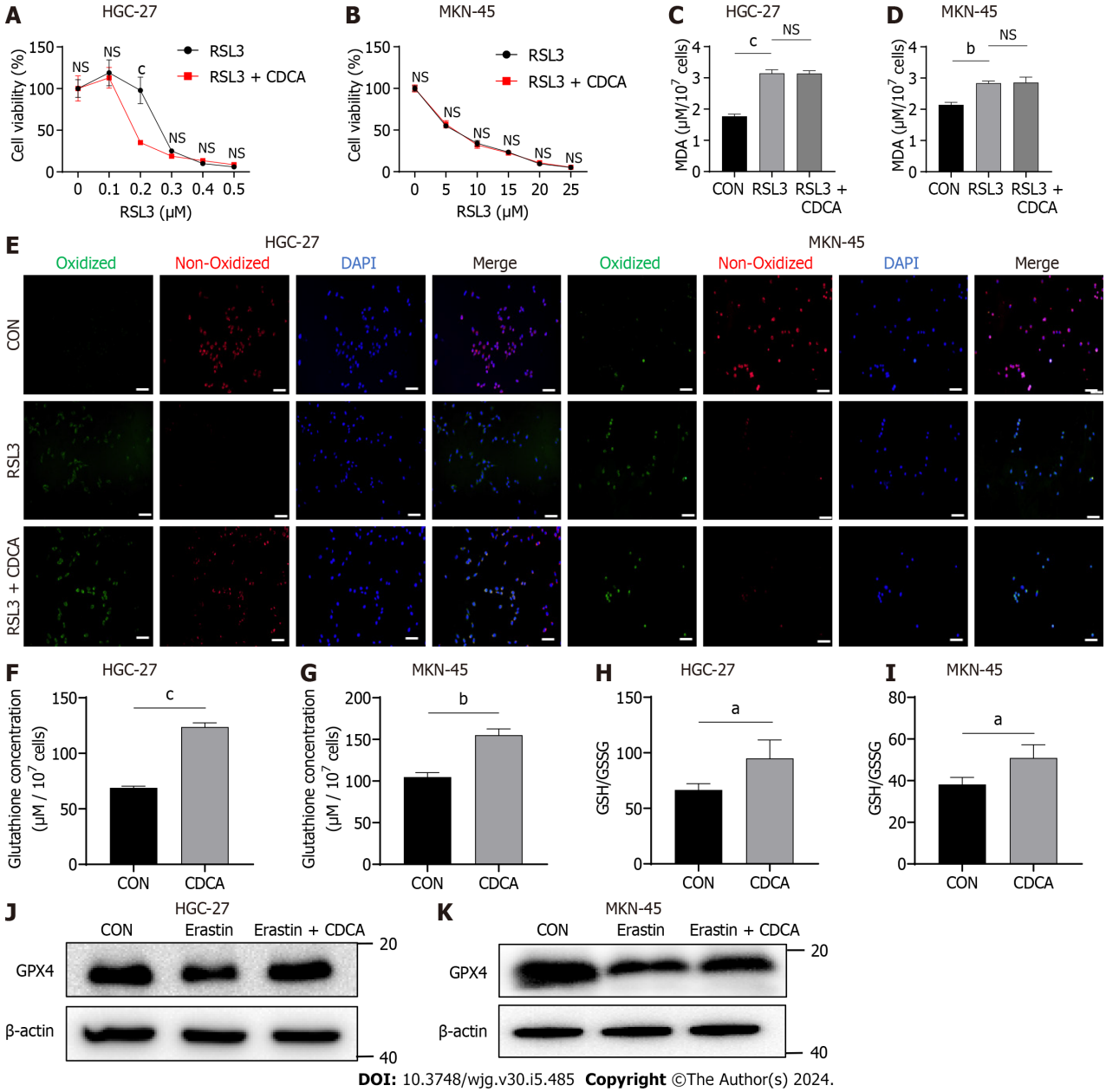

DOI: 10.3748/wjg.v30.i5.485

Figure 2 Bile acids significantly upregulated glutathione and glutathione peroxidase 4 in gastric cancer cells. A and B: Cell viability assay of two gastric cancer cell lines treated with RSL3 together with chenodeoxycholic acid (CDCA) or control; C and D: Malondialdehyde production in HGC-27 and MKN-45 cells treated with RSL3 (0.2 μM for HGC-27, 10 μM for MKN-45) followed by CDCA or control; E: BODIPY-589/591 C11 staining to identify lipid reactive oxygen species in the cell lines treated with RSL3 (0.2 μM for HGC-27, 10 μM for MKN-45) followed by CDCA or control; F and G: The glutathione (GSH) concentrations were measured in cells treated with CDCA; H and I: The GSH/oxidized GSH ratio was measured in cells treated with CDCA; J and K: Western blot analysis of GSH peroxidase 4 protein expression in HGC-27 and MKN-45 cells under different stimuli. Scale bar: 100 μm. $^{a}P < 0.05$, $^{b}P < 0.01$, $^{c}P < 0.001$. These experiments were repeated three times. CDCA: Chenodeoxycholic acid; MDA: Malondialdehyde; GPX4: Glutathione peroxidase 4; NS: Not significant.

BAs exerted its anti-ferroptosis sensitivity function in GC cells by activating FXR

CDCA is the strongest FXR agonist in the human body[12]. Therefore, we hypothesized that CDCA acted through activating FXR to inhibit the sensitization of GC cells to ferroptosis. We firstly used GW4064, an *in vitro* agonist of FXR, and found that the ferroptosis sensitivity of GC cells treated with GW4064 was significantly reduced (Figure 3A and B). Subsequently, we transfected shFXR and its control plasmid in HGC-27 and MKN-45 cells, constructing a cellular knockdown model of FXR to be successfully constructed by WB analysis (Figure 3C and D). Our data showed that after knocking down FXR, CDCA-induced erastin resistance was not observed (Figure 3E and F) and it could no longer reverse the onset of erastin-induced ferroptosis (Figure 3G-I). We further constructed an overexpression model of FXR in HGC-27 and MKN-45 cells (Figure 3J and K). FXR overexpression resulted in a significant enhancement of resistance to erastin-induced cell death in HGC-27 and MKN-45 (Figure 3L and M), as well as a significant reversal of ferroptosis (Figure 3N-P).

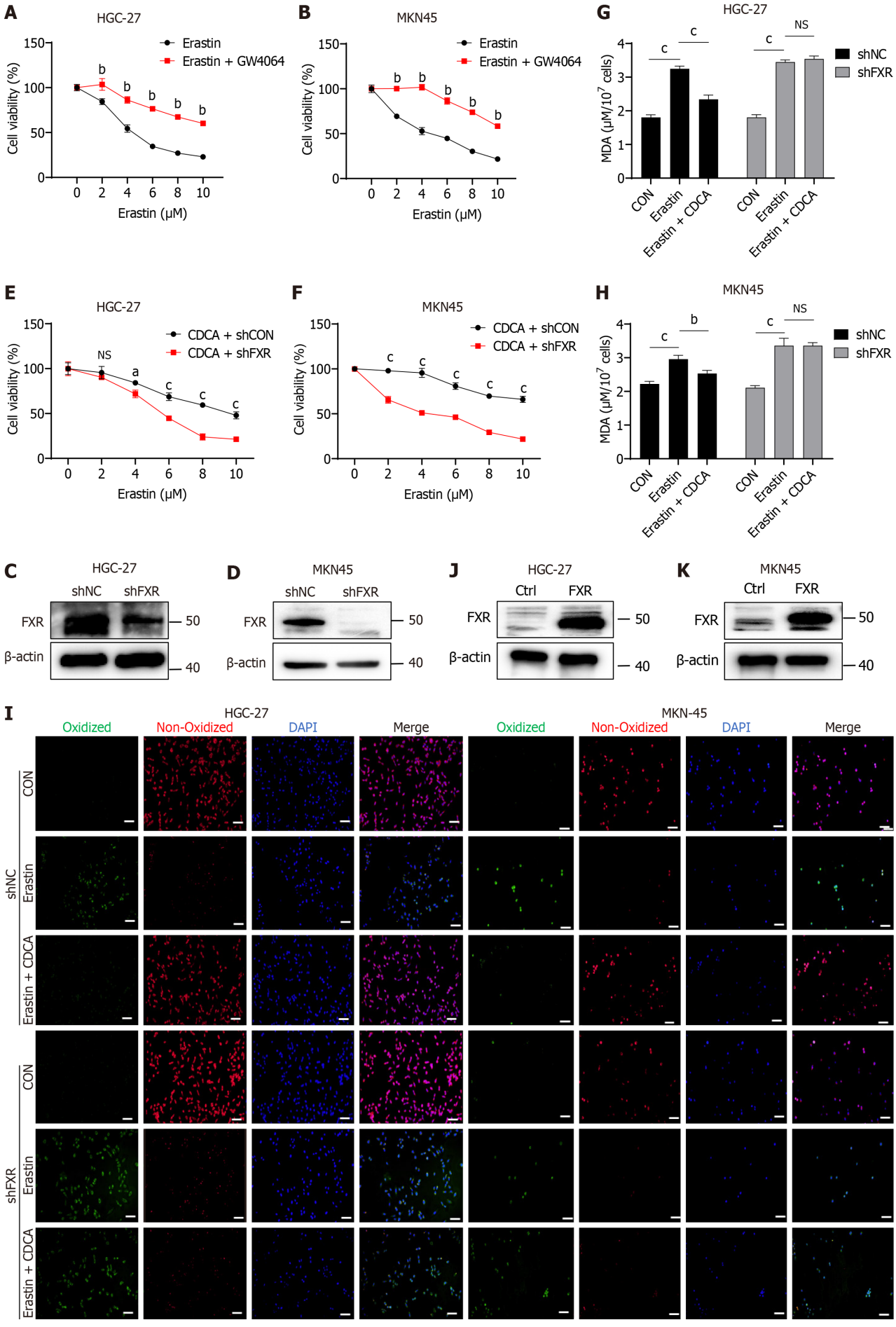
A
HGC-27
Erastin
Erastin + GW4064
Cell viability (%)
Erastin (μM)
B
MKN45
G
HGC-27
MDA (μM/10^7 cells)
shNC
shFXR
CON
Erastin
Erastin + CDCA
NS
E
HGC-27
CDCA + shCON
CDCA + shFXR
F
MKN45
H
MKN45
C
HGC-27
shNC
shFXR
FXR
β-actin
D
MKN45
J
HGC-27
Ctrl
FXR
K
MKN45
I
HGC-27
MKN-45
Oxidized
Non-Oxidized
DAPI
Merge

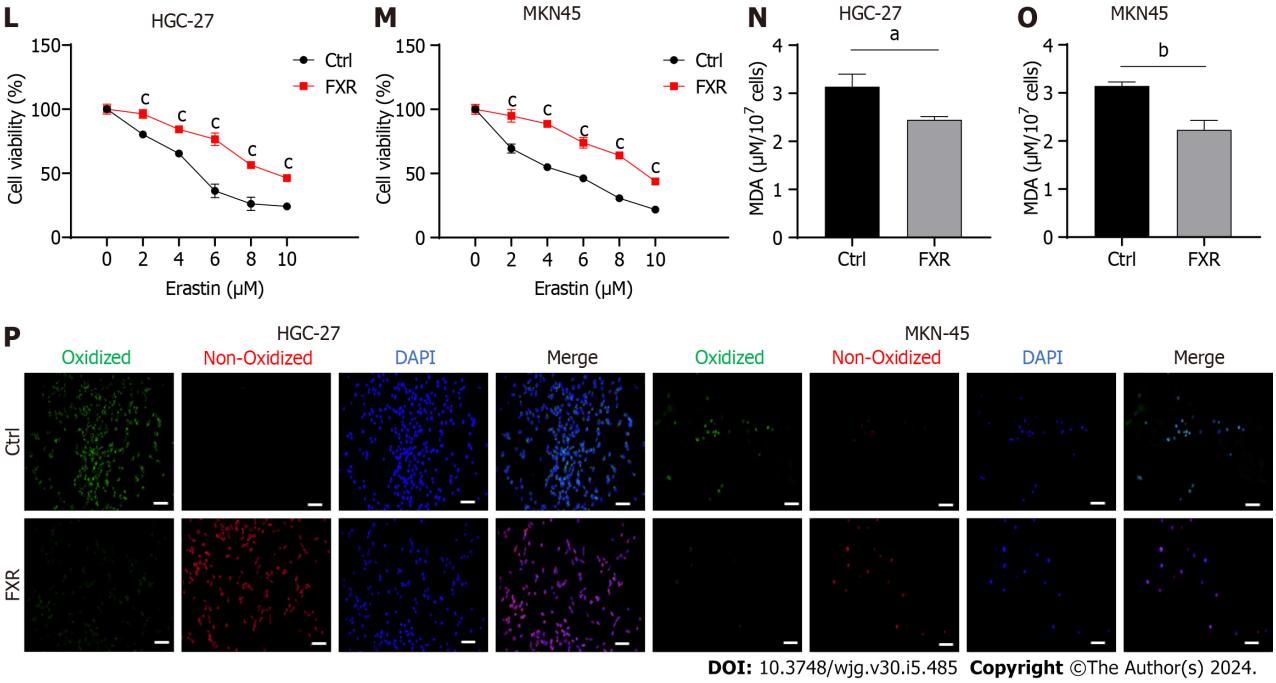

DOI: 10.3748/wjg.v30.i5.485

Figure 3 Bile acids inhibited ferroptosis sensitivity of gastric cancer cells by activating farnesoid X receptor. A and B: Cell viability of erastin-treated HGC-27 and MKN-45 cells with or without GW4064 treatment; C and D: HGC-27 and MKN-45 cells were transfected with shFXR or shNC plasmid. Successful construction was confirmed by western blot analysis; E and F: Cell viability assay of GC cells treated with different concentrations of erastin and CDCA (50 μM) transfected with shFXR or shNC for 24 h; G-I: Malondialdehyde (MDA) production and BODIPY-589/591 C11 staining of GC cells transfected with shFXR or shNC plasmid and treated with erastin together with or without CDCA for 24 h; J and K: GC cells were transfected with control or FXR-coding plasmid and confirmed through western blot analysis; L and M: Cell viability assay of GC cells treated with different concentrations of erastin and CDCA (50 μM) transfected with control or FXR-coding plasmid for 24 h.; N-P: MDA production and BODIPY-589/591 C11 staining of GC cells transfected with control or FXR-coding plasmid and treated with erastin together with or without CDCA for 24 h. Scale bar: 100 μm. $^{a}P < 0.05$, $^{b}P < 0.01$, $^{c}P < 0.001$. These experiments were repeated three times. FXR: Farnesoid X receptor; NC: Negative control; CDCA: Chenodeoxycholic acid; MDA: Malondialdehyde; NS: Not significant.

FXR significantly promoted GSH synthesis in GC cells

To investigate whether FXR could likewise increase intracellular GSH concentrations, we examined the effect of FXR on GSH levels. The results showed that GSH concentrations were significantly reduced after FXR knockdown in HGC-27 and MKN-45 cells (Figure 4A and B). The GSH/GSSG ratio, an indicator of cellular antioxidant capacity, was also significantly decreased after FXR knockdown (Figure 4C and D). We next examined the effect of FXR on the protein expression levels of GSH synthesis-related enzymes in GC cells using WB analysis, finding that FXR knockdown significantly reduced the expression of GSH synthases, including GCLC, GCLM and GSS. It also affected GPX4 expression levels, which used GSH as a substrate (Figure 4E and F). To further validate these observations, we repeated the above experiments using the FXR overexpression HGC-27 and MKN-45 cells. The results showed that overexpressing FXR in these GC cells led to increased GSH concentrations (Figure 4G and H), GSH/GSSG ratio (Figure 4I and J), and GSH synthase and GPX4 expression levels (Figure 4K and L).

FXR exerted its anti-ferroptosis and pro-GSH synthesis effects correlating with inhibiting BACH1 in GC cells

Recently, FXR was shown to inhibit heme catabolism and increase heme levels by repressing HO-1 transcription[29]. Heme in high concentrations can inhibit BACH1, which can lead to decreased expression of GSH synthases[30,31]. Therefore, BACH1 is potentially a crucial bridge through which FXR exerted its effects. We firstly detected BACH1 protein expression using WB analysis in HCG-27 and MKN-45 cells with overexpression or knockdown of FXR expression. The results showed that knocking down FXR indeed significantly elevated BACH1 protein levels (Figure 5A and B), while overexpressing FXR significantly downregulated BACH1 expression (Figure 5C and D). To further validate the role of BACH1 in this system, we constructed overexpression models of BACH1 in HGC-27 and MKN-45 cells and verified (Figure 5E and F). We then transfected cells with the FXR overexpression plasmid together with the BACH1 overexpression plasmid and erastin treatment. This rescue experiment suggested that overexpression of BACH1 Led to a significant reduction in ferroptosis resistance mediated by FXR, as seen with the MDA assay and BODIPY-589/591 C11 staining results (Figure 5G-I). Simultaneously, FXR-mediated enhancements of GSH concentrations (Figure 5J and K), GSH/GSSG ratio (Figure 5L and M), GSH synthase expression including GCLC, GCLM, GSS, and GPX4 (Figure 5N and O) were significantly reversed by overexpressed BACH1.

FXR significantly promoted GC cells proliferation

To further determine the role of FXR in GC progression, we analyzed its biological functions in GC cells. As described above, knockdown models of FXR in HGC-27 and MKN-45 cells were constructed (Figure 3C and D). Subsequently, cell

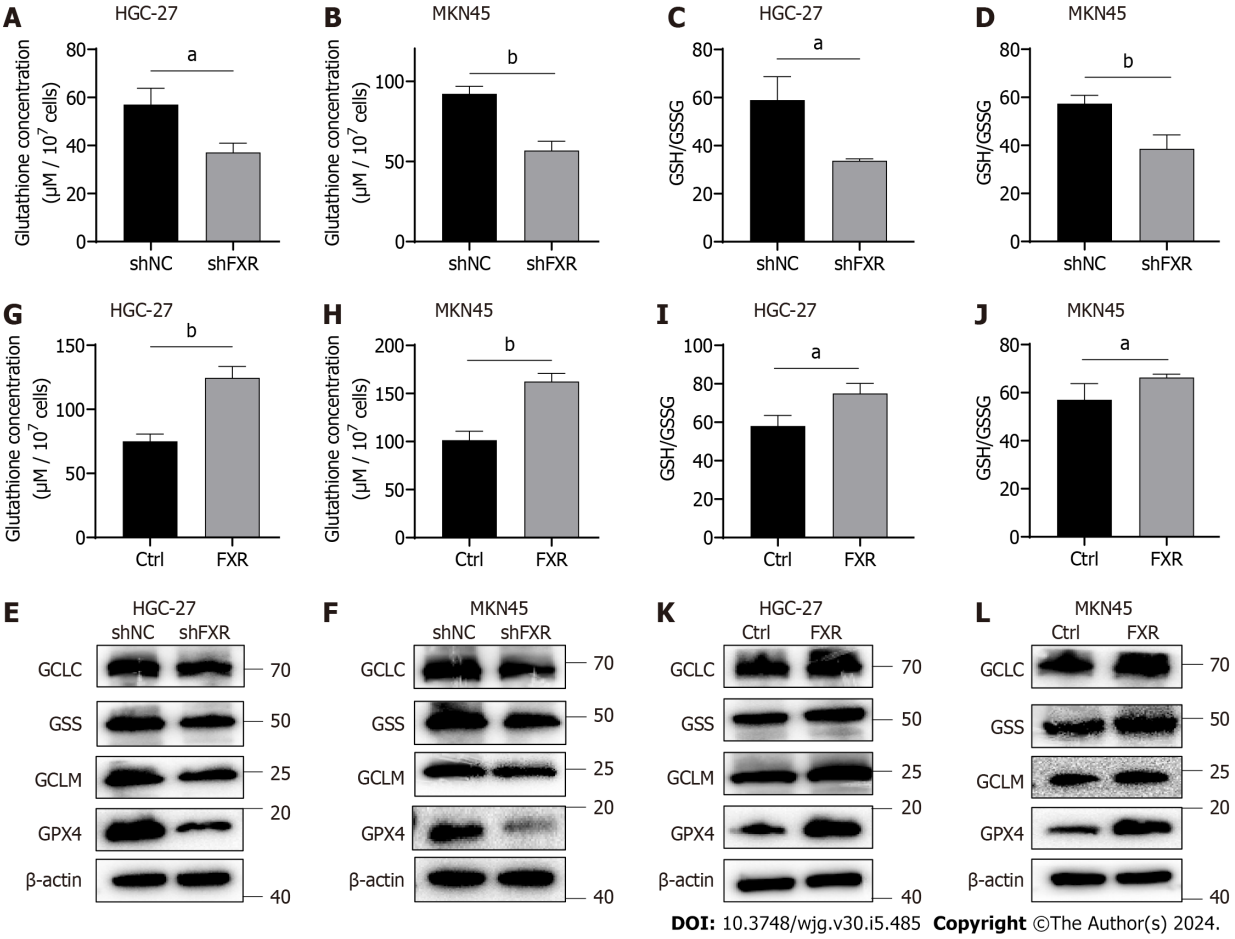

DOI: 10.3748/wjg.v30.i5.485

Figure 4 Farnesoid X receptor significantly promoted the synthesis of glutathione **and the level of glutathione peroxidase 4 in gastric cancer cells.** A-D: Alterations of glutathione (GSH) concentrations and the GSH/oxidized GSH (GSSG) ratio in HGC-27 and MKN-45 cells transfected with the shNC or shFXR plasmid; E and F: Protein expression of GCLC, GSS, GCLM, and GSH peroxidase 4 (GPX4) in HGC-27 and MKN-45 cells transfected with the shNC or shFXR plasmid; G-J: Alterations of GSH concentrations and the GSH/GSSG ratio in HGC-27 and MKN-45 cells transfected with the control or farnesoid X receptor (FXR)-coding plasmid; K and L: Protein expression of GCLC, GSS, GCLM, and GPX4 in HGC-27 and MKN-45 cells transfected with the control or FXR-coding plasmid. $^{a}P < 0.05$, $^{b}P < 0.01$. These experiments were repeated three times. FXR: Farnesoid X receptor; GPX4: Glutathione peroxidase 4.

viability assays showed that GC cell proliferation rates were significantly reduced after FXR knockdown (Figure 6A and B). This was also confirmed by EdU staining, which showed that the proportion of actively proliferating GC cells was significantly reduced with lower FXR expression levels (Figure 6C and D). Additional assays likewise revealed that the colony formation ability of GC cells was significantly decreased after knocking down FXR (Figure 6E and F). Experiments with the overexpression model showed that FXR promoted GC cell proliferation (Figure 6G and H), facilitated the capacity of DNA replication (Figure 6I and J), and enhanced the colony formation ability (Figure 6K and L).

DISCUSSION

GC is a major cause of cancer-related mortality in East Asia[32], but the molecular mechanisms and regulatory systems involved still need to be further elucidated. In the present study, we provided evidence that BAs can promote GC progression by inhibiting the ferroptosis sensitivity of GC, then explored the related mechanism in more detail.

BAs are essential small-molecule metabolites that can act as signaling molecules in the onset and progression of many diseases in humans, including various cancers[33]. For example, BAs can promote gastric carcinogenesis *via* the IL-6/JAK1/STAT3 axis[5]. Since the discovery of ferroptosis, numerous studies have focused on its potential use as a therapeutic target in cancer, including in GC[34]. For instance, activation of the Wnt/beta-catenin signaling pathway significantly enhanced ferroptosis resistance in GC[35]. ACTL6A inhibits the onset of ferroptosis in GC by upregulating GCLC[36]. However, only a few studies have explored whether BAs can affect GC through regulation of ferroptosis. Our data indicated that several BAs, especially CDCA, significantly inhibit erastin-induced GC cell death. Additionally, we confirmed that erastin induced cell death through ferroptosis. Subsequently, we found that the BAs did not reverse cell death induced by RSL3, a ferroptosis inducer that targeted GPX4. This suggested that BAs may exert their anti-ferroptosis activity through GSH, which is downstream of the erastin target xCT and upstream of GPX4. Indeed, both the GSH concentration and the GSH/GSSG ratio were significantly elevated following treatment of GC cells with BAs. This

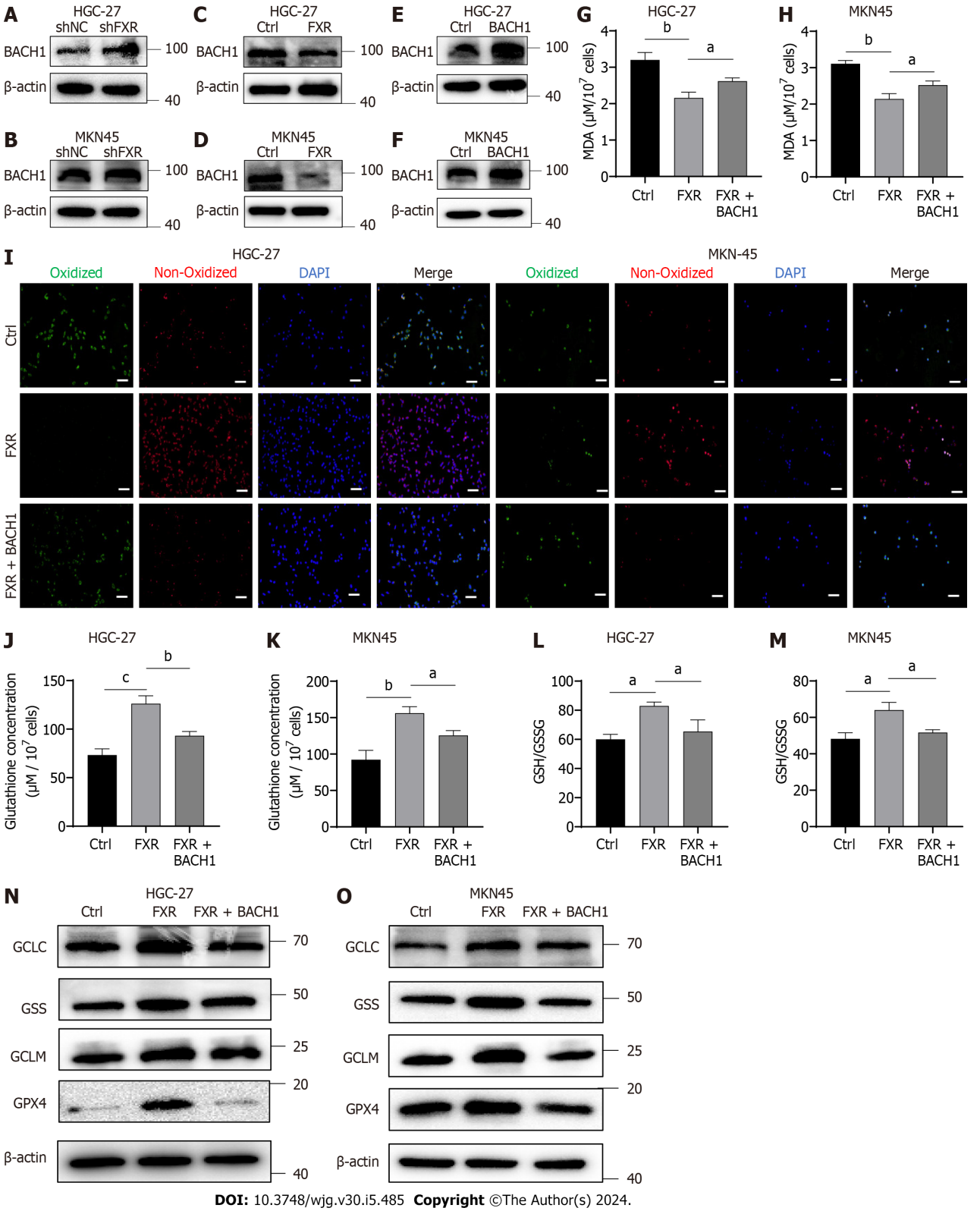

DOI: 10.3748/wjg.v30.i5.485

Figure 5 Farnesoid X receptor exerted anti-ferroptosis effects by inhibiting BTB and CNC homology 1. A and B: Protein expression of BTB and CNC homology 1 (BACH1) in gastric cancer (GC) cells transfected with the shNC or shFXR plasmid for 24 h; C and D: Western blot (WB) analysis of BACH1 protein expression in GC cells transfected with the shNC or shFXR plasmid for 24 h; E and F: HGC-27 and MKN-45 cells were transfected with the control or BACH1-coding plasmid and confirmed through WB analysis; G-I: Malondialdehyde production and BODIPY-589/591 C11 staining of GC cells after transfection with the farnesoid X receptor (FXR)-coding plasmid together with or without the BACH1-coding plasmid and erastin treatment (5 μM) for 24 h; J-M: Alterations of glutathione (GSH) concentrations and the GSH/oxidized GSH ratio in HGC-27 and MKN-45 cells after transfection with the FXR-coding plasmid together with or without the BACH1-coding plasmid; N and O: WB analysis of GCLC, GSS, GCLM, and GSH peroxidase 4 protein expression after transfection with the FXR-coding plasmid together with or without the BACH1-coding plasmid. Scale bar: 100 μm. $^{a}P < 0.05$, $^{b}P < 0.01$, $^{c}P < 0.001$. These experiments were repeated three times. FXR: Farnesoid X receptor; BACH1: BTB and CNC homology 1; GSH: Glutathione; GSSG: Oxidized glutathione; GPX4: Glutathione peroxidase 4.

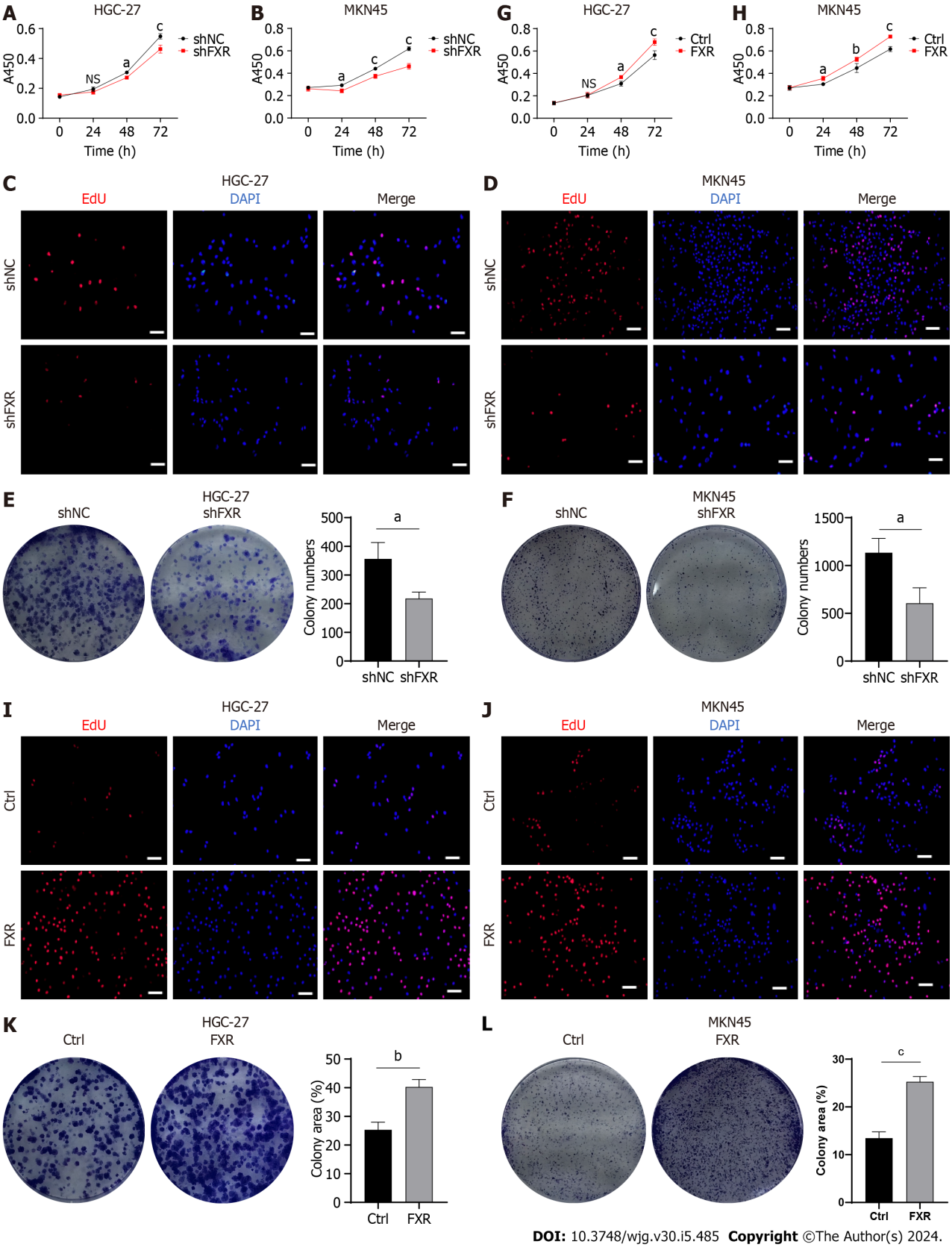

DOI: 10.3748/wjg.v30.i5.485

Figure 6 Farnesoid X receptor promoted proliferation of gastric cancer cells. A-F: Malignant proliferation assays, including cell viability (A and B), 5-ethynyl-2'-deoxyuridine (Edu) staining (C and D), andcolony formation assays (E and F), were performed in gastric cancer (GC) cells after transfection with the shNC or shFXR plasmid; G-L: Cell viability (G and H); Edu staining (I and J), andcolony formation assays (K and L) were performed in GC cells after transfection with the control or farnesoid X receptor-coding plasmid. Scale bar: 100 μm. $^{a}P < 0.05$, $^{b}P < 0.01$, $^{c}P < 0.001$. These experiments were repeated three times. FXR: Farnesoid X receptor; Edu: 5-ethynyl-2'-deoxyuridine; NC: Negative control; NS: Not significant.

suggested that the BAs increased both GSH and GPX4 levels in GC cells, resulting in resistance to ferroptosis.

We hypothesized that CDCA regulates ferroptosis in GC cells by acting through FXR. FXR is a member of the nuclear hormone receptor superfamily, for which BAs are physiological ligands. Of these, CDCA has the strongest *in vivo* affinity for FXR[11,37]. Previous work demonstrated that FXR promotes gastric intestinal metaplasia, a precancerous lesion that can lead to GC development, *via* the FXR/SNAI2/miR-1 axis[38]. However, the role played by FXR in GC progression, and especially in ferroptosis, remained unknown. We found that GW4064, a classical *in vitro* FXR agonist, had similar effects on GC cell death as BAs. Subsequently, we performed FXR gain and loss of function assays and found that the anti-ferroptosis effect of the BAs was almost completely abolished by FXR knockdown, while FXR overexpression in the absence of BAs decreased GC cell ferroptosis. In addition, our data suggested that FXR can increase the expression of GSH synthases, including GSS, GCLC, and GCLM, as well as significantly increase the GSH concentration, GSH/GSSG ratio, and GPX4 expression in GC cells. These results suggest that BAs may inhibit ferroptosis by promoting GSH synthesis *via* FXR activation.

To clarify the mechanism by which FXR exerts its effects in the context of GC, we reviewed relevant studies and found that FXR suppresses the expression of HO-1, which can degrade heme, leading to inhibition of BACH1[29]. BACH1 belongs to the CNC b-Zip family of proteins and can inhibit intracellular synthesis of GSH[30,31,39]. Therefore, we considered whether BACH1 acts as a bridge between GSH synthesis and FXR. Our data indicated that FXR and BACH1 expression levels were inversely related, suggesting that FXR inhibits BACH1 expression. Subsequent functional rescue experiments revealed that BACH1 overexpression partially counteracted the pro-GSH synthesis and anti-ferroptosis effects of FXR. Finally, we investigated the effect of FXR on GC cell growth and found that FXR has marked oncogenic capacity, as it significantly increased GC cell proliferation rates, which may be closely related to the inhibition of GC cell ferroptosis by FXR.

This study had some limitations. Because of experimental restrictions, we were unable to perform *in vivo* experiments to validate our *in vitro* results. Additionally, we did not investigate the molecular mechanism by which FXR regulates BACH1; this requires further research.

CONCLUSION

Overall, our study illustrates a novel strategy by which BAs regulate ferroptosis in GC cells, and provides new insights into the molecular mechanisms underlying BA-mediated promotion of GC progression. We found that ferroptosis plays an influential role in GC progression, raising the possibility that treatments targeting FXR and BACH1 could improve the outcomes of GC patients with BAs reflux.

ARTICLE HIGHLIGHTS

Research background

Gastric cancer (GC) is the fifth most common cancer worldwide and the third leading cause of cancer-related deaths because of the difficulties associated with early diagnosis. Bile acids (BAs) reflux, as an etiologic factor for GC, is receiving more attentions. BAs are engaged in the regulation of metabolism, and the latter is closely related to the ferroptosis. Thus BAs may be potentially relevant to the regulation of ferroptosis.

Research motivation

To elaborate the relationship between BAs and ferroptosis in GC and to providing new insights into the precise treatment of GC patients with BAs reflux.

Research objectives

In this study, we aimed to explore the role of BAs in regulating ferroptosis in GC and to investigate the underlying molecular mechanisms. The present study helps to further elucidate the pathophysiologic mechanisms in GC patients with BAs reflux.

Research methods

The research methods are as follows: cell transfection, cell viability assay, glutathione (GSH) and Malondialdehyde assay quantification, lipid reactive oxygen species assay, 5-ethynyl-2′-deoxyuridine staining, colony formation assay, Western blot.

Research results

Firstly, we found that BAs can promote GC cell proliferation and inhibit erastin-induced ferroptosis sensitivity through upregulate GSH and GSH peroxidase 4 (GPX4). Secondly, BAs exerted its anti-ferroptosis sensitivity function in GC cells by activating farnesoid X receptor (FXR) which significantly promoted GSH synthesis. Subsequently, BTB and CNC homology 1 (BACH1) provided an essential bridging role in BAs and FXR facilitating GSH synthesis. Finally, the notable oncogenic effects of FXR were discovered.

Research conclusions

BAs could inhibit ferroptosis sensitivity through the FXR-BACH1-GSH-GPX4 axis in GC cells.

Research perspectives

The findings of this basic study will be validated in *in vivo* experiments and clinical specimens to clarify whether FXR and BACH1 can serve as therapeutic targets for GC patients with BAs reflux.

FOOTNOTES

Author contributions: Zhong MW, Zhu JK and Zhang GY designed and coordinated the study; Liu CX, Gao Y, Jin X and Zhang Y performed the experiments, acquired and analyzed data; Liu CX, Xu Q and Ding HX, interpreted the data; Liu CX, Li BJ, Du FK, Li LC and Zhang GY wrote the manuscript; Xu XF revised this study; all authors approved the final version of the article.

Supported by the Major Basic Research Project of Natural Science Foundation of Shandong Province, No. ZR2020ZD15.

Institutional review board statement: This basic study did not involve human and/or animal subjects.

Conflict-of-interest statement: The authors declare that the research was conducted in the absence of any commercial or financial relationships that could be construed as a potential conflict of interest.

Data sharing statement: No additional data are available.

Country/Territory of origin: China

ORCID number: Chu-Xuan Liu 0009-0008-8039-3161; Ying Gao 0009-0001-7011-8958; Qian Xu 0000-0002-6174-3348; Ming-Wei Zhong 0000-0002-6548-550X; Jian-Kang Zhu 0000-0001-5007-9528; Guang-Yong Zhang 0000-0001-5308-0129.

S-Editor: Lin C
L-Editor: A
P-Editor: Zhao S

REFERENCES

1 **Bray F**, Ferlay J, Soerjomataram I, Siegel RL, Torre LA, Jemal A. Global cancer statistics 2018: GLOBOCAN estimates of incidence and mortality worldwide for 36 cancers in 185 countries. *CA Cancer J Clin* 2018; **68**: 394-424 [PMID: 30207593 DOI: 10.3322/caac.21492]
2 **Smyth EC**, Nilsson M, Grabsch HI, van Grieken NC, Lordick F. Gastric cancer. *Lancet* 2020; **396**: 635-648 [PMID: 32861308 DOI: 10.1016/S0140-6736(20)31288-5]
3 **Oba M**, Miwa K, Fujimura T, Harada S, Sasaki S, Hattori T. Chemoprevention of glandular stomach carcinogenesis through duodenogastric reflux in rats by a COX-2 inhibitor. *Int J Cancer* 2008; **123**: 1491-1498 [PMID: 18646190 DOI: 10.1002/ijc.23742]
4 **Collins SL**, Stine JG, Bisanz JE, Okafor CD, Patterson AD. Bile acids and the gut microbiota: metabolic interactions and impacts on disease. *Nat Rev Microbiol* 2023; **21**: 236-247 [PMID: 36253479 DOI: 10.1038/s41579-022-00805-x]
5 **Wang S**, Kuang J, Zhang H, Chen W, Zheng X, Wang J, Huang F, Ge K, Li M, Zhao M, Rajani C, Zhu J, Zhao A, Jia W. Bile Acid-Microbiome Interaction Promotes Gastric Carcinogenesis. *Adv Sci (Weinh)* 2022; **9**: e2200263 [PMID: 35285172 DOI: 10.1002/advs.202200263]
6 **Dixon MF**, Mapstone NP, Neville PM, Moayyedi P, Axon AT. Bile reflux gastritis and intestinal metaplasia at the cardia. *Gut* 2002; **51**: 351-355 [PMID: 12171955 DOI: 10.1136/gut.51.3.351]
7 **Hang S**, Paik D, Yao L, Kim E, Trinath J, Lu J, Ha S, Nelson BN, Kelly SP, Wu L, Zheng Y, Longman RS, Rastinejad F, Devlin AS, Krout MR, Fischbach MA, Littman DR, Huh JR. Bile acid metabolites control T(H)17 and T(reg) cell differentiation. *Nature* 2019; **576**: 143-148 [PMID: 31776512 DOI: 10.1038/s41586-019-1785-z]
8 **McIlvride S**, Dixon PH, Williamson C. Bile acids and gestation. *Mol Aspects Med* 2017; **56**: 90-100 [PMID: 28506676 DOI: 10.1016/j.mam.2017.05.003]
9 **Mikó E**, Kovács T, Sebő É, Tóth J, Csonka T, Ujlaki G, Sipos A, Szabó J, Méhes G, Bai P. Microbiome-Microbial Metabolome-Cancer Cell Interactions in Breast Cancer-Familiar, but Unexplored. *Cells* 2019; **8** [PMID: 30934972 DOI: 10.3390/cells8040293]
10 **Watanabe M**, Houten SM, Mataki C, Christoffolete MA, Kim BW, Sato H, Messaddeq N, Harney JW, Ezaki O, Kodama T, Schoonjans K, Bianco AC, Auwerx J. Bile acids induce energy expenditure by promoting intracellular thyroid hormone activation. *Nature* 2006; **439**: 484-489 [PMID: 16400329 DOI: 10.1038/nature04330]
11 **Režen T**, Rozman D, Kovács T, Kovács P, Sipos A, Bai P, Mikó E. The role of bile acids in carcinogenesis. *Cell Mol Life Sci* 2022; **79**: 243 [PMID: 35429253 DOI: 10.1007/s00018-022-04278-2]
12 **Makishima M**, Okamoto AY, Repa JJ, Tu H, Learned RM, Luk A, Hull MV, Lustig KD, Mangelsdorf DJ, Shan B. Identification of a nuclear

receptor for bile acids. *Science* 1999; **284**: 1362-1365 [PMID: 10334992 DOI: 10.1126/science.284.5418.1362]
13 **Sun L**, Cai J, Gonzalez FJ. The role of farnesoid X receptor in metabolic diseases, and gastrointestinal and liver cancer. *Nat Rev Gastroenterol Hepatol* 2021; **18**: 335-347 [PMID: 33568795 DOI: 10.1038/s41575-020-00404-2]
14 **Martínez-Reyes I**, Chandel NS. Cancer metabolism: looking forward. *Nat Rev Cancer* 2021; **21**: 669-680 [PMID: 34272515 DOI: 10.1038/s41568-021-00378-6]
15 **Liang D**, Minikes AM, Jiang X. Ferroptosis at the intersection of lipid metabolism and cellular signaling. *Mol Cell* 2022; **82**: 2215-2227 [PMID: 35390277 DOI: 10.1016/j.molcel.2022.03.022]
16 **Dixon SJ**, Lemberg KM, Lamprecht MR, Skouta R, Zaitsev EM, Gleason CE, Patel DN, Bauer AJ, Cantley AM, Yang WS, Morrison B 3rd, Stockwell BR. Ferroptosis: an iron-dependent form of nonapoptotic cell death. *Cell* 2012; **149**: 1060-1072 [PMID: 22632970 DOI: 10.1016/j.cell.2012.03.042]
17 **Jiang X**, Stockwell BR, Conrad M. Ferroptosis: mechanisms, biology and role in disease. *Nat Rev Mol Cell Biol* 2021; **22**: 266-282 [PMID: 33495651 DOI: 10.1038/s41580-020-00324-8]
18 **Zheng J**, Conrad M. The Metabolic Underpinnings of Ferroptosis. *Cell Metab* 2020; **32**: 920-937 [PMID: 33217331 DOI: 10.1016/j.cmet.2020.10.011]
19 **Stockwell BR**, Jiang X, Gu W. Emerging Mechanisms and Disease Relevance of Ferroptosis. *Trends Cell Biol* 2020; **30**: 478-490 [PMID: 32413317 DOI: 10.1016/j.tcb.2020.02.009]
20 **Yang WS**, SriRamaratnam R, Welsch ME, Shimada K, Skouta R, Viswanathan VS, Cheah JH, Clemons PA, Shamji AF, Clish CB, Brown LM, Girotti AW, Cornish VW, Schreiber SL, Stockwell BR. Regulation of ferroptotic cancer cell death by GPX4. *Cell* 2014; **156**: 317-331 [PMID: 24439385 DOI: 10.1016/j.cell.2013.12.010]
21 **Ouyang S**, Li H, Lou L, Huang Q, Zhang Z, Mo J, Li M, Lu J, Zhu K, Chu Y, Ding W, Zhu J, Lin Z, Zhong L, Wang J, Yue P, Turkson J, Liu P, Wang Y, Zhang X. Inhibition of STAT3-ferroptosis negative regulatory axis suppresses tumor growth and alleviates chemoresistance in gastric cancer. *Redox Biol* 2022; **52**: 102317 [PMID: 35483272 DOI: 10.1016/j.redox.2022.102317]
22 **Lin Z**, Song J, Gao Y, Huang S, Dou R, Zhong P, Huang G, Han L, Zheng J, Zhang X, Wang S, Xiong B. Hypoxia-induced HIF-1α/lncRNA-PMAN inhibits ferroptosis by promoting the cytoplasmic translocation of ELAVL1 in peritoneal dissemination from gastric cancer. *Redox Biol* 2022; **52**: 102312 [PMID: 35447413 DOI: 10.1016/j.redox.2022.102312]
23 **Li T**, Guo H, Li H, Jiang Y, Zhuang K, Lei C, Wu J, Zhou H, Zhu R, Zhao X, Lu Y, Shi C, Nie Y, Wu K, Yuan Z, Fan DM, Shi Y. MicroRNA-92a-1-5p increases CDX2 by targeting FOXD1 in bile acids-induced gastric intestinal metaplasia. *Gut* 2019; **68**: 1751-1763 [PMID: 30635407 DOI: 10.1136/gutjnl-2017-315318]
24 **Lee JY**, Nam M, Son HY, Hyun K, Jang SY, Kim JW, Kim MW, Jung Y, Jang E, Yoon SJ, Kim J, Seo J, Min JK, Oh KJ, Han BS, Kim WK, Bae KH, Song J, Huh YM, Hwang GS, Lee EW, Lee SC. Polyunsaturated fatty acid biosynthesis pathway determines ferroptosis sensitivity in gastric cancer. *Proc Natl Acad Sci U S A* 2020; **117**: 32433-32442 [PMID: 33288688 DOI: 10.1073/pnas.2006828117]
25 **Bannai S**. Exchange of cystine and glutamate across plasma membrane of human fibroblasts. *J Biol Chem* 1986; **261**: 2256-2263 [PMID: 2868011]
26 **Tang D**, Chen X, Kang R, Kroemer G. Ferroptosis: molecular mechanisms and health implications. *Cell Res* 2021; **31**: 107-125 [PMID: 33268902 DOI: 10.1038/s41422-020-00441-1]
27 **Chen X**, Li J, Kang R, Klionsky DJ, Tang D. Ferroptosis: machinery and regulation. *Autophagy* 2021; **17**: 2054-2081 [PMID: 32804006 DOI: 10.1080/15548627.2020.1810918]
28 **Shin D**, Kim EH, Lee J, Roh JL. Nrf2 inhibition reverses resistance to GPX4 inhibitor-induced ferroptosis in head and neck cancer. *Free Radic Biol Med* 2018; **129**: 454-462 [PMID: 30339884 DOI: 10.1016/j.freeradbiomed.2018.10.426]
29 **Kim DH**, Choi HI, Park JS, Kim CS, Bae EH, Ma SK, Kim SW. Farnesoid X receptor protects against cisplatin-induced acute kidney injury by regulating the transcription of ferroptosis-related genes. *Redox Biol* 2022; **54**: 102382 [PMID: 35767918 DOI: 10.1016/j.redox.2022.102382]
30 **Wiel C**, Le Gal K, Ibrahim MX, Jahangir CA, Kashif M, Yao H, Ziegler DV, Xu X, Ghosh T, Mondal T, Kanduri C, Lindahl P, Sayin VI, Bergo MO. BACH1 Stabilization by Antioxidants Stimulates Lung Cancer Metastasis. *Cell* 2019; **178**: 330-345.e22 [PMID: 31257027 DOI: 10.1016/j.cell.2019.06.005]
31 **Nishizawa H**, Yamanaka M, Igarashi K. Ferroptosis: regulation by competition between NRF2 and BACH1 and propagation of the death signal. *FEBS J* 2023; **290**: 1688-1704 [PMID: 35107212 DOI: 10.1111/febs.16382]
32 **Huang J**, Lucero-Prisno DE 3rd, Zhang L, Xu W, Wong SH, Ng SC, Wong MCS. Updated epidemiology of gastrointestinal cancers in East Asia. *Nat Rev Gastroenterol Hepatol* 2023; **20**: 271-287 [PMID: 36631716 DOI: 10.1038/s41575-022-00726-3]
33 **Jia W**, Xie G, Jia W. Bile acid-microbiota crosstalk in gastrointestinal inflammation and carcinogenesis. *Nat Rev Gastroenterol Hepatol* 2018; **15**: 111-128 [PMID: 29018272 DOI: 10.1038/nrgastro.2017.119]
34 **Hassannia B**, Vandenabeele P, Vanden Berghe T. Targeting Ferroptosis to Iron Out Cancer. *Cancer Cell* 2019; **35**: 830-849 [PMID: 31105042 DOI: 10.1016/j.ccell.2019.04.002]
35 **Wang Y**, Zheng L, Shang W, Yang Z, Li T, Liu F, Shao W, Lv L, Chai L, Qu L, Xu Q, Du J, Liang X, Zeng J, Jia J. Wnt/beta-catenin signaling confers ferroptosis resistance by targeting GPX4 in gastric cancer. *Cell Death Differ* 2022; **29**: 2190-2202 [PMID: 35534546 DOI: 10.1038/s41418-022-01008-w]
36 **Yang Z**, Zou S, Zhang Y, Zhang J, Zhang P, Xiao L, Xie Y, Meng M, Feng J, Kang L, Lee MH, Fang L. ACTL6A protects gastric cancer cells against ferroptosis through induction of glutathione synthesis. *Nat Commun* 2023; **14**: 4193 [PMID: 37443154 DOI: 10.1038/s41467-023-39901-8]
37 **Forman BM**, Goode E, Chen J, Oro AE, Bradley DJ, Perlmann T, Noonan DJ, Burka LT, McMorris T, Lamph WW, Evans RM, Weinberger C. Identification of a nuclear receptor that is activated by farnesol metabolites. *Cell* 1995; **81**: 687-693 [PMID: 7774010 DOI: 10.1016/0092-8674(95)90530-8]
38 **Wang N**, Wu S, Zhao J, Chen M, Zeng J, Lu G, Wang J, Zhang J, Liu J, Shi Y. Bile acids increase intestinal marker expression *via* the FXR/SNAI2/miR-1 axis in the stomach. *Cell Oncol (Dordr)* 2021; **44**: 1119-1131 [PMID: 34510400 DOI: 10.1007/s13402-021-00622-z]
39 **Sun J**, Brand M, Zenke Y, Tashiro S, Groudine M, Igarashi K. Heme regulates the dynamic exchange of Bach1 and NF-E2-related factors in the Maf transcription factor network. *Proc Natl Acad Sci U S A* 2004; **101**: 1461-1466 [PMID: 14747657 DOI: 10.1073/pnas.0308083100]

World Journal of Gastroenterology

Submit a Manuscript: https://www.f6publishing.com

World J Gastroenterol 2024 February 7; 30(5): 499-508

DOI: 10.3748/wjg.v30.i5.499

ISSN 1007-9327 (print) ISSN 2219-2840 (online)

CASE REPORT

Dynamic ultrasonography for optimizing treatment position in superior mesenteric artery syndrome: Two case reports and review of literature

Nobuaki Hasegawa, Akihiko Oka, Muyiwa Awoniyi, Yuri Yoshida, Hiroshi Tobita, Norihisa Ishimura, Shunji Ishihara

Specialty type: Gastroenterology and hepatology

Provenance and peer review: Unsolicited article; Externally peer reviewed.

Peer-review model: Single blind

Peer-review report's scientific quality classification

Grade A (Excellent): 0
Grade B (Very good): B
Grade C (Good): 0
Grade D (Fair): 0
Grade E (Poor): 0

P-Reviewer: Govindarajan KK, India

Received: October 2, 2023
Peer-review started: October 2, 2023
First decision: November 24, 2023
Revised: December 11, 2023
Accepted: January 12, 2024
Article in press: January 12, 2024
Published online: February 7, 2024

Nobuaki Hasegawa, Akihiko Oka, Norihisa Ishimura, Shunji Ishihara, Department of Internal Medicine II, Shimane University Faculty of Medicine, Izumo 693-8501, Shimane, Japan

Muyiwa Awoniyi, Department of Gastroenterology, Hepatology and Nutrition, Digestive Disease and Surgery Institute, Hepatology Section, Cleveland Clinic, Cleveland, OH 44195, United States

Yuri Yoshida, Clinical Laboratory Division, Shimane University Hospital, Izumo 693-8501, Shimane, Japan

Hiroshi Tobita, Division of Hepatology, Shimane University Hospital, Izumo 693-8501, Japan

Corresponding author: Akihiko Oka, MD, PhD, Assistant Professor, Department of Internal Medicine II, Shimane University Faculty of Medicine, 89-1, Izumo 693-8501, Shimane, Japan. aoka@med.shimane-u.ac.jp

Abstract

BACKGROUND

Superior mesenteric artery (SMA) syndrome is a rare cause of duodenal obstruction by extrinsic compression between the SMA and the aorta (SMA-Ao). Although the left lateral recumbent position is considered effective in the treatment of SMA syndrome, individual variations in the optimal patient position have been noted. In this report, we present two elderly cases of SMA syndrome that exhibited rapid recovery due to ultrasonographic dynamic evaluation of the optimal position for each patient.

CASE SUMMARY

Case 1: A 90-year-old man with nausea and vomiting. Following diagnosis of SMA syndrome by computed tomography (CT), ultrasonography (US) revealed the SMA-Ao distance in the supine position (4 mm), which slightly improved in the lateral position (5.7–7.0 mm) without the passage of duodenal contents. However, in the sitting position, the SMA-Ao distance was increased to 15 mm accompanied by improved content passage. Additionally, US indicated enhanced passage upon abdominal massage on the right side. By day 2, the patient could eat comfortably with the optimal position and massage. Case 2: An 87-year-old woman with vomiting. After the diagnosis of SMA syndrome and aspiration

pneumonia by CT, dynamic US confirmed the optimal position (SMA-Ao distance was improved to 7 mm in forward-bent position, whereas it remained at 5 mm in the supine position). By day 7 when her pneumonia recovered, she could eat with the optimal position.

CONCLUSION
The optimal position for SMA syndrome varies among individuals. Dynamic US appears to be a valuable tool in improving patient outcomes.

Key Words: Superior mesenteric artery syndrome; Wilkie's syndrome; Cast syndrome; Aorto-mesenteric compass syndrome; Ultrasonography; Case report

Core tip: Superior mesenteric artery (SMA) syndrome is a rare cause of duodenal obstruction by extrinsic compression between the SMA and aorta. While the left lateral recumbent position has traditionally been recommended as conservative therapy for facilitating duodenal passage, recent studies have highlighted variations in the optimal position among patients. Here, we present two cases of SMA syndrome where rapid recovery was achieved through ultrasonographic dynamic evaluation of the individualized optimal positions. This pioneering report includes valuable images and a video of dynamic ultrasonography, contributing to improved prognosis by averting potentially life-threatening complications such as shock, pancreatitis, perforation, and hypokalemia.

Citation: Hasegawa N, Oka A, Awoniyi M, Yoshida Y, Tobita H, Ishimura N, Ishihara S. Dynamic ultrasonography for optimizing treatment position in superior mesenteric artery syndrome: Two case reports and review of literature. *World J Gastroenterol* 2024; 30(5): 499-508
URL: https://www.wjgnet.com/1007-9327/full/v30/i5/499.htm
DOI: https://dx.doi.org/10.3748/wjg.v30.i5.499

INTRODUCTION

Superior mesenteric artery (SMA) syndrome is a rare cause of duodenal obstruction by extrinsic compression between the SMA and the aorta (SMA-Ao)[1-4]. Left untreated, it can lead to potentially lethal complications, including sudden death, shock, pancreatitis, gastric perforation, malnutrition and hypokalemia[5-9]. Hence, early diagnosis and treatments are imperative[10,11]. However, its nonspecific symptoms, such as nausea, appetite loss, and abdominal discomfort often lead to underdiagnosis in clinical practice[10-12]. Additionally, due to its rarity, therapeutic guidelines have not been established. While the left lateral recumbent position is generally considered to be effective in the treatment of SMA syndrome, literature on the optimal patient position is scarce[4,13-18]. Some reports suggest that the optimal position may not be limited to the lateral position but could include right recumbent and sitting positions, depending on the course of the SMA in relation to the aorta[14,15,17,18]. Therefore, the optimal position might differ for each patient, and we hypothesize that dynamic observation of the SMA-Ao distance by ultrasonography (US) is ideal to determine the optimal therapeutic position. Dynamic US has recently emerged as a valuable technique offering real-time and dynamic evaluation, as well as safe and quick access[19,20]. In this report, we present two cases of SMA syndrome that exhibited prompt recovery through ultrasonographic dynamic evaluation of the optimal position.

CASE PRESENTATION

Chief complaints

Case 1: A 90-year-old man arrived in the emergency department in our hospital with complaints of nausea, vomiting, and abdominal distention for several hours.

Case 2: An 87-year-old woman arrived in the emergency department in our hospital with complaints of nausea and recurrent vomiting.

History of present illness

Case 1: The patient had been treated with continuous positive airway pressure (CPAP) for sleep apnea syndrome since 2019. After CPAP therapy had started, he sometimes woke up with nausea and vomiting. During sleep, he remained mainly in the supine position because of CPAP. Several hours before his visit to our hospital in 2022, he received dental treatment in the supine position for 2 h, after which nausea and abdominal distension occurred.

Case 2: The patient had infectious diarrhea several months before coming to our hospital and lost 5 kg of body weight. The diarrhea recovered with conservative therapy. On the day coming to our hospital, she vomited frequently after dinner for several hours, then visited the emergency department in our hospital.

History of past illness

Case 1: The patient had undergone a right hemicolectomy for ascending colon cancer in 2009, with no recurrence. In the same year, he also underwent right ureteral reconstruction for right ureteral injury. Since 2019, he had been receiving CPAP therapy for mild sleep apnea syndrome. He had been on medications for hypertension, Alzheimer's disease, and paroxysmal atrial fibrillation since 2016.

Case 2: The patient had taken medication for hypertension.

Personal and family history

Case 1: There was no significant personal and family history.

Case 2: There was no significant personal and family history.

Physical examination

Case 1: The patient was 166 cm in height and 52.0 kg in weight [body mass index (BMI), 18.9, there had been no body weight loss for several recent years]. The vital signs were normal: consciousness, clear; blood pressure, 146/66 mmHg; heart rate, 53 beats/min; body temperature, 36.4 °C; respiratory rate, 16 breaths/min. The saturation of percutaneous oxygen (SpO_2) was 96% at room air. His abdomen was slightly distended with mild epigastric tenderness. There was no rebound tenderness. The abdominal sound was almost normal peristalsis. Surgical scars from right hemicolectomy were visible in the midline abdominal incision site for ascending colon cancer, located at the center and right of the abdomen.

Case 2: The patient was 161 cm in height and 42.4 kg in weight (BMI, 16.4). The vital signs were as follows: Consciousness, clear; blood pressure, 130/80 mmHg; heart rate, 100 beats/min; body temperature, 36.8 °C; respiratory rate, 24 breaths/min. SpO_2 was 94% at room air. Her abdomen was moderately distended with mild epigastric tenderness. There was no rebound tenderness. The abdominal sound was almost normal peristalsis.

Laboratory examinations

Case 1: Routine blood analyses showed no significant abnormalities: white blood cell (WBC) count, 5170 cells/μL; total bilirubin (TBil), 0.6 mg/dL; aspartate aminotransferase (AST), 20 IU/L; alanine aminotransferase (ALT), 13 IU/L; alkaline phosphatase (ALP), 66 IU/L; γ-glutamyl transpeptidase, 12 IU/L; serum amylase, 141 IU/L; blood urea nitrogen (BUN), 22.0 mg/dL; creatinine (Cr), 0.88 mg/dL; $Na^+/K^+/Cl^+$ levels, 138/3.8/101 mmol/L; and C-reactive protein (CRP), 0.04 mg/dL. Blood pH was within the normal range (7.394).

Case 2: Elevated WBC count (8680 cells/μL) and CRP (3.59 mg/dL) indicated systemic inflammation. Elevated BUN (29.0 mg/dL) and Cr (1.29 mg/dL) indicated dehydration. Except for the elevated serum amylase (255 IU/L), other routine blood analyses were in normal range: TBil, 1.3 mg/dL; AST, 24 IU/L; ALT, 11 IU/L; ALP, 262 IU/L; $Na^+/K^+/Cl^+$, 138/4.4/105 mmol/L. The blood pH was normal (7.366).

Imaging examinations

Case 1: Computed tomography (CT) demonstrated compression of the third portion of the duodenum between the SMA-Ao, as well as markedly dilated duodenum and stomach (Figure 1). Arteriosclerosis of the abdominal aorta and SMA was also observed. Abdominal US revealed that, in the supine position, the distance between SMA-Ao was shortened to 4 mm and the angle of SMA-Ao decreased to 15° (Figure 2). Additionally, real-time US observation showed no passage of contents through the SMA-Ao site, along with the to-and-fro sign at the oral side of this location (Video).

Case 2: CT showed a frosted shadow in the lower lobe of the right lung and compression of the third portion of the duodenum between SMA-Ao, as well as a markedly dilated duodenum and stomach (Figure 3). Arteriosclerosis of the abdominal aorta and SMA was also observed. US demonstrated the SMA-Ao distance was narrowed to 5 mm in the supine position without the passage of duodenal contents (Figure 4A). The angle of SMA-Ao decreased to 18° (Figure 4B).

Further diagnostic work-up

Case 1: We performed a position change with dynamic observation using US (Figure 5). In the left lateral position, which is traditionally recommended for the patients with SMA syndrome, the SMA-Ao distance was 4 mm (no change compared to that in the supine position). In the right lateral position, US showed that the SMA-Ao distance increased to 7 mm and intestinal gas passed through the compression site of the duodenum. In the sitting position, SMA-Ao distance increased to 15 mm and gas and fluid content passed through the site. Real-time US revealed that pushing by hand on his right upper abdomen enhanced the passage of duodenal contents through the site (Video).

Case 2: Dynamic US with a change in body position revealed dynamic changes in the SMA-Ao distance, measuring 5.3 mm in the supine position, 5.3 mm in the left lateral position, 6.6 mm in the right lateral position, and 7.0 mm in the sitting position (Figure 6).

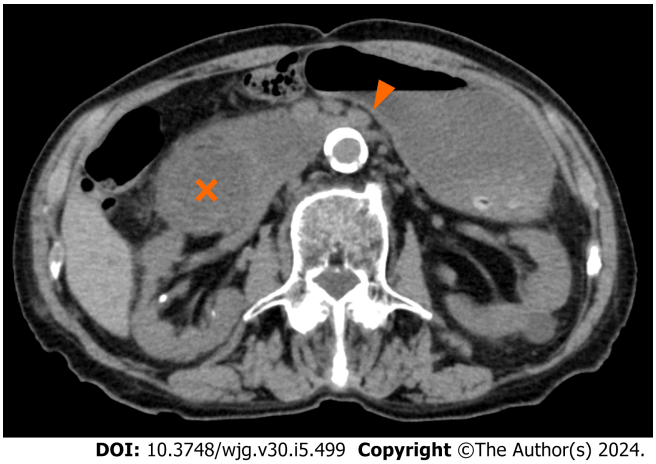

DOI: 10.3748/wjg.v30.i5.499

Figure 1 Computed tomography images of case 1. The axial view of computed tomography showed the compression of the third portion of the duodenum between the superior mesenteric artery and the aorta (arrowhead) as well as markedly dilated duodenum (cross) and stomach.

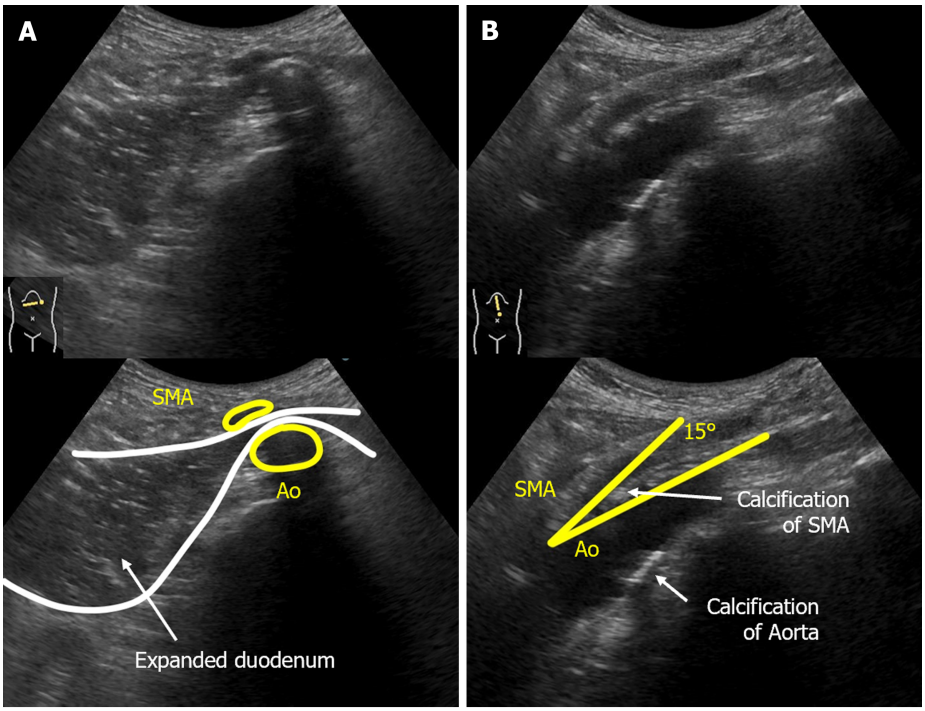

DOI: 10.3748/wjg.v30.i5.499

Figure 2 Abdominal ultrasonography images of case 1. A: The supine position of ultrasonography epigastric transverse scan confirmed expansion of the third part of the duodenal lumen and extrinsic compression of the duodenum by the superior mesenteric artery (SMA). The distance between the SMA and the aorta (Ao) was narrowed to 4 mm; B: Epigastric longitudinal scan showed that the angle of SMA-Ao decreased to 15°. Calcifications (arteriosclerosis) of the aorta and the root of SMA was also observed. SMA: Superior mesenteric artery; Ao: Aorta.

FINAL DIAGNOSIS

Case 1

The final diagnosis was SMA syndrome based on the CT and US findings.

Case 2

The final diagnosis was SMA syndrome with aspiration pneumonia as an SMA syndrome-related complication based on her medical history and CT and US findings.

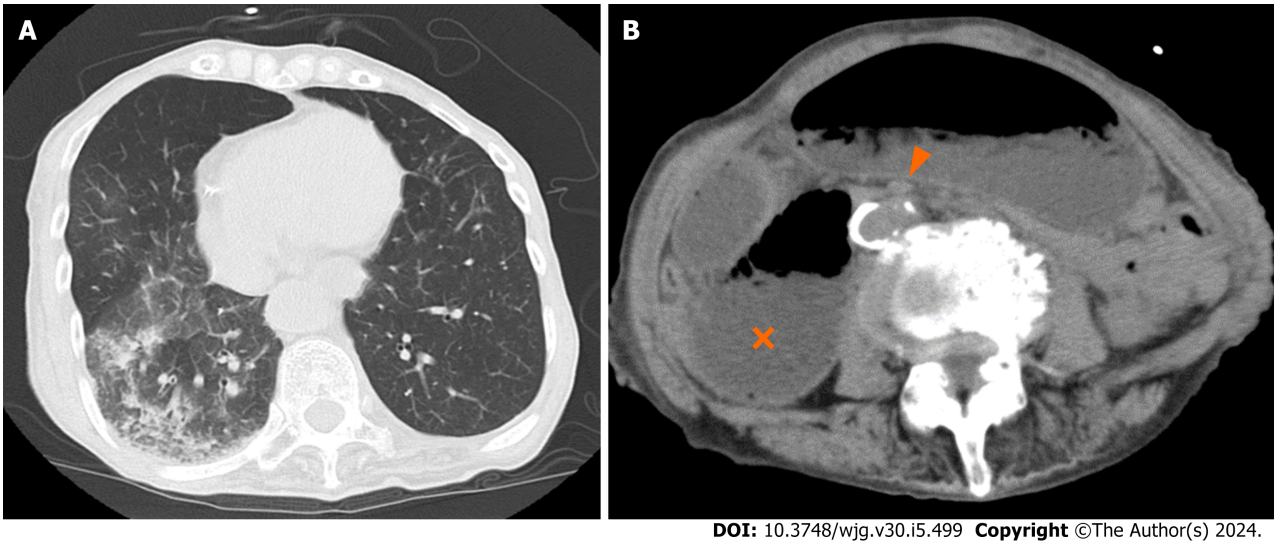

DOI: 10.3748/wjg.v30.i5.499

Figure 3 Computed tomography images of case 2. A: The axial view of thoracic computed tomography (CT) indicated aspiration pneumonia; B: The axial view of abdominal CT demonstrates extensive dilatation of stomach and proximal duodenum (cross), between the superior mesenteric artery (arrow head) and the aorta.

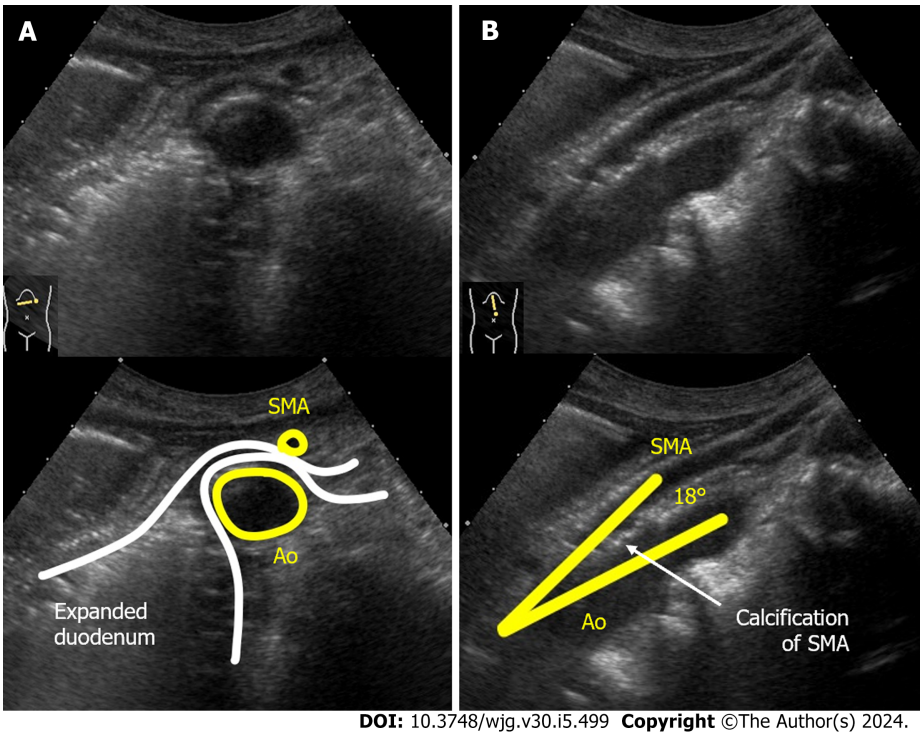

DOI: 10.3748/wjg.v30.i5.499

Figure 4 Dynamic ultrasonography images of case 2. A: The supine position of ultrasonography confirmed expansion of the third part of the duodenal lumen and extrinsic compression of the duodenum by the superior mesenteric artery (SMA). The distance between the SMA and the aorta (Ao) was narrowed to 5 mm; B: Epigastric longitudinal scan showed that the angle of SMA-Ao decreased to 18°. Calcifications (arteriosclerosis) of the aorta and the root of SMA was also observed. SMA: Superior mesenteric artery; Ao: Aorta.

TREATMENT

Case 1

On day 1 of hospitalization, fasting and peripheral venous nutrition started. Based on the findings of dynamic US, the patient kept his postprandial position in the right lateral or sitting as much as possible.

Case 2

On the day 1 of hospitalization, fasting and peripheral venous nutrition started. Based on the findings of dynamic US, she was instructed to keep the optimal body position after a meal. Aspiration pneumonia was treated with intravenous

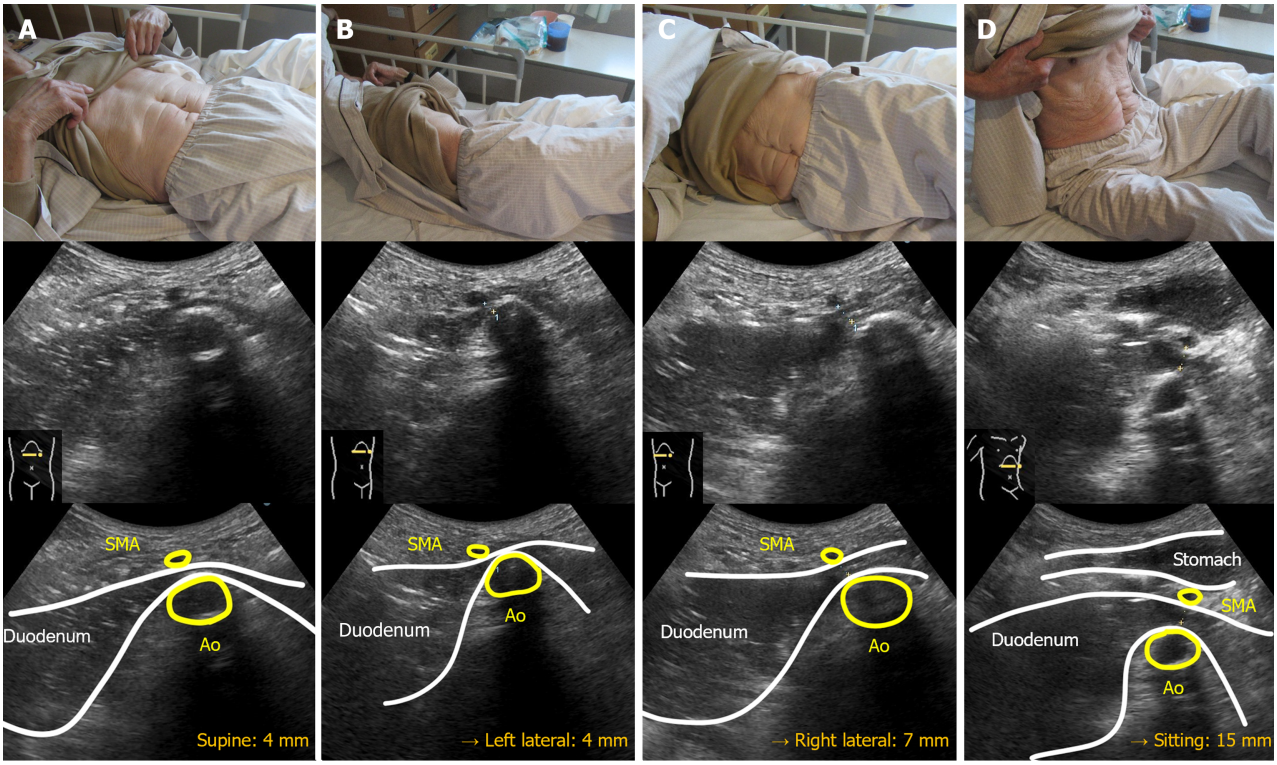

DOI: 10.3748/wjg.v30.i5.499

Figure 5 Dynamic ultrasonography images of case 1. A: Narrowed superior mesenteric artery-aorta (SMA-Ao) distance (4 mm); B: Left lateral position did not improve the SMA-Ao distance (4 mm); C: Right lateral position increased the SMA-Ao distance to 7 mm and the duodenal gas could pass through; D: Sitting position (Fowler's position) dramatically improved the SMA-Ao distance to 15 mm and the passage of duodenal contents. SMA: Superior mesenteric artery; Ao: Aorta.

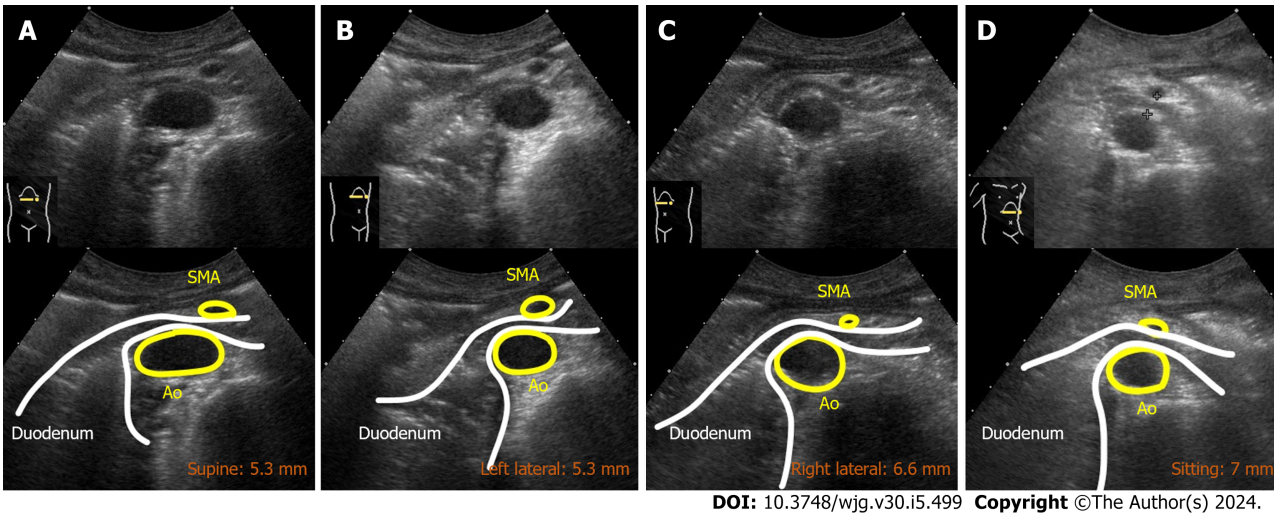

DOI: 10.3748/wjg.v30.i5.499

Figure 6 Dynamic ultrasonography images of case 2. A: Supine position showed the narrowed superior mesenteric artery-aorta (SMA-Ao) distance (5.3 mm); B: Left lateral position did not improve the SMA-Ao distance (5.3 mm); C and D: Right lateral position and sitting position increased the SMA-Ao distance to 6.6 and 7.0 mm, respectively. SMA: Superior mesenteric artery; Ao: Aorta.

antibiotics for 10 d.

OUTCOME AND FOLLOW-UP

Case 1

By day 2, all of the patient's symptoms had vanished, and US confirmed significant improvements in stomach and duodenal dilatation. Consequently, he could eat without recurrence. Upon discharge from the hospital on day 3, he was

advised to maintain positions such as sitting or the right lateral position after meals, and also to assume the right-side supine position when using CPAP during sleep. He was also instructed to apply manual pressure (massage) to his right upper abdomen if he experienced any symptoms related to SMA syndrome. There have been no recurrences in the two years since the incident.

Case 2

On day 7, the patients could start eating without recurrence. On day 32, she was discharged and there was no recurrence in the 12 years since the incident.

DISCUSSION

SMA syndrome (also known as Wilkie's syndrome, cast syndrome, mesenteric duodenal obstruction, or aorto-mesenteric compass syndrome) is a rare duodenal obstruction caused by compression between the SMA-Ao[1,21]. Recent reviews indicate a wide age range of patients affected by SMA syndrome, with a notable increase in elderly patients[1,21]. Indeed, the present two patients were very old and required more prompt and careful management to avoid age-related complications, including aspiration pneumonia, functional decline, and malnutrition[22]. Fortunately, dynamic US could determine the optimal position for individualized duodenal passage, thus obviating the need for nasogastric tube placement, a common intervention for decompression and nutritional support in SMA syndrome[1-4]. However, nasogastric tubes can introduce additional complications, such as aspiration pneumonia and intestinal injuries[23,24].

The etiology of SMA syndrome might be different between younger and older patients[21]. In older patients (> 40 years), post-abdominal surgery emerges as the most common etiology, followed by weight loss. In contrast, younger patients (< 40 years) predominantly experience scoliosis-related cases, such as those following spinal fusion surgery and body casting, also accompanied by weight loss. Case 1 had multiple histories of abdominal surgery, suggesting surgical adhesion pulled on the mesentery or restricted the SMA mobility[1]. Furthermore, the presence of atherosclerosis affecting both the SMA and the Ao, as observed in both cases, might further impede SMA mobility[25,26]. Given these restrictions of the SMA mobility, confirming the SMA mobility by dynamic US should be helpful; or, the absence of SMA mobility could suggest early surgical intervention. CT is considered the gold standard for diagnosing SMA syndrome by visualizing duodenal compression by the SMA, along with dilation of the proximal duodenum and stomach[1,27]. Three-dimensional CT has emerged as a valuable tool for visualizing the anatomy of the SMA, Ao, and duodenum[28]. Under normal circumstances, the SMA-Ao angle and distance measure 38–65 and 10–33 mm, respectively[29-31]. The cutoff value was reported as 22 on the SMA-Ao angle and 8 mm distance with 42.8% sensitivity and 100% specificity[30]. While CT undoubtedly offers valuable and objective diagnostic information, it is typically performed in a single body position, usually supine. In contrast, US can potentially be conducted in various postures and provides dynamic assessments of luminal content and vascular movement. As demonstrated in this report, dynamic US is instrumental in identifying the most suitable position for facilitating luminal content passage. Historically, barium X-ray series were used for diagnosis and evaluation of luminal content passage in SMA syndrome[1,32]. However, due to the associated radiation exposure risks, US assessments offer a safer and more effective alternative for managing SMA syndrome. The diagnostic sensitivity of US for SMA syndrome has been validated in comparative studies with CT findings[30]. In addition, because it can be performed at the bedside, it can easily evaluate gastroduodenal dilatation and the distance between the SMA-Ao during follow-up. In light of these advantages, we believe dynamic US represents the most valuable tool for determining the optimal position for each patient with SMA syndrome. The absence of SMA movement, possibly due to calcification at the SMA root or post-abdominal surgery, could be indicative of the need for early surgical intervention[1]. While US findings may potentially be influenced by operator bias and interobserver variation, dynamic observation places greater emphasis on subjective focus compared to static images. To the best of our knowledge, this report constitutes the first documentation of dynamic US in SMA syndrome, complete with detailed images and a video. We anticipate that this report will be valuable for US practitioners aiming to enhance their understanding of SMA syndrome diagnosis.

The treatment for SMA syndrome is initiated by conservative methods, such as gastric and duodenal decompression by postural change and/or nasogastric tube suction[22,33]. If the conservative treatment fails, surgery may be necessary [1,34]. Although it is believed that positioning the patient in the left lateral position is effective in the treatment of SMA syndrome, there is little evidence[13,16]. The optimal body position for each patient may vary because recent studies found a variation in the SMA position and movement[14,15,17]. Case 1 in our report demonstrated better content passage in the right lateral position than the left, corroborating the findings of Khan *et al*[15]. Miyata *et al*[17] reported a variation in position of SMA demonstrating that major position was the right side along with the aorta[17]. No study has reported the optimal position in SMA syndrome[1]. As such, we conducted an evaluation of the optimal body position in 14 individuals, including our two SMA syndrome cases and nine healthy controls, using abdominal US (Figure 7). In cases where duodenal detection proved challenging, subjects ingested 200 mL of water, modifying the drinking US test[35]. While the left lateral position, which is generally thought to be an optimal position, was significantly effective (long distance of SMA-Ao) as expected, the right lateral position was also significantly effective (Figure 7A). The best position varies from case to case: the left lateral position was effective in some cases while the right lateral recumbent position and the sitting position were more effective in other cases (Figure 7B). Further prospective cohort studies are warranted to explore the effectiveness of dynamic US in identifying ideal positions for SMA syndrome patients. Although recent surgical interventions for SMA syndrome have demonstrated safety and efficacy[1,36], surgery and anesthesia inherently pose risks to elderly patients, particularly those with pulmonary risk factors, as demonstrated by our cases[37]. Dynamic US offers a promising avenue to enhance the effectiveness of non-surgical treatments and prevent unnecessary surgical

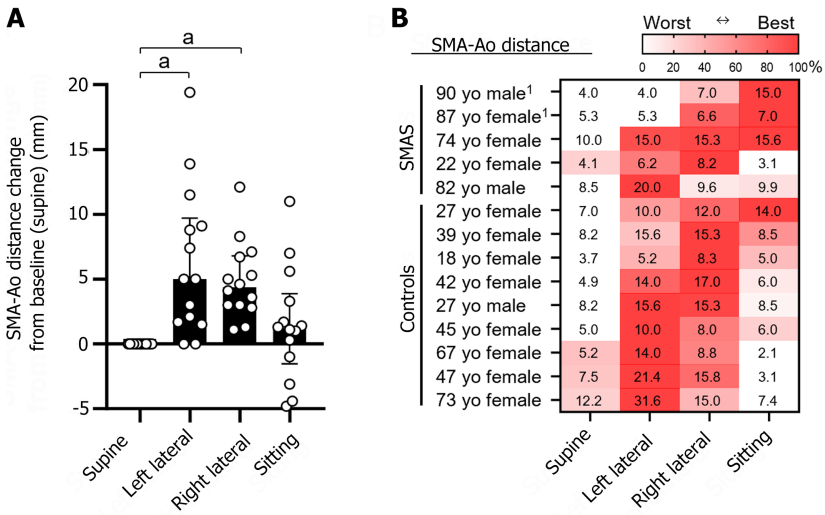

DOI: 10.3748/wjg.v30.i5.499

Figure 7 Superior mesenteric artery-aorta distance in four body positions in eight individuals. A: Distance change of superior mesenteric artery-aorta (SMA-Ao) from the baseline position (supine position). Dots indicate individual results. Bars indicate median with interquartile range; B: Fourteen individuals included five cases of superior mesenteric artery syndrome and nine healthy controls (age, sex, and absolute distance of SMA-Ao mm). The absolute distance of SMA-Ao (mm) in thirteen individuals were shown in each position. The SMA-Ao distances were measured by ultrasonography. If it was difficult to detect the duodenum, the subjects ingested 200 mL of water which is a modified method of drinking-ultrasonography test. Statistical analysis was performed by GraphPad Prism version 10.0.2 with Dunn's multiple comparisons tests with ANOVA. [1]Indicates the present case. [a]$P < 0.01$. The heat map indicates the best and worst positions of the SMA-Ao distance in each individual. SMA: Superior mesenteric artery; Ao: Aorta; SMAS: Superior mesenteric artery syndrome.

procedures.

CONCLUSION

We presented two cases of SMA syndrome in elderly patients in which US proved invaluable for determining optimal positioning. Given the variability of optimal body positions in SMA syndrome among patients, dynamic assessment of the optimal body position *via* bedside positioning using dynamic US emerged as a minimally invasive and effective option.

ACKNOWLEDGMENTS

We thank Keiko Masuzaki and Yuriko Adachi for collecting references and Maki Watanabe for collaborating with the ethics committee.

FOOTNOTES

Author contributions: Hasegawa N, Oka A, and Awoniyi M contributed to drafting of manuscript; Hasegawa N, Oka A, and Yoshida Y contributed to assessment of ultrasonography; Tobita H, Ishimura N, and Ishihara S contributed to supervisor of study; All the authors solely contributed to this paper.

Informed consent statement: This publication of case reports was approved by the Shimane University Hospital review board (approval No. 6612) in adherence to the Helsinki Declaration. Each patient provided informed consent for publication.

Conflict-of-interest statement: All the authors report no relevant conflicts of interest for this article.

CARE Checklist (2016) statement: The authors have read CARE Checklist (2016), and the manuscript was prepared and revised according to CARE Checklist (2016).

Country/Territory of origin: Japan

ORCID number: Nobuaki Hasegawa 0000-0002-7449-5259; Akihiko Oka 0000-0001-6451-8413; Muyiwa Awoniyi 0000-0002-5811-070X; Yuri Yoshida 0000-0002-4123-786X; Hiroshi Tobita 0000-0003-2408-2023; Norihisa Ishimura 0000-0001-8039-3155; Shunji Ishihara 0000-0002-8228-1912.

Corresponding Author's Membership in Professional Societies: The Japanese Society of Gastroenterology.

S-Editor: Li L
L-Editor: Kerr C
P-Editor: Cai YX

REFERENCES

1 **Oka A**, Awoniyi M, Hasegawa N, Yoshida Y, Tobita H, Ishimura N, Ishihara S. Superior mesenteric artery syndrome: Diagnosis and management. *World J Clin Cases* 2023; **11**: 3369-3384 [PMID: 37383896 DOI: 10.12998/wjcc.v11.i15.3369]
2 **Wilkie DPD**. Chronic duodenal ileus. *Am J Med Sci* 1927; **173**: 643-648 [DOI: 10.1097/00000441-192705000-00006]
3 **Hines JR**, Gore RM, Ballantyne GH. Superior mesenteric artery syndrome. Diagnostic criteria and therapeutic approaches. *Am J Surg* 1984; **148**: 630-632 [PMID: 6496852 DOI: 10.1016/0002-9610(84)90339-8]
4 **Evarts CM**. The cast syndrome. Report of a case after spinal fusion for scoliosis. *Clin Orthop Relat Res* 1971; **75**: 164-166 [PMID: 5554620 DOI: 10.1097/00003086-197103000-00022]
5 **Murakami C**, Irie W, Sasaki C, Nakamaru N, Sakamoto M, Nagato J, Satoh F. Extensive gastric necrosis secondary to acute gastric dilatation: A case report. *Leg Med (Tokyo)* 2019; **36**: 85-88 [PMID: 30448603 DOI: 10.1016/j.legalmed.2018.11.007]
6 **Mohammad Kazmin NE**, Kamaruzaman L, Wong Z, Fong VK, Mohd R, Mustafar R. Acute Kidney Injury Caused by Superior Mesenteric Artery Syndrome. *Case Rep Nephrol* 2020; **2020**: 8364176 [PMID: 32328326 DOI: 10.1155/2020/8364176]
7 **Petrosyan M**, Estrada JJ, Giuliani S, Williams M, Rosen H, Mason RJ. Gastric perforation and pancreatitis manifesting after an inadvertent nissen fundoplication in a patient with superior mesenteric artery syndrome. *Case Rep Med* 2009; **2009**: 426162 [PMID: 19730743 DOI: 10.1155/2009/426162]
8 **Thieme ET**, Postmus R. Superior mesenteric artery syndrome. *Ann Surg* 1961; **154**: 139-143 [PMID: 13920640 DOI: 10.1097/00000658-196112000-00017]
9 **Shajani-Yi Z**, Lee HK, Cervinski MA. Hyponatremia, Hypokalemia, Hypochloremia, and Other Abnormalities. *Clin Chem* 2016; **62**: 898 [PMID: 27235468 DOI: 10.1373/clinchem.2015.249292]
10 **Elbadaway MH**. Chronic superior mesenteric artery syndrome in anorexia nervosa. *Br J Psychiatry* 1992; **160**: 552-554 [PMID: 1571759 DOI: 10.1192/bjp.160.4.552]
11 **Mandarry MT**, Zhao L, Zhang C, Wei ZQ. A comprehensive review of superior mesenteric artery syndrome. *Eur Surg* 2010; **42**: 229-236 [DOI: 10.1007/s10353-010-0561-y]
12 **Kawanishi K**, Shojima K, Nishimoto M, Abe H, Kakimoto T, Yasuda Y, Hara T, Kato J. Superior Mesenteric Artery Syndrome May Be Overlooked in Women with Functional Dyspepsia. *Intern Med* 2017; **56**: 2549-2554 [PMID: 28883239 DOI: 10.2169/internalmedicine.8647-16]
13 **Evarts CM**, Winter RB, Hall JE. Vascular compression of the duodenum associated with the treatment of scoliosis. Review of the literature and report of eighteen cases. *J Bone Joint Surg Am* 1971; **53**: 431-44 passim [PMID: 5580004 DOI: 10.2106/00004623-197153030-00002]
14 **Dounas GD**, Cundy TP, Smith ML, Gent R, Antoniou G, Sutherland LM, Cundy PJ. The coronal aorto-mesenteric orientation theory for post-operative nausea and vomiting following scoliosis surgery in children: a pilot study. *ANZ J Surg* 2021; **91**: 174-178 [PMID: 33244810 DOI: 10.1111/ans.16438]
15 **Khan H**, Al-Jabbari E, Shroff N, Barghash M, Shestopalov A, Bhargava P. Coexistence of superior mesenteric artery syndrome and nutcracker phenomenon. *Radiol Case Rep* 2022; **17**: 1927-1930 [PMID: 35401899 DOI: 10.1016/j.radcr.2022.03.063]
16 **Neri S**, Signorelli SS, Mondati E, Pulvirenti D, Campanile E, Di Pino L, Scuderi M, Giustolisi N, Di Prima P, Mauceri B, Abate G, Cilio D, Misseri M, Scuderi R. Ultrasound imaging in diagnosis of superior mesenteric artery syndrome. *J Intern Med* 2005; **257**: 346-351 [PMID: 15788004 DOI: 10.1111/j.1365-2796.2005.01456.x]
17 **Miyata J**, Eshak ES, Yoshioka T, Iso H. Movement of the superior mesenteric artery in patients with superior mesenteric artery syndrome: A case-reference study. *Clin Anat* 2022; **35**: 891-898 [PMID: 35417615 DOI: 10.1002/ca.23885]
18 **Choi SH**, Pfalzer FA Jr. Superior mesenteric artery syndrome. *N Y State J Med* 1976; **76**: 986-988 [PMID: 1064781]
19 **Wu WT**, Lin CY, Shu YC, Chen LR, Özçakar L, Chang KV. Subacromial Motion Metrics in Painful Shoulder Impingement: A Dynamic Quantitative Ultrasonography Analysis. *Arch Phys Med Rehabil* 2023; **104**: 260-269 [PMID: 36055380 DOI: 10.1016/j.apmr.2022.08.010]
20 **Shu YC**, Lo YC, Chiu HC, Chen LR, Lin CY, Wu WT, Özçakar L, Chang KV. Deep learning algorithm for predicting subacromial motion trajectory: Dynamic shoulder ultrasound analysis. *Ultrasonics* 2023; **134**: 107057 [PMID: 37290256 DOI: 10.1016/j.ultras.2023.107057]
21 **Oka A**, Hasegawa N, Yoshida Y, Tobita H, Awoniyi M, Ishimura N, Ishihara S. Ep129 superior mesenteric artery syndrome -a systematic review of 2,453 cases in the literature. *Gastroenterology* 2023; **164**: S-1215 [DOI: 10.1016/S0016-5085(23)03812-X]
22 **Merrett ND**, Wilson RB, Cosman P, Biankin AV. Superior mesenteric artery syndrome: diagnosis and treatment strategies. *J Gastrointest Surg* 2009; **13**: 287-292 [PMID: 18810558 DOI: 10.1007/s11605-008-0695-4]
23 **McCann C**, Cullis PS, McCabe AJ, Munro FD. Major complications of jejunal feeding in children. *J Pediatr Surg* 2019; **54**: 258-262 [PMID: 30528177 DOI: 10.1016/j.jpedsurg.2018.10.078]
24 **Miura T**, Nakamura J, Yamada S, Miura T, Yanagi M, Tani Y, Nishihara M, Takahashi T. A Fatal Aortoesophageal Fistula Caused by Critical Combination of Double Aortic Arch and Nasogastric Tube Insertion for Superior Mesenteric Artery Syndrome. *Case Rep Gastroenterol* 2010; **4**: 198-203 [PMID: 20805944 DOI: 10.1159/000316633]
25 **Beita AKV**, Whayne TF. The Superior Mesenteric Artery: From Syndrome in the Young to Vascular Atherosclerosis in the Old. *Cardiovasc Hematol Agents Med Chem* 2019; **17**: 74-81 [PMID: 31538906 DOI: 10.2174/1871525717666190920100518]

26 **Kitaura K**, Harima K. Superior mesenteric artery syndrome with vascular calcification in a maintenance hemodialysis patient. *Clin Nephrol* 2009; **71**: 228-230 [PMID: 19203523 DOI: 10.5414/CNP71228]

27 **Lamba R**, Tanner DT, Sekhon S, McGahan JP, Corwin MT, Lall CG. Multidetector CT of vascular compression syndromes in the abdomen and pelvis. *Radiographics* 2014; **34**: 93-115 [PMID: 24428284 DOI: 10.1148/rg.341125010]

28 **Raman SP**, Neyman EG, Horton KM, Eckhauser FE, Fishman EK. Superior mesenteric artery syndrome: spectrum of CT findings with multiplanar reconstructions and 3-D imaging. *Abdom Imaging* 2012; **37**: 1079-1088 [PMID: 22327421 DOI: 10.1007/s00261-012-9852-z]

29 **Hearn JB**. Duodenal ileus; with reference to superior mesenteric artery compression. *Md State Med J* 1965; **14**: 65-68 [PMID: 14267372 DOI: 10.1148/86.2.305]

30 **Unal B**, Aktaş A, Kemal G, Bilgili Y, Güliter S, Daphan C, Aydinuraz K. Superior mesenteric artery syndrome: CT and ultrasonography findings. *Diagn Interv Radiol* 2005; **11**: 90-95 [PMID: 15957095]

31 **Le D**, Stirparo JJ, Magdaleno TF, Paulson CL, Roth KR. Point-of-care ultrasound findings in the diagnosis and management of Superior Mesenteric Artery (SMA) syndrome. *Am J Emerg Med* 2022; **55**: 233.e1-233.e4 [PMID: 35241297 DOI: 10.1016/j.ajem.2022.02.018]

32 **Hutchinson DT**, Bassett GS. Superior mesenteric artery syndrome in pediatric orthopedic patients. *Clin Orthop Relat Res* 1990; 250-257 [PMID: 2293937]

33 **Lee TH**, Lee JS, Jo Y, Park KS, Cheon JH, Kim YS, Jang JY, Kang YW. Superior mesenteric artery syndrome: where do we stand today? *J Gastrointest Surg* 2012; **16**: 2203-2211 [PMID: 23076975 DOI: 10.1007/s11605-012-2049-5]

34 **Shin MS**, Kim JY. Optimal duration of medical treatment in superior mesenteric artery syndrome in children. *J Korean Med Sci* 2013; **28**: 1220-1225 [PMID: 23960451 DOI: 10.3346/jkms.2013.28.8.1220]

35 **Kato M**, Nishida U, Nishida M, Hata T, Asaka R, Haneda M, Yamamoto K, Imai A, Yoshida T, Ono S, Shimizu Y, Asaka M. Pathophysiological classification of functional dyspepsia using a novel drinking-ultrasonography test. *Digestion* 2010; **82**: 162-166 [PMID: 20588028 DOI: 10.1159/000308363]

36 **Pottorf BJ**, Husain FA, Hollis HW Jr, Lin E. Laparoscopic management of duodenal obstruction resulting from superior mesenteric artery syndrome. *JAMA Surg* 2014; **149**: 1319-1322 [PMID: 25353279 DOI: 10.1001/jamasurg.2014.1409]

37 **Turrentine FE**, Wang H, Simpson VB, Jones RS. Surgical risk factors, morbidity, and mortality in elderly patients. *J Am Coll Surg* 2006; **203**: 865-877 [PMID: 17116555 DOI: 10.1016/j.jamcollsurg.2006.08.026]

World Journal of Gastroenterology

Submit a Manuscript: https://www.f6publishing.com

World J Gastroenterol 2024 February 7; 30(5): 509-511

DOI: 10.3748/wjg.v30.i5.509

ISSN 1007-9327 (print) ISSN 2219-2840 (online)

LETTER TO THE EDITOR

Prevention of hepatitis B reactivation in patients with hematologic malignancies treated with novel systemic therapies: Who and Why?

Matteo Tonnini, Clara Solera Horna, Luca Ielasi

Specialty type: Gastroenterology and hepatology

Provenance and peer review: Unsolicited article; Externally peer reviewed.

Peer-review model: Single blind

Peer-review report's scientific quality classification

Grade A (Excellent): 0
Grade B (Very good): B, B
Grade C (Good): 0
Grade D (Fair): 0
Grade E (Poor): 0

P-Reviewer: Lun YZ, China; Said ZNA, Egypt

Received: November 1, 2023
Peer-review started: November 1, 2023
First decision: December 7, 2023
Revised: December 15, 2023
Accepted: January 11, 2024
Article in press: January 11, 2024
Published online: February 7, 2024

Matteo Tonnini, Department of Medical and Surgical Sciences, University of Bologna, Bologna 40138, Italy

Matteo Tonnini, Division of Internal Medicine, Hepatobiliary and Immunoallergic Diseases, IRCCS Azienda Ospedaliero-Universitaria di Bologna, Bologna 40138, Italy

Clara Solera Horna, Infectious Disease Unit, Azienda USL-IRCCS di Reggio Emilia, Reggio Emilia 42123, Italy

Luca Ielasi, Department of Internal Medicine, Ospedale degli Infermi di Faenza, Faenza 48018, Italy

Corresponding author: Luca Ielasi, MD, Doctor, Department of Internal Medicine, Ospedale degli Infermi di Faenza, Viale Stradone, 9, Faenza 48018, Italy. luca.ielasi.kr@gmail.com

Abstract

The risk of reactivation in patients with chronic or past/resolved hepatitis B virus (HBV) infection receiving chemotherapy or immunosuppressive drugs is a well-known possibility. The indication of antiviral prophylaxis with nucleo(t)side analogue is given according to the risk of HBV reactivation of the prescribed therapy. Though the advent of new drugs is occurring in all the field of medicine, in the setting of hematologic malignancies the last few years have been characterized by several drug classes and innovative cellular treatment. As novel therapies, there are few data about the rate of HBV reactivation and the decision of starting or not an antiviral prophylaxis could be challenging. Moreover, patients are often treated with a combination of different drugs, so evaluating the actual role of these new therapies in increasing the risk of HBV reactivation is difficult. First results are now available, but further studies are still needed. Patients with chronic HBV infection [hepatitis B surface antigen (HBsAg) positive] are reasonably all treated. Past/resolved HBV patients (HBsAg negative) are the actual area of uncertainty where it could be difficult choosing between prophylaxis and pre-emptive strategy.

Key Words: Hepatitis B reactivation; Hepatitis B virus; Antiviral prophylaxis; Hematologic malignancies; Chimeric antigens receptor-T cell therapy; Immune checkpoint inhibitors

Core Tip: In the last few years, the advent of several new therapies has characterized the therapeutic scenario of hematologic malignancies. There is now the open issue of assessing the risk of hepatitis B virus reactivation in these patients in order to decide which patients should undergo antiviral prophylaxis.

Citation: Tonnini M, Solera Horna C, Ielasi L. Prevention of hepatitis B reactivation in patients with hematologic malignancies treated with novel systemic therapies: Who and Why? *World J Gastroenterol* 2024; 30(5): 509-511
URL: https://www.wjgnet.com/1007-9327/full/v30/i5/509.htm
DOI: https://dx.doi.org/10.3748/wjg.v30.i5.509

TO THE EDITOR

We read with interest the article recently published by Mak *et al*[1] reviewing prevention and management of hepatitis B virus (HBV) reactivation in the setting of hematologic malignancies in the era of new targeted therapies. They well differentiated two entities as HBV reactivation: Exacerbation of hepatitis B surface antigen (HBsAg) positive chronic hepatitis B (CHB) or reactivation of past/resolved HBV infection (HBsAg negative and hepatitis B core antibody positive).

They subsequently analyzed the risk of reactivation and therefore the need for antiviral prophylaxis associated with monoclonal antibodies and the novel targeted therapies in the hematological setting for both CHB and past/resolved HBV infection. For HBsAg positive patients there is a consensus, as also described in the review of Mustafayev and Torres[2] that patients treated with drugs which have a moderate (1%-10%) to high risk (> 10%) of reactivation, such as B-cell depleting drugs, immune checkpoint inhibitors (ICIs) and targeted therapies, should be given an antiviral prophylaxis as soon as the treatment has started[1].

The recent guidelines of Asian-Pacific Association for the study of the liver also recommend starting antiviral prophylaxis in HBsAg positive patients who need to undergo an immunosuppressive treatment due to a moderate-high risk of HBV reactivation[3]. An exception is made for patients receiving traditional immunosuppressants (*e.g.*, azathioprine and methotrexate), which is also confirmed by Shi and Zheng[4].

On the other hand, for resolved HBV infection the risk of reactivation associated with these new drugs is still a matter of debate. The current review by Mak *et al*[1], as well as the one by Mustafayev and Torres[2], agree on a moderate/high risk of HBV reactivation and therefore a need of antiviral prophylaxis for patients undergoing a B cell-depleting regimen, an allogenic stem cell transplantation or an anthracyclines based chemotherapy, but a certain degree of uncertainty remains for chimeric antigens receptor (CAR)-T cell therapies and ICIs.

The issue of HBV reactivation for patients receiving CAR-T cell therapy remains unexplored and further investigations are needed, though an antiviral prophylaxis for resolved HBV seems reasonable. A recent meta-analysis of Papatheodoridis *et al*[5] showed an HBV reactivation rate of 4% in 112 patients undergoing CAR-T cell therapy and not receiving nucleo(t)side analogue (NA). Despite very limited data, they suggest starting antiviral prophylaxis in this group of patients[5].

Regarding ICIs, the risk of HBV reactivation and therefore the need of an antiviral prophylaxis is differentiated between chronic and past/resolved HBV infection. In HBsAg positive patients the meta-analysis of Papatheodoridis *et al* [5] showed a pooled rate of reactivation in patients not receiving NA prophylaxis of 6%-11%, confirming these patients as at moderate/high risk of HBV reactivation. Instead, HBsAg negative not receiving NA prophylaxis have a pooled rate of reactivation of 0.2%, so a pre-emptive strategy is suggested[5]. A more recent meta-analysis of Ding *et al*[6], focused on HBV reactivation in patients undergoing ICIs, showed similar results and proposed the same recommendations of antiviral prophylaxis for CHB patients and pre-emptive strategy for past/resolved HBV patients. The actual mechanism of HBV reactivation induced by ICIs is still unclear. On the other hand, there are several ongoing clinical trials on the potential role of ICIs as a curative treatment for CHB based on their activity in regain the original immunosurveillance capacity of exhausted CD8+ T cells[7].

Regarding the preferred antiviral prophylaxis regimen, as recommended by the main HBV management guidelines, all the available nucleot(s)ide analogue are possible options for past/resolved HBV infection[8,9]. In this setting of patients with not detectable HBV-DNA, even a low barrier to HBV resistance agent, such as lamivudine, may be used safely and it is cost-effective. Patients with CHB or HBsAg negative with detectable HBV-DNA should instead be treated with agents with high barrier to HBV resistance such as entecavir, tenofovir disoproxil-fumarate and tenofovir alafenamide.

In conclusion, the review of Mak *et al*[1] well resumed the risk of HBV reactivation in patients with hematologic malignancies undergoing novel therapies. In the cited studies, the populations are very heterogeneous dealing with patients with both solid and hematologic tumors, the latter representing generally a smaller part of the sample size. Authors' conclusions are reasonably suitable in these group of patients, but solid results are still lacking.

FOOTNOTES

Author contributions: Tonnini M, Solera Horna C and Ielasi L conceived the manuscript; Tonnini M reviewed the literature and wrote the original draft; Tonnini M and Ielasi L reviewed and edited the manuscript; Solera Horna C supervised; and all authors read and agreed to the published version of the manuscript.

Conflict-of-interest statement: All the authors report no relevant conflicts of interest for this article.

Country/Territory of origin: Italy

ORCID number: Luca Ielasi 0000-0003-4162-2319.

S-Editor: Wang JJ
L-Editor: A
P-Editor: Zhao S

REFERENCES

1 **Mak JWY**, Law AWH, Law KWT, Ho R, Cheung CKM, Law MF. Prevention and management of hepatitis B virus reactivation in patients with hematological malignancies in the targeted therapy era. *World J Gastroenterol* 2023; **29**: 4942-4961 [PMID: 37731995 DOI: 10.3748/wjg.v29.i33.4942]

2 **Mustafayev K**, Torres H. Hepatitis B virus and hepatitis C virus reactivation in cancer patients receiving novel anticancer therapies. *Clin Microbiol Infect* 2022; **28**: 1321-1327 [PMID: 35283317 DOI: 10.1016/j.cmi.2022.02.042]

3 **Lau G**, Yu ML, Wong G, Thompson A, Ghazinian H, Hou JL, Piratvisuth T, Jia JD, Mizokami M, Cheng G, Chen GF, Liu ZW, Baatarkhuu O, Cheng AL, Ng WL, Lau P, Mok T, Chang JM, Hamid S, Dokmeci AK, Gani RA, Payawal DA, Chow P, Park JW, Strasser SI, Mohamed R, Win KM, Tawesak T, Sarin SK, Omata M. APASL clinical practice guideline on hepatitis B reactivation related to the use of immunosuppressive therapy. *Hepatol Int* 2021; **15**: 1031-1048 [PMID: 34427860 DOI: 10.1007/s12072-021-10239-x]

4 **Shi Y**, Zheng M. Hepatitis B virus persistence and reactivation. *BMJ* 2020; **370**: m2200 [PMID: 32873599 DOI: 10.1136/bmj.m2200]

5 **Papatheodoridis GV**, Lekakis V, Voulgaris T, Lampertico P, Berg T, Chan HLY, Kao JH, Terrault N, Lok AS, Reddy KR. Hepatitis B virus reactivation associated with new classes of immunosuppressants and immunomodulators: A systematic review, meta-analysis, and expert opinion. *J Hepatol* 2022; **77**: 1670-1689 [PMID: 35850281 DOI: 10.1016/j.jhep.2022.07.003]

6 **Ding ZN**, Meng GX, Xue JS, Yan LJ, Liu H, Yan YC, Chen ZQ, Hong JG, Wang DX, Dong ZR, Li T. Hepatitis B virus reactivation in patients undergoing immune checkpoint inhibition: systematic review with meta-analysis. *J Cancer Res Clin Oncol* 2023; **149**: 1993-2008 [PMID: 35767193 DOI: 10.1007/s00432-022-04133-8]

7 **Su M**, Ye T, Wu W, Shu Z, Xia Q. Possibility of PD-1/PD-L1 inhibitors for the treatment of patients with chronic hepatitis B infection. *Dig Dis* 2023 [PMID: 37820605 DOI: 10.1159/000534535]

8 **European Association for the Study of the Liver**. EASL 2017 Clinical Practice Guidelines on the management of hepatitis B virus infection. *J Hepatol* 2017; **67**: 370-398 [PMID: 28427875 DOI: 10.1016/j.jhep.2017.03.021]

9 **Terrault NA**, Lok ASF, McMahon BJ, Chang KM, Hwang JP, Jonas MM, Brown RS Jr, Bzowej NH, Wong JB. Update on prevention, diagnosis, and treatment of chronic hepatitis B: AASLD 2018 hepatitis B guidance. *Hepatology* 2018; **67**: 1560-1599 [PMID: 29405329 DOI: 10.1002/hep.29800]

World Journal of Gastroenterology

Submit a Manuscript: https://www.f6publishing.com

World J Gastroenterol 2024 February 7; 30(5): 512-515

DOI: 10.3748/wjg.v30.i5.512

ISSN 1007-9327 (print) ISSN 2219-2840 (online)

LETTER TO THE EDITOR

Can serum immunoglobulin G4 levels and age serve as reliable predictors of relapse in autoimmune pancreatitis?

Jun-Min Song, Si-Yu Sun

Specialty type: Gastroenterology and hepatology

Provenance and peer review: Unsolicited article; Externally peer reviewed.

Peer-review model: Single blind

Peer-review report's scientific quality classification

Grade A (Excellent): A
Grade B (Very good): B
Grade C (Good): 0
Grade D (Fair): 0
Grade E (Poor): 0

P-Reviewer: Altonbary AY, Egypt; Salvadori M, Italy

Received: December 11, 2023
Peer-review started: December 11, 2023
First decision: December 22, 2023
Revised: December 23, 2023
Accepted: January 12, 2024
Article in press: January 12, 2024
Published online: February 7, 2024

Jun-Min Song, Si-Yu Sun, Department of Gastroenterology, Shengjing Hospital of China Medical University, Shenyang 110004, Liaoning Province, China

Corresponding author: Si-Yu Sun, MD, PhD, Professor, Department of Gastroenterology, Shengjing Hospital of China Medical University, No. 36 Sanhao Street, Shenyang 110004, Liaoning Province, China. sunsy@sj-hospital.org

Abstract

We are writing in response to the paper published in the *World Journal of Gastroenterology* by Zhou *et al*. The authors identified higher serum immunoglobulin (Ig) G4 levels and age over 55 years as independent risk factors for disease relapse. Despite notable strengths, it is crucial to address potential biases. Firstly, the cohort study included 189 patients with autoimmune pancreatitis (AIP) type 1 (with higher IgG4 seropositivity and higher relapse) and 24 with type 2 (with lower IgG4 seropositivity and lower relapse). Consequently, most, if not all, AIP type 2 patients were assigned to the normal group, possibly inflating the association of higher serum IgG4 levels with relapse and potentially exaggerating the association of older age with relapse. Secondly, the authors did not provide sufficient details regarding AIP diagnosis, such as the ratio of definitive *vs* probable cases and the proportion of biopsies. In cases where histological evidence is unavailable or indeterminate, AIP type 2 may be misdiagnosed as definitive type 1, and type 1 may also be misdiagnosed as probable type 2, particularly in cases with normal or mildly elevated serum IgG4 levels. Lastly, in this retrospective study, approximately one-third of the consecutive patients initially collected were excluded for various reasons. Accordingly, the impact of non-random exclusion on relapse outcomes should be carefully considered. In conclusion, the paper by Zhou *et al* offers plausible, though not entirely compelling, evidence suggesting a predictive role of elevated serum IgG4 levels and advanced age in AIP relapse. The foundation for future investigations lies in ensuring a reliable diagnosis and accurate disease subtyping, heavily dependent on obtaining histological specimens. In this regard, endoscopic ultrasound-guided fine-needle biopsy emerges as a pivotal component of the diagnostic process, contributing to mitigating biases in future explorations of the disease.

Key Words: Autoimmune pancreatitis; Immunoglobulin; Endoscopic ultrasound; Relapse; Age

Core Tip: This paper assesses the strengths and potential biases of the provided study. Accurate diagnosis and subtyping are crucial for both clinical practice and research. In this context, endoscopic ultrasound-guided fine-needle biopsy emerges as a pivotal component of the diagnostic process, playing a key role in mitigating the introduction of various biases in future investigations of autoimmune pancreatitis.

Citation: Song JM, Sun SY. Can serum immunoglobulin G4 levels and age serve as reliable predictors of relapse in autoimmune pancreatitis? *World J Gastroenterol* 2024; 30(5): 512-515
URL: https://www.wjgnet.com/1007-9327/full/v30/i5/512.htm
DOI: https://dx.doi.org/10.3748/wjg.v30.i5.512

TO THE EDITOR

We are writing in response to the recent clinical research paper published in the *World Journal of Gastroenterology* by Zhou *et al*[1]. In their study, the authors presented a cohort of 213 patients diagnosed with autoimmune pancreatitis (AIP), assigned to two groups based on serum immunoglobulin (Ig) G4 levels. Specifically, 148 patients were assigned to the abnormal group with serum IgG4 levels exceeding 2-fold the upper limit of the reference range, while 65 patients belonged to the normal group with serum IgG4 levels at or below this threshold. Through a comprehensive comparison of clinical characteristics and outcomes between these two groups, Zhou *et al*[1] identified higher serum IgG4 levels and age over 55 years as independent risk factors for disease relapse.

The significance of this large-sample study, considering the relative rarity of AIP, lies in its potential to contribute valuable insights to the management of patients with AIP. The findings suggest that monitoring serum IgG4 levels, particularly when exceeding 2-fold the upper limit of the reference range, can serve as a useful predictive indicator for disease relapse. Furthermore, the identification of age over 55 years as an independent risk factor adds dimension to the prognostic considerations for AIP. The implications of these results are noteworthy, as they may guide clinicians in developing more targeted and effective management strategies for AIP patients. The study conducted by Zhou *et al*[1] provides a solid foundation for further discussions and investigations in the field of AIP, shedding light on potential paths for improved patient care and outcomes.

AIP represents a distinctive form of chronic pancreatitis triggered by aberrant autoimmune or inflammatory reactions. The disease encompasses two clinical subtypes, namely type 1 (histologically defined as lymphoplasmacytic sclerosing pancreatitis) and type 2 (histologically defined as idiopathic duct-centric pancreatitis). Despite sharing indistinguishable imaging manifestations and exhibiting a complete response to steroid treatments, these two subtypes display distinct clinical, histological, and prognostic features[2]. Notably, patients with AIP type 1 exhibit higher IgG4 seropositivity (60%-80%)[3-5] and a more elevated relapse rate (up to 60%)[4] compared to those with type 2, where IgG4 seropositivity is lower (approximately 20%)[4,5], and the relapse rate is correspondingly reduced (approximately 20%)[6,7]. Additionally, individuals with type 1 are, on average, two decades older than their type 2 counterparts[2].

One of the outstanding challenges in clinical practice is identifying reliable risk factors associated with the relapse of AIP type 1. Presently, the most pertinent factors include proximal bile duct involvement (*vs* no involvement), diffuse pancreatic enlargement (*vs* focal enlargement), and initial treatment with steroids (*vs* surgical resection)[8]. However, the role of elevated serum IgG4 levels and older age remains contentious, as discussed in this paper and other sources[8]. The primary contribution of this study is to underscore the significance of elevated serum IgG4 levels and older age in predicting relapse. However, it is crucial to interpret this contribution cautiously due to potential biases. Firstly, the cohort study included 189 patients with AIP type 1 and 24 with type 2, resulting in a proportion of type 2 patients of approximately 10%, consistent with an international multicenter study[9]. Consequently, most, if not all, AIP type 2 patients (with lower IgG4 seropositivity and lower relapse rates) were assigned to the normal group, possibly inflating the association of higher serum IgG4 levels with relapse. Similarly, the abnormal group mostly comprised AIP type 1 patients with older age (as indicated in the study, male patients in the abnormal group were older than their normal group counterparts) and higher IgG4 seropositivity, potentially exaggerating the association of older age with relapse. Secondly, the authors did not provide sufficient details regarding AIP diagnosis, such as the ratio of definitive *vs* probable cases and the proportion of biopsies. According to international consensus diagnostic criteria, biopsy is mandatory for AIP type 2 but not for type 1[10]. However, in cases where histological evidence is unavailable or indeterminate, AIP type 2 may be misdiagnosed as definitive type 1[11], and type 1 may also be misdiagnosed as probable type 2, particularly in cases with normal or mildly elevated serum IgG4 levels. Lastly, in this retrospective study, a total of 308 consecutive patients were initially collected, but 95 patients (approximately one-third) were excluded for various reasons. As the exclusion was not random (*e.g.*, patients with no relapse were more likely to be excluded due to incomplete follow-up data), the impact of exclusion on relapse outcomes should be carefully considered.

In conclusion, the clinical research paper authored by Zhou *et al*[1] provides plausible, albeit not entirely compelling, evidence suggesting a predictive role of elevated serum IgG4 levels and advanced age in the relapse of AIP. These findings, while intriguing, warrant further validation through prospective, multi-center studies with larger sample sizes.

The cornerstone of such investigations lies in ensuring a reliable diagnosis and accurate disease subtyping, a task heavily reliant on obtaining histological specimens. In this regard, endoscopic ultrasound (EUS)-guided fine needle aspiration (FNA) and biopsy (FNB) emerge as pivotal components of the diagnostic process. While EUS-FNA proves valuable in distinguishing between the two subtypes of AIP, particularly in seronegative cases[12], the overall performance of FNB surpasses that of FNA. A recent clinical research paper published in the *Endoscopic Ultrasound* by Thomsen *et al*[13] sheds light on this aspect. Their examination of 852 consecutive pancreatic EUS-SharkCore FNB procedures, spanning both benign and malignant lesions, revealed the successful acquisition of sufficient tissue cylinders for histological diagnosis in 93.4% (796/852) of cases. Despite immediate and late complications occurring in 5.4% and 4.7% of procedures, respectively, only 0.2% required intervention. Notably, among the FNB procedures from 15 patients with AIP (10 type 1 and 5 type 2), the study reported a sensitivity of 83.3%, a specificity of 99.5%, and an accuracy of 99.2%. Furthermore, EUS, especially ultrasound elastography, provides distinctive features that enhance the diagnosis of AIP, while concurrently aiding in its differentiation from pancreatic cancer[14,15]. Collectively, these studies underscore the potential of EUS-FNB as an optimal approach for diagnosing and subtyping AIP, offering a high level of efficacy and safety. This contributes to mitigating the introduction of various biases in future explorations of the disease.

FOOTNOTES

Author contributions: Sun SY contributed to the paper framework; Song JM authored the manuscript; both authors collaborated on finalizing the manuscript before submission.

Conflict-of-interest statement: There are no conflicts of interest to report.

Country/Territory of origin: China

ORCID number: Si-Yu Sun 0000-0002-7308-0473.

S-Editor: Chen YL
L-Editor: A
P-Editor: Cai YX

REFERENCES

1 **Zhou GZ**, Zeng JQ, Wang L, Liu M, Meng K, Wang ZK, Zhang XL, Peng LH, Yan B, Pan F. Clinical characteristics and outcome of autoimmune pancreatitis based on serum immunoglobulin G4 level: A single-center, retrospective cohort study. *World J Gastroenterol* 2023; **29**: 5125-5137 [PMID: 37744294 DOI: 10.3748/wjg.v29.i35.5125]

2 **Li Y**, Song H, Meng X, Li R, Leung PSC, Gershwin ME, Zhang S, Sun S, Song J. Autoimmune pancreatitis type 2 (idiopathic duct-centric pancreatitis): A comprehensive review. *J Autoimmun* 2023; **140**: 103121 [PMID: 37826920 DOI: 10.1016/j.jaut.2023.103121]

3 **Masamune A**, Kikuta K, Hamada S, Tsuji I, Takeyama Y, Shimosegawa T, Okazaki K; Collaborators. Nationwide epidemiological survey of autoimmune pancreatitis in Japan in 2016. *J Gastroenterol* 2020; **55**: 462-470 [PMID: 31872350 DOI: 10.1007/s00535-019-01658-7]

4 **Sah RP**, Chari ST, Pannala R, Sugumar A, Clain JE, Levy MJ, Pearson RK, Smyrk TC, Petersen BT, Topazian MD, Takahashi N, Farnell MB, Vege SS. Differences in clinical profile and relapse rate of type 1 *vs* type 2 autoimmune pancreatitis. *Gastroenterology* 2010; **139**: 140-8; quiz e12 [PMID: 20353791 DOI: 10.1053/j.gastro.2010.03.054]

5 **Kamisawa T**, Chari ST, Giday SA, Kim MH, Chung JB, Lee KT, Werner J, Bergmann F, Lerch MM, Mayerle J, Pickartz T, Lohr M, Schneider A, Frulloni L, Webster GJ, Reddy DN, Liao WC, Wang HP, Okazaki K, Shimosegawa T, Kloeppel G, Go VL. Clinical profile of autoimmune pancreatitis and its histological subtypes: an international multicenter survey. *Pancreas* 2011; **40**: 809-814 [PMID: 21747310 DOI: 10.1097/MPA.0b013e3182258a15]

6 **Tacelli M**, Celsa C, Magro B, Barresi L, Guastella S, Capurso G, Frulloni L, Cabibbo G, Cammà C. Risk Factors for Rate of Relapse and Effects of Steroid Maintenance Therapy in Patients With Autoimmune Pancreatitis: Systematic Review and Meta-analysis. *Clin Gastroenterol Hepatol* 2019; **17**: 1061-1072.e8 [PMID: 30312787 DOI: 10.1016/j.cgh.2018.09.051]

7 **Nikolic S**, Lanzillotta M, Panic N, Brismar TB, Moro CF, Capurso G, Della Torre E, Löhr JM, Vujasinovic M. Unraveling the relationship between autoimmune pancreatitis type 2 and inflammatory bowel disease: Results from two centers and systematic review of the literature. *United European Gastroenterol J* 2022; **10**: 496-506 [PMID: 35526270 DOI: 10.1002/ueg2.12237]

8 **Hart PA**, Zen Y, Chari ST. Recent Advances in Autoimmune Pancreatitis. *Gastroenterology* 2015; **149**: 39-51 [PMID: 25770706 DOI: 10.1053/j.gastro.2015.03.010]

9 **Hart PA**, Kamisawa T, Brugge WR, Chung JB, Culver EL, Czakó L, Frulloni L, Go VL, Gress TM, Kim MH, Kawa S, Lee KT, Lerch MM, Liao WC, Löhr M, Okazaki K, Ryu JK, Schleinitz N, Shimizu K, Shimosegawa T, Soetikno R, Webster G, Yadav D, Zen Y, Chari ST. Long-term outcomes of autoimmune pancreatitis: a multicentre, international analysis. *Gut* 2013; **62**: 1771-1776 [PMID: 23232048 DOI: 10.1136/gutjnl-2012-303617]

10 **Shimosegawa T**, Chari ST, Frulloni L, Kamisawa T, Kawa S, Mino-Kenudson M, Kim MH, Klöppel G, Lerch MM, Löhr M, Notohara K,

Okazaki K, Schneider A, Zhang L; International Association of Pancreatology. International consensus diagnostic criteria for autoimmune pancreatitis: guidelines of the International Association of Pancreatology. *Pancreas* 2011; **40**: 352-358 [PMID: 21412117 DOI: 10.1097/MPA.0b013e3182142fd2]

11 **Ikeura T**, Detlefsen S, Zamboni G, Manfredi R, Negrelli R, Amodio A, Vitali F, Gabbrielli A, Benini L, Klöppel G, Okazaki K, Vantini I, Frulloni L. Retrospective comparison between preoperative diagnosis by International Consensus Diagnostic Criteria and histological diagnosis in patients with focal autoimmune pancreatitis who underwent surgery with suspicion of cancer. *Pancreas* 2014; **43**: 698-703 [PMID: 24681878 DOI: 10.1097/MPA.0000000000000114]

12 **Ishikawa T**, Itoh A, Kawashima H, Ohno E, Matsubara H, Itoh Y, Nakamura Y, Hiramatsu T, Nakamura M, Miyahara R, Ohmiya N, Goto H, Hirooka Y. Endoscopic ultrasound-guided fine needle aspiration in the differentiation of type 1 and type 2 autoimmune pancreatitis. *World J Gastroenterol* 2012; **18**: 3883-3888 [PMID: 22876041 DOI: 10.3748/wjg.v18.i29.3883]

13 **Thomsen MM**, Larsen MH, Di Caterino T, Hedegaard Jensen G, Mortensen MB, Detlefsen S. Accuracy and clinical outcomes of pancreatic EUS-guided fine-needle biopsy in a consecutive series of 852 specimens. *Endosc Ultrasound* 2022; **11**: 306-318 [PMID: 35708361 DOI: 10.4103/EUS-D-21-00180]

14 **Tacelli M**, Zaccari P, Petrone MC, Della Torre E, Lanzillotta M, Falconi M, Doglioni C, Capurso G, Arcidiacono PG. Differential EUS findings in focal type 1 autoimmune pancreatitis and pancreatic cancer: A proof-of-concept study. *Endosc Ultrasound* 2022; **11**: 216-222 [PMID: 35142701 DOI: 10.4103/EUS-D-21-00111]

15 **Cui XW**, Li KN, Yi AJ, Wang B, Wei Q, Wu GG, Dietrich CF. Ultrasound elastography. *Endosc Ultrasound* 2022; **11**: 252-274 [PMID: 35532576 DOI: 10.4103/EUS-D-21-00151]

Published by **Baishideng Publishing Group Inc**
7041 Koll Center Parkway, Suite 160, Pleasanton, CA 94566, USA
Telephone: +1-925-3991568
E-mail: office@baishideng.com
Help Desk: https://www.f6publishing.com/helpdesk
https://www.wjgnet.com